uOttawa

Sustainable Polymer Reaction Engineering: Towards Fully Renewable Pressure-Sensitive Adhesives

By

Vida A. Gabriel

A thesis submitted in partial fulfillment of the requirements for the

Doctorate in Philosophy degree in Chemical Engineering

Department of Chemical and Biological Engineering, Faculty of Engineering

University of Ottawa, Ottawa, Canada

Abstract

This thesis has as its principal goal the development of sustainable pressure-sensitive adhesives (PSAs). To that end, we examined polymer reaction engineering practices and polymer formulations through the lens of the *12 Principles of Green Chemistry*. To begin with, we employed emulsion polymerization as our polymer synthesis method because of its use of water instead of hazardous solvents. We also replaced various petroleum-based components with bio-based alternatives (e.g., starch, cellulose nanocrystals), thereby reducing synthesis hazards, increasing product safety and increasing the amount of sustainably sourced raw materials in the PSA. However, changing the synthetic method as well as key components in the formulation presented significant challenges to maintaining PSA performance. This thesis illustrates the challenging path taken towards developing a fully renewable PSA.

PSAs should display a specific balance of adhesion and cohesion. Typically, petroleum-based additives (which are often hazardous/toxic) such as tackifiers, cross-linkers, chain transfer agents and rheology modifiers are added to tailor latex properties to fit the intended application. However, because of their inherently opposing effects, an additive used to increase adhesion will weaken the cohesive forces of the polymer, and vice versa. Cellulose nanocrystals (CNCs) are sustainable nanomaterials that have been shown to be effective to resolve the adhesion/cohesion conundrum. In the first part of this project, we developed a new technique to increase CNC loading in emulsion-based PSA formulations beyond the 1-2% limits previously encountered due to high latex viscosity, colloidal instability, and poor film properties. The higher CNC loadings were shown to continuously improve shear strength but resulted in eventual decreases to tack and peel strength.

In the second part of this project, we replaced the sulfated CNCs with carboxylated CNCs (cCNCs), which are produced by a process using a “greener” catalyst (i.e., hydrogen peroxide instead of sulfuric acid). The cCNCs’ carboxylate surface groups interacted strongly with the polymer matrix, ultimately leading to catastrophic coagulation. The interactions between cCNCs and other standard latex components were studied and through the creative manipulation of the emulsion polymerization process, a reproducible method to incorporate the cCNCs in a seeded semi-batch reaction yielded stable, high-quality latexes. In the third part of this project, the effect

of the cCNCs on the adhesive properties of the nanocomposite latex films was studied and compared to the effects of the sulfated CNCs. AFM imaging revealed that cCNCs interact with latex particles and each other; thus, omitting ultrasonication at the preparation stage was shown to preserve these interactions and lead to greater property enhancements.

In the fourth part of this project, starch nanoparticles (SNPs) were used to displace some of the petroleum-based monomer in the production of core-shell (SNP cores, acrylic shell) latexes. SNPs are renewably sourced, inexpensive, and biodegradable. The challenge of locating the SNPs into the particle cores was overcome by crosslinking the SNPs using a food grade cross-linker (sodium trimetaphosphate) and functionalizing them using a sugar-based monomer (EcoMer™). To tune the PSA properties to rival a range of commercial tapes, a method to incorporate CNCs to the SNP-latexes *in situ* was developed. In addition, because monomers such as 2-octyl acrylate (2OA), styrene, and acrylic acid can be bio-sourced, they were selected as the acrylic shell monomers to encapsulate the SNPs in the nanocomposite latexes. Due to supply chain challenges, n-octyl acrylate was used as a model monomer for 2OA to produce latexes with ~80% bio-content that rivaled commercial Post-It™ notes, masking tapes, and duct tapes.

After addressing the sustainability of the polymerization method and polymer components, we posed the question: what are the effects of using renewably sourced and bio-sourced materials on the end-of-life of the PSAs? Because the infrastructure for biodegradation studies at the lab scale via composting does not exist in Canada (to our knowledge), we designed an in-house aerobic composting set-up consisting of a series of bioreactors and sensors capable of measuring the aerobic biodegradability of our polymers in a simulated composting environment. Although not fully tested, the composting setup was designed, and its construction was begun. Steps to complete the construction and validate its operation are detailed.

The path towards sustainability is often long and complex. In this four-year study, the re-design of an adhesive synthesis process using a more sustainable approach, emulsion polymerization, along with an 80% bio-sourced formulation required significant corrective measures. Overcoming the technical challenges required mustering all the polymer reaction engineering tools at our disposal. Despite the time and effort required, achieving a more sustainable process is indeed within our grasp.

Résumé

L’objectif principal de cette thèse fut le développement durable d'adhésifs sensibles à la pression (ASP). Nous avons employé la polymérisation en émulsion comme méthode de synthèse car il s’agit d’une méthode écologique en raison de son utilisation d'eau au lieu de solvants. Nous avons également remplacé divers composants à base de pétrole par des alternatives biosourcées (ex. amidon, cellulose) d’augmenter la sécurité des produits et la quantité de matières premières d'origine durable. Cependant, l’utilisation de la polymérisation en émulsion et la modification des composants clés de nos latex (c.-à-d, polymères dispersés dans de l’eau) ont mené des défis importants vis-à-vis la qualité et performance des ASP. Cette thèse illustre la voie difficile empruntée pour développer des ASP entièrement renouvelables.

Les ASP doivent démontrés un équilibre spécifique d'adhésion et de cohésion. Généralement, des additifs à base de pétrole (qui sont souvent dangereux/toxiques, ex., des agents collants, de réticulation, de transfert de chaîne, modificateurs de rhéologie,) sont rajoutés pour adapter les propriétés du latex à l'application prévue. Pourtant, en raison de leurs effets opposés, un additif utilisé pour augmenter l'adhérence affaiblira les forces de cohésion du polymère, et vice versa. Les nanocristaux de cellulose (NCC) sont des nanomatériaux durables qui se sont avérés efficaces pour résoudre l'énigme adhérence/cohésion. Dans la première partie de ce projet, nous avons développé une nouvelle technique pour augmenter la charge des NCC dans les formulations d’ASP au-delà des limites de 1 à 2 % précédemment rencontrées. Les charges CNC plus élevées améliorent continuellement la résistance au cisaillement, mais entraînent éventuellement une diminution de la résistance au « tack » et au pelage.

Dans la deuxième partie de ce projet, nous avons remplacé les NCC sulfatés par des NCC carboxylés (NCCc), qui sont synthétisés par une voie plus écologique (par l’emploi du peroxyde d'hydrogène au lieu de l'acide sulfurique). Les groupes de surface carboxylate des NCCc furent déstabilisés par les autres composantes du latex induisant par conséquence une coagulation catastrophique. Les interactions entre les NCCc et d'autres composants de latex standard ont été étudiées et une méthode reproductible pour incorporer les NCCc dans une réaction en semi-continu a abouti des latex stables et de haute qualité. Dans la troisième partie de ce projet, l'effet des NCCc sur les propriétés adhésives des films de latex a été étudié et comparé aux effets des

NCC sulfatés. L'imagerie microscope à force atomique a révélé que les NCCc interagissent avec les particules de latex et entre elles. L'omission de la dispersion ultrasonique préservait ces interactions menant à de plus grandes améliorations des propriétés des films.

Dans la quatrième partie de ce projet, des nanoparticules d'amidon (NPA) ont été utilisées pour remplacer une partie du monomère dans la production de latex coque-noyaux (noyaux NPA, coque acrylique). Les NPA sont renouvelable, peu coûteux et biodégradables. Le défi de délimiter les NPA dans les noyaux des particules a été surmonté en réticulant les NPA avec un réticulant alimentaire (trimétaphosphate de sodium) et en les fonctionnalisant à l'aide d'un monomère à base de sucre (EcoMer™). Pour ajuster les propriétés NPA pour rivaliser avec des rubans commerciaux, une méthode pour incorporer des NCC aux latex NPA *in situ* a été développée. De plus, comme des monomères tels que l'acrylate de 2-octyle (2OA), le styrène et l'acide acrylique peuvent être biosourcés, ils ont été sélectionnés pour former la coque acrylique. En raison des défis et retards de la chaîne d'approvisionnement, l'acrylate de n-octyle a été utilisé comme monomère modèle pour 2OA afin de produire des latex avec une teneur en bio d'environ 80 % qui rivalisait avec les adhésifs commerciaux (Post-It™, rubans de masquage, rubans d'emballage).

Après avoir abordé la durabilité du mode de polymérisation et des composants du polymère, nous avons posé la question : quels sont les effets de l'utilisation de matériaux bio et biosourcés sur la fin de vie des ASP ? Parce que l'infrastructure pour les études de biodégradation à l'échelle du laboratoire via le compostage n'existe pas au Canada (à notre connaissance), nous avons conçu un appareil de compostage aérobie capable de mesurer la biodégradabilité aérobie de nos polymères dans un environnement de compostage. Bien qu'elle n'ait pas été entièrement testée, l'installation de compostage a été conçue et sa construction a commencé. Les étapes pour terminer la construction et valider son fonctionnement sont détaillées.

Le chemin vers la durabilité est souvent long et complexe. Dans cette étude la ré-conception de la synthèse d'adhésifs avec une approche plus durable, la polymérisation en émulsion, associée à une formulation à 80% biosourcée a nécessité d'importantes mesures correctives. Pour surmonter les défis techniques, il a fallu rassembler tous les outils d'ingénierie de la réaction des polymères à notre disposition. Malgré le temps et les efforts requis, la réalisation d'un processus plus durable est en effet à notre portée.

Preface

Dedications

I dedicate my thesis first and foremost to my parents, Iman and Albert, who have showered me in their love and prayers all my life. Mom and dad, you have given me everything I could ever need and instilled in me a fierce curiosity and thirst for knowledge from a very young age. Thank you for your unwavering support and encouragement that has enabled me to complete a doctorate degree in Chemical and Biological Engineering. Thank you for teaching me that I can do anything that I set my mind to (and for also teaching me that I can't do *everything*). Leading by example, you have helped me grow into a kind, confident, and effective leader (in my opinion anyway). Thank you for nurturing me into the person I am today. I love you both so much.

I likewise dedicate this thesis to my sisters, Grace and Shaina. To Grace; If it weren't for you teaching me how to read and rite English many years ago, I'd be in a lot of troble! Your deep understanding and passion in your field along with your academic ambitions and success have inspired me to want to deepen my knowledge in my own field. Thank you for having encouraged me to pursue post-graduate studies and for your help in preparing my grad school and NSERC applications. To Shaina; I am so fortunate and happy that you decided to study in Ottawa. I have benefitted from your sound advice and astute perspectives on many occasions. You have such a unique way of making me laugh and love life, and I always have so much fun when we hang out! Thank you for making me laugh until my cheeks hurt, for your emotional support and for your wholesome and warm company. Thank you for taking me salsa dancing, suffering through Madfit workouts with me, enabling some epic food adventures, and for keeping me alive when I was sick. I love you both so much.

Acknowledgements

I would like to acknowledge those with who without their guidance, support, advice, encouragement and inspiration through my studies at the University of Ottawa, this thesis would not have been possible.

With much earnestness, I would like to express my deepest gratitude to my supervisor (and mentor, and therapist…), Prof. Marc A. Dubé. You have been part of my academic and personal journey since 2013 where you taught my first ever chemical engineering course (CHG 1525), and at least one other course each year thereafter (the department really needs more French speaking professors… haha!). Thank you for your enthusiastic encouragement, patient guidance and useful critiques through the planning and completion of this work. Thank you for all of the time you have invested in me. You have created the environment that has allowed me to learn and grow as a researcher and as a person and for providing the opportunities for me to succeed. Your strong leadership skills have fostered a research group in which I felt motivated, encouraged, and confident. You have also helped me grow as a leader. The last 5-6 years of my life have been truly exceptional, and in many ways I have you to thank for that. Last but not least, thank you for being a kind, compassionate, and trustworthy adult that I could turn to for personal advice.

I would also like to sincerely express my deepest gratitude and love to my partner, Sean M.W. Wilson. Your curiosity, entrepreneurial traits, and constant thirst for knowledge are truly admirable and over the years you have inspired me to become more curious and daring on an academic and personal level. Thank you for engaging me in countless debates and fruitful conversations about polymer degradation, time management, and life priorities. Watching how you prioritized your family and stayed true to your values throughout your studies taught me how to establish meaningful work-life balances and made me questions and redefine my own priorities and life goals. Thank you for introducing me to the world of prototyping and for sharing your knowledge, skills, and experience with me freely; your input during the design and in-house construction of the biodegradation set-up was invaluable. Thank you for taking care of me during my graduate studies (e.g., pep-talks, indulging me with French baguettes, pizzas, pulled-pork,

chocolate castella cakes, chocolate mousse, then forcing me to get some exercise) and for enabling me to live my best life. I cherish all of the memories we made throughout our studies, quarantined during COVID, and traveling (New-Brunswick, Australia, France, the USA, Finland, Croatia). You are truly a remarkable human being, and I cannot imagine a life without you in it. I am eager to embark on this journey (i.e., life) with you and to experience lifelong adventure, learning and growth alongside you.

I must express my love and sincere gratitude to my brother-in-law, Patrick M.J. Szell, who likewise played a critical part in my journey. Pat, as my TA (#bestTAever), you inspired me. Your confidence, mentoring and teaching abilities, critical thinking, lab experience, charisma and general mannerisms gave you this aura that was so fascinating to me; I wanted to be like you. I mark the start of this entire journey when you helped me switch from Biotechnology to Chemical Engineering. Thereafter, your impact in my academic and personal journeys compounded as you transitioned from TA to mentor, friend, and then family. Thank you for your continuous encouragement and praise and for being an active part of my life. The fact that you enthusiastically believed in me made me believe that I could accomplish anything. You are one of a kind Pat, and I can't wait for our future children to grow up together.

I would like to take the time to thank my colleagues, Yujie Zhang and Amir S. Pakdel. Yujie; thank you for showing me the ropes of polymer reaction engineering. From day one you were there with me on the battlefield of CBY D404 and you are the person with whom I loved doing research with the most. You taught me that problems and challenges encountered in the lab were just learning opportunities in disguise. Thank you for blasting Coldplay and Imagine Dragons in the lab while we worked; you showed me how fun research can be even if we were cleaning coagulum. I am so fortunate and grateful to have a friend like you in my life. Amir; your knowledge and creative thinking never ceased to amaze me. I have learned so much from you; talking through my research challenges with you over the years always left me energized and motivated to move forward. Thank you for being so easy to laugh with, for always greeting me with a smile and for being a part of my academic journey. Despite the experience, maturity and knowledge gap between us, you always treated me as an equal and though you may not know it, it did wonders to my confidence.

I would like to take the time to thank some of my Ottawa family. To Debbie and Tim Wilson; thank you for welcoming me into your beautiful family. Knowing that we will get together every Sunday for dinner kept me going during the week. Thank you for generously sharing your knowledge and time with me, and for organizing such wholesome awesome New Brunswick vacations. To Marie Faure; you are a fierce and wonderful human. Thank you for letting me be a part of your life, and for enriching mine in indescribable ways. Your advice and perspectives on problems and life in general are enormously valuable to me. I love you more than words can describe, and I will always be there for you (get ready to babysit my 10+ children!) To Dominique Thérien and Josée Gravelle (a.k.a. Mama T); thank you for always being the first to congratulate me and for believing in me, even before I started graduate school. Dominique, your friendship is priceless. Thank you for letting me be a part of so many of your milestones (graduation, wedding, starting a family). Thank you both for stealing me away from my busy world and taking me various oases (e.g., the spa, Bekta, La Belle et La Boeuf, Pizzaro's, the movies (#FantasticBeasts), Cirque du Soleil, your cottage) and for helping me not fall behind when I got sick in 4th year. I love you all so much!

I would like to thank Prof. Emily D. Cranston for her involvement in all my work. Thank you for introducing me to the world of CNCs and for coming up with the titles of basically all of our collaborative work. Your input and guidance through some of my stickiest situations (hehe) was invaluable. Your academic achievements are remarkable and each of your students that I have interacted with were so bright, kind, driven, knowledgeable and helpful which attests to your abilities as a leader, teacher and supervisor.

I would like to acknowledge the amazing team at Anomera Inc., notably, Dr. Timothy Morse, Dr. Nathan Hordy, Dr. Amir Khabibullin, Dr. Zhen (Justin) Hu and Michael Kiriakou for all their help and input when working with the carboxylated cellulose nanocrystals. Tim, turns out that the flavour of Salmiaki has grown on me too!

Finally, I would like to thank the Faculty of Engineering for partial funding of my graduate studies through the academic excellence scholarships and for the Natural Sciences and Engineering Research Council for their financial support through the CGS-D scholarship.

Statement of Contributions

I would like to acknowledge Prof. Emily D. Cranston from the University of British Columbia for her research guidance and editorial help in the writing of the manuscript entitled "Pushing the Limits with Cellulose Nanocrystal Loadings in Latex-Based Pressure-Sensitive Adhesive Nanocomposites."

Prof. Michael Cunningham from Queen's University provided editorial comments and general experimental guidance with the work done with the carboxylated cellulose nanocrystals. Prof. Pascale Champagne from Queen's University likewise participated in discussions for that work. Mathieu N. Tousignant (University of Ottawa) performed AFM and Dr. Sean M.W. Wilson (TerraFixing Inc.) and Dr. Marie D.M. Faure (University of Ottawa) assisted in the manipulation and interpretation of the AFM data. Prof. Benoît Lessard (University of Ottawa) provided the funds for the AFM measurements.

Dr. S.W. Wilson assisted the bioreactor prototyping (including the electrical components) and translated the physical bioreactor design to SolidWorks (i.e., produced the schematics for their construction).

My supervisor Prof. Marc A. Dubé provided scientific guidance and support, and contributed to the revisions and editing of the manuscripts presented here.

Statement of Originality

I certify that the research presented in this thesis is of my own work, and all referenced work performed by others is explicitly stated using standard methods.

Table of Contents

List of Figures

List of Tables

Nomenclature

2OA	2-Octyl acrylate
AA	Acrylic acid
AFM	Atomic force microscopy
AIBN	2,2'-Azobisisobutyronitrile
ASTM	American Society for Testing and Materials
ATR-FTIR	Attenuated total reflectance-Fourier transform infrared spectroscopy
BA	Butyl acrylate
BVE	Butyl vinyl ether
CNC	Cellulose nanocrystal
cCNC	Carboxylated CNC
CTA	Chain transfer agent
CTAB	Cetyltrimethylammonium bromide
DDW	Distilled deionized water
DLS	Dynamic light scattering
DMA	Dynamic mechanical analysis
DSC	Differential scanning calorimetry
EP	Emulsion polymerization
FSM	Functionalized sugar-based monomer
HCl	Hydrochloric acid
ISO	International Organization for Standardization
KPS	Potassium persulfate
M_c	Molecular weight between crosslink points
M_e	Molecular weight between entanglements
MMA	Methyl methacrylate
mSNP	Modified starch nanoparticles
M_w	Molecular weight
MWD	Molecular weight distribution
$NaHCO_3$	Sodium bicarbonate, buffer
NaOH	Sodium hydroxide
NMR	Nuclear magnetic resonance spectroscopy
nOA	n-Octyl acrylate
phm	Parts per hundred parts of monomer (by mass)
PNC	Polymer nanocomposites
PSA	Pressure-sensitive adhesive
PSD	Particle size distribution
PSTC	Pressure Sensitive Tape Council
SEM	Scanning electron microscopy
SNC	Starch nanocrystal
SNP	Starch nanoparticle
SS	Stainless steel
STMP	Sodium trimetaphosphate
STY	Styrene
TEM	Transmission electron microscopy
T_g	Glass transition temperature
THF	Tetrahydrofuran
wt.%	Weight percent

Chapter 1

Introduction

1.1 Sustainable polymer reaction engineering

1.1.1 What do we mean by "sustainable polymer"?

Polymers are a class of materials with an exceedingly broad range of applications. Although their light weight, flexibility, versatility, and low cost have provided unparalleled benefits to humanity, their manufacture, ubiquity, and durability has resulted in their accumulation in nature and in causing serious harm to our ecosystems. When tackling environmental concerns, sustainability is often the first criteria addressed. The definition of "sustainability", in its general sense, refers to the continued capacity to function at the necessary level to maintain the desired benefits.[1] In the context of this thesis, sustainability also encompasses the notion of considering future consequences of present processes or actions. The definition of polymer sustainability has been the subject of much debate because it is often defined in a relative manner, that is, by comparison to current or traditional practices. For example, if a plastic product contains renewable materials, is produced via an eco-friendlier method or can degrade (even if just partially), it can be called a "sustainable polymer". Ideally, for a polymer to be labelled as sustainable, each element of its lifecycle (i.e., material extraction, manufacturing, packaging and transportation, use, and end-of-life) should be sustainable. Thus, when discussing "sustainable polymers", we are henceforth referring to a polymer that:

1. Is produced in an eco-friendly process (e.g., has no harmful by-products, does not generate waste, requires minimal water resources and energy (preferably, renewable energy), does not impart negative environmental consequences),
2. Is produced using renewable feedstock (e.g., waste materials, plant or other naturally occurring matter), and
3. Can be reintegrated into the environment after its useful life without any detrimental effects to humans, animals, or the environment.

An important aside: Although the terms bio-based, bio-sourced, renewably-sourced, renewable and sustainable share some similarities, they are not interchangeable. Each have key elements that make them distinguishable from the other, thus, for clarity, they are defined in Table 1.1 (note that the word "material" can be replaced with monomer, polymer, etc.).

Table 1.1 Helpful term distinctions and definitions.

Term	**Definition**
Bio-based material	A material that is *obtained directly* from natural resources
Bio-sourced material	A material that is *derived* from natural resources
Renewably-sourced material	A material that is obtained via an ecological (renewable) process
Renewable material	A material made from natural resources (bio-based or bio-sourced) that can be replenished and/or cycled back to its origin
Sustainable material	A material that is renewably-sourced and renewable

Figure 1.1 is an effective approach for the development of sustainable polymers. Waste prevention at the production stage, using catalysts, avoiding chemical derivatives, maximizing atom economy, analyzing in real time, and minimizing potential for accidents (principles 1, 5-7, 9, 11 and 12, respectively) are arguably well addressed in industry due to the economic benefits that they offer. On the other hand, the principles with the greatest potential impact on sustainability include (2) designing safer products, (3) designing less hazardous synthesis, (4) using renewable feedstock, (8) using safer solvents and reaction conditions, and (10) designing products to degrade after use.[2, 3]

Figure 1.1 The 12 Principles of Green Chemistry.[4]

In this thesis, we use emulsion polymerization (discussed in detail later), a well-known polymer production process. It is considered to be an environmentally friendly method of producing polymers largely because its bulk medium is water as opposed to the volatile and toxic solvents used in many commercial processes.[5] Principles 2, 3, and 8 are addressed when switching to emulsion polymerization because the resulting products are safer (e.g., no solvent off-gassing), it is a less hazardous polymer production method (e.g., low reaction pressure, good heat transfer), and the absence of solvents improves overall reaction safety conditions.

Producing polymeric materials from renewable feedstock (i.e., principle 4) has an enormous environmental impact because the majority of polymer formulations consist of monomers, which typically, are derived from fossil fuels. Renewable monomers have been available for decades[6–9] and their abundance in nature provides a baseline for economical and environmentally-friendly use. Common monomers such as methacrylic acid, styrene, and acrylic acid can be bio-sourced,[10–14] thus, using renewably-sourced monomers can improve polymer sustainability dramatically. In addition, using a renewable feedstock can provide further impact on other "green" principles. For instance, vegetable oils, lignin, cellulose, chitin, starch, and other natural polymers have been used to produce polymeric materials[6, 15–18]and because they are largely nontoxic, the resulting products are safer (principle 2). Furthermore, renewably-sourced nanoparticles, such as cellulose nanocrystals (CNCs, discussed later), can be used as polymer property modifiers[19–24] and are a safer alternative to typical, toxic property modifiers.[25] Thus, employing green nanoparticles in lieu of traditional petrochemical additives can reduce overall synthesis hazards (i.e., principle 3).

Finally, the use of renewable feedstock may enable the design of polymers that can degrade after use (principle 10). Starch nanoparticles (SNPs) are renewably-sourced and biobased nanomaterials and can be used as fillers in emulsion-based polymers.[26–28] When used to fill polymer particle cores, SNPs not only displace fossil fuel-based materials (i.e., monomer), but they increase the polymer bio-content and introduce a biodegradable component to the resulting material. Nonetheless, petroleum-based monomers still form a significant part of polymer formulations, thus, we have an opportunity (and a duty) to displace higher amounts of monomer and other toxic components with bio- or sustainably-sourced alternatives.

1.1.2 Challenges to sustainable practice

The main challenge in the production of more sustainable adhesives lies in the use of emulsion polymerization. In the first place, many commercial adhesives are prepared via solution polymerization and conversion to an emulsion polymerization process will lead to product performance changes.[2, 20, 21, 29, 30] The heterogeneous (i.e., multi-phase) nature of the emulsion polymerization process, compared to the single phase in a solution polymerization, is responsible for these changes. Specifically, a solution polymerization will yield a homogeneous, continuous network that provides cohesive strength to the adhesive when cast as a film on a substrate. On the other hand, because of the compartmentalized nature of an emulsion polymerization (a suspension of polymer particles or latex), a continuous network is harder to achieve during film formation because it relies on diffusion of polymer chains from particle to particle. In addition, because of the replacement of such a significant amount of components in the formulation with renewable materials, the polymerization kinetics and the resulting product properties will inevitably be affected. In particular, the colloidal stability of the latex can be disrupted; colloidal dispersions are sensitive to their specific chemical environments and thus, every component present in the reaction mixture is prone to interactions with other components. To overcome such significant changes to the polymerization process and formulation, we will need to exploit many techniques in our polymer reaction engineering toolbox, which include when and how to add components to the formulation (e.g., via semi-batch addition), and adjusting the particle size, particle size distribution, pH, solids content, and polymer microstructure.

Two of the renewable materials selected for this study, CNCs and SNPs, are hydrophilic and incorporating them in a hydrophobic polymer matrix poses additional technical challenges, especially in an emulsion polymerization (i.e., a water-based process).[19, 27] Regardless, the addition of SNPs allows for a higher bio-content while CNCs have been shown to improve adhesive properties.[20, 21, 27] A number of techniques have been developed to overcome these challenges including chemical modification of the CNCs and SNPs.[26, 31–36] At the same time, the loading of these materials, relative to the bulk monomer, is limited due to their effect on adhesive performance. Thus, replacing the remaining petroleum-based monomer with renewably-sourced alternatives becomes an appealing option.

Given that our long-term goal is to design a completely renewable PSA, we must replace the most impactful components (i.e., monomers) with greener counterparts. There are many options available, but most of these are either too expensive or are obtained through unsustainable pathways, which defeats the purpose of this work. Plant-based oils have been explored as a cheaper, potential source of greener monomers due to the presence of double bonds in their structure. However, the triglyceride building blocks in these oils are often inert and pushing them to react in a conventional free-radical emulsion polymerization is difficult.[15, 16, 37, 38] Monomer options for the production of high-performance, sustainable PSAs are particularly constrained because they should simultaneously 1- be compatible with waterborne polymerization methods, 2- be biobased, bio-sourced or biodegradable, 3- be able to participate in free-radical polymerization (i.e., have a vinyl group), and 4- have a low homopolymer T_g. Therefore, deriving widely used monomers, traditionally prepared from fossil resources, from renewable feedstock is an appealing option because the above criteria can be met without affecting reaction kinetics or product performance.

Acrylic acid (AA) and methacrylic acid (MAA) are among the cornerstone building blocks for common acrylic monomers and although it is not yet the standard in industry, AA and MAA can be synthesized from glycerol with high yields and selectivity.[39] 2-octyl acrylate (2OA), which can be derived from bio-sourced AA, has been gaining popularity in the realm of PSAs because it is a low T_g acrylic monomer. In 2008, 3M™ patented the use of 2OA for adhesive applications and launched its Scotch® Magic™ Greener tape in 2009, made from 65% plant-based and recycled materials.[40] A year later, the Post-It® Greener note was released which uses 100% recycled paper fibres and 67% plant-based adhesives.[41] In this work, we sought to increase the biocontent of our emulsion-based PSAs therefore, 2OA, STY and AA were selected as co-monomers because each of them can be biosourced.[11, 12, 42, 43] Note that nOA (same molecular weight a 2OA) was used as a model monomer for 2OA because of its availability during the COVID-19 pandemic.

Finally, while there has been significant research on the use of renewable materials in polymer formulations,[6, 44–50] analysis regarding polymer end of life is lacking. Despite the availability of standardized and internationally recognized testing methods[51–54] and the vast

amounts of resources and data addressing polymer degradation, little has been reported about the degradability of adhesives (with the exception of research focused on adhesives for medical applications).[55] For reasons described in Chapter 7, our hypothesis is that the probability for polymer (bio)degradation is highest in a composting environment, thus we are interested in testing the aerobic biodegradability of our PSAs in a composting environment. Unfortunately, to our knowledge, the infrastructure for testing biodegradation in a composting environment at the lab scale does not exist in Canada. Chapter 7 details the design and construction of an apparatus capable of simulating a composting environment to determine the aerobic biodegradation of plastic materials under controlled composting conditions (compliant to the American standard testing method (ASTM) D5338).[51] Ultimately, this simulated composting environment is the missing tool that we need in our engineering toolbox to design truly sustainable PSAs.

1.2 Objectives, hypothesis, and thesis structure

The objective of this thesis was to use sustainable methods to produce high-performance adhesives composed of a maximal amount of renewable material. We hypothesize that by combining the unique qualities of SNPs and CNCs as a nanocomposite material with renewably-sourced monomers (e.g., 2-octyl acrylate, acrylic acid, styrene), we can deliver high performance and high bio-content latexes for adhesive applications with equivalent or superior properties to their commercially available equivalents.

This thesis includes a total of 8 chapters, described below:

Chapter 2 provides a background on adhesives and adhesion, discusses the emulsion polymerization process, and introduces the renewable nanomaterials (i.e., CNCs and SNPs) used to produce our polymer nanocomposites.

Chapter 3 was published in the Macromolecular Reaction Engineering journal[56] and explores the effects of higher loadings of sulfated CNCs in latex-based PSA films. When added in an emulsion polymerization reaction, sulfated CNCs are commonly loaded at concentrations of 0.5 – 1% (relative to monomer) for latex property enhancements due to the experimental challenges encountered with higher CNC loadings.[19–22] Because our objectives included producing high-performance PSAs and increasing the quantity of renewable materials in our

formulations, we developed a method to overcome the colloidal instabilities related to high CNC loadings and measured the effect of high CNC loadings (up to 4%) on the adhesive properties.

Chapter 4, published in The Canadian Journal of Chemical Engineering,[57] explores the use of a novel nanomaterial, carboxylated CNCs (cCNCs) in latex-based PSAs. The cCNCs can be obtained in a wet form (i.e., cCNCs suspended in water) and as a spray-dried powder. Due to their carboxylated surface groups, the cCNCs interacted strongly with the polymer particles, which made their incorporation via emulsion polymerization challenging. Chapter 4 details the creative manipulation of the emulsion polymerization process that enabled the production of nanocomposite PSA latexes with cCNCs.

Chapter 5 was published in the Macromolecular Reaction Engineering journal[58] and discusses the effects of cCNCs on PSA performance properties (i.e., peel strength, tack, and shear strength) of latex films. In that published work, we took a closer look at the effects of cCNCs on PSA film formation via atomic force microscopy. Therein, we uncovered the mechanisms by which cCNCs improve PSA performance.

Chapter 6 features a manuscript submitted to the ACS Sustainable Chemistry and Engineering journal. The chapter describes how we increased the renewable material loading by displacing the polymer cores of our PSAs with SNPs. We developed methods to incorporate sulfated CNCs into the PSA formulation for property performance enhancement. This is the first instance of the combination of SNPs and CNCs in a latex, to our knowledge. In that work we used a model monomer system for an ~80% bio-based PSA formulation and demonstrated that commercially competitive PSAs with high renewable feedstock content is possible.

Chapter 7 provides a brief overview of current methods for assessing polymer degradation and highlights the opportunities and potential benefits of designing polymers that can biodegrade in a composting environment. We present a bioreactor design, which simulates a composting environment. Though the apparatus is not yet in operation, its status and action plan for its completion are detailed.

Chapter 8 provides a general discussion and summarizes the most important findings in this thesis. The discussion concludes by proposing new, more effective approaches for the production of sustainable polymers.

Finally, Appendix I-III contain supporting information related to chapters 3, 5 and 7 respectively, Appendix IV provides a report on health and safety considerations for this project and Appendix V contains a list of publications and conference attendance.

1.3 References

[1] S. Wiltsey Stirman, J. Kimberly, N. Cook, A. Calloway, F. Castro, and M. Charns, "The sustainability of new programs and innovations: a review of the empirical literature and recommendations for future research," *Implementation Science*, vol. 7, no. 1, p. 17, Dec. 2012, doi: 10.1186/1748-5908-7-17.

[2] M. A. Dubé and S. Salehpour, "Applying the Principles of Green Chemistry to Polymer Production Technology," *Macromolecular Reaction Engineering*, vol. 8, no. 1, pp. 7–28, Jan. 2014, doi: 10.1002/mren.201300103.

[3] Y. Zhang and M. A. Dubé, "Green Emulsion Polymerization Technology," in *Advances in Polymer Science*, vol. 280, 2017, pp. 65–100. doi: 10.1007/12_2017_8.

[4] J. C. Anastas, P.T.; Warner, "Green Chemistry: theory and Practice, 12 Principles of Green Chemistry," *Oxford University Press*, 1998.

[5] D. C. Sherrington, "Emulsion polymerization and emulsion polymers," *Reactive and Functional Polymers*, vol. 36, no. 1, pp. 104–105, Feb. 1998, doi: 10.1016/S1381-5148(97)84204-6.

[6] A. Gandini and T. M. Lacerda, "From monomers to polymers from renewable resources: Recent advances," *Progress in Polymer Science*, vol. 48, pp. 1–39, 2015, doi: 10.1016/j.progpolymsci.2014.11.002.

[7] J. J. Bozell, "Feedstocks for the Future: Using Technology Development as a Guide to Product Identification," pp. 1–12, 2009, doi: 10.1021/bk-2006-0921.ch001.

[8] K. Yao and C. Tang, "Controlled Polymerization of Next-Generation Renewable Monomers and Beyond," 2013, doi: 10.1021/ma3019574.

[9] M. de Geus, I. van der Meulen, B. Goderis, K. van Hecke, M. Dorschu, and H. van Der, "Performance polymers from renewable monomers : high molecular weight poly (pentadecalactone) for fiber applications," pp. 525–533, 2010, doi: 10.1039/b9py00360f.

[10] R. Beerthuis, G. Rothenberg, and N. R. Shiju, "Catalytic routes towards acrylic acid, adipic acid and ε-caprolactam starting from biorenewables," *Green Chemistry*, vol. 17, no. 3, pp. 1341–1361, 2015, doi: 10.1039/c4gc02076f.

[11] J. Spekreijse, J. le Nôtre, J. van Haveren, E. L. Scott, and J. P. M. Sanders, "Simultaneous production of biobased styrene and acrylates using ethenolysis," *Green Chemistry*, vol. 14, no. 10, pp. 2747–2751, 2012, doi: 10.1039/c2gc35498e.

[12] J. G. H. Hermens, A. Jensma, and B. L. Feringa, "Highly Efficient Biobased Synthesis of Acrylic Acid," *Angewandte Chemie*, vol. 134, no. 4, pp. 1–6, 2022, doi: 10.1002/ange.202112618.

[13] E. ben Ayed, R. Cochereau, C. Dechancé, I. Capron, T. Nicolai, and L. Benyahia, "Water-In-Water Emulsion Gels Stabilized by Cellulose Nanocrystals," *Langmuir*, vol. 34, no. 23, pp. 6887–6893, 2018, doi: 10.1021/acs.langmuir.8b01239.

[14] J. Lebeau, J. P. Efromson, and M. D. Lynch, "A Review of the Biotechnological Production of Methacrylic Acid," *Frontiers in Bioengineering and Biotechnology*, vol. 8, no. March, pp. 1–10, Mar. 2020, doi: 10.3389/fbioe.2020.00207.

[15] F. Habib and M. Bajpai, "Synthesis and Characterization of Acrylated Epoxidized Soybean Oil for Uv Cured Coatings," *Chemistry and Chemical Technology*, vol. 5, no. 3, pp. 317–326, 2011.

[16] Y. Li *et al.*, "Copolymers from epoxidized soybean oil and lactic acid oligomers for pressure-sensitive adhesives," *RSC Adv.*, vol. 5, no. 35, pp. 27256–27265, 2015, doi: 10.1039/C5RA02075A.

[17] Y. Lu and R. C. Larock, "Novel polymeric materials from vegetable oils and vinyl monomers: Preparation, properties, and applications," *ChemSusChem*, vol. 2, no. 2, pp. 136–147, 2009, doi: 10.1002/cssc.200800241.

[18] L. Jiang and J. Zhang, *Biodegradable Polymers and Polymer Blends*, no. 2011. Elsevier, 2012. doi: 10.1016/B978-1-4557-2834-3.00006-9.

[19] Z. Dastjerdi, E. D. Cranston, and M. A. Dubé, "Synthesis of Poly(n -butyl acrylate/methyl methacrylate)/CNC Latex Nanocomposites via In Situ Emulsion Polymerization," *Macromolecular Reaction Engineering*, vol. 11, no. 6, p. 1700013, Dec. 2017, doi: 10.1002/mren.201700013.

[20] Z. Dastjerdi, E. D. Cranston, and M. A. Dubé, "Pressure sensitive adhesive property modification using cellulose nanocrystals," *International Journal of Adhesion and Adhesives*, vol. 81, pp. 36–42, Mar. 2018, doi: 10.1016/j.ijadhadh.2017.11.009.

[21] A. Ouzas, E. Niinivaara, E. D. Cranston, and M. A. Dubé, "In Situ Semibatch Emulsion Polymerization of 2-Ethyl Hexyl Acrylate/ n -Butyl Acrylate/Methyl Methacrylate/Cellulose Nanocrystal Nanocomposites for Adhesive Applications," *Macromolecular Reaction Engineering*, vol. 12, no. 3, p. 1700068, Jun. 2018, doi: 10.1002/mren.201700068.

[22] A. Ouzas, E. Niinivaara, E. D. Cranston, and M. A. Dubé, "Synthesis of poly(isobutyl acrylate/n-butyl acrylate/methyl methacrylate)/CNC nanocomposites for adhesive applications via in situ semi-batch emulsion polymerization," *Polymer Composites*, vol. 40, no. 4, pp. 1365–1377, Apr. 2019, doi: 10.1002/pc.24869.

[23] A. S. Pakdel, V. Gabriel, R. M. Berry, C. Fraschini, E. D. Cranston, and M. A. Dubé, "A sequential design approach for in situ incorporation of cellulose nanocrystals in emulsion-based pressure sensitive adhesives," *Cellulose*, vol. 27, no. 18, pp. 10837–10853, Dec. 2020, doi: 10.1007/s10570-020-03060-6.

[24] A. S. Pakdel, E. Niinivaara, E. D. Cranston, R. M. Berry, and M. A. Dubé, "Cellulose Nanocrystal (CNC)–Latex Nanocomposites: Effect of CNC Hydrophilicity and Charge on Rheological, Mechanical, and Adhesive Properties," *Macromolecular Rapid Communications*, vol. 42, no. 3, p. 2000448, Feb. 2021, doi: 10.1002/marc.202000448.

[25] J. D. Ede, K. J. Ong, M. Goergen, A. Rudie, C. A. Pomeroy-Carter, and J. A. Shatkin, "Risk analysis of cellulose nanomaterials by inhalation: Current state of science," *Nanomaterials*, vol. 9, no. 3, pp. 1–18, 2019, doi: 10.3390/nano9030337.

[26] S. Cummings, Y. Zhang, N. Smeets, M. Cunningham, and M. Dubé, "On the Use of Starch in Emulsion Polymerizations," *Processes*, vol. 7, no. 3, p. 140, 2019, doi: 10.3390/pr7030140.

[27] Y. Zhang, M. F. Cunningham, N. M. B. Smeets, and M. A. Dubé, "Starch nanoparticle incorporation in latex-based adhesives," *European Polymer Journal*, vol. 106, no. June, pp. 128–138, 2018, doi: 10.1016/j.eurpolymj.2018.07.014.

[28] Y. Zhang, M. F. Cunningham, N. M. B. Smeets, and M. A. Dubé, "Increasing Starch Nanoparticle Content in Emulsion Polymer Latexes," *Industrial & Engineering Chemistry Research*, 2019, doi: 10.1021/acs.iecr.9b00332.

[29] S. Roberge and M. A. Dubé, "The effect of particle size and composition on the performance of styrene/butyl acrylate miniemulsion-based PSAs," *Polymer*, vol. 47, no. 3, pp. 799–807, Jan. 2006, doi: 10.1016/j.polymer.2005.12.024.

[30] L. Que and M. A. Dubé, "Manipulation of chain transfer agent and cross-linker concentration to modify latex micro-structure for pressure-sensitive adhesives," *European Polymer Journal*, vol. 46, no. 6, pp. 1225–1236, 2010, doi: 10.1016/j.eurpolymj.2010.02.014.

[31] N. Lin, J. Huang, P. R. Chang, D. P. Anderson, and J. Yu, "Preparation, modification, and application of starch nanocrystals in nanomaterials: A review," *Journal of Nanomaterials*, vol. 2011, 2011, doi: 10.1155/2011/573687.

[32] M. Morits *et al.*, "Polymer Brushes on Cellulose Nanofibers: Modification, SI-ATRP, and Unexpected Degradation Processes," *ACS Sustainable Chemistry and Engineering*, vol. 5, no. 9, pp. 7642–7650, 2017, doi: 10.1021/acssuschemeng.7b00972.

[33] T. Abitbol, H. Marway, and E. D. Cranston, "Surface Modification of Cellulose Nanocrystals with Cetyltrimethylammonium Bromide," *Nordic Pulp & Paper Research Journal*, vol. 29, no. 1, pp. 46–57, 2014.

[34] Y. Habibi, "Key Advances in the Chemical Modification of Nanocelluloses," *Chem Soc Rev*, vol. 43, no. 5, pp. 1519–42, Mar. 2014, doi: 10.1039/c3cs60204d.

[35] D. Saidane, E. Perrin, F. Cherhal, F. Guellec, and I. Capron, “Some modification of cellulose nanocrystals for functional Pickering emulsions,” *Philosophical Transactions of the Royal Society A: Mathematical, Physical and Engineering Sciences*, vol. 374, no. 2072, 2016, doi: 10.1098/rsta.2015.0139.

[36] J. C. Cazotti, A. T. Fritz, O. Garcia-Valdez, N. M. B. Smeets, M. A. Dubé, and M. F. Cunningham, “Graft Modification of Starch Nanoparticles Using Nitroxide-Mediated Polymerization and the ‘Grafting to’ Approach,” *Biomacromolecules*, vol. 21, no. 11, pp. 4492–4501, 2020, doi: 10.1021/acs.biomac.0c00462.

[37] R. P. Wool *et al.*, “Development and application of triglyceride-based polymers and composites,” *Journal of Applied Polymer Science*, vol. 82, no. 3, pp. 703–723, 2002, doi: 10.1002/app.1897.

[38] C. M. Klapperich, C. L. Noack, J. D. Kaufman, L. Zhu, L. Bonnaillie, and R. P. Wool, “A novel biocompatible adhesive incorporating plant-derived monomers,” *Journal of Biomedical Materials Research - Part A*, vol. 91, no. 2, pp. 378–384, 2009, doi: 10.1002/jbm.a.32250.

[39] J. L. Dubois and G. Patience, “Method for preparing acrylic acid from glycerol,” 2007

[40] “Scotch® Magic™ Greener Tape, 812-2P-C, 3/4 in x 25 yd (19 mm x 22.8 m), 2 per pack | 3M Canada.” https://www.3mcanada.ca/3M/en_CA/p/d/v000148956/ (accessed Mar. 2022).

[41] “Post-it® Greener Notes 653-RP-A, Helsinki Collection, 1 3/8 in x 1 7/8 in (34.9 mm x 47.6 mm), 100 Notes/Pack, 12 Pads/Pack | 3M Canada.” https://www.3mcanada.ca/3M/en_CA/p/d/v101143019/ (accessed Mar. 2022).

[42] J. T. Claypool, D. R. Raman, L. R. Jarboe, and D. R. Nielsen, “Technoeconomic evaluation of bio-based styrene production by engineered Escherichia coli,” *Journal of Industrial Microbiology and Biotechnology*, vol. 41, no. 8, pp. 1211–1216, 2014, doi: 10.1007/s10295-014-1469-5.

[43] C. v. Pramod, R. Fauziah, K. Seshan, and J. P. Lange, “Bio-based acrylic acid from sugar via propylene glycol and allyl alcohol,” *Catalysis Science and Technology*, vol. 8, no. 1, pp. 289–296, 2018, doi: 10.1039/c7cy01416c.

[44] D. L. Kaplan, *Biopolymers from Renewable Resources*. Berlin: Springer, 1998.

[45] Y. Zhu, C. Romain, and C. K. Williams, “Sustainable polymers from renewable resources,” *Nature*, vol. 540, no. 7633, pp. 354–362, Dec. 2016, doi: 10.1038/nature21001.

[46] A. J. F. Carvalho, *Monomers, Polymers and Composites from Renewable Resources*. Elsevier, 2008. doi: 10.1016/B978-0-08-045316-3.X0001-4.

[47] A. Gandini, “Epoxy Polymers Based on Renewable Resources,” *Epoxy Polymers: New Materials and Innovations*, pp. 55–78, 2010, doi: 10.1002/9783527628704.ch4.

[48] G. Lligadas, J. C. Ronda, M. Galià, and V. Cádiz, “Renewable polymeric materials from vegetable oils: A perspective,” *Materials Today*, vol. 16, no. 9, pp. 337–343, 2013, doi: 10.1016/j.mattod.2013.08.016.

[49] M. A. R. Meier, J. O. Metzger, and U. S. Schubert, “Plant oil renewable resources as green alternatives in polymer science,” *Chemical Society Reviews*, vol. 36, no. 11, pp. 1788–1802, 2007, doi: 10.1039/b703294c.

[50] A. Gandini and M. N. Belgacem, *The State of the Art of Polymers from Renewable Resources*, no. 2008. Elsevier, 2012. doi: 10.1016/B978-1-4557-2834-3.00004-5.

[51] ASTM International, “ASTM D5338-15 : Standard Test Method for Determining Aerobic Biodegradation of Plastic Materials Under Controlled Composting Conditions, Conditions, Incorporating Thermophilic Temperatures,” *ASTM Standards.* pp. 1–7, 2015. doi: 10.1520/D5338-15.2.

[52] ASTM International, “ASTM D7475: Standard Test Method for Determining the Aerobic Degradation and Anaerobic Biodegradation of Plastic Materials under Accelerated Bioreactor Landfill Conditions 1,” *Annual Book of ASTM Standards*, pp. 1–9, 2014, doi: 10.1520/D7475-11.only.

[53] ASTM Standard D5988, “Standard Test Method for Determining Aerobic Biodegradation of Plastic Materials in,” *ASTM International*, pp. 1–6, 2012, doi: 10.1520/D5988-12.2.

[54] R. Jayasekara, I. Harding, I. Bowater, and G. Lonergan, “Biodegradability of a selected range of polymers and polymer blends and standard methods for assessment of biodegradation,” *Journal of Polymers and the Environment*, vol. 13, no. 3, pp. 231–251, 2005, doi: 10.1007/s10924-005-4758-2.

[55] Z. Czech, K. Wilpiszewska, B. Tyliszczak, and X. Jiang, “Biodegradable self-adhesive tapes with starch carrier,” *International Journal of Adhesion and Adhesives*, vol. 44, pp. 195–199, 2013, doi: 10.1016/j.ijadhadh.2013.03.002.

[56] V. A. Gabriel, E. D. Cranston, and M. A. Dubé, “Pushing the Limits with Cellulose Nanocrystal Loadings in Latex-Based Pressure-Sensitive Adhesive Nanocomposites,” *Macromolecular Reaction Engineering*, vol. 14, no. 6, p. 2000027, Dec. 2020, doi: 10.1002/mren.202000027.

[57] V. A. Gabriel, P. Champagne, M. F. Cunningham, and M. A. Dubé, “In-situ addition of carboxylated cellulose nanocrystals in seeded semi-batch emulsion polymerization,” *The Canadian Journal of Chemical Engineering*, vol. 100, no. 4, pp. 767–779, Apr. 2022, doi: 10.1002/cjce.24299.

[58] V. A. Gabriel *et al.*, “Improving Latex-Based Pressure-Sensitive Adhesive Properties Using Carboxylated Cellulose Nanocrystals,” *Macromolecular Reaction Engineering*, p. 2100051, Jan. 2022, doi: 10.1002/mren.202100051.

Chapter 2

Background

A background on adhesive theory and characterization, emulsion polymerization and nanocomposites is presented below. Note that a general discussion of CNCs and SNPs in polymer nanocomposites is discussed here and that details pertaining to sulfated or carboxylated CNCs are discussed in Chapter 3, and Chapters 4 and 5 respectively. A background on degradation will be addressed in Chapter 7.

2.1 Adhesives and adhesion

Adhesives are non-metallic materials used to bond matter together through surface interactions such as adhesion and cohesion. Adhesion is defined by the bonding of one material to another and describes the forces that are operating across an interface, whereas cohesion refers to the intermolecular interactions between molecules of a same material.[1]

2.1.1 Pressure-sensitive adhesives (PSAs)

PSAs are polymeric materials that instantaneously bond to a surface upon light contact pressure and differ from traditional adhesives in that the material remains in a fluid state after adhesion.[1] Furthermore, they can be easily removed with a light pulling force without leaving a residue on the substrate. Global demands from the automotive, packaging, construction, electronics, medical, and general consumer industry have shaped a multibillion dollar PSA industry which is expected to grow from $9.8 billion (in 2020) to 17.6 billion USD in 2030.[2, 3] Water-based, hot melt, and solvent-based PSAs can be used for a variety of applications such as graphics, medical, tapes and labels.

Polymers are employed for PSA fabrication as they display high shear strength and peel adhesion without leaving residue upon debonding – both characteristics are paramount but can act against one another. The distinctive balance between adhesive and cohesive forces is possible due to a polymer's viscoelastic profile; it facilitates PSA flowability and energy dissipation during

the bonding process via interfacial and interstitial crosslinking, and polymer chain entanglement.[1, 4]

2.1.2 PSA formulation and performance

Polymers with a low glass-transition temperature (T_g), preferably ranging from -20 to -60 °C,[1] are commonly used in PSA formulations because they can maintain their fluidity and tackiness at room temperature. Low T_g polymers are achieved by combining "soft" monomers (i.e., monomers with < 0°C homopolymer T_g) with "hard" monomers (monomers with > 0°C homopolymer T_g). The T_g of polymer samples can be measured via differential scanning calorimetry (DSC). Manipulation of the copolymer microstructure (e.g., molecular weight, crosslinking) also plays a role in PSA performance. Examples of the impact of difference chemical and physical factors on PSA properties are included in Table 2.1.

Table 2.1 Impact of chemical and physical factors on tack, peel strength and shear strength of PSAs.[1, 5]

Factors	Tack force	Peel strength	Shear strength
Chemical			
"Soft" monomers	↑	↓	↓
"Hard" monomers	↓	⎴↑↓	↑
Polar monomers	↓	⎴↑↓	↑
Crosslinkers	↓	⎴↑↓	↑
Tackifiers	↑	⎴↑↓	↓
Peel Modifiers	↑	↑	↓
Physical			
Film thickness	↑	↑	↓
Temperature	↑	↑	↓

↑ = increases, ↓ = decreases, ⎴↑↓ = increases to a maximum, then decreases

PSAs are conventionally characterized by tack force (or simply, tack), peel adhesion and shear resistance. Tack refers to the separation energy after a short contact time and low pressure (Figure 2.1A), peel adhesion measures the material's ability to resist removal through peeling (Figure 2.1B) and shear resistance is the ability that a material has to resist a constant shear force (Figure 2.1C).[1, 4, 6–8] Tack and peel tests typically involve a bonding and a debonding step where the loading rate is important, whereas shear strength is measured in a static manner.

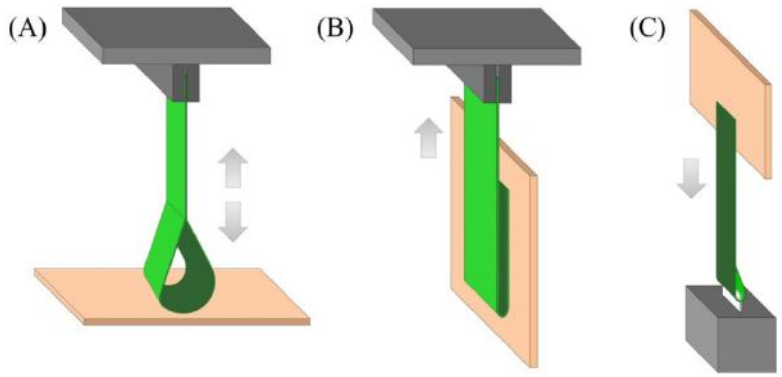

Figure 2.1 Loop tack (A), peel strength (B) and shear strength (C) testing representations.[9]

Benedek and Heymans showed that a decrease in particle size increases tack and peel strength.[1, 10] They explained this effect by noting that smaller particles pack more tightly during the film forming process, thereby increasing the contact area between the adhesive and substrate. In a similar way, the latex particle size distribution (PSD) can influence particle packing during film formation and affect adhesive-substrate contact. In the case of tack, a lower adhesive viscosity is favoured because the material is able to wet the surface more intimately due to better viscous flow and elastic deformation. Thus, with higher fluidity, the force required to separate the adhesive from the substrate is higher.[1] Peel strength is similar to tack in that it also implies a bonding and debonding step, but the influence of adhesive viscosity on its strength is less critical because the debonding time for peel strength measurement lasts longer.[1] Nonetheless, the increase in adhesive strength from the lowered viscosity is often accompanied by a decrease in cohesive strength (shear strength) and thus, balanced PSDs and viscosities need to be attained to obtain optimal adhesion and cohesion.

As noted earlier, the polymer microstructure is another important determining factor for adhesive properties. The molecular weight distribution (MWD) is governed by the chemical nature of the monomer systems and can be modified using, for example, chain-transfer agents (CTAs) and/or crosslinkers. These modifiers can affect the molecular weight (M_w), the molecular weight between entanglements (M_e), and the molecular weight between crosslink points (M_c), which all affect adhesive performance.[11] Generally speaking, the M_w should be limited for polymers intended for adhesive applications so that they can retain their fluidity – increasing the molecular weight of polymers in an emulsion tends to decrease the fluidity of the polymer, which increases the shear strength to the detriment of tack and peel strength.

Depending on the formulation (e.g., monomers, property modifiers), the latex's gel content (i.e., the portion of polymer that is crosslinked) can change, which drastically affects PSA properties. In general, with increasing gel content, the shear strength increases while the tack and peel strength decrease. This is due to the increased cohesive strength introduced by the polymer-gel matrix, which in turn decreases the ability of the material to adhere to the substrate. Monomers with functional groups, such as acrylic acid (AA), are commonly used in formulations to increase the shear strength of PSAs by increasing their gel content.[10, 11] The M_w, M_e and M_c must also be considered for their effect on adhesive properties. For instance, in a higher gel containing polymer, M_w and M_e affect the peel strength and tack, whereas the network morphology (M_c) governs the shear strength.[12] For low gel containing polymers, higher peel strengths are seen for cases where M_e is high, while lower M_e (with constant M_w) shows an improved shear strength due to higher degrees of entanglement, for a constant M_w.[11] As noted above, the MWD, M_w, M_e and M_c can be tuned in an emulsion polymerization using CTAs and crosslinkers,[37,36] often without affecting reaction rate or provoking colloidal instabilities.

2.2 Emulsion polymerization

Emulsion polymerization is a heterogeneous polymerization process involving monomer droplets dispersed in a continuous aqueous phase to form a latex polymer. It is widely used to produce resins with various colloidal and physicochemical properties and is considered as a more sustainable approach to polymer production because it uses water as its suspending medium.[13]

Eliminating the need for solvents or other toxic suspending agents renders emulsion polymerization safer and more sustainable as opposed to solution polymerization.

The main components in an emulsion polymerization are water, monomer, surfactant, initiator, buffer (optional) and other property modifiers. The water acts as the chief dispersant which comprises 40-50% of the reaction volume (hence, latexes typically have a 50-60% solids content), acting as a heat sink.[14] Many polymerization techniques are accompanied by heat transfer challenges arising from the highly exothermic polymerization reaction, yet emulsion polymerization overcomes these challenges because of its lower viscosity. Emulsion polymerization allows for high-solids and low-viscosity latexes, which are two great benefits for commercial use.[14]

Emulsion polymerizations can be performed in batch, semi-batch, or continuous modes. In the batch process, all the components are initially loaded to the reactor. Upon radical formation, particle nucleation and growth happen simultaneously, allowing for little control over the polymerization. Using a semi-batch process allows for much more control because it is performed in two stages: a latex seeding stage followed by a monomer feeding stage. The seed stage determines the overall number of particles whereas the particle growth rate, and thus heat removal rate, copolymer composition and even particle morphology, can be controlled during the monomer feeding stage. Industrially, some commodity emulsion polymers are produced in a series of stirred tank reactors in continuous mode to provide high reaction rates and uniform quality production for large-scale needs.[14, 15] Acrylic polymer latex films are an example of materials produced by conventional emulsion polymerization and due to its versatile nature, the formulation can be modified to yield a polymer suitable for a vast range of applications such as high-impact polymers, latex paints, paper coatings, textiles, sealants and adhesives.[14, 15]

The main components in the emulsion polymer formulation are the monomer(s), initiator and surfactant. Water soluble initiators such as persulfates are widely used in emulsion polymerization and are the source of free-radicals used to initiate the chain growth polymerization reactions of the monomers. Typically, in free-radical polymerization, the radicals target the carbon-carbon double bond on the monomer. The surfactant provides colloidal stability to the various particle species in the latex. Anionic surfactants are most commonly used

because they are inexpensive and provide good particle stabilization. When the concentration is greater than the critical micelle concentration (CMC), surfactant molecules aggregate to form micelles of about 50-150 Å in diameter.

Upon mixing the water, monomer(s) and surfactant together, the surfactant-micelles swell with monomer; the number density of the monomer-swollen micelles is typically on the order of 10^{17} to 10^{18} L^{-1}. The majority of the monomer is partitioned into large droplets, usually in the range of 1 – 10 µm with a number density of 10^{9} to 10^{11} L^{-1}. Note that the monomer-swollen micelles become the main locus for polymer particle nucleation because of their much higher number density relative to the monomer droplets.[15] Although monomers are commonly hydrophobic, a small amount of monomer is dissolved in the water phase.

Figure 2.2 illustrates the progression of a conventional emulsion polymerization reaction (note that the components are not to scale). Firstly, surfactant is mixed into a water-monomer mixture in a reactor and migrates to the aqueous/organic interface to reduce interfacial tension. The surfactant stabilizes the monomer droplets and forms monomer-swollen micelles. (Figure 2.2i) After the addition of a water-soluble initiator, (Figure 2.2ii) the few monomer molecules dissolved in the aqueous phase, polymerize to form oligoradicals (i.e., short-chain polymers) (Figure 2.2iii). When an oligoradical reaches a certain critical length (usually between 10-20 monomer units), it becomes too hydrophobic to remain in the water phase and is absorbed into a monomer-swollen micelle, thus nucleating a latex particle (Figure 2.2iv). There are other variations in nucleation mechanisms, but it is worth noting that the main locus of particle nucleation is typically in the monomer-swollen micelles rather than the monomer droplets because of the significant difference in surface area. Both the particle number and polymerization rate increase with time until all the micelles are nucleated. Thereafter, in a conventional emulsion polymerization, the number of particles in the latex does not change, indicating the completion of the seeding (i.e., initiation) stage. As the reaction proceeds, oligoradicals enter the polymer particles. The presence of a radical in the particle leads to immediate termination of the polymerization due to the presence of another radical. Another oligoradical entering the particle, resumes the polymerization and so on. Next, the particle size increases due to the growing polymer particles. The monomer concentration in the particles

remains constant due to rapid diffusion from the monomer droplets and as a result, the polymerization rate during the feeding stage is constant. The final stage of the polymerization begins when the polymerization rate starts to decrease due to the depletion of monomer droplets (Figure 2.2v). The remaining monomer in the particles continues to react until completely consumed (Figure 2.2vi).

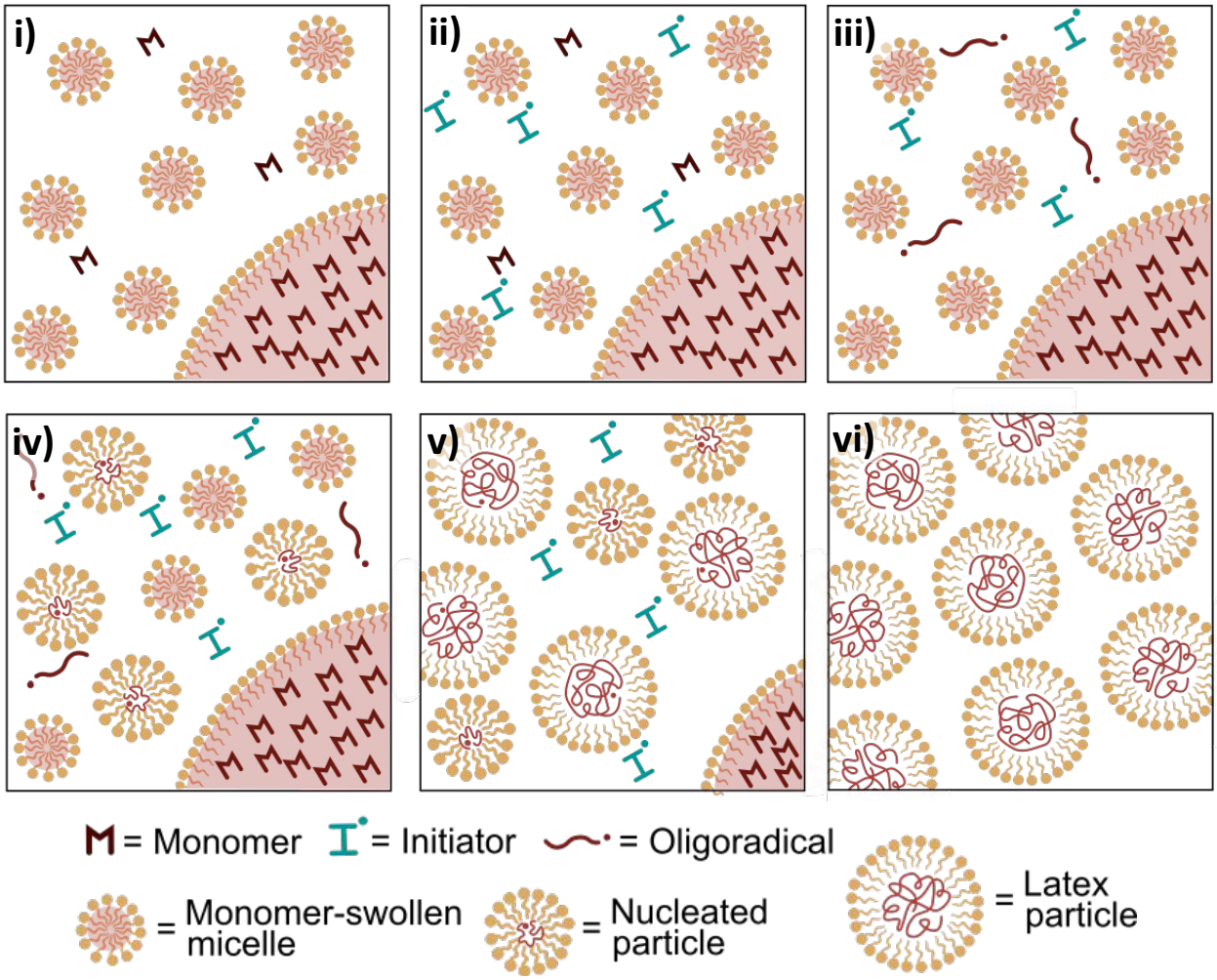

Figure 2.2 Illustration of the progression of a conventional emulsion polymerization reaction. Note that the components are not to scale.

2.3 Polymer nanocomposites

Inert and reinforcing fillers can be added to polymer matrices to enhance their physical, thermodynamic and processing characteristics and have been shown to improve chemical and mechanical performance.[16] Nanoparticles in polymer composite materials have been the focus of many advancements in recent years and are referred to as polymer nanocomposites. To date,

nanoparticles such as carbon nanotubes, nanosilica, nanoclay and nanotin-oxide have been shown to positively influence composite material properties.[17–24] For instance, adding as little as 0.3 wt.% of surface modified carbon nanotubes greatly improved the viscoelastic properties and adhesion energy of PSAs produced by emulsion polymerization by 65 and 85%, respectively.[18] Attempts were also made to improve the adhesive properties of a PSA with nanosilica, which increased the tack by 250 and 300% with 2 and 4 wt.% loadings, respectively. [23] With nanosilica, however, the peel strength decreased at higher loadings. The utility of nanoparticles provides opportunities for diverse commercial applications especially given their high impact despite low volumes (1-10 wt.%) as opposed to the traditional micro-scale inorganic fillers whose loadings can be quite high (15-40 wt.%), thereby negatively affecting properties.[16]

Despite the excellent performance impact of many nanomaterials, the question of their negative impact on the environment persists. Bio-sourced nanomaterials such as cellulose nanocrystals (CNCs) are an interesting alternative and have been shown to be safe.[25–27]

2.3.1 Cellulose nanocrystals (CNCs)

Cellulose is a linear chain of glucose molecules (containing β-1,4 glycosidic bonds, right side of Figure 2.3) which is produced mainly by plants and is most commonly extracted from wood pulp.[28–30] Cellulose nanocrystals (CNCs) can be extracted from the crystalline regions of microfibrils of natural cellulose via chemical processing and form stable aqueous colloids making them compatible with water-based systems, such as emulsion polymerization. To isolate CNCs from cellulose fibres found in plants, a strong-acid-catalyzed hydrolysis (typically, with sulfuric acid) is performed, leaving only the highly ordered and regular rod-like nanocrystals suspended in the aqueous medium.[31] The morphology of plant fibers is illustrated in Figure 2.3.

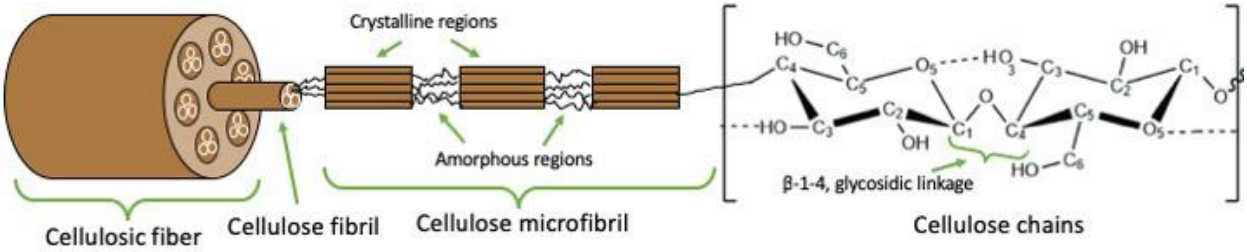

Figure 2.3 Schematic of hierarchical morphology of a plant cellulose fiber.[32–34]

The performance of polymer nanocomposites is largely determined by the shape, dispersion quality, and functionality of the nanomaterial added. Many nanomaterials that have been studied are spherical. When extracted, CNCs have an anisotropic rod-like shape (Figure 2.4) and their high length to width ratio (i.e., aspect ratio) is responsible for their remarkable strength effects on polymer nanocomposites.[17, 20] CNCs are safely produced,[25] non-toxic,[26] pose low potential health hazards,[27] and are generally compostable and biocompatible.[35, 36] CNC surface chemistry can vary and is largely determined by the acid used for its isolation. For example, wood pulp treated with sulphuric acid yields CNCs with sulphate half-ester surface groups,[37, 38] and oxidative hydrogen peroxide treatments yield CNCs with carboxylate surface groups.[39] The first reported uses of CNCs took advantage of their flexibility and high mechanical strength, providing a greater axial elastic modulus than Kevlar.[40] Recent work in our laboratory, including work herein, indicate the highly advantageous effects of CNCs on adhesive properties. [9, 41–45]

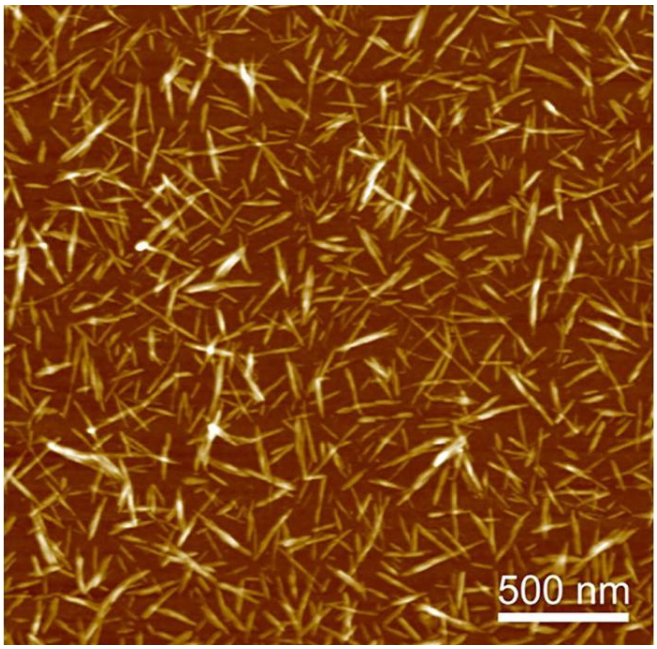

Figure 2.4 Tapping mode AFM image of CNCs. Reproduced with permission.[46] Copyright 2018, Elsevier.

CNCs are compatible with water-based systems and can be suspended in aqueous media.[47] This makes the dispersion of the CNCs in an emulsion polymerization, for example, relatively straightforward. Stable CNC-latex dispersions were first reported using miniemulsion

polymerization, where CNCs improved the storage modulus of nanocomposite films in the rubbery state.[32, 48] A recent study showed significant improvement of polymeric films cast from styrene-butyl acrylate latex formulations with CNCs.[49] Our research group has pioneered the use of sulphated CNCs in latex-based adhesive formulations and experimental methods describing ways to incorporate CNCs for the production of latexes for adhesive applications are readily found.[41, 44, 50] An important finding was that the PSA films obtained from conventional free-radical emulsion polymerization demonstrated a concurrent enhancement of shear strength, tack, and peel strength with increasing CNC content, thus overcoming some of the challenges in PSA properties noted earlier.[41, 42, 44] Moreover, the performance enhancement for PSAs prepared with CNCs *in situ* as opposed to *ex situ* (i.e., post-reaction blending) was substantially greater.[41]

2.3.2 Starch and starch nanoparticles (SNPs)

Starch is a polysaccharide produced by most green plants as energy storage and is a good candidate for the production of sustainable polymer nanocomposites because it is naturally occurring, abundant, non-toxic, cheap and biodegradable.[51, 52] The shape and particle size of starch granules (graphical representation in Figure 2.5) largely depend on its botanic origin and due to the strong nature of the starch granules, crystalline starch moieties (that make up 15 to 45% of native starch)[52] can be readily extracted via physical or chemical treatments.[51–53] Typically, starch is composed of 70-80% amylose (possessing primarily α-1,4 glycosidic bonds) and 20-30% branched amylopectin (possessing both α–1,4 and α–1,6 glycosidic bonds, Figure 2.6), both of which are forms of glucose.[52, 54]

Despite the promising evidence that starch can reduce the use of synthetic monomers and increase overall process sustainability, incorporating starch in latex formulations can disrupt the colloidal stability (because it is water soluble), which would impart negative effects on the end-use properties. Some of these challenges can be overcome by modifying native starch into its nanocrystal or nanoparticle form through acid hydrolysis.[55] Starch nanoparticles (SNPs) have been used as nano-fillers to improve mechanical and barrier properties, to improve stability in emulsion systems, and as binders in paper.[53, 56–58] SNPs can be further modified via SNPs to increase crosslinking, vinyl functionalization, anionic/cationic charging or even hydrophobization

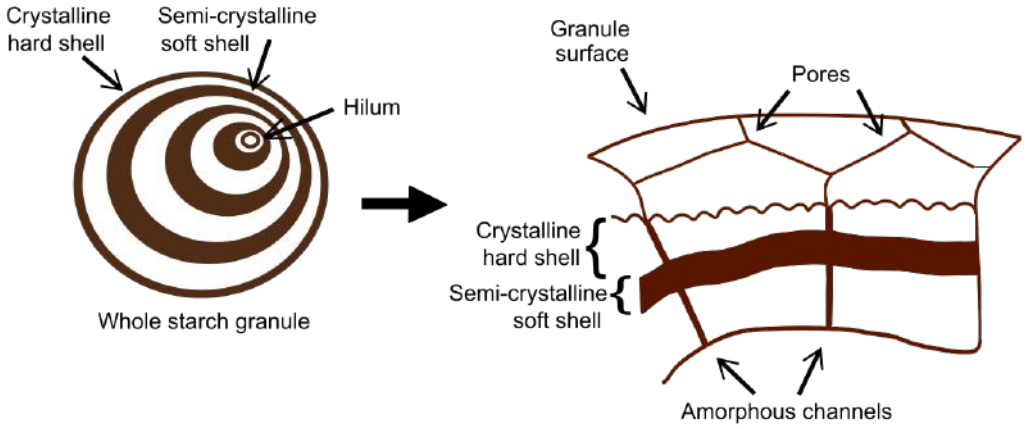

Figure 2.5 Illustration of starch granule structure.[51]

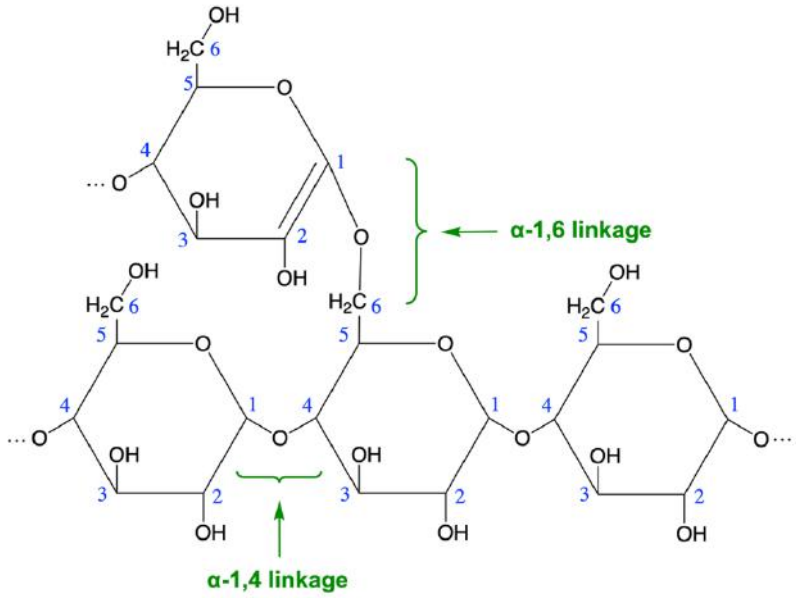

Figure 2.6 Illustration of the α-1,4 and α-1,6 glycosidic bonds of starch.[54]

to tune their surface groups and alter their behaviour.[59, 60] For example, SNPs modified with functional groups have been used as Pickering stabilizers and as monomers in emulsion polymerization to make starch-based latexes.[56, 57, 61] Most recently, Zhang et al.[59] developed a method to incorporate SNPs into the core of latex particles produced for PSA applications. Using a series of modifications including crosslinking, vinyl functionalization and the use of a bridging monomer, they were able to locate the SNPs in the hydrophobic polymer matrix as a particle core rather than at the particle shell-water interface or even in the water phase. In this way, they used the biocontent of the latex while maintaining the adhesive properties of the resulting films.[59]

Put another way, by restricting the SNPs to the latex particle cores, the adhesive film surfaces were largely comprised of acrylic polymer, thereby displaying the properties of the acrylic shell polymers as opposed to that of the SNPs in the hidden cores.

2.4 Conclusion

The goal of this thesis is to practice as many of the 12 Principles of Green Chemistry to design a more sustainable PSA. Synthesizing our polymers via the emulsion polymerization process whilst replacing as many petroleum-based components with more bio-based and bio-sourced counterparts will inevitably pose some technical challenges. Thus, we will employ as many techniques as are needed from our engineering toolbox to counteract the colloidal instabilities and product performance changes that these substitutions might cause. The successful displacement of monomer and additives with greener counterparts will significantly improve PSA sustainability.

Despite the clear advantages of using CNCs for PSA property engineering and SNPs to increase biocontent, the discussion of recycling, disposal and degradation of the adhesive is not commonly addressed. Often, it is assumed that with increased biocontent, the degradability of the material would also improve; however, for PSAs this has largely been untested. This discussion will be presented in Chapter 7.

2.5 References

[1] I. Benedek, *Pressure-Sensitive Adhesives and Applications*. 2004.

[2] C. Bilagi, N. Mittal, and E. Prasad, “Pressure Sensitive Adhesives Market Size, Share | Growths 2030,” Jul. 2021. https://www.alliedmarketresearch.com/pressure-sensitive-adhesives-market (accessed Oct. 2021).

[3] Grand View Research, “Global Pressure Sensitive Adhesives Market Size Report, 2019-2025.” https://www.grandviewresearch.com/industry-analysis/pressure-sensitive-adhesives-market (accessed May 2021).

[4] C. Creton, “Pressure-sensitive adhesives: an introductory course,” *Materials Research Society*, pp. 434–439, Dec. 2003, Accessed: May 13, 2018. [Online]. Available: https://patents.google.com/patent/US4243500A/en

[5] R. Jovanović and M. A. Dubé, "Emulsion-Based Pressure-Sensitive Adhesives: A Review," *Journal of Macromolecular Science, Part C: Polymer Reviews*, vol. 44, no. 1, pp. 1–51, Dec. 2004, doi: 10.1081/MC-120027933.

[6] "ASTM D3654-06 (Reapproved 2011) Standard Test Methods for Shear Adhesion of Pressure-Sensitive Tapes." 2006. doi: 10.1520/D3654.

[7] "ASTM D3330-04 (Reapproved 2018) Standard Test Method for Peel Adhesion of Pressure-Sensitive Tape." 2004. doi: 10.1520/D3330.

[8] "ASTM D6463-06 (Reapproved 2012) Standard Test Method for Time to Failure of Pressure Sensitive Articles Under Sustained Shear Loading." 2012. doi: 10.1520/D6463.

[9] A. S. Pakdel, V. Gabriel, R. M. Berry, C. Fraschini, E. D. Cranston, and M. A. Dubé, "A sequential design approach for in situ incorporation of cellulose nanocrystals in emulsion-based pressure sensitive adhesives," *Cellulose*, vol. 27, no. 18, pp. 10837–10853, Dec. 2020, doi: 10.1007/s10570-020-03060-6.

[10] S. Roberge and M. A. Dubé, "The effect of particle size and composition on the performance of styrene/butyl acrylate miniemulsion-based PSAs," *Polymer (Guildf)*, vol. 47, no. 3, pp. 799–807, Jan. 2006, doi: 10.1016/j.polymer.2005.12.024.

[11] L. Que and M. A. Dubé, "Manipulation of chain transfer agent and cross-linker concentration to modify latex micro-structure for pressure-sensitive adhesives," *European Polymer Journal*, vol. 46, no. 6, pp. 1225–1236, 2010, doi: 10.1016/j.eurpolymj.2010.02.014.

[12] S. D. Tobing and A. Klein, "Molecular parameters and their relation to the adhesive performance of emulsion acrylic pressure-sensitive adhesives. II. Effect of crosslinking," *Journal of Applied Polymer Science*, vol. 79, no. 14, pp. 2558–2564, 2001, doi: 10.1002/1097-4628(20010401)79:14<2558::AID-APP1065>3.0.CO;2-Y.

[13] D. C. Sherrington, "Emulsion polymerization and emulsion polymers," *Reactive and Functional Polymers*, vol. 36, no. 1, pp. 104–105, Feb. 1998, doi: 10.1016/S1381-5148(97)84204-6.

[14] J. M. Asua, "Emulsion polymerization: From fundamental mechanisms to process developments," *Journal of Polymer Science Part A: Polymer Chemistry*, vol. 42, no. 5, pp. 1025–1041, Mar. 2004, doi: 10.1002/pola.11096.

[15] P. A. Lovell and M. S. El-Aasser, Eds., *Emulsion Polymerization and Emulsion Polymers*. Chichester: John Wiley and Sons, 1981.

[16] R. A. Vaia and J. F. Maguire, "Polymer Nanocomposites with Prescribed Morphology: Going beyond Nanoparticle-Filled Polymers," *Chemical Materials*, vol. 26, no. 19, pp. 2736–2751, 2007, doi: 10.1021/cm052765h.

[17] P. K. Rana, S. K. Swain, and P. K. Sahoo, "Synthesis, characterization, and properties of intercalated poly(2-ethyl hexylacrylate)/silicate nanocomposites: XRD, TEM, IR, TGA, superabsorbency, pressure-

sensitive adhesion, and biodegradation," *Journal of Applied Polymer Science*, vol. 93, no. 3, pp. 1007–1011, 2004, doi: 10.1002/app.20568.

[18] T. Wang *et al.*, "Waterborne, Nanocomposite Pressure-Sensitive Adhesives with High Tack Energy, Optical Transparency, and Electrical Conductivity," *Advanced Materials*, vol. 18, no. 20, pp. 2730–2734, Oct. 2006, doi: 10.1002/adma.200601335.

[19] T. Wang, P. J. Colver, S. A. F. Bon, and J. L. Keddie, "Soft polymer and nano-clay supracolloidal particles in adhesives: synergistic effects on mechanical properties," *Soft Matter*, vol. 5, pp. 3842–3849, 2009, doi: 10.1039/b904740a.

[20] J. Kajtna, M. Krajnc, and J. Golob, "The role of components in waterbased microsphere acrylic PSA adhesive properties," *Macromolecular Symposia*, vol. 243, pp. 132–146, 2006, doi: 10.1002/masy.200651114.

[21] S. Patel, A. Bandyopadhyay, A. Ganguly, and A. K. Bhowmick, "Synthesis and properties of nanocomposite adhesives," *Journal of Adhesion Science and Technology*, vol. 20, no. 4, pp. 371–385, Jan. 2006, doi: 10.1163/156856106776381794.

[22] Y. Yamamoto, S. Fujii, K. Shitajima, K. Fujiwara, S. Hikasa, and Y. Nakamura, "Soft polymer-silica nanocomposite particles as filler for pressure-sensitive adhesives," *Polymer (Guildf)*, vol. 70, pp. 77–87, Jul. 2015, doi: 10.1016/j.polymer.2015.06.006.

[23] M. Khalina, M. Sanei, H. S. Mobarakeh, and A. R. Mahdavian, "Preparation of acrylic/silica nanocomposites latexes with potential application in pressure sensitive adhesive," *International Journal of Adhesion and Adhesives*, vol. 58, pp. 21–27, Apr. 2015, doi: 10.1016/j.ijadhadh.2014.12.007.

[24] S.-W. Lee *et al.*, "Optical properties and UV-curing behaviors of optically clear PSA-TiO 2 nano-composites," *International Journal of Adhesion and Adhesives*, vol. 44, pp. 200–208, 2013, doi: 10.1016/j.ijadhadh.2013.03.001.

[25] B. O'Connor, R. Berry, and R. Goguen, "Commercialization of Cellulose Nanocrystal (NCC^{TM}) Production: A Business Case Focusing on the Importance of Proactive EHS Management," in *Nanotechnology Environmental Health and Safety: Risks, Regulation, and Management: Second Edition*, Elsevier Inc., 2014, pp. 225–246. doi: 10.1016/B978-1-4557-3188-6.00010-4.

[26] M. Roman, "Toxicity of cellulose nanocrystals: A review," *Industrial Biotechnology*, vol. 11, no. 1, pp. 25–33, 2015, doi: 10.1089/ind.2014.0024.

[27] J. D. Ede, K. J. Ong, M. Goergen, A. Rudie, C. A. Pomeroy-Carter, and J. A. Shatkin, "Risk analysis of cellulose nanomaterials by inhalation: Current state of science," *Nanomaterials*, vol. 9, no. 3, pp. 1–18, 2019, doi: 10.3390/nano9030337.

[28] S. Camarero Espinosa, T. Kuhnt, E. J. Foster, and C. Weder, "Isolation of Thermally Stable Cellulose Nanocrystals by Phosphoric Acid Hydrolysis," *Biomacromolecules*, vol. 14, no. 4, pp. 1223–1230, Apr. 2013, doi: 10.1021/bm400219u.

[29] H.-Y. Yu, D.-Z. Zhang, F.-F. Lu, and J. Yao, "New Approach for Single-Step Extraction of Carboxylated Cellulose Nanocrystals for Their Use As Adsorbents and Flocculants," *ACS Sustainable Chemistry & Engineering*, vol. 4, no. 5, pp. 2632–2643, May 2016, doi: 10.1021/acssuschemeng.6b00126.

[30] O. M. Vanderfleet *et al.*, "Insight into thermal stability of cellulose nanocrystals from new hydrolysis methods with acid blends," *Cellulose*, vol. 26, no. 1, pp. 507–528, Jan. 2019, doi: 10.1007/s10570-018-2175-7.

[31] A. Gandini and T. M. Lacerda, "From monomers to polymers from renewable resources: Recent advances," *Progress in Polymer Science*, vol. 48, pp. 1–39, 2015, doi: 10.1016/j.progpolymsci.2014.11.002.

[32] A. ben Mabrouk, H. Kaddami, A. Magnin, M. N. Belgacem, A. Dufrensne, and S. Boufi, "Preparation of Nanocomposite Dispersions Based on Cellulose Whiskers and Acrylic Copolymer by Miniemulsion Polymerization: Effect of the Silane Content Ayman," *Polymer Engineering and Science*, 2011, doi: 10.1002/pen.21778.

[33] A. Dufresne, *Cellulose-Based Composites and Nanocomposites*. Elsevier, 2008. doi: 10.1016/B978-0-08-045316-3.00019-3.

[34] N. Lavoine, I. Desloges, A. Dufresne, and J. Bras, "Microfibrillated cellulose - Its barrier properties and applications in cellulosic materials: A review," *Carbohydrate Polymers*, vol. 90, no. 2, pp. 735–764, 2012, doi: 10.1016/j.carbpol.2012.05.026.

[35] K. J. de France *et al.*, "Tissue Response and Biodistribution of Injectable Cellulose Nanocrystal Composite Hydrogels," *ACS Biomaterials Science and Engineering*, vol. 5, no. 5, pp. 2235–2246, 2019, doi: 10.1021/acsbiomaterials.9b00522.

[36] B. Jia *et al.*, "Effect of microcrystal cellulose and cellulose whisker on biocompatibility of cellulose-based electrospun scaffolds," *Cellulose*, vol. 20, no. 4, pp. 1911–1923, 2013, doi: 10.1007/s10570-013-9952-0.

[37] E. J. Foster *et al.*, "Current characterization methods for cellulose nanomaterials," *Chemical Society Reviews*, vol. 47, no. 8, pp. 2609–2679, 2018, doi: 10.1039/C6CS00895J.

[38] R. S. Reiner and A. W. Rudie, "Process Scale-Up of Cellulose Nanocrystal Production to 25 kg per Batch at the Forest Products Laboratory," in *Production and Applications of Cellulose Nanomaterials*, no. June 2013, M. T. Postek, R. J. Moon, A. W. Rudie, and M. A. Bilodeau, Eds. Peachtree Corners: TAPPI Press, 2014, pp. 21–24.

[39] M. P. Andrews, T. Morse, A. Khabibullin, M. Farooque, and M. Rak, "WO 2020/163948 A1 Nanoredispersible microparticles of dried cellulose nanocrystals and method of production thereof," 2020

[40] R. J. Moon, A. Martini, J. Nairn, J. Simonsen, and J. Youngblood, "Cellulose nanomaterials review: structure, properties and nanocomposites," *Chemical Society Reviews*, vol. 40, no. 7, p. 3941, Jun. 2011, doi: 10.1039/c0cs00108b.

[41] Z. Dastjerdi, E. D. Cranston, and M. A. Dubé, "Pressure sensitive adhesive property modification using cellulose nanocrystals," *International Journal of Adhesion and Adhesives*, vol. 81, pp. 36–42, Mar. 2018, doi: 10.1016/j.ijadhadh.2017.11.009.

[42] Z. Dastjerdi, E. D. Cranston, and M. A. Dubé, "Synthesis of Poly(n -butyl acrylate/methyl methacrylate)/CNC Latex Nanocomposites via In Situ Emulsion Polymerization," *Macromolecular Reaction Engineering*, vol. 11, no. 6, p. 1700013, Dec. 2017, doi: 10.1002/mren.201700013.

[43] A. Ouzas, E. Niinivaara, E. D. Cranston, and M. A. Dubé, "Synthesis of poly(isobutyl acrylate/n-butyl acrylate/methyl methacrylate)/CNC nanocomposites for adhesive applications via in situ semi-batch emulsion polymerization," *Polymer Composites*, vol. 40, no. 4, pp. 1365–1377, Apr. 2019, doi: 10.1002/pc.24869.

[44] A. Ouzas, E. Niinivaara, E. D. Cranston, and M. A. Dubé, "In Situ Semibatch Emulsion Polymerization of 2-Ethyl Hexyl Acrylate/ n -Butyl Acrylate/Methyl Methacrylate/Cellulose Nanocrystal Nanocomposites for Adhesive Applications," *Macromolecular Reaction Engineering*, vol. 12, no. 3, p. 1700068, Jun. 2018, doi: 10.1002/mren.201700068.

[45] A. S. Pakdel, E. Niinivaara, E. D. Cranston, R. M. Berry, and M. A. Dubé, "Cellulose Nanocrystal (CNC)–Latex Nanocomposites: Effect of CNC Hydrophilicity and Charge on Rheological, Mechanical, and Adhesive Properties," *Macromolecular Rapid Communications*, vol. 42, no. 3, p. 2000448, Feb. 2021, doi: 10.1002/marc.202000448.

[46] D. Klemm *et al.*, "Nanocellulose as a natural source for groundbreaking applications in materials science: Today's state," *Materials Today*, vol. 21, no. 7, pp. 720–748, 2018, doi: 10.1016/j.mattod.2018.02.001.

[47] S. A. Kedzior, V. A. Gabriel, M. A. Dubé, and E. D. Cranston, "Nanocellulose in Emulsions and Heterogeneous Water-Based Polymer Systems: A Review," *Advanced Materials*. Wiley-VCH Verlag, 2020. doi: 10.1002/adma.202002404.

[48] A. ben Elmabrouk, T. Wim, A. Dufrensne, and S. Boufi, "Preparation of Poly(styrene-co-hexylacrylate)/Cellulose Whiskers Nanocomposites via Miniemulsion Polymerization," *Polymers and Polymer Science*, no. 7, pp. 449–456, 2009, doi: 10.1002/app.30886.

[49] F. Bettaieb, R. Khiari, A. Dufresne, M. F. Mhenni, and M. N. Belgacem, "Mechanical and thermal properties of Posidonia oceanica cellulose nanocrystal reinforced polymer," *Carbohydrate Polymers*, vol. 123, pp. 99–104, 2015, doi: 10.1016/j.carbpol.2015.01.026.

[50] S. A. Kedzior *et al.*, "Incorporating Cellulose Nanocrystals into the Core of Polymer Latex Particles via Polymer Grafting," *ACS Macro Letters*, vol. 7, no. 8, pp. 990–996, 2018, doi: 10.1021/acsmacrolett.8b00334.

[51] A. J. F. Carvalho, *Monomers, Polymers and Composites from Renewable Resources*. Elsevier, 2008. doi: 10.1016/B978-0-08-045316-3.X0001-4.

[52] D. le Corre, J. Bras, and A. Dufresne, "Starch Nanoparticles: A Review," *Biomacromolecules*, vol. 11, no. 5, pp. 1139–1153, May 2010, doi: 10.1021/bm901428y.

[53] H. Y. Kim, S. S. Park, and S. T. Lim, "Preparation, characterization and utilization of starch nanoparticles," *Colloids and Surfaces B: Biointerfaces*, vol. 126, pp. 607–620, 2015, doi: 10.1016/j.colsurfb.2014.11.011.

[54] D. J. ; Thomas and W. A. Atwell, "Chapter 1: Starch Structure," in *Starches*, 1999, pp. 1–11.

[55] S. Cummings, Y. Zhang, N. Smeets, M. Cunningham, and M. Dubé, "On the Use of Starch in Emulsion Polymerizations," *Processes*, vol. 7, no. 3, p. 140, 2019, doi: 10.3390/pr7030140.

[56] C. Li, P. Sun, and C. Yang, "Emulsion stabilized by starch nanocrystals," *Starch/Starke*, vol. 64, no. 6, pp. 497–502, 2012, doi: 10.1002/star.201100178.

[57] S. B. Haaj, W. Thielemans, A. Magnin, and S. Boufi, "Starch nanocrystal stabilized pickering emulsion polymerization for nanocomposites with improved performance," *ACS Applied Materials and Interfaces*, vol. 6, no. 11, pp. 8263–8273, 2014, doi: 10.1021/am501077e.

[58] A. Sorrentino, G. Gorrasi, and V. Vittoria, "Potential perspectives of bio-nanocomposites for food packaging applications," *Trends in Food Science and Technology*, vol. 18, no. 2, pp. 84–95, 2007, doi: 10.1016/j.tifs.2006.09.004.

[59] Y. Zhang, M. F. Cunningham, N. M. B. Smeets, and M. A. Dubé, "Starch nanoparticle incorporation in latex-based adhesives," *European Polymer Journal*, vol. 106, no. June, pp. 128–138, 2018, doi: 10.1016/j.eurpolymj.2018.07.014.

[60] H. Namazi, F. Fathi, and A. Heydari, "Nanoparticles Based on Modified Polysaccharides," in *The Delivery of Nanoparticles*, IntechOpen, 2012.

[61] X. Pei *et al.*, "Synthesis of monodisperse starch-polystyrene core-shell nanoparticles via seeded emulsion polymerization without stabilizer," *Polymer (Guildf)*, vol. 108, pp. 78–86, 2017, doi: 10.1016/j.polymer.2016.11.035.

Chapter 3

Pushing the Limits with Cellulose Nanocrystal Loadings in Latex-Based Pressure-Sensitive Adhesive Nanocomposites

Vida A. Gabriel,[a] Emily D. Cranston,[b] and Marc A. Dubé[a]

[a]Department of Chemical and Biological Engineering, Centre for Catalysis Research and Innovation, University of Ottawa, 161 Louis Pasteur Pvt, Ottawa, Ontario K1N 6N5, Canada
[b]Department of Wood Science, University of British Columbia, 2424 Main Mall, Vancouver, British Columbia V6T 1Z4, Canada

This chapter is a manuscript published in Macromolecular Reaction Engineering (2020; 14,8: 2000027)

3.1 Abstract

Cellulose nanocrystals (CNCs) are a naturally sourced, non-toxic, nanoparticle known to improve tack, peel strength and shear resistance simultaneously when incorporated into nanocomposite latexes produced for pressure-sensitive adhesive (PSA) applications. In this study, methods for incorporating CNCs into a butyl acrylate/styrene/acrylic acid (91.5/4.5/4.0 wt%) seeded semi-batch emulsion polymerization for the production of PSAs are presented. Past work revealed a limit of 1.0-2.0 wt% (based on monomer) CNC loadings due to latex instability. In this work, CNC loadings of up to 4.0 wt% in a stable latex with 40 wt% solids are achieved by utilizing all of the available water in the formulation to maximize CNC redispersion. The CNC addition method is studied (i.e., in the seed, in the feed, or partitioned in both) and adhesive performance results indicate that there are no significant benefits to where the CNCs are dispersed *in situ* during polymerization. However, the quality of the CNC-water dispersion is pivotal to ensuring latex homogeneity and therefore, adhesive film quality. Though CNCs did improve adhesive strength at low concentrations, their enhancing effects are modest when used with a commercially competitive base-case PSA formulation.

Keywords: Emulsion polymerization, cellulose nanocrystals, pressure-sensitive adhesives, nanocomposites, latex

3.2 Introduction

Reinforcing fillers are added to polymer matrices to enhance their physical, thermodynamic and processing characteristics and have been shown to improve chemical and mechanical performance.[1] Nanoparticle fillers such as carbon nanotubes, nanosilica, nanoclay and nanotin-oxide have been shown to positively influence polymer composite material properties.[2–7] Generally, nanocomposites are produced using physical or chemical processing methods. Physical methods, namely blending, include solvent processing, melt processing, latex blends and so on. In these cases, simple mixing is usually insufficient for adequate nanoparticle dispersion leading to sub-optimal performance, thus product heterogeneity often poses a challenge.[8] Chemical methods comprise the addition of the nanofiller via polymerization[9] (e.g., solution polymerization, suspension polymerization, emulsion polymerization, intercalative polymerization). By using *in situ* methods, the nanoparticles are more easily dispersed in the continuous or monomer phase, allowing them to be present during the polymerization, or to participate therein, to produce a homogeneous polymer nanocomposite.[10–12]

Emulsion polymerization is considered to be a more sustainable approach to polymer production, largely because its bulk medium is water as opposed to the volatile and toxic solvents used in solution polymerization.[13] Emulsion polymerization provides specific advantages over other polymerization technologies such as low reaction viscosity, which facilitates mixing and nanoparticle dispersion, as well as improved heat transfer.[14] In addition, in emulsion polymerization, molecular weight is decoupled from reaction rate and high productivity can yield high molecular weight polymers, unlike for example, bulk polymerization.

With greater urgency, research on more sustainable polymer production is increasing.[15] This involves replacing various components of polymer nanocomposites, including the reinforcing fillers, with less toxic alternatives. In recent years, nanocellulose has received significant interest due to its renewability, non-toxicity and availability. Cellulose nanocrystals (CNCs) in particular are quite advantageous due to their rod-like morphology, which gives them a high aspect ratio.[16] This characteristic, along with their compatibility with waterborne polymerization systems, such as emulsion polymerization, enables the CNCs to form a network at an interface or in the continuous phase of a matrix instead of forming the typical close-packed

monolayer that spherical nanomaterials often exhibit.[17] CNCs also have accessible and abundant surface groups that provide opportunities for functionalization, meaning that the nanocrystals can be tuned and compatibilized for dispersion in both hydrophilic and hydrophobic systems.[18, 19] For example, latexes produced via emulsion polymerization for adhesive applications were enhanced with CNCs using both physical (blending)[12, 20] and chemical (*in situ*) methods[12, 21] and showed simultaneous improvements in tack, peel strength and shear strength up to a concentration of 1.0 wt% (based on solids). In the referenced studies, adhesive property improvements were demonstrated using initial base case formulations (i.e., without CNCs), which had relatively weak adhesive strength compared to commercially available tapes. In these limited cases, CNC concentrations beyond 1.0 – 2.0 wt% caused colloidal instabilities during the seeded semi-batch emulsion polymerization process.[20]

In this study, a PSA formulation made of butyl acrylate, styrene and acrylic acid (BA/STY/AA, 91.5/4.5/4.0 wt%) yielding adhesive properties at commercially competitive levels was used to investigate different means of incorporating CNCs into latex polymers *in situ*. CNC loadings in the formulation were increased until physical limits, inflicted by dispersion limitations, were reached. Finally, the adhesive properties of films produced from these CNC-saturated latexes were tested.

3.3 Experimental

3.3.1 Materials

Butyl acrylate (BA), styrene (STY) and acrylic acid (AA) (all >99% purity and stabilized by 20-200 ppm hydroquinone) were purchased from Sigma Aldrich. BA was purified by passing it through an inhibitor removal column and the other monomers were used as received. The sodium dodecyl sulfate surfactant (SDS, ACS Reagent >99%), potassium persulfate initiator (KPS, ACS Reagent >99%), and n-dodecyl mercaptan chain transfer agent (NDM, >95.5%), were purchased from Sigma Aldrich and used as received. CNCs were obtained from CelluForce Inc. (Windsor, Quebec), produced via sulfuric acid hydrolysis of bleached Kraft pulp and provided as a spray-dried powder in the sodium salt form (dimensions: length = 183 ± 88, cross-section 6 ± 2 nm; nominal sulfate half-ester surface charge content of 250 mmol kg^{-1} CNC).[22] Distilled,

deionized water (DDW) was used to prepare the CNC dispersions, pre-emulsion solution and initiator solution. Tetrahydrofuran (THF, ACS grade, Sigma Aldrich) was used as supplied for gel content analysis.

3.3.2 Seeded semi-batch emulsion polymerization

Polymerization reactions were conducted in a 1.25 L jacketed stainless-steel Mettler Toledo LabMax Automatic Lab Reactor equipped with an anchor stirrer, a reflux condenser with a vent line, and two separate feed lines. The reactor was purged with N_2 (Linde, Canada) throughout the reaction and the temperature and stir rate were maintained at 60 °C and 250 rpm, respectively. A general formulation is shown in Table 3.1.

Table 3.1 Base formulation for a 40 wt% solids (total mass = 650 g) nanocomposite latex.

Component	Seed stage (g)	Feed stage (g)
Monomer	26.00	234.00
KPS	0.08	0.82
SDS	0.6 - 0.65	7.10 - 7.15
Buffer	-	0.14
NDM	-	0.63
CNC	0 - 2.60	0 – 7.15
DDW	180.00[a]	210.00[a]

[a]Includes total water content from KPS solution, SDS solution and CNC dispersion (if used).

Latex nanocomposites were produced via a seeded semi-batch emulsion polymerization technique. In the seed stage, the polymer particles were nucleated. The seed particles grew as a result of monomer (and initiator) fed to the reactor as a pre-emulsion during the feed stage. Table 3.2 describes the seed and feed stage mixtures and specifies how and when these mixtures were incorporated. Additional details of the seeded semi-batch emulsion polymerization technique can be found elsewhere.[11] At the end of the feed stage, the reactor contents were mixed for an additional 30 min at 60°C to ensure that all residual monomer or free radicals (if any) were consumed.

Table 3.2 Components in the seed and feed stages of a 40 wt% solids latex formulation with 2 phm CNC (divided equally in the seed and feed stages).

	Mixture	Description	Component	Amount (g)
Seed stage	Emulsifier	Surfactant solution initially loaded into reactor, mixed at 250 rpm, and heated to 60 °C. Reactor temperature maintained at ± 1 °C throughout polymerization.	CNC	2.60
			SDS	0.60
			DDW	175.50
	Monomer	Seed monomer (~10% of total monomer) added to heated emulsifier solution and mixed for 5 min.	STY	1.17
			BA	23.79
	Initiator 1	Small volume of initiator injected as a shot to commence seed stage, which lasts 30 min.	KPS	0.078
		Measurements for "initial" particle size were taken at the end of this 30 min period.	DDW	3.90
Feed stage	Pre-emulsion	Components emulsified via vigorous mixing in a beaker using magnetic stirring. Pre-emulsion solution fed to reactor at 1.37 g min^{-1} for 240 min, after completion of seed stage, for particle growth. When present, CNCs were separately dispersed in water prior to emulsification with other components.	CNC	2.56
			DDW	128.70
			AA	10.40
			STY	10.53
			BA	214.11
			SDS	7.15
			NDM	0.65
	Initiator 2	Initiator 2 solution fed to reactor at same time as pre-emulsion solution at 0.3 g min^{-1} for 270 min total.	KPS	0.82
			DDW	81.90
			Buffer	0.14

3.3.3 CNC Redispersion

CNC dispersions were prepared by mixing CNC powder with fresh DDW overnight (in a covered beaker) with a magnetic stir bar on a stir plate. The dispersion was probe sonicated (Fisher Scientific 550 sonic dismembrator) whilst submerged in an ice bath the day of the reaction

for 15 min (three 5-min intervals with 5-min rest in between) at 75% amplitude. The dispersions were suction filtered (110 mm, particle retention of >2.7 μm) thrice to remove any impurities and used immediately. In runs where CNCs were added at both the seed stage and pre-emulsion feed, the water-CNC mixtures were dispersed and sonicated separately. Note that at concentrations above ~17.0 g_{CNC} L^{-1}_{water}, the dispersions could not be suction filtered and were therefore used as is.

3.3.4 Characterization

Samples (~3 g) were taken at 30-60 min intervals from a sampling valve at the bottom of the reactor. All samples were characterized for conversion (by gravimetry), particle size and distribution (three measurements via dynamic light scattering (DLS), Malvern NanoS Zetasizer), and pH (via Fisher Scientific/Acumet Research AR50 Dual Channel pH/Ion/Conductivity probe). The final latexes were characterized for conversion, particle size, pH, viscosity (via Thermo Scientific HAAKE Viscotester, Model D), glass transition temperature (T_g, via differential scanning calorimetry (DSC) TA Instruments, Model Q1000), gel content (three measurements), water and diiodomethane contact angle (six measurements via VCA Optima, AST Productions Inc.), and adhesive properties (i.e., tack, peel strength and shear strength, using an Instron 3000 Universal Tester, five repeat measurements each). The error bars in the figures represent the standard deviation of the measurements. Details of each method are provided in Appendix I.

3.4 Results and discussion

3.4.1 Maximizing CNC loading

Using the general formulation from Table 3.2, a BA/STY/AA (91.5/4.5/4.0 wt%) terpolymer latex was produced using the seeded semi-batch emulsion polymerization formulation described above. A series of preliminary experiments was run to identify a high-performance adhesive formulation. Details of these experiments are found in Appendix I. The resulting 40 wt% solids base case formulation contained 0.25 phm NDM (a commonly used chain transfer agent) and 0.5:1.0 (mol:mol) of buffer:initiator because these additives led to significant improvement in the peel strength and tack of the adhesive films (see Figure AI.1, AI.2, and Table AI.1 of Appendix I). Acrylic acid was omitted from the seed stage of the reaction because it decreased the media's

pH leading to CNC aggregation and ultimately, latex coagulation (see Table AI.2 of the Appendix I). As discussed in Appendix I, the CNC concentration affected the latex particle size and consequently the adhesive strength (Figure AI.3 of Appendix I). Therefore, the SDS concentration was varied depending on the CNC loading to maintain similar initial and final particle sizes, thereby eliminating any particle size effects on film formation and thus, on adhesive properties.[23] Furthermore, the total monomer mass was adjusted to account for other solids (e.g., initiator, surfactant) to ensure that the targeted solids content of 40% was reached. All latexes achieved final conversions of >99 wt.% (Figures AI.4 to AI.15 of Appendix I).

The quality (i.e., density and homogeneity) of the network that CNCs can form, and consequently the magnitude of their reinforcing effects, depends on the processing conditions (e.g., the dispersion or redispersion process).[24] For PSAs in particular, the addition of CNCs *in situ* is preferred over *ex situ* (i.e., blending) because the *in situ* addition allows for better dispersion of the nanomaterial.[10–12] Moreover, adding pre-dispersed nanomaterials during the polymerization process eliminates the need for post-synthesis operations (e.g., blending), which reduces production time and therefore cost.

CNCs were dispersed in the water reserved for the seed stage of the polymerization and an *in situ* loading limit of 1.25 phm CNCs was observed, which is low compared to other studies. For example, Dastjerdi et al.[20] reached an *in situ* loading of 2.0 phm CNCs in the seed stage, but with a different monomer system. Although more than 1.25 phm CNCs could be dispersed in the water reserved for the seed's emulsifier solution, preparing a seed with higher CNC concentrations interfered with particle nucleation and resulted in reaction failure (i.e., coagulation). The observed colloidal instabilities can be explained in part by the increased emulsion viscosity caused by the addition of CNCs[17] and in part by the possible CNC-component interactions and aggregation in the seed stage of the reaction. In an attempt to mitigate the instability, the surfactant concentration was increased, but this had no discernible effect on stability (data not shown).

To understand why these colloidal instabilities occur, the CNCs behaviour in a dispersion must be understood. When properly dispersed (e.g., via ultrasonication), the CNCs form a metastable aqueous colloid in water due to the electrostatic repulsion between their surface

sulfate half-ester groups, which helps surmount the attractive van der Waals forces that would otherwise aggregate them, in accordance with DLVO theory.[22] In addition, their rod-like morphology allows them to form a network in water above a critical concentration; which is governed by a percolation mechanism between the nanocrystals.[25] Cherhal et al.[26] discussed the aggregation mechanism of rod-like particles and studied the effects of ionic strength and surface charge density on the agglomeration of CNC dispersions. For charged CNCs with the same aspect ratio and surface groups as the CNCs used in this study, they found that CNC dispersions above 2.5 $g_{CNC}\ L^{-1}_{water}$ can become metastable (e.g., the dispersion is susceptible to collapse, under gravity for example).[26] Because the dispersion concentrations used in this study were above 2.5 $g_{CNC}\ L^{-1}_{water}$ for every latex, the possibility of small CNC agglomerates is possible.

Considering the CNC behaviour in a dispersion, the 1.25 phm CNC loading limit can be re-examined. For a 650 g latex with 40 wt% solids, a total of 390 g of water is available in the polymerization; approximately 180 g of which are reserved for the seed stage (Table 3.2). Thus, 1.25 phm CNCs, the equivalent of 3.10 g, were dispersed in the emulsifier solution, resulting in a *local* CNC concentration of approximately 17.14 $g_{CNC}\ L^{-1}_{water}$, which is considered relatively high. Thus, to continue adding CNCs to the latex while avoiding any interference with particle nucleation, the CNC concentration in the seed solution should be capped, and any additional CNCs should be dispersed elsewhere in the formulation where water is available, notably, in the pre-emulsion solution. In other words, additional CNCs can be incorporated in the latex by dispersing them in the water of the pre-emulsion solution and fed to the reactor in the feed stage. A seed latex containing 1.0 phm CNCs (i.e., 13.75 $g_{CNC}\ L^{-1}_{water}$, Run A3, Table 3.3) was used as a starting point rather than the maximum 1.25 phm concentration because feeding a CNC-filled pre-emulsion solution to a seed with greater than 1.0 phm CNC resulted in an unstable final latex (i.e., there was formation of coagulum or grit in the latex when cooled to room temperature). In this manner, a latex produced with up to 3.0 phm CNCs (or 23.31 $g_{CNC}\ L^{-1}_{water}$ total) was possible when the equivalent of 1.0 phm was added during the seed stage, and the remainder through the feed stage. The local CNC concentrations in both the seed and feed solutions are shown in Table 3.3.

Table 3.3 Latex viscosity and particle size for increasing CNC concentrations (described in phm and $g_{CNC}\ L^{-1}_{water}$).

Run	[CNC] (phm)			[CNC] ($g_{CNC}\ L^{-1}_{water}$)			Viscosity	Particle size (nm)	
	[Seed]	[Feed]	[Total]	[Seed]	[Feed]	[Total]	(cP)	Initial	Final
A1	-	-	-	-	-	-	45	76.1	126.7
A2	0.5	-	0.5	6.88	-	3.89	270	72.4	134.4
A3	1.0	-	1.0	13.75	-	7.77	525	86.0	142.0
A3'	-	1.0	1.0	-	17.87	7.77	445	82.8	144.0
A3''	0.5	0.5	1.0	6.88	9.02	7.77	432	73.9	146.3
B4	1.25	-	1.25	17.14	-	9.71	830	79.6	156.6
C1	1.0	0.5	1.5	13.75	9.02	11.66	745	66.9	134.0
C2	1.0	1.0	2.0	13.75	17.87	15.54	866	79.6	155.0
C2'	-	2.0	2.0	-	34.10	15.54	824	76.2	139.9
C3	1.0	2.0	3.0	13.76	34.10	23.31	1392	71.5	142.5
C3'	-	3.0	3.0	-	36.49	23.31	1142	73.0	143.7
C4	1.0	3.0	4.0	15.78	34.10	31.08	1514	73.8	138.7

In a final attempt to load more CNCs into the latex, some water was displaced from the "Initiator 2" solution to the "Pre-emulsion" solution allowing for the dispersion of 3.0 phm CNCs (23.31 $g_{CNC}\ L^{-1}_{water}$) into the pre-emulsion feed. Note that the feed rates of "Initiator 2" and "Pre-emulsion" solutions were adjusted to maintain the reaction rate (and thus, reaction kinetics). Thus, a maximum CNC loading in a latex with 40 wt% solids was found to be 31.08 $g_{CNC}\ L^{-1}_{water}$ total or 4.0 phm. Table 3.3 summarizes the latex particle sizes and viscosities in order of CNC loading; CNC concentrations are presented in both phm and $g_{CNC}\ L^{-1}_{water}$. Overall, the CNCs did not impact the initial or final latex particle sizes, conversion or pH trajectories but had significant impacts on latex viscosity. Conversion, pH, particle size and solid content versus time data can be found in Appendix I (Figure AI.4 to AI.15).

The latex viscosity (Table 3.3) increased with CNC loading regardless of its placement (seed vs. feed stage) due in part to the increase in CNC-latex particle interactions and in part to the CNC loading itself. When comparing runs B4 and C1, there was a small decrease in latex viscosity

despite the increase of CNC loading, suggesting a better dispersion of the CNCs relative to the latex when they were added to the feed stage. Interestingly, the latex viscosity in the entire range showed a positive linear trend (Figure 3.1d), suggesting that the final latex viscosity is a function of *total* CNC loading and was not significantly impacted by the *local* CNC concentrations.

3.4.2 Effect of CNC loading on adhesive performance

CNCs have been shown to improve latex-based adhesive properties, albeit for formulations with low base case performance.[10–12, 20] It remains unknown however, if these improvements would likewise be present for high-performance latexes (i.e., formulations whose tack and peel strength were equal to or greater than that of commercial products). The adhesive properties of the latexes from Table 3.3 were tested and reported in Figure 3.1. Note that the data labeled as "masking tape" represent adhesive performance of Uline™ general purpose 1" masking tape using identical test conditions.

3.4.2.1 CNCs loaded in the seed stage only (runs A1, A2, A3 and B4)

Generally, for tack and peel strength, the PSA films with 0 to 2.0 phm CNCs outperform Uline general purpose 1" masking tape, referred to hereafter as "commercial masking tape" (Figure 3.1a and 3.1b). Adhesive performance trends are similar to those in the literature,[10–12, 20] specifically for experiments where CNCs were loaded in the *seed* stage (runs A1-A3 and B4 of Figure 3.1a and 3.1b). In other words, for latexes prepared by dispersing CNCs in the seed only, the adhesive strength reaches a maximum at about 0.5 – 1.0 phm for peel and 0.5 phm for tack, and then sharply decreases with higher loadings. To explain these trends, the CNC-water dispersion concentrations from Table 3.2 can be re-examined. Recall that concentrations above 2.5 $g_{CNC}\ L^{-1}_{water}$, are possible but can aggregate beyond a certain point. At 0.5 phm (e.g., run A2 with 6.88 $g_{CNC}\ L^{-1}_{water}$ in the seed), the CNC network remains stable due to the constant mixing in the reactor. The CNC hydrophilicity (due to their surface hydroxyl groups) improves the wettability of the films, which enables the dry polymer film to more intimately wet the testing substrate, thereby improving adhesive strength.[12, 27] With the current formulation, the peel strength and tack reach their peaks at 1.0 and 0.5 phm CNC respectively (Figure 3.1a and 3.1b), due in part to the improvement in film wettability. However, for higher CNC levels, the *local* CNC concentration exceeded the ability of mechanical mixing to keep the CNCs well dispersed during

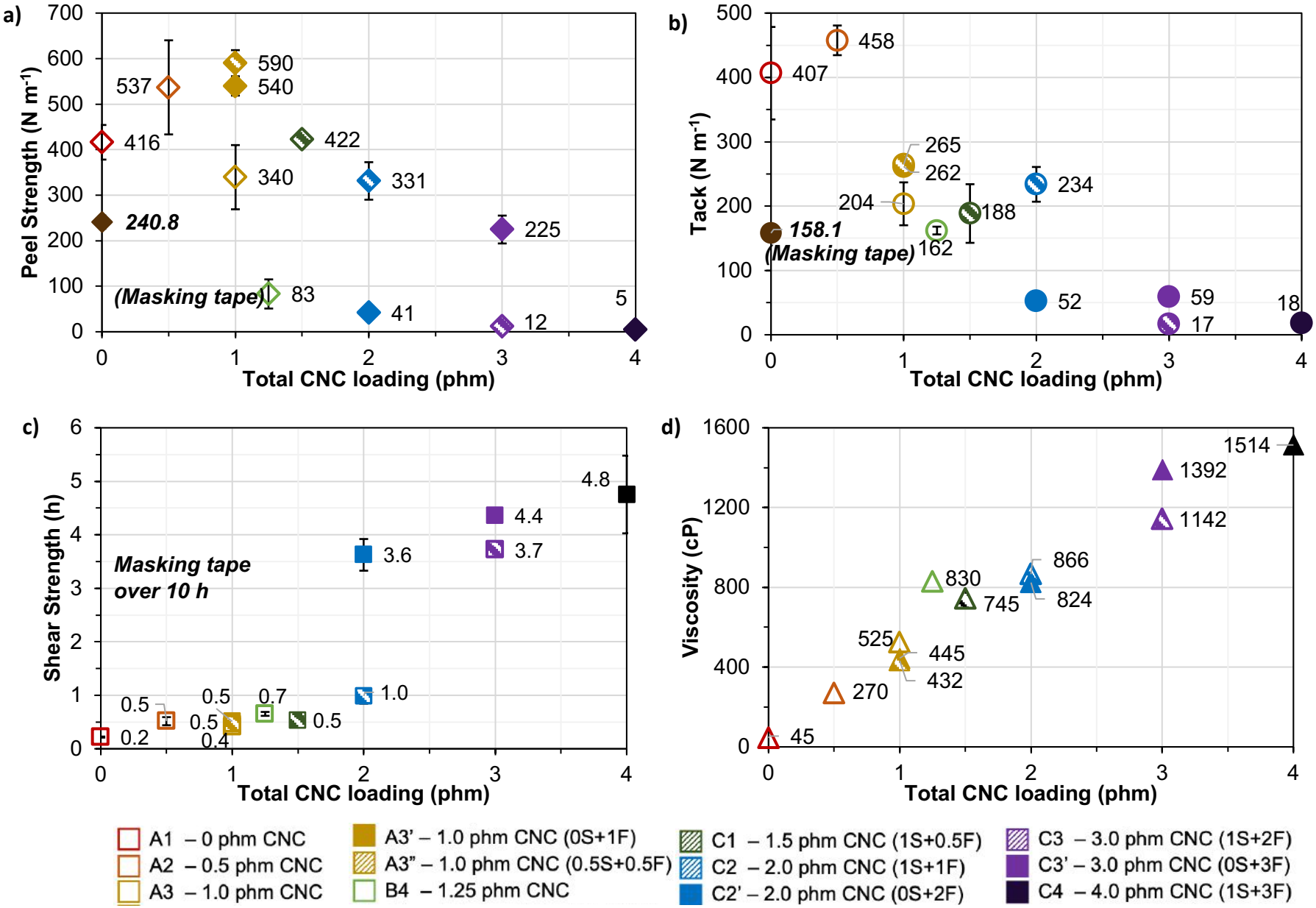

Figure 3.1 a) Peel strength, b) tack c) shear strength of adhesive films and d) latex viscosity with increasing CNC loading ("S" = seed and "F" = feed). Hollow symbols = latexes prepared by dispersing CNCs in the seed stage only; striped symbols = latexes prepared by dispersing CNCs in both the seed and feed stages; solid symbols = latexes prepared by dispersing CNCs in the feed stage only. Error bars represent the standard deviation.

the seed stage due to their interactions with other components of the emulsion. Thus, the addition of CNCs in the seed stage beyond 1.0 phm can start to negatively affect the adhesive properties. TEM images of latexes from previous work containing 1.0 phm CNCs showed some mild CNC agglomerates indicating film heterogeneity, which is known to diminish adhesive strength.[11] This is the case for run B4 in particular, where 1.25 phm CNCs is loaded during the seed stage and the film's peel strength drops substantially (from over 500 down to 83.1 N m^{-1}) with just a 0.25 phm increase in the CNC concentration. At the same time, the tack was also reduced relative to the base case. Thus, if the local CNC-water concentration is capped at 13.75 g_{CNC} L^{-1}_{water} in the seed, tack and peel strength can remain higher than that of the commercial masking tape, even with higher CNC loadings.

3.4.2.2 CNCs loaded in the seed & feed stages and in the feed stage only (runs A3', A3'', C1, C2, C2', C3, C3' and C4)

When going beyond 1.0 phm CNCs by dispersing CNCs in the feed as well as the seed stage, the tack and peel strength do not sharply plummet after reaching their peak - rather, they decrease gradually. For instance, the peel strength from films containing 1.0, 1.5, 2.0 and 3.0 phm (runs A3", C1, C2 and C3, respectively) decreases linearly with increasing CNC loading (Figure 3.1a).

With a total of 1.0 phm CNCs in the formulation, adhesive property improvements were greater when the CNCs were partitioned between the seed and feed stages (run A3') relative to when the total amount was dispersed entirely in the seed stage (run A3) or entirely in the feed stage (run A3"). Dividing the CNCs between the seed and feed stages allowed for lower local CNC concentrations (6.88 and 9.02 g_{CNC} L^{-1}_{water} in the seed and feed stages, respectively) which helped the CNCs remain well-dispersed during the polymerization and exhibit their typical performance improvements. Nevertheless, the peel strength of these adhesives decreased with higher loadings because of the increased latex viscosity (due in part to the addition of CNCs and in part to the CNC-latex particle interactions), which affected film formation and therefore, the quality of adhesive films.[28] In other words, with higher CNC loadings, the CNC-latex particle interactions inhibit good particle coalescence leading to a non-uniform polymer entanglement density thereby producing a non-homogeneous film. Although the peel strength with 1.5 or 2.0 phm CNC

loading was low relative to the base case, dividing the CNCs between the seed and feed stages allowed the adhesive performance to exceed that of commercial masking tape. However, as is seen for tack, loading 2.0 phm CNCs entirely in the feed significantly decreased the peel strength due to the formation of CNC agglomerates as well as chain immobilization caused by the high local concentration (15.54 g_{CNC} L^{-1}_{water}).

For tack, regardless of the CNC incorporation stage (i.e., seed stage vs. feed stage vs. seed *and* feed stages), any levels beyond 0.5 phm decreased adhesive performance compared to the peak tack with CNCs and the base case. The formation, elongation and failure of an adhesive's fibrils at a given debonding rate are the most important mechanisms that contribute to adhesive bond strength.[29] Thus, sharper decreases in tack are observed with the addition of CNCs due to their impact on an adhesive's viscoelastic properties.[10–12, 20, 21] Specifically, CNCs increase the elasticity of the polymer matrix (or decrease its fluidity) due to their rod-like morphology because the formation of a network reduces polymer chain mobility. This suggests that the adhesive's ability to elongate and resist an applied force was reduced relative to the base case formulation (run A1), which explains the decrease in tack beyond 0.5 phm CNCs. Despite these reductions, the tack remained comparable to that of commercial masking tape for total concentrations of up to 2.0 phm CNCs (Figure 3.1b).

Between 1.0 – 2.0 phm CNC loadings, regardless of how the CNC was added, the tack remained in the range of 162-264 N m^{-1} (statistically the same within experimental error). This is because the immobilizing effects of the CNCs which affect tack are more dependent on the total CNC concentration than the local concentrations. For 1.0 phm CNC loadings divided between the seed and feed stages (run A3"), only slight improvements in tack were observed versus loading the CNCs entirely in the feed stage (run A3') relative to improvements observed in peel strength, which were much more significant (Figure 3.1a). Adding 1.25 phm in the seed stage (run B4) did not have as severe an impact on tack as it did on peel strength for the same reasons. When adding 1.5 (run C1) or 2.0 (run C2) phm CNCs divided in the seed and feed stages, film tackiness was unchanged due to good CNC-water dispersion thanks to the acceptable CNC-water concentrations (that is, up to 13.75 g_{CNC} L^{-1}_{water} in the seed and 17.87 g_{CNC} L^{-1}_{water} in the feed). When adding the entire 2.0 phm CNCs in the feed stage (run C2'), the local CNC-water

concentration was much too high (34.01 g_{CNC} L^{-1}_{water}) resulting in a dramatic decrease in tack. In summary, for tack and peel strength, so long as the total CNC-water concentration is less than 15.54 g_{CNC} L^{-1}_{water}, adhesion outperforms that of commercial masking tape. Nonetheless, it is recommended to cap the seed concentration at 13.75 g_{CNC} L^{-1}_{water} and the feed concentration at 17.87 g_{CNC} L^{-1}_{water} to maintain a good CNC dispersion.

For higher CNC loadings (3.0 phm in runs C3, C3' and 4.0 phm in run C4, respectively), adhesive properties of the resulting films were poor. Although sonication cycles were performed for all CNC dispersions, at concentrations above 17.87 g_{CNC} L^{-1}_{water}, filtering the CNCs was challenging because the dispersion formed a gel and could not be suction filtered. Thus, unlike the instances in which CNCs were sonicated *and* filtered, it cannot be assumed that the CNCs were fully dispersed at the onset of the reaction. For runs C3 and C4 (containing 3.0 and 4.0 phm CNCs, respectively), the final latexes resembled a thick jelly, similar to mayonnaise, and contained bubbles even after cooling to room temperature. Casting films from these latexes also had some issues due to the remarkably lower flowability (i.e., the latex had to be scooped onto the Mylar films rather than pipetted).

The tack and peel strength were similar in runs A3, C1 and C2 despite their differing total CNC concentrations of 1.0 phm, 1.5 phm and 2.0 phm, respectively. This is because the seed solutions of these higher CNC-containing latexes were made with 1.0 phm CNCs and so it was no surprise that the adhesive performance for C1 and C2 (with 1.5 and 2.0 phm total CNC loadings) was similar to that of A3. Incorporating additional CNCs in the feed stage allowed for a higher *total* CNC loading while maintaining a good CNC-dispersion because the *local* CNC concentrations were still within acceptable ranges. Furthermore, because the CNCs were being mixed into two separate suspensions, their sonication and filtration cycles were done separately, to ensure good dispersion in both the seed and feed stages and ultimately, a more stable CNC-water network.

Generally, the shear strength of a PSA is influenced by its T_g, molecular weight and degree of crosslinking, which are intrinsic properties of the polymer, governed primarily by the formulation. Other property modifiers such as CTAs or cross-linkers can be added to manipulate the microstructural properties of the polymer and are often used together to balance their individual effects.[30] The base case formulation (no CNCs, run A1) showed the lowest shear

strength and very high tack and peel strength (Figure 3.1), which was not surprising given that high tack and peel strength are often achieved at the expense of diminishing shear strength.[29] At low CNC loadings, the time to shear failure did not show significant improvement compared to other studies,[10–12, 20] averaging 0.2-1 h (Figure 3.1c). The highest time to shear failure, 4.75 h, was observed for PSAs with 4.0 phm CNCs. With the addition of a stiff nanocrystal, a reinforced network with interconnected rigid micro-domains between soft polymer particles was possible, and improved the rigidity of the polymer matrix.[21] This allowed for stronger cohesive forces within the matrix and therefore, improved shear resistance. In previous work, the shear strength of PSA films prepared with different monomer systems likewise continually increased with higher CNC loadings.[10–12, 20, 21] In our case, the manifestation of this effect only occurred when the CNC concentration was high. This was because the base case polymer was exceptionally soft, due to the 0.25 phm chain transfer agent (i.e., NDM) in the formulation, which reduced the polymer molecular weight. Because of the shorter polymer chains, the CNCs have less opportunity to become entangled with chains protruding from the polymer particles.[21] Nonetheless, the use of a cross-linker in addition to the chain transfer agent is recommended to improve shear strength.

The gel content (Figure 3.2a), representing the insoluble cross-linked portion of the polymer, is extremely low for all composite latexes relative to previous, similar work.[10–12, 20, 21] Though it increased, the gel content ranged between 3 – 8% for CNC loadings between 0 – 2.0 phm and at its maximum, the gel content only reached 11 – 15% at CNC loadings of 3.0 – 4.0 phm (Figure 3.2c, runs C3, C3’ and C4). Low gel content can be attributed to the addition of chain transfer agent, which led to shorter overall polymer chain lengths and greatly reduced potential polymer cross-linking.[21, 30] In some cases, it has been shown that increasing the CNC loading can lead to an increase in gel content due to CNC-polymer cross-linking in the polymer matrix.[20] However, because the T_g remained between -40.8 and -38.6 ^oC regardless of CNC loading (Table AI.3 of Appendix I), there is no evidence supporting extensive CNC-polymer cross-linking. If there were any cross-linking reactions, their effects were completely outweighed by the effect of the chain transfer agent (i.e., NDM). The increase of gel content in runs C3, C3’ and C4 (with 3.0 – 4.0 phm CNCs) can be attributed to the CNCs whose 3-D network likely entrapped polymer particles or swelled during gel content testing. As the CNC loading increased, so did the experimental error

related to gel content. This suggests that the CNCs in the latex samples were not uniformly dispersed, as some samples had a higher gel fraction than others. Because of this, the gel content showed no statistical change between 1.5 and 2.0 phm, nor between 3.0 and 4.0 phm despite the increase in viscosity and changes in shear strength.

Lastly, contact angle measurements were conducted to investigate the effect of CNCs on film hydrophilicity/hydrophobicity and work of adhesion. With the increase in CNC loading, the PSA film's hydrophilicity was expected to increase because the CNCs, which should reside outside of the polymer particles, are hydrophilic. However, for increased CNC loadings in the seed stage (i.e., runs A1, A2 A3 and B4), both the water and the diiodomethane contact angles remained largely statistically unchanged (Figure 3.2b and 3.2c). This intriguing behaviour can be explained by film formation theory. During the PSA film preparation (see Appendix I), the latex was cast on a Mylar film and was left to dry under controlled conditions (i.e., temperature and humidity). Because the water evaporated from the film's surface, CNCs were drawn upward and tended to reside at the film surface, whereas the polymer particles settled nearer to the substrate. If not well distributed in the polymer matrix, CNCs can agglomerate during film formation, however, if CNCs are anchored to the polymer matrix, they can remain more uniformly dispersed.[31] Regardless of the potential of polymer-CNC anchoring, PSA films would have had a high enough CNC concentration even at 'lower' CNC loadings to allow a significant CNC accumulation at the surface of the prepared films. The abundance of CNCs in the formulation in addition to the use of acrylic acid led to the production of overall hydrophilic PSA films[21] and thus, low and relatively uniform water and diiodomethane contact angles.

In previous work, increasing CNC loading helped to improve the film's wettability and in turn, the work of adhesion.[10, 12] The work of adhesion (Figure 3.2d) was calculated using the water and diiodomethane contact angles and the Owens-Wendt equation[32] (Appendix I). Relative to other studies,[10, 12] the work of adhesion is high, ranging between 419-522 mN m^{-1}, and follows no particular trend with increasing the total CNC loading. In our case, the addition of CNCs has minimal impact on the work of adhesion relative to the intrinsic adhesive qualities of the bulk polymer, determined by the formulation. In other words, because the base case latex adhesive strength is high, the addition of CNCs had less of an impact on the work of adhesion

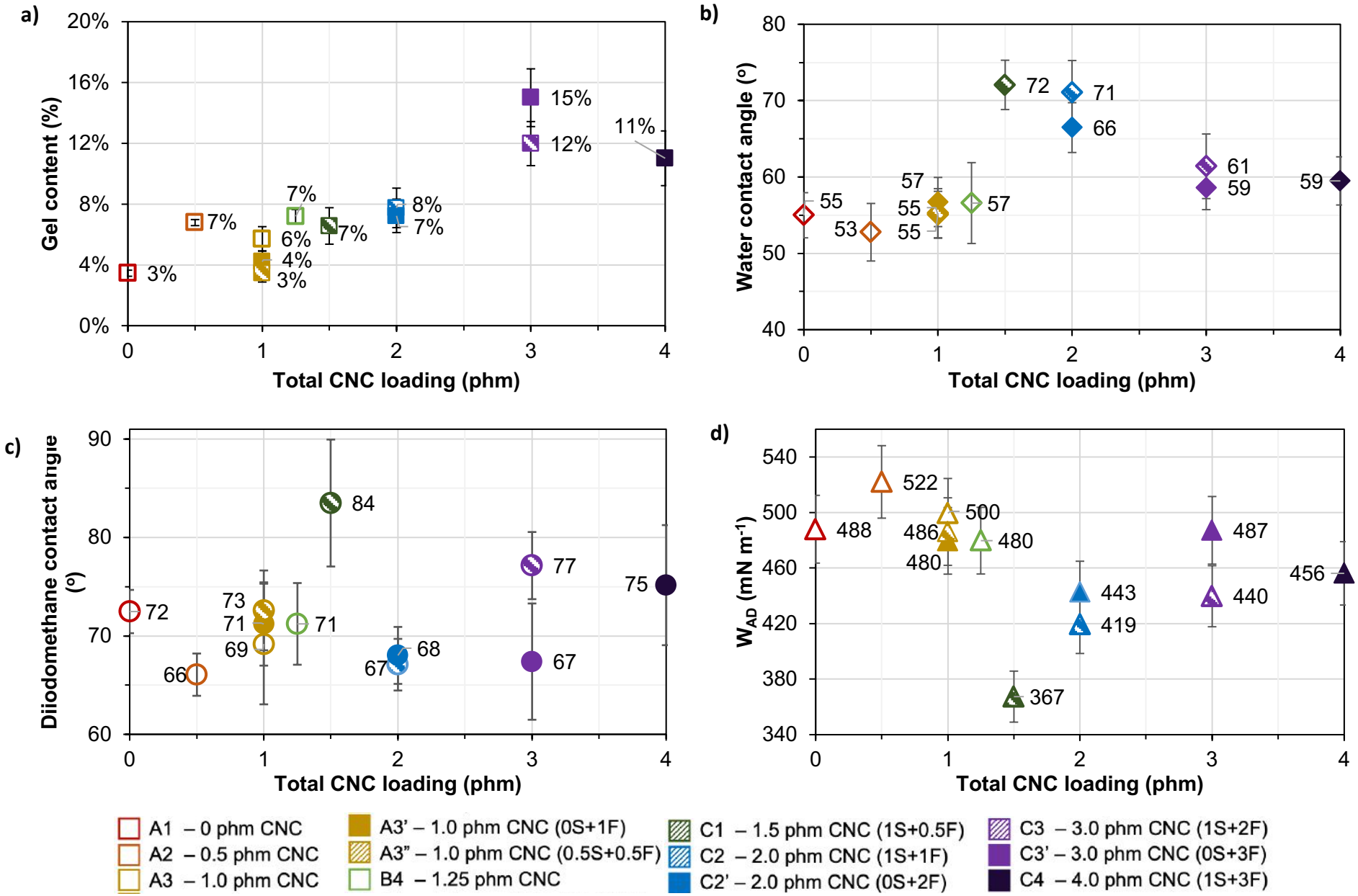

Figure 3.2 a) Gel content, b) water contact angle, c) diiodomethane contact angle, and d) work of adhesion of adhesive films. Error bars represent the standard deviation.

Overall.

3.5 Conclusion

Generally, CNCs need to be fully dispersed in water if they are to be properly incorporated into a latex polymerization. Knowing the limitations for CNC dispersion while keeping in mind the desire for high solids concentrations in emulsion polymerizations, presents additional constraints. In this work, we explored new ways of increasing the CNC loading *in situ* in a seeded semi-batch emulsion polymerization. An unprecedented CNC concentration of 4.0 phm, or 31.08 $g_{CNC}\ L^{-1}_{water}$ was achieved in a stable latex with 40 wt% total solids. This was accomplished by utilizing all of the available water in the formulation for CNC re-dispersion, allowing the CNCs to be loaded in both the emulsifier solution (used for the seed stage) and in the pre-emulsion solution (added in the feed stage).

The next question becomes "what is the impact of maximizing the CNC content in a latex formulation?". The application of interest in this work was PSAs. Starting with what can be considered a good PSA in terms of tack and peel strength, exceeding that of a commercial masking tape, the addition of CNCs to the formulation showed only modest improvements to these properties at low loadings. At higher loadings, the tack and peel strengths decreased while shear resistance increased. Nevertheless, for loadings up to 2.0 phm CNCs, the tack and peel strengths of our nanocomposites outperformed that of a commercial masking tape.

Comparing the incorporation method of the CNCs (i.e., in the seed, in the feed, or partitioned in both) indicated that there are no specific advantages to dispersing the CNCs in the seed solution vs. the feed solution or dividing them in both. Rather, the quality of the CNC dispersion and the local CNC-water concentration in a given phase is crucial; if the local concentration is high in the emulsifier solution (i.e., in the seed), the CNCs impede on particle nucleation and disrupt the colloidal stability in the emulsion, and if too high in the pre-emulsion solution (i.e., in the feed), the CNCs do not remain well dispersed thereby reducing the adhesive strength in the dried latex composite films. Thus, it was found that acceptable maximum CNC-water concentration in the seed and feed were 13.75 $g_{CNC}\ L^{-1}_{water}$ and 17.87 $g_{CNC}\ L^{-1}_{water}$, respectively in a BA/STY/AA latex PSA.

It is worth mentioning that PSAs are not the only applications of latex polymers. As we know, changes to the monomer formulation (e.g., using monomers yielding higher T_g polymers) can result in a wide range of products, for instance, for coatings applications. Clearly this work shows that higher loadings of CNCs led to monotonically increasing cohesion in the films (i.e., shear strength) which may be similarly advantageous in other latex nanocomposite applications. The examination of the impact of CNCs on these many other applications is only beginning. One can certainly keep in mind their impact on viscosity and other mechanical properties. Thus, we have presented a pathway towards higher CNC loadings that may be of interest for these other applications.

3.6 Supporting Information

Supporting Information is reproduced in Appendix I.

3.7 Acknowledgments

The authors are obliged to CelluForce Inc. for providing the unmodified CNC starting material. E.D.C. is grateful for financial support and recognition through the Early Researcher awards from the Ontario Ministry of Research and Innovation, the Canada Research Chairs program, and the University of British Columbia's President's Excellence Chair initiative. McMaster University (Faculty of Engineering), the University of British Columbia (Faculty of Applied Science and Faculty of Forestry) and the Bioproducts Institute (bpi.ubc.ca) are gratefully acknowledged for support. This work was funded through the Natural Sciences and Engineering Research Council of Canada (NSERC) Discovery Grant RGPIN-2017-05252 to E.D.C. and RGPIN-2019-03946 to M.A.D. V.A.G. is a recipient of a NSERC CGS-D Scholarship.

3.8 References

[1] R. A. Vaia and J. F. Maguire, "Polymer Nanocomposites with Prescribed Morphology: Going beyond Nanoparticle-Filled Polymers," *Chemical Materials*, vol. 26, no. 19, pp. 2736–2751, 2007, doi: 10.1021/cm052765h.

[2] P. K. Rana, S. K. Swain, and P. K. Sahoo, “Synthesis, characterization, and properties of intercalated poly(2-ethyl hexylacrylate)/silicate nanocomposites: XRD, TEM, IR, TGA, superabsorbency, pressure-sensitive adhesion, and biodegradation,” *Journal of Applied Polymer Science*, vol. 93, no. 3, pp. 1007–1011, 2004, doi: 10.1002/app.20568.

[3] T. Wang *et al.*, “Waterborne, Nanocomposite Pressure-Sensitive Adhesives with High Tack Energy, Optical Transparency, and Electrical Conductivity,” *Advanced Materials*, vol. 18, no. 20, pp. 2730–2734, Oct. 2006, doi: 10.1002/adma.200601335.

[4] T. Wang, P. J. Colver, S. A. F. Bon, and J. L. Keddie, “Soft polymer and nano-clay supracolloidal particles in adhesives: synergistic effects on mechanical properties,” *Soft Matter*, vol. 5, pp. 3842–3849, 2009, doi: 10.1039/b904740a.

[5] J. Kajtna, M. Krajnc, and J. Golob, “The role of components in waterbased microsphere acrylic PSA adhesive properties,” *Macromolecular Symposia*, vol. 243, pp. 132–146, 2006, doi: 10.1002/masy.200651114.

[6] Y. Yamamoto, S. Fujii, K. Shitajima, K. Fujiwara, S. Hikasa, and Y. Nakamura, “Soft polymer-silica nanocomposite particles as filler for pressure-sensitive adhesives,” *Polymer (Guildf)*, vol. 70, pp. 77–87, Jul. 2015, doi: 10.1016/j.polymer.2015.06.006.

[7] M. Khalina, M. Sanei, H. S. Mobarakeh, and A. R. Mahdavian, “Preparation of acrylic/silica nanocomposites latexes with potential application in pressure sensitive adhesive,” *International Journal of Adhesion and Adhesives*, vol. 58, pp. 21–27, Apr. 2015, doi: 10.1016/j.ijadhadh.2014.12.007.

[8] J. I. Hong, K. S. Cho, C. I. Chung, L. S. Schadler, and R. W. Siegel, “Retarded cross-linking in ZnO-low-density polyethylene nanocomposites,” 2002.

[9] B. A. Bhanvase and S. H. Sonawane, “Ultrasound assisted in situ emulsion polymerization for polymer nanocomposite: A review,” *Chemical Engineering and Processing: Process Intensification*, vol. 85, pp. 86–107, 2014, doi: 10.1016/j.cep.2014.08.007.

[10] Z. Dastjerdi, E. D. Cranston, and M. A. Dubé, “Pressure sensitive adhesive property modification using cellulose nanocrystals,” *International Journal of Adhesion and Adhesives*, vol. 81, pp. 36–42, Mar. 2018, doi: 10.1016/j.ijadhadh.2017.11.009.

[11] A. Ouzas, E. Niinivaara, E. D. Cranston, and M. A. Dubé, “In Situ Semibatch Emulsion Polymerization of 2-Ethyl Hexyl Acrylate/ n -Butyl Acrylate/Methyl Methacrylate/Cellulose Nanocrystal Nanocomposites for Adhesive Applications,” *Macromolecular Reaction Engineering*, vol. 12, no. 3, p. 1700068, Jun. 2018, doi: 10.1002/mren.201700068.

[12] A. Ouzas, E. Niinivaara, E. D. Cranston, and M. A. Dubé, “Synthesis of poly(isobutyl acrylate/n-butyl acrylate/methyl methacrylate)/CNC nanocomposites for adhesive applications via in situ semi-batch

emulsion polymerization," *Polymer Composites*, vol. 40, no. 4, pp. 1365–1377, Apr. 2019, doi: 10.1002/pc.24869.

[13] D. C. Sherrington, "Emulsion polymerization and emulsion polymers," *Reactive and Functional Polymers*, vol. 36, no. 1, pp. 104–105, Feb. 1998, doi: 10.1016/S1381-5148(97)84204-6.

[14] J. M. Asua, "Emulsion polymerization: From fundamental mechanisms to process developments," *Journal of Polymer Science Part A: Polymer Chemistry*, vol. 42, no. 5, pp. 1025–1041, Mar. 2004, doi: 10.1002/pola.11096.

[15] M. A. Dubé, V. A. Gabriel, A. S. Pakdel, and Y. Zhang, "Sustainable polymer reaction engineering: Are we there yet? (Submitted)," *Canadian Journal of Chemical Engineering*, 2020.

[16] S. Mondal, "Review on Nanocellulose Polymer Nanocomposites," *Polymer - Plastics Technology and Engineering*, vol. 57, no. 13, pp. 1377–1391, 2018, doi: 10.1080/03602559.2017.1381253.

[17] R. J. Moon, A. Martini, J. Nairn, J. Simonsen, and J. Youngblood, "Cellulose nanomaterials review: structure, properties and nanocomposites," *Chemical Society Reviews*, vol. 40, no. 7, p. 3941, Jun. 2011, doi: 10.1039/c0cs00108b.

[18] Y. Habibi, "Key Advances in the Chemical Modification of Nanocelluloses," *Chem Soc Rev*, vol. 43, no. 5, pp. 1519–42, Mar. 2014, doi: 10.1039/c3cs60204d.

[19] A. Dufresne, *Cellulose-Based Composites and Nanocomposites*. Elsevier, 2008. doi: 10.1016/B978-0-08-045316-3.00019-3.

[20] Z. Dastjerdi, E. D. Cranston, and M. A. Dubé, "Synthesis of Poly(n -butyl acrylate/methyl methacrylate)/CNC Latex Nanocomposites via In Situ Emulsion Polymerization," *Macromolecular Reaction Engineering*, vol. 11, no. 6, p. 1700013, Dec. 2017, doi: 10.1002/mren.201700013.

[21] A. S. Pakdel, V. Gabriel, R. M. Berry, C. Fraschini, E. D. Cranston, and M. A. Dubé, "A sequential design approach for in situ incorporation of cellulose nanocrystals in emulsion-based pressure sensitive adhesives," *Cellulose*, vol. 27, no. 18, pp. 10837–10853, Dec. 2020, doi: 10.1007/s10570-020-03060-6.

[22] M. S. Reid, M. Villalobos, and E. D. Cranston, "Cellulose nanocrystal interactions probed by thin film swelling to predict dispersibility," *Nanoscale*, vol. 8, no. 24, pp. 12247–12257, 2016, doi: 10.1039/c6nr01737a.

[23] S. Roberge and M. A. Dubé, "The effect of particle size and composition on the performance of styrene/butyl acrylate miniemulsion-based PSAs," *Polymer (Guildf)*, vol. 47, no. 3, pp. 799–807, 2006, doi: 10.1016/j.polymer.2005.12.024.

[24] P. Hajji, J. Y. Cavaillé, V. Favier, C. Gauthier, and G. Vigier, "Tensile Behavior of Nanocomposites From Latex and Cellulose Whiskers," *Polymer Composites*, vol. 7, no. 4, pp. 612–619, 1996.

[25] V. Favier, G. R. Canova, S. C. Shrivastava, and J. Y. Cavaillé, "Mechanical percolation in cellulose whisker nanocomposites," *Polymer Engineering and Science*, vol. 37, no. 10, pp. 1732–1739, 1997, doi: 10.1002/pen.11821.

[26] F. Cherhal, F. Cousin, and I. Capron, "Influence of charge density and ionic strength on the aggregation process of cellulose nanocrystals in aqueous suspension, as revealed by small-angle neutron scattering," *Langmuir*, vol. 31, no. 20, pp. 5596–5602, 2015, doi: 10.1021/acs.langmuir.5b00851.

[27] Z. Ajelou, N. Nikfarjam, and N. Taheri-Qazvini, "In-situ modified cellulose nanocrystals as water droplet stabilizer in polystyrene beads targeted for water expanded foam," *European Polymer Journal*, vol. 121, no. July, p. 109343, 2019, doi: 10.1016/j.eurpolymj.2019.109343.

[28] A. ben Elmabrouk, T. Wim, A. Dufrensne, and S. Boufi, "Preparation of Poly(styrene-co-hexylacrylate)/Cellulose Whiskers Nanocomposites via Miniemulsion Polymerization," *Polymers and Polymer Science*, no. 7, pp. 449–456, 2009, doi: 10.1002/app.30886.

[29] R. Jovanović and M. A. Dubé, "Emulsion-Based Pressure-Sensitive Adhesives: A Review," *Journal of Macromolecular Science - Polymer Reviews*, vol. 44, no. 1, pp. 1–51, 2004, doi: 10.1081/MC-120027933.

[30] L. Que and M. A. Dubé, "Manipulation of chain transfer agent and cross-linker concentration to modify latex micro-structure for pressure-sensitive adhesives," *European Polymer Journal*, vol. 46, no. 6, pp. 1225–1236, 2010, doi: 10.1016/j.eurpolymj.2010.02.014.

[31] A. ben Mabrouk, H. Kaddami, A. Magnin, M. N. Belgacem, A. Dufrensne, and S. Boufi, "Preparation of Nanocomposite Dispersions Based on Cellulose Whiskers and Acrylic Copolymer by Miniemulsion Polymerization: Effect of the Silane Content Ayman," *Polymer Engineering and Science*, 2011, doi: 10.1002/pen.21778.

[32] D. Sowa, Z. Czech, and Ł. Byczyński, "Peel adhesion of acrylic pressure-sensitive adhesives on selected substrates versus their surface energies," *International Journal of Adhesion and Adhesives*, vol. 49, pp. 38–43, 2014, doi: 10.1016/j.ijadhadh.2013.12.013.

Chapter 4

In situ Addition of Carboxylated Cellulose Nanocrystals in Seeded Semi-Batch Emulsion Polymerization

Vida A. Gabriel,[1] Pascale Champagne,[2] Michael F. Cunningham,[2] Marc A. Dubé[1]

[1]Department of Chemical and Biological Engineering, Centre for Catalysis Research and Innovation, University of Ottawa, Ottawa, Ontario, Canada

[2]Department of Chemical Engineering, Queen's University, Kingston, Ontario, Canada

This chapter is a manuscript published in The Canadian Journal of Chemical Engineering (2022; 100,4: 767-779)

4.1 Abstract

Nanocellulosic materials can be used as green materials for property modification in latex polymers. In particular, cellulose nanocrystals (CNCs) can be incorporated in latexes *in situ* – a preferable method to *ex situ* addition because it ensures latex homogeneity and better performance enhancements. DextraCel™ is a commercial CNC with carboxylate surface groups, henceforth referred to as "cCNC". The interactions between cCNCs and other standard latex components are studied, and experiments reveal that cCNCs can be sensitive to the ionic strength of the aqueous phase of the latex. A reproducible method to incorporate cCNCs *in situ* in a seeded semi-batch emulsion polymerization is developed for the production of latexes for adhesive applications by varying the surfactant-initiator systems in the seed stage and the feed stage. Sodium dodecyl sulphate (SDS) and potassium persulphate (KPS), negatively charged surfactant and initiator respectively, are used for the seeding reaction, and Triton X-405 and 2,2'-azobisisobutyronitrile (AIBN) (uncharged surfactant and initiator) are used in the feed to preserve low ionic strength of the latex, thereby producing stable latexes.

Keywords: Emulsion polymerization, latex, nanocomposites, cellulose nanocrystals, carboxylated cellulose nanocrystals

4.2 Introduction

In an effort to design safer polymer products and to manufacture them in a more sustainable way, there has been a shift towards the use of water-based production methods, such as emulsion polymerization (EP).[1] EP affords numerous technical, environmental, and safety advantages relative to solvent-based production methods. For example, using water as a dispersing agent not only eliminates the risks associated with the usage of organic solvents, but it is a more economical and sustainable process.[2, 3] Following several decades of development, EP is a major production method for several commodity products (e.g., paints, coatings, adhesives).

EP is a heterogeneous system in which organic and inorganic phases co-exist. EP allows for the simultaneous increase of polymer molecular weight and reaction rate (desirable to maximize productivity), unlike the case for polymers produced in bulk or solution polymerization where high molecular weights can only be achieved at lower reaction rates, and vice versa.[4–6] Furthermore, the viscosity of a given latex is, for the most part, not governed by the polymer molecular weight and thus, high solids content latexes can be obtained without affecting the polymer microstructure. Finally, the water in an EP helps to reduce the reaction viscosity and simultaneously acts as a heat sink allowing for efficient heat transfer and therefore better overall temperature control.

Compared to single-phase systems, EP can benefit from a broader range of property modifiers because both hydrophilic and hydrophobic materials can be incorporated into the polymer latex. In the last few decades, nanomaterials such as nanosilica,[7–10] nanoclays,[11, 12] and carbon nanotubes[13–16] have been used increasingly to improve polymer properties (e.g., thermodynamic, structural, mechanical) because very small amounts (e.g., 1-2%) can cause dramatic property improvements. In particular, nanocellulosic materials (i.e., nanomaterials derived from a natural cellulosic source) exhibit unique properties due to their structure and surface chemistry. They are promising alternatives to synthetic and petroleum-based property modifiers because of their ability to assemble at air-water[17] and oil-water interfaces,[18] typical of heterogeneous systems. As such, nanocellulose incorporation via EP has yielded composite latexes with greater wettability, stability, and mechanical and adhesive performance.[18]

Cellulose nanocrystals (CNCs), a subclass of nanocellulose, are commonly extracted from wood pulp or cotton plants via acid hydrolysis.[19–22] The chemical process used to isolate the CNCs directly affects their dimensions and surface chemistry, which in turn impacts their properties. Sulphuric acid treatment of plant-based cellulose is the most popular route for obtaining CNCs and typically yields high aspect ratio, rod-like particles that are 100 to 200 nm long and 5 to 10 nm wide, with sulphate half-ester surface groups on the crystal surface.[23, 24] Though commonly available in powder form after spray-drying, generally, CNCs can be redispersed in water to form a stable colloid[25–28] and have been incorporated in a number of water-based systems in their dispersed form. For example, when up to 2 wt.% CNCs were added to latexes via mechanical blending, the mechanical properties,[29–32] shear modulus,[29, 33] thermal stability,[33–35] matrix reinforcement,[36, 37] and adhesive strength[38–43] of the nanocomposite films were enhanced. When incorporated via an *in situ* process in an EP (i.e., added to the formulation prior to or during the reaction), CNCs have shown similar improvements.[38–43]

An important consideration in EP is maintaining a stable dispersion; the addition of nanomaterials *in situ* can be disruptive to latex stability. Moreover, the many components in a latex formulation (e.g., monomers, surfactants, initiators, modifiers) also impact latex stability and can play a role in how nanomaterials and, in this case, CNCs affect latex stability and performance. Although CNCs will be partitioned in the water phase of an emulsion, monomers which are slightly water-soluble (e.g., butyl acrylate, vinyl acetate) can help to maintain a good CNC dispersion in a latex.[38, 39, 41, 43] On the other hand, water-soluble components in a latex formulation (e.g., buffers, acidic monomers, initiators) can affect the pH and/or ionic strength and destabilize the CNC dispersion; the type of the charged species is also important. For example, the electrostatic stability of CNC dispersions in seeded semi-batch EP was compromised when a cationic surfactant (e.g., CTAB) interacted with the CNCs, thereby destabilizing the latex, whereas anionic surfactants (e.g., SDS) did not.[44, 45]

Due to their surface groups, CNCs can easily undergo a number of chemical modifications allowing one to control their surface activity and tune their functionality, thereby greatly broadening their scope of use in novel applications. Surface modified CNCs in the form of carboxylated CNCs,[46] acetylated CNCs,[47] aldehyde CNCs,[48] polymer-grafted CNCs,[49] and CNCs

modified with alkyl chains of varying lengths[46, 50] were used in suspension polymerization to enhance the stability of monomer droplets/polymer particles. EP product properties can be tailored to specific applications by introducing functional groups to the latex via the formulation components present (e.g., monomers, surfactants, initiators, fillers). For example, the drying rate of latex based films can be modified with the addition of carboxyl groups to the latex formulation, which in turn can affect their optical quality.[51]

Unlike the typical sulphated CNCs, Anomera Inc. manufactures carboxylated CNCs, called DextraCel™. In a recent benchmarking paper, Delepierre et al.[52] compared CNCs extracted by conventional sulphuric acid hydrolysis to DextraCel™. DextraCel™ CNCs are 100 to 200 nm in length, 5 nm in width, and form stable colloidal suspensions in water. They have lower surface charges and are also shorter than CNCs made by sulphuric acid hydrolysis or other commercial CNCs.[53] These differences result in a significant impact on nanomaterial performance. For instance, DextraCel™ CNCs are more thermally stable in both their acid and sodium-form than sulphated CNCs, in part, because of their lower surface charge. In particular, when comparing the degradative thermogravimetry curves for the two types of CNCs (in their acid form), the onset of thermal degradation for sulphated CNCs occurs at 150^{o}C, whereas that of carboxylated CNCs only begins at 250^{o}C.[52]

The *in situ* addition of CNCs in emulsion-based polymers is challenging and methods developed for *in situ* CNC addition are specific to the nature of the CNCs, and the components of the EP. To date, no studies have investigated the addition of carboxylated CNCs in EP reactions. In this work, a reproducible method for the incorporation of DextraCel™ (henceforth referred to as “carboxylated CNCs” or “cCNCs”) in a colloidally stable *in situ* seeded semi-batch EP formulation is developed. To that end, the interactions of the cCNCs with various components of the EP formulation (e.g., surfactants and initiators) were studied.

4.3 Experimental

4.3.1 Materials

Butyl acrylate (BA) and methyl methacrylate (MMA) (both >99% pure and stabilized by 20-200 ppm hydroquinone) were purchased from Sigma-Aldrich and purified before use by

passing them dropwise through an inhibitor removal column. All the surfactants, namely, sodium dodecyl sulphate (SDS, ACS Reagent >99%), Triton X-405 (liquid, 70% concentration) and cetyltrimethylammonium bromide (CTAB, Fisher Scientific, technical grade) were used as received. The initiators, potassium persulphate (KPS, >99%) and 2,2'-azobisisobutyronitrile (AIBN, 98%) were purchased from Sigma-Aldrich and used as received. DextraCel™ (i.e., carboxylated CNCs or cCNCs) was obtained from Anomera Inc. (Montreal, Canada) in a 'never-dried' form (a 4.5 wt.% dispersion in water). The apparent cCNC size, via dynamic light scattering (DLS), was found to be 81 ± 0.4 nm and the length and cross-section determined by atomic force microscopy[52] was 150 ± 30 nm and 5 ± 1 nm, respectively; they were supplied with Na+ counterions (pH ≈ 7.5) and the carboxylate surface group content was determined to be 141 ± 10 mmol/kg cCNC.[52] Distilled deionized water (DDW) with a resistivity of 18.0 ± 0.2 MΩ-cm was used for the emulsion polymerization reactions as well as for all dispersions, suspensions, solutions, and for characterization purposes.

4.3.2 Seeded semi-batch emulsion polymerization

A copolymer formulation containing a 'hard' and 'soft' monomer (MMA and BA, whose homopolymer glass transition temperatures are 105°C and -54°C respectively)[54] was used in anticipation of future work to produce latexes for adhesive applications. The ratio of these monomers, 90:10 BA:MMA, was selected according to previous work[39, 40] in order to make direct comparisons with sulphated or otherwise modified CNCs. Preliminary experiments revealed that loading the CNCs to the seed of the EP reaction (as is done traditionally)[39–42] caused significant gelling due to the high local SDS-cCNC concentration (discussed in section 4.4.2) which perturbed the seeding reaction, ultimately leading to coagulation. Although the addition of CNCs into the formulation of a seeded semi-batch EP has a remarkable impact on final latex properties, previous work revealed that their addition protocol (i.e., added at the seed stage vs. feed stage) did not affect the degree of property enhancement.[38] In other words, CNCs can be added in the seed or in the feed stage, provided that they are well dispersed. Thus, the cCNCs were added to the pre-emulsion of the feed stage, rather than the seeding stage to ensure the formation of a stable polymer seed. A 500 mL RC1e glass reactor (Mettler-Toledo) equipped with a Hastelloy stirrer, two feeding pumps, a thermometer and nitrogen purge line (a needle inlet) were used for

all polymerization reactions to produce latexes with 40 wt.% solids. Three approaches were used, which are described as “classical”, “modified” and “hybrid” in terms of which surfactants and initiators were used.

Classical starved-feed semi-batch emulsion polymerization: Table 4.1 describes the polymerization sequence and partitioning of the components in a typical reaction. Water and surfactant were loaded to the reactor, were heated to 60°C under constant stirring (250 rpm), and were purged with nitrogen for 25 min. Next, 10% of the total monomer was added to the reactor and left to stir for 5 min before adding a shot of KPS in DDW (0.062 g KPS in 2.25 g DDW) to initiate the seeding reaction. After the 30-min seeding reaction was complete, two separate solutions were fed to the reactor via pumps in a feeding stage: 1- a pre-emulsion containing the monomers, DDW, SDS, and cCNCs, if any; and 2- an initiator solution containing DDW and KPS. The pre-emulsion was fed to the reactor for a total of 240 min, whereas the initiator solution was fed for 30 min longer (i.e., 270 min). At the end of the feeding stage, the latex was left to “cook” at 250 rpm at 60°C for an additional 30 min to allow residual monomer to react. Samples were taken throughout the runs and were characterized for particle size, zeta-potential, conversion, and solids content.

Table 4.1 Classical starved-fed semi-batch emulsion polymerization formulation and reaction sequence to produce a 40 wt.% solids latex with 1.0 phm cCNCs.

	Mixture	**Description**	**Component**	**Amount (g)**
Seed stage	Emulsifier	Surfactant solution mixed at 250 rpm and heated to 60°C over 25 min. Reactor purged with nitrogen and maintained within 1°C of set temperature and mixing at 250 rpm for the duration of the reaction.	DDW	48.25
			SDS	0.43
	Monomer	Seed monomer (~10 wt.% of total monomer) added to heated emulsifier solution and left to mix and heat for 5 min.	BA	15.30
			MMA	1.70
	Initiator 1	Initiator dissolved in DDW injected to reactor to initiate seeding stage, lasting 30 min.	KPS	0.062
			DDW	2.25

Feed stage	Pre-emulsion	Monomer, surfactant and DDW are mixed vigorously using a magnetic stir bar until emulsified. This pre-emulsion solution is fed to reactor at 1.33 g/min for 240 min after the completion of the seed stage. When present, cCNCs added to the pre-emulsion.	BA	145.8
			MMA	18.0
			DDW	113.3
			SDS	1.944
			cCNC	40.0
	Initiator 2	Initiator 2 solution fed in parallel with pre-emulsion solution at 0.25 g/min for 270 min total.	KPS	0.54
			DDW	67.5
Cook stage		Reactor contents left to mix at 60°C for additional 30 min to ensure conversion of residual monomer.		

Modified starved-feed semi-batch emulsion polymerization: For reasons discussed in detail in Section 4.4, a different surfactant and initiator were used to produce a stable latex with the cCNCs *in situ*. Because the cCNCs were sensitive to the ionic strength of the aqueous phase of the growing polymer colloid, Triton X-405, a non-ionic surfactant, and AIBN, an oil-soluble initiator, were used to replace the SDS and KPS, respectively, and reduce the electrolyte concentration in the water phase of the polymerization where the cCNCs reside. Instead of adding a shot of initiator solution to initiate the seeding reaction, the AIBN initiator was dissolved in the seed monomer to initiate the reaction, because it is oil-soluble. Furthermore, the partitioning of the components in the two feeds was altered; the monomer and initiator were fed to the reactor as a solution together, and the emulsifier solution (water and surfactant) were fed via the second feed line. Both feeds lasted for 270 min. All other elements of the EP procedure remained the same as the “classical” case (Table 4.2).

Table 4.2 Modified starved-fed semi-batch emulsion polymerization formulation and reaction sequence to produce a 40 wt.% solids latex with 1.0 phm cCNCs.

	Mixture	Description	Component	Amount (g)
Seed stage	Emulsifier 1	Surfactant solution mixed at 250 rpm and heated to 60°C over 25 min. Reactor purged with nitrogen and maintained within 1°C of set temperature and mixing at 250 rpm for the duration of the reaction.	DDW	42.50
			Triton X-405	0.93
	Monomer + Initiator 1	Seed monomer (~10 wt.% of total monomer) and initiator added to heated emulsifier solution to initiate seeding stage, lasting 30 min.	BA	15.30
			MMA	1.70
			AIBN	0.054
Feed stage	Monomer + Initiator 2	Monomer and initiator are fed to reactor at 0.57 g/min for 270 min after the completion of the seed stage. Mixing rate increased to 300 rpm.	BA	137.70
			MMA	15.30
			AIBN	1.56
	Emulsifier 2	DDW and surfactant are fed to reactor at 0.79 g/min for 270 min after the completion of the seed stage. When present, cCNCs added to the Emulsifier 2 solution. Mixing rate increased to 300 rpm.	DDW	167.90
			Triton X-405	6.57
			cCNC	40.0
Cook stage		Reactor contents left to mix at 60°C for additional 30 min to ensure conversion of residual monomer.		

Hybrid starved-feed semi-batch emulsion polymerization: Although using the "modified" technique and formulation in Table 4.2 did not lead to coagulation, there were other complications, discussed in detail in Section 4.4. The mixing rate was increased to 300 rpm avoid the generation of aggregates and samples were carefully taken with a syringe without pausing the mixing. Furthermore, the initial and final particle sizes were hard to control using the AIBN + Triton X-405 combination of surfactant and initiator. Thus, to overcome the stability issues while simultaneously maintaining control of the initial and final particle sizes, it was found that stable nanocomposite latexes could be obtained by producing a conventional seed (i.e., with SDS and

KPS) and then changing the surfactant-initiator system to AIBN + Triton X-405 at the onset of the feeding stage. To ensure high final conversion, a shot of initiator solution (0.25 g KPS in 2.25 g DDW) was added at the onset of the cook stage. Table 4.3 describes the component partitioning of this "hybrid" method. Because the AIBN initiator was oil soluble, it could not be fed to the reactor separately from the monomer. Thus, the following feed solutions were prepared: 1- a monomer and initiator solution and 2- a water, surfactant and cCNC (when used) solution.

Table 4.3 Hybrid starved-fed semi-batch emulsion polymerization formulation and reaction sequence for a 40 wt.% solids latex with 1.0 phm cCNC.

	Mixture	**Description**	**Component**	**Amount (g)**
Seed stage	Emulsifier 1	Surfactant solution mixed at 250 rpm and heated to 60°C over 25 min. Reactor purged with nitrogen and maintained within 1°C of set temperature and mixing at 250 rpm for the duration of the reaction.	DDW	48.25
			SDS	0.43
	Monomer	Seed monomer (~10 wt.% of total monomer) added to heated emulsifier solution and left to mix and heat for 5 min.	BA	15.30
			MMA	1.70
	Initiator 1	Initiator dissolved in DDW injected to reactor to initiate seeding stage, lasting 30 min.	KPS	0.062
			DDW	2.75
Feed stage	Monomer + Initiator	Monomer and initiator are fed to reactor at 0.57 g/min for 270 min after the completion of the seed stage. Mixing rate increased to 300 rpm.	BA	137.70
			MMA	15.30
			AIBN	1.024
	Emulsifier 2	DDW and surfactant are fed to reactor at 0.77 g/min for 270 min after the completion of the seed stage. When present, cCNCs added to the Emulsifier 2 solution. Mixing rate increased to 300 rpm.	DDW	165.17
			Triton X-405	4.74
			cCNC	37.78

Cook stage	Initiator dissolved in DDW injected to reactor to boost final conversion. Reactor contents left to mix at 60°C for additional 30 min to ensure conversion of residual monomer.	KPS	0.25
		DDW	2.50

4.3.3 Latex characterization

2 mL samples were taken from the reactor at 30- or 60-min intervals to characterize the latex. Instantaneous and cumulative conversions were measured gravimetrically using standard methods.[43]

Particle size and distribution, and zeta-potential were measured using a Malvern Zetasizer 2000. Dynamic light scattering (DLS) was used to measure the average particle size and distribution of polymer particles; ~2 mL of diluted latex sample (0.1 – 0.2 g_{latex}/g_{water}) was loaded to a disposable polystyrene cuvette and measured at a scattering angle of 173^{o} and at 25°C. The reported particle sizes are an intensity-weighed mean diameter value (z-average) obtained from three measurements of 12 to 15 scans, and the PDI is a measure of the breadth of the particle size distribution derived from the cumulant analyses. For the zeta-potential measurements, prepared samples were loaded in a folded capillary cell. The Smoluchowski approximation, based on the electrophoretic mobility of the charged particles, was used to calculate the zeta-potential. For the zeta-potential of latex, ~3 mL of diluted latex sample (0.1 – 0.2 g_{latex}/g_{water}) was injected to a folded capillary cell using a syringe. For the zeta-potential of other solutions (i.e., DDW + KPS, DDW + cCNCs, DDW + surfactant), no dilutions were performed. The viscosity of the final latex was measured at 100 rpm using spindles R2 or R3 in a Thermo Scientific HAAKE Viscotester (Model D).

4.4 Results and discussion

4.4.1 Preliminary experiments using “classical” approach

When cCNCs were first introduced via the pre-emulsion solution in a “classical” starved-feed semi-batch emulsion polymerization, coagulation occurred approximately 120 min into the feed stage. In general, the addition of any charged species to the formulation of an emulsion-

based polymer can lead to coagulation because it can interfere with the particles' electrical double layer, ultimately destabilizing the colloid. In addition, all types of CNCs typically increase reaction viscosity, which in turn can lead to coagulation, but increasing the amount of surfactant in the formulation can mitigate this effect, ultimately yielding a stable latex.[38] However, upon increasing the amount of SDS in the current formulation from 1.35 phm (2.97 g total, Table 4.1) to 1.75 phm (3.85 g), coagulation occurred in a shorter time frame. The pH, initial and final particle sizes, as well as the reaction temperature, were varied in a series of troubleshooting experiments but latex stability continued to be problematic. Kedzior et al.[55] noted that surfactant adsorption to CNCs is strongly dependant on the CNC surface charge and counterions present in the continuous phase, and such interactions could lead to the destabilization of a CNC dispersion. Thus, the next logical step was to study the interactions between cCNCs and all ionic components of the emulsion formulation, namely, the surfactant and initiator. Three different surfactants (SDS - anionic, Triton X-405 - non-ionic, and CTAB - cationic) were studied to reveal any potential interactions with the cCNCs. The KPS initiator was likewise studied.

4.4.2 cCNC – surfactant and cCNC – KPS interactions

cCNCs were diluted in DDW to form 0.5 wt.% and 1.0 wt.% dispersions. A predetermined amount of surfactant was added to the cCNC dispersions to produce solutions that were 0.2, 0.5, 1, 2, 5, 10 and 15 times the critical micelle concentration (CMC) of each respective surfactant in water (i.e., 8.25 mM for SDS,[56] 0.86 mM for Triton X-405,[57] and 0.89 mM for CTAB).[58] Likewise, KPS was mixed with the cCNC dispersions of 0.5 wt.% and 1.0 wt.% at concentrations of 15, 30, 40, 50, 60, 70 and 80 mM. In order to study the interactions between each of the aforementioned components with cCNCs, the apparent diameter and zeta-potential of the cCNC dispersions were measured (Figure 4.1 and 4.2, respectively).

In general, DLS is better suited for characterizing spherical particles thus, measurements for rod-like particles, like CNCs, is not accurate. Rather, DLS provides an apparent diameter of samples and can be used as a point of comparison between CNCs within a study. Because the apparent cCNC diameter was approximately 80 nm (81 ± 0.4 nm)[52] any particle size readings above, ~100 nm, suggested that the DLS was measuring cCNC aggregates. In Figure 4.1A, SDS loadings beyond 20 mM for 1.0 wt.% cCNC and beyond 40 mM for 0.5 wt.% cCNC yielded

(A)

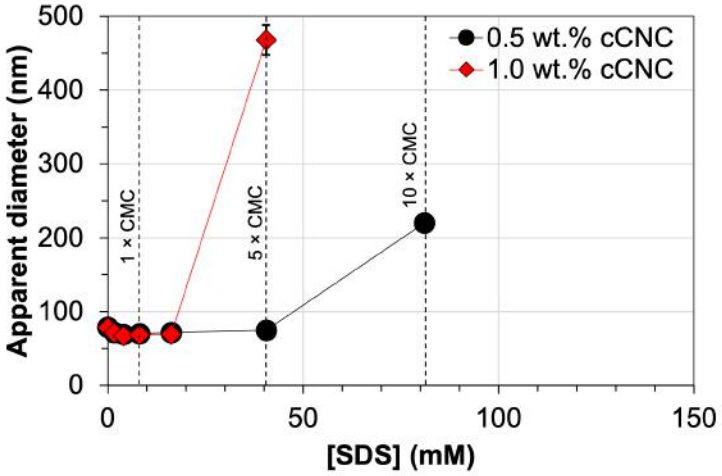

(B)

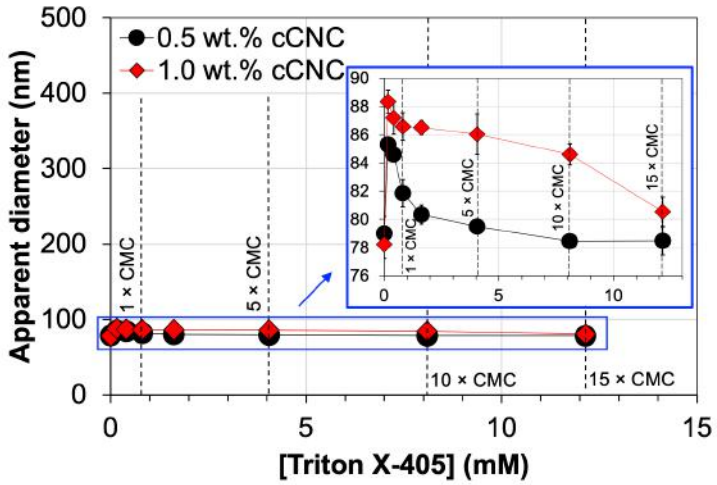

(C)

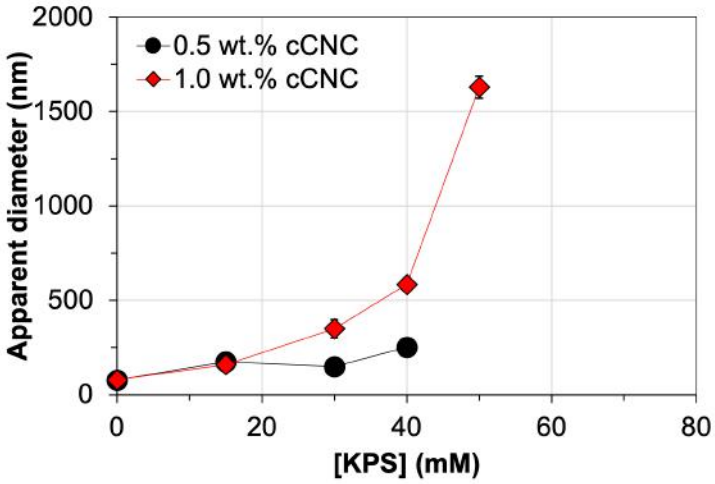

Figure 4.1 Apparent particle diameter (z-average) of cCNCs in suspension vs. concentration of (A) SDS, (B) Triton X-405, and (C) KPS. Each point is an average of three measurements and the error bars represent the standard deviation. Lines drawn between points are provided as a guide.

apparent particle diameters above 100 nm, thereby indicating the onset of cCNC aggregation. CNCs can form stable dispersions in water due to their anionic surface charges, which mutually repulse neighbouring particles and keep them in suspension.[18, 52, 53, 59] However, as the ionic strength of the medium is increased, the dispersion stability can be disrupted due to compression of the charged double layer near the CNC surface (SDS, in addition to being a surfactant, is also a salt). With increasing SDS concentration, the inherent negative charges that stabilized the cCNCs were no longer sufficient to prevent particle aggregation and thus, some aggregation occurred.

In contrast to the SDS case, the apparent diameter of the cCNCs barely changed with the addition of Triton X-405. The apparent diameter of cCNC dispersions with Triton X-405 initially increased by 6-8 nm, and then decreased gradually as the surfactant reached its CMC (Figure 4.1B). Once at the CMC (0.86 mM),[57] the apparent diameter returned to its original value (~80 nm). Due to the ease of sample preparation and quality of the particle diameter readings, non-ionic surfactants were deemed suitable stabilizers for cCNCs as they did not negatively interact with the cCNCs.

For the CTAB-cCNC dispersions, the apparent diameter of the oppositely charged cCNC-surfactant combinations was expected to increase due to surfactant binding. However, the apparent particle size of cCNC samples in the presence of CTAB could not be measured via DLS when adding even as little as 0.2 mM due to sample cloudiness and/or precipitation. These observations are explained by the cCNC surface charge neutralization that the CTAB induced, and by the hydrophilization of the cCNC surface with the increase in CTAB loading. More specifically, as the CTAB (or more precisely, CTA+) concentration increased, the cationic surfactant heads neutralized the carboxylic ions. Then, other CTA+ heads interacted with the hydrophobic tails of the already adsorbed surfactant molecules chain-wise until the nanoparticles became hydrophobic and precipitated.[60–62] These strong surface interactions ultimately led to poor dispersions, and thus, measurements via DLS were not possible. We concluded that CTAB was not a suitable surfactant for formulations containing cCNCs.

Similar to SDS-cCNC interactions, the addition of KPS increased the apparent cCNC diameter due to the increase in ionic strength of the solution (Figure 4.1C). At KPS concentrations of ~30 mM for both cCNC loadings, the apparent cCNC diameters increased, but the dispersion

remained stable enough to obtain adequate DLS readings. However, beyond 40 and 50 mM KPS in cCNC dispersions of 1.0 wt.% and 0.5 wt.%, respectively, reliable readings could not be obtained due to aggregation made evident by sample cloudiness. Thus, KPS and cCNCs were deemed to be compatible at low concentrations, approximately 30 and 40 mM for 0.5 wt.% and 1.0 wt.% cCNC dispersions, respectively. Beyond that point, similar to the SDS-cCNC case, the ionic strength of the medium became high enough to destabilize the dispersions.

Zeta-potential values were measured and plotted against surfactant and initiator concentrations to uncover any trends in surface charge (Figure 4.2). As an approximate guideline, a zeta-potential greater than |10 mV| can be sufficient to maintain adequate electrostatic repulsion, and thus latex stability.[63]

With the addition of up to five times the CMC of SDS (i.e., ~40.5 mM SDS), the magnitude of the zeta-potential of the cCNC dispersions remained statistically unchanged (Figure 4.2A). At higher concentrations (i.e., 10 and 15 times the CMC), the magnitude of the negative charge increased slightly, indicating some additional electrostatic repulsion. For the Triton X-405 case, the magnitude of the zeta-potential of the cCNC dispersions decreased steadily, from about -50 to -30 mV (Figure 4.2B). This decrease could be explained by the increase in Triton X-405 concentration; with the addition of neutral charges, the surface charge density, and therefore the surface electrostatic potential, decreased in magnitude.

For the CTAB (cationic) dispersions with cCNC, as the CTAB concentration reached its CMC (0.89 mM),[58] the magnitude of the zeta-potential increased from about -50 to -75 mV (Figure 4.2C). Once the concentration increased beyond the CMC, the zeta-potential moved sharply in the opposing direction, passing into the positive zeta-potential region. The initial decrease in zeta-potential is due to CTAB's behaviour at a solid-liquid interface above and below the CMC. The CTA+ head groups of the CTAB adsorb via electrostatic interaction to the cCNCs' negative surface carboxyl groups. At low CTAB concentrations (e.g., below the CMC), adsorption remained low despite the presence of a relatively high amount of available negative charges because at the onset of adsorption, CTAB's hydrocarbon tails lie flat on the cCNCs and reduce their contact area with water to minimize their interfacial energy.[64] Thus, at low concentrations, a relatively high cCNC surface area was occupied by CTAB, which initially hindered adsorption of additional CTAB

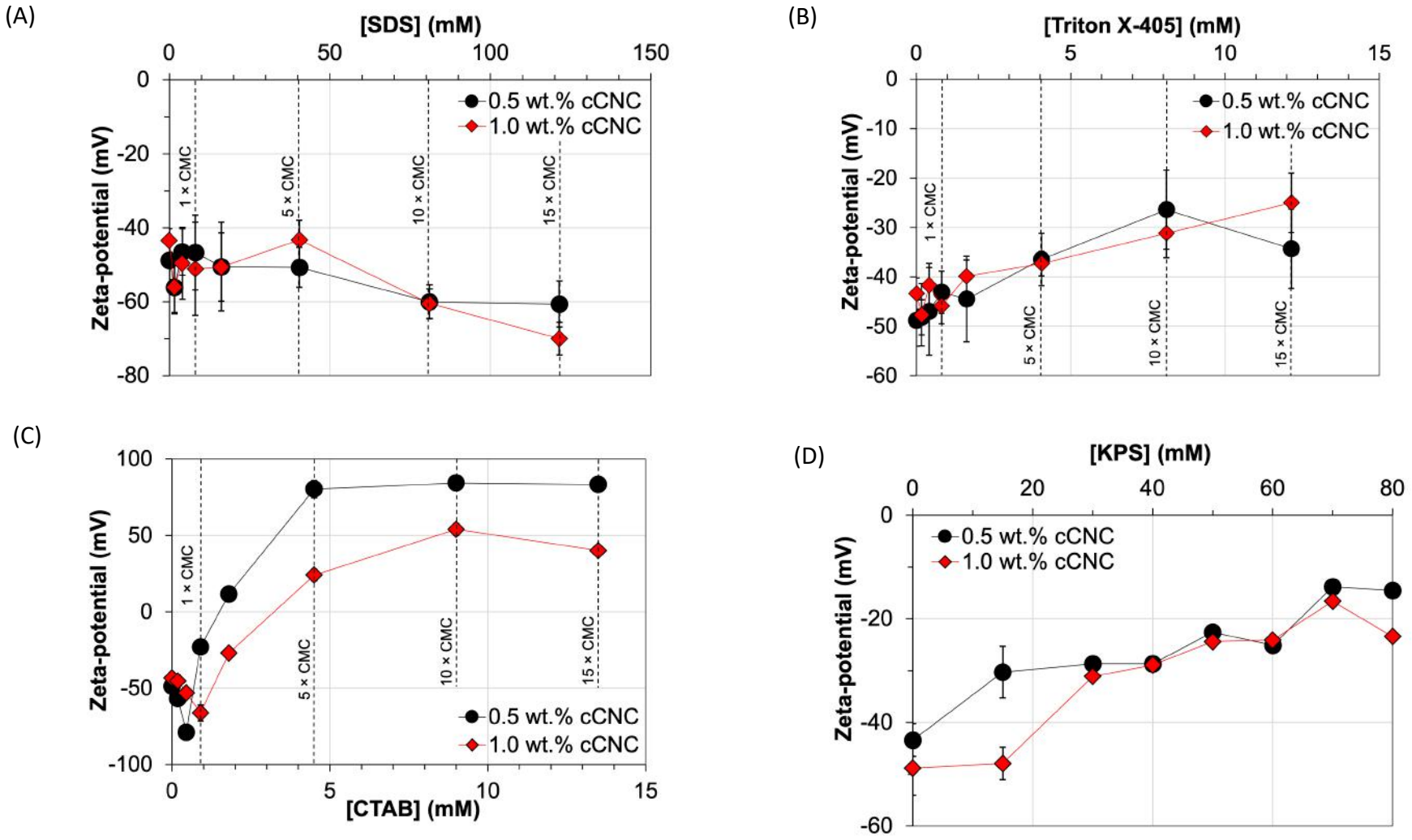

Figure 4.2 Zeta-potential of cCNCs dispersions vs. concentration of (A) SDS, (B) Triton X-405, (C) CTAB, and (D) KPS. Each point is an average of three measurements and the error bars represent the standard deviation. Lines drawn between points are provided as a guide.

molecules – it was in this region (between 0 to 1 mM CTAB, Figure 4.2C) that the zeta-potential decreased slightly despite the addition of a cationic surfactant. Subsequently, as the CTAB concentration increased, the hydrocarbons' orientation changed from a flat to a perpendicular orientation.[64] Thus, above the CMC, the anionic surface charges on the cCNCs were neutralized by the cationic surfactant heads due to the high electrostatic attraction of the positive CTAB and negative cCNC charges. After passing through zero, the zeta-potential continued to grow in the positive range due to surfactant aggregation on the cCNC surfaces. This conforms to previous reports in the literature[24, 55, 65] and suggests that the cationic surfactant bound ionically to the cCNC surface groups. The electrostatic attraction and surfactant aggregation to the cCNC provided additional evidence that CTAB was not a suitable surfactant choice when using cCNCs.

The addition of KPS led to an overall increase in zeta-potential (Figure 4.2D). Specifically, the magnitude of the negative zeta-potential decreased with higher KPS loadings. Unlike SDS, which forms a monovalent ion in solution and has a hydrophobic moiety, KPS forms divalent ions, which dissociate completely in solution and do not form micelles past a critical concentration. The increase in zeta-potential with high KPS loadings was likely due to a compression of the electrical double layer on the particles, which reduced their overall surface charge density. Although no precipitates were visible, the cCNC-KPS samples ranged from cloudy to opaque. Furthermore, when the samples were re-examined after 24 h, a white rim had formed at the liquid-air interface. These observations suggest that the cCNCs and KPS aggregated and came out of solution, thereby lowering the magnitude of the zeta-potential of the KPS-cCNC solution. A summary of the experimental findings from the cCNC – surfactant and cCNC – initiator study (i.e., the concentration thresholds of each of the surfactants and initiator relative to the cCNC dispersions) is presented in Table 4.4. Although the concentration recommendations of Table 4.4 are useful for troubleshooting, one needs to consider that the cCNCs in an EP interact with all ions present in the medium. In other words, the total electrolyte concentration, or ionic strength of the medium as a whole, should be considered when confronting stability issues. We address this in the next section.

Table 4.4 Maximum recommended concentrations of SDS, Triton X-405, CTAB, and KPS in 0.5 wt.% and 1.0 wt.% cCNC dispersions.

cCNC dispersion (wt.%)	Maximum recommended concentrations (mM)			
	SDS	Triton X-405	CTAB	KPS
0.5	< 80 (<~10 × CMC)	>13 (>15 × CMC)	Not compatible	< ~30
1.0	< 30 (<~4 × CMC)	>13 (>15 × CMC)	Not compatible	<~18

4.4.3 Ionic strength of the medium

The ionic strength, I, of an aqueous phase can be calculated as follows:

$$I = \frac{1}{2} * \sum_{i=1}^{n} C_i * z_i^2 \qquad \text{(Eq 4.1)}$$

where i represents the ion in solution, n is the number of ionic species in the mixture, C is the electrolyte concentration in g/mol, and z is the valence of the ion. As such, the ionic strength of the last stable sample taken from EPs before they coagulated in the preliminary experiments was calculated and plotted against cCNC concentration (Figure 4.3; referred to as 'Metastable latex samples') along with the stable SDS-cCNC and KPS-cCNC dispersions. In addition to these data, we derived an empirical model based on the lowest ionic strength of the metastable latex samples and added it to Figure 4.3 as a guide to represent an *approximate* ionic strength threshold below which a stable latex could exist. The empirical model was:

$$[I] = -3.2[cCNC] + 65 \qquad \text{(Eq 4.2)}$$

where $[I]$ is the maximum recommended ionic strength, and $[cCNC]$ is the concentration of cCNCs in the aqueous phase of the formulation. As the cCNC concentration increased, the Na+ counterion concentration and carboxyl content likewise increased, which intrinsically increased the ionic strength of the water phase. It is for this reason that the ionic strength threshold decreased with increasing cCNC concentration. Thus, to reduce the ionic strength of the latex below the threshold line in Figure 4.3, we modified the formulation by reducing and/or replacing the components contributing to the ionic strength, as discussed in the next section.

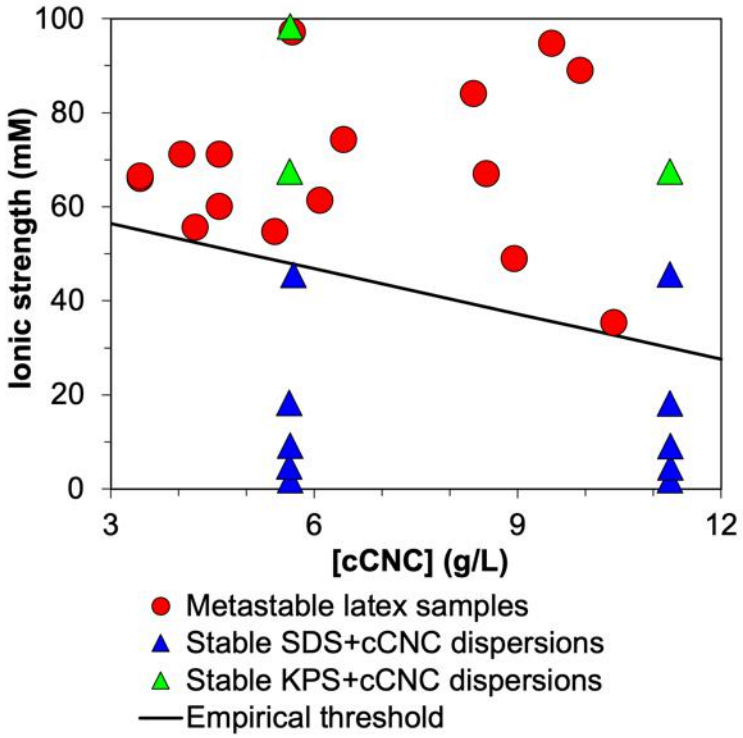

Figure 4.3 Ionic strength versus cCNC concentration of metastable latex samples (i.e., the last stable sample of a latex, which eventually coagulated) as well as the ionic strength of stable SDS-cCNC and KPS-cCNC dispersions. The model represents a recommended ionic strength limit, below which a stable latex could exist.

4.4.4 "Modified" experimental approach

In order to reduce the ionic strength of the latex below the threshold line in Figure 4.3 (Eq 4.2), a "modified" formulation was developed in which the aqueous phase was free of added ions from the initiator or surfactant: the initiator (KPS) and surfactant (SDS) were replaced with AIBN and Triton X-405, respectively (Table 4.2). Despite being able to carry out the EP to completion, the polymerizations did not follow expected conversion trajectories and presented challenges in controlling particle size. Results for a typical run are shown in Figure 4.4.

In a classical semi-batch EP, the conversion at the end of the seed stage should be high (>80%),[5] whereas the seed produced with Triton X-405 and AIBN only reached 30% conversion (t = 0 min, Figure 4.4A) even for cases when the seeding time was extended beyond the usual 30 min. Additional AIBN was added to the seed stage in an attempt to increase conversion, but this resulted in polymer coagulum on the impeller. EP reaction kinetics are correlated with the partitioning of the non-ionic surfactant between the oil and aqueous phase and it is known that

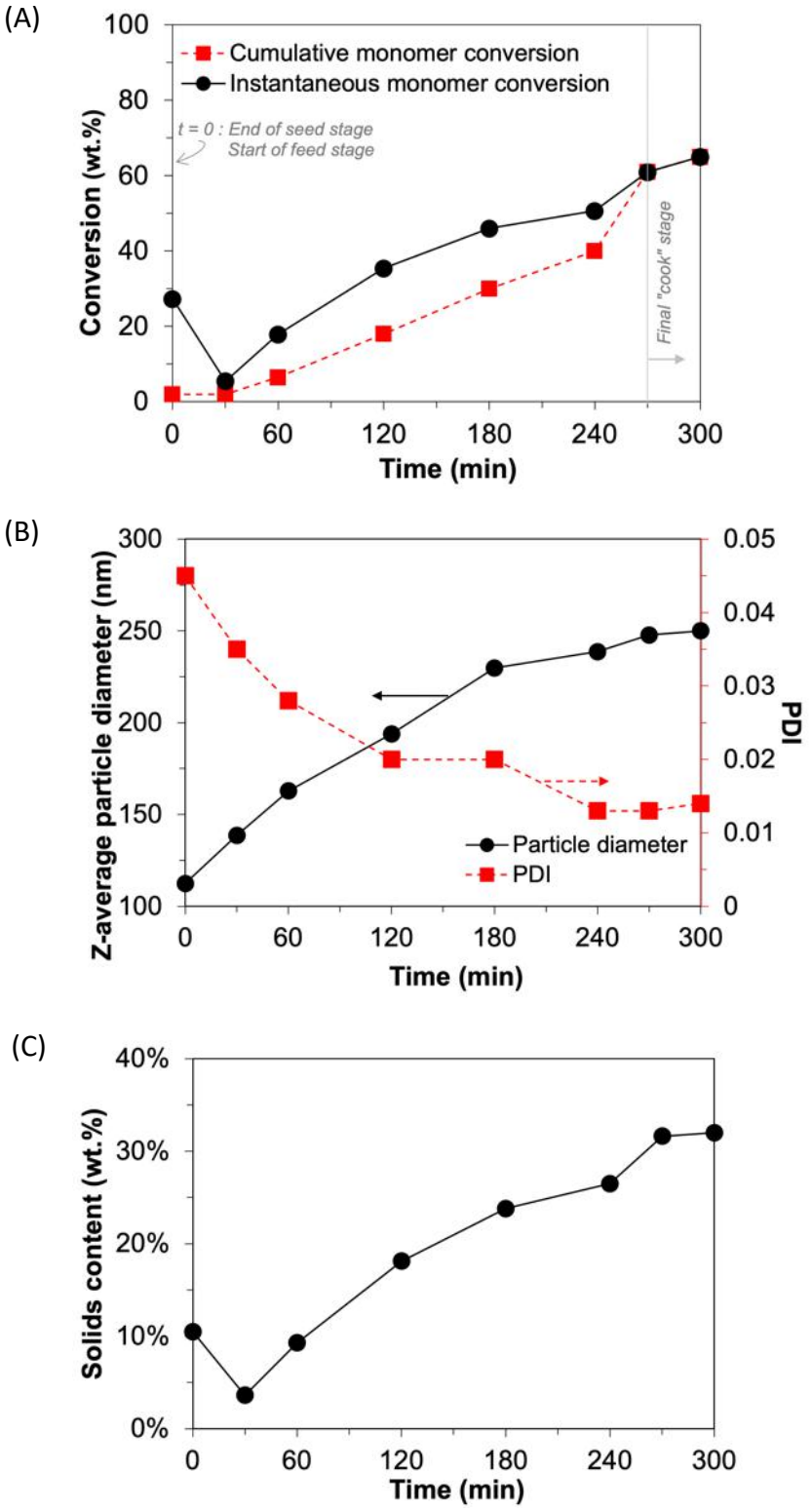

Figure 4.4 (A) Conversion vs. time, (B) z-average particle diameter vs. time, and (C) solids content vs. time for a 40 wt.% solids latex with 1.0 phm cCNCs using AIBN as initiator and Triton X-405 as surfactant. See Table 4.2 for formulation and polymerization details.

surfactant partitioning depends on both the surfactant concentration and its interactions with other ionic components in the mixture.[57, 66–68] Surfactant partitioning can be mitigated by dissolving the surfactant in the water charged to the reactor and then slowly feeding the neat monomer, in contrast to the conventional approach of charging all ingredients simultaneously.[67] In our case, because the reactions were seeded by adding neat monomer to an aqueous surfactant solution (i.e., DDW + Triton X-405), the nucleation mechanism was likely micellar. Nonetheless, the reaction rates throughout the experiments were low compared to experiments conducted using SDS and KPS.

Another distinguishing factor for the "modified" latexes was that the seed particles were large relative to seed particles obtained from the "classical" formulations stabilized with an anionic surfactant; typical "classical" experiments yielded seed particles in the 60 to 80 nm range.[38, 42, 43] However, the seed particles obtained using the "modified" formulation were over 110 nm (Figure 4.4B). Generally, latexes produced with non-ionic surfactants will produce particles as much as an order of magnitude larger than latexes stabilized with ionic surfactants (at the same concentration relative to the CMC), due to the nature of the particle stabilization mechanism.[68–71] Although particle diameters in that range are not inherently problematic, latex particle size does impact film formation and ultimately, performance properties. In order to eliminate the effects of particle size on film formation, the initial and final latex particle sizes should be controlled and maintained from latex to latex,[38, 72] which proved difficult to do with Triton X-405 in the current study. Lastly, the final conversion was below 70% (Figure 4.4A) and the solids content only reached 32% (Figure 4.4C). Any increase in AIBN concentration led to the accumulation of polymer gel on the impeller, suggesting monomer droplet nucleation. Thus, further addition of initiator to boost conversion was avoided. The next challenge was to simultaneously increase monomer conversion, control the initial and final particle diameters, and maintain the ionic strength of the reaction mixture below the threshold (Figure 4.3).

4.4.5 "Hybrid" experimental approach

Because the cCNC dispersion did remain stable under a range of ionic strengths, it was decided to produce a "classical" seed using SDS and KPS (Table 4.1) and to continue the particle growth in the feed stage with the "modified" formulation using Triton X-405 and AIBN (Table

4.2). This approach was inspired by the common industrial practice to use mixed surfactant systems; although this is typically added as a mixture throughout the polymerization. This so-called “hybrid” formulation (Table 4.3) was preferred because: 1- water-soluble initiators are generally favoured for EP seeding reactions, and 2- using Triton X-405 as surfactant ensures that the growing particles remain colloidally stable without increasing the ionic strength of the reaction mixture. Thus, the proposed “hybrid” formulation enabled better control of the particle size and kept the reaction mixture in an acceptable ionic strength range. With the “hybrid” formulation, the final latex conversion and solids content were improved to 89% and 35%, respectively (Figure 4.5A and 4.5C). The initial (76 ± 3 nm) and final (163 ± 5 nm) particle sizes were consistent between experiments and the latexes could be cast to form continuous films for adhesive applications. The latex viscosity of a 40 wt.% solids latex with 1.0 phm cCNC loading was 167 mPa·s, which is significantly lower than latexes produced with other CNCs at the same solids content and CNC loading.[38, 42]

Non-ionic/ionic surfactant mixtures have been utilized in the past and studies addressing SDS-Triton X-405 combinations reveal that the synergistic effects of the combined surfactants render the overall CMC hard to predict.[68–70] The observed CMC of surfactant mixtures has been reported to be non-additive because of the interactions between different molecules in micelle formation.[71] This ultimately leads to difficulties in controlling particle size, predicting particle stability and determining whether the nucleation mechanism is micellar, coagulative, or a combination of the two. In our “hybrid” formulation, because the seeding stage contained only SDS (ionic surfactant) and KPS (water-soluble initiator), the nucleation mechanism was undoubtedly micellar. This ensured that stability issues could be avoided in the early, more critical stages of the polymerization. Continuing the reaction with Triton X-405 (nonionic surfactant) and AIBN (monomer-soluble initiator) proved to be effective. Monomer droplet nucleation and/or secondary nucleation is possible when using oil-soluble initiators in EPs.[5, 73] In our case, there was an accumulation of polymer gel on the impeller suggesting that some monomer droplet nucleation did occur. Because we could not achieve a solids content higher than 35 wt.% (recall our 40 wt.% target), we estimated that 5 wt.%, i.e., roughly 13% of the total monomer weight, was subject to monomer droplet nucleation. Nevertheless, the monomodal

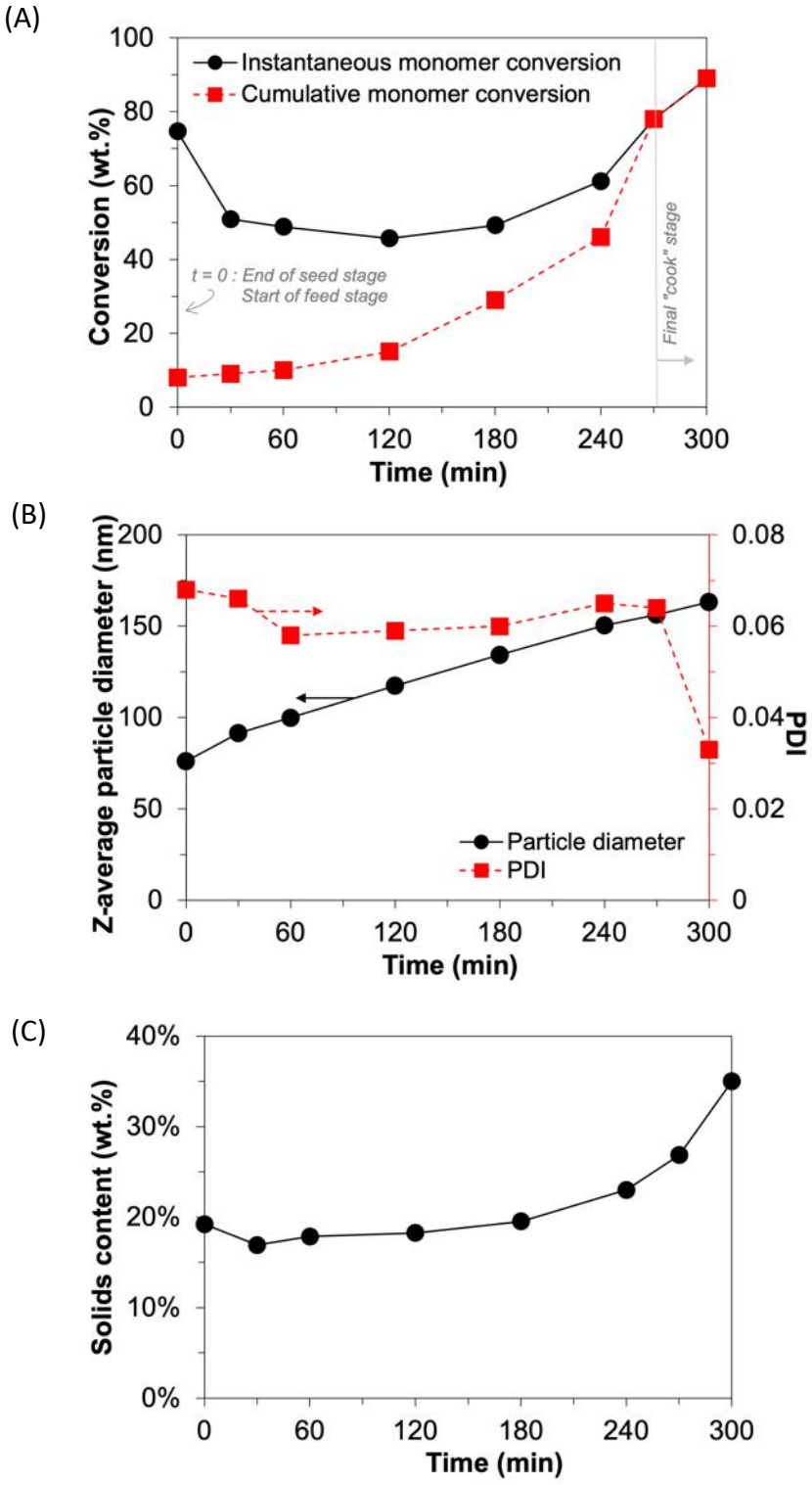

Figure 4.5 (A) Conversion vs. time, (B) z-average particle diameter vs. time, and (C) solids content vs. time for a 40 wt.% solids latex with 1.0 phm cCNCs using SDS (surfactant) and KPS (initiator) in the seed, and Triton X-405 (surfactant) and AIBN (initiator) in the feed as surfactant. See Table 4.3 for formulation and polymerization details.

PSD obtained via DLS and the low PDI (Figure 4.5B) suggested that any nucleated monomer droplets were completely separate from the latex and thus, the final latex was of good quality and could be fully characterized.

4.5 Conclusion

The path towards more sustainable polymer reaction engineering is facilitated with the use of EP. This water-based approach provides several economic and technical advantages while also yielding environmental benefit – the displacement of organic solvents from the polymerization process. In so doing, however, product performance is necessarily altered to achieve the same polymer properties. One such approach is the use of nanomaterials to prepare nanocomposites. Health and safety concerns normally associated to nanomaterials are greatly reduced when using cellulose-based materials such as CNCs.

We have shown that in an *in situ* EP, the cCNC dispersion can be destabilized by the high ionic strength of the aqueous phase. After a careful study of the interactions between cCNCs and the various EP components, alternative approaches in terms of formulation and component partitioning during the semi-batch addition were developed and tested. Ultimately, to facilitate the addition of cCNCs *in situ*, a novel "hybrid" semi-batch EP method was used in which a "classical" seed was formed (using KPS and SDS), followed by the addition of a "modified" feed solution (using Triton X-405 and AIBN) containing the cCNC dispersion. With this creative polymerization method, cCNCs were incorporated into latex formulations *in situ* as a green alternative to petroleum-based property modifiers for performance improvements.

4.6 Acknowledgements

The authors thank Anomera Inc. (Montreal, QC) for providing the DextraCel™ (i.e., cCNCs, carboxylated CNCs), and also to Dr. Amir Khabibullin, Dr. Timothy Morse, Dr. Nathan Hordy and Dr. Zhen (Justin) Hu from Anomera Inc., for beneficial discussions. The authors thank Prof. Emily D. Cranston for her helpful input. This work was funded through the MITACS Accelerate program. V.A.G is a recipient of a NSERC CGS-D Scholarship. Prof. Dubé is grateful for the co-supervision of Prof. O'Driscoll (along with Prof. Penlidis) during his MASc thesis, back in 1987-89.

4.7 References

[1] Y. Zhang and M. A. Dubé, "Green Emulsion Polymerization Technology," in *Advances in Polymer Science*, vol. 280, 2017, pp. 65–100. doi: 10.1007/12_2017_8.

[2] M. A. Dubé, V. A. Gabriel, A. S. Pakdel, and Y. Zhang, "Sustainable polymer reaction engineering: Are we there yet?," *The Canadian Journal of Chemical Engineering*, vol. 99, no. 1, pp. 31–60, Jan. 2021, doi: 10.1002/cjce.23865.

[3] M. A. Dubé and S. Salehpour, "Applying the Principles of Green Chemistry to Polymer Production Technology," *Macromolecular Reaction Engineering*, vol. 8, no. 1, pp. 7–28, Jan. 2014, doi: 10.1002/mren.201300103.

[4] J. M. Asua, "Emulsion polymerization: From fundamental mechanisms to process developments," *Journal of Polymer Science Part A: Polymer Chemistry*, vol. 42, no. 5, pp. 1025–1041, Mar. 2004, doi: 10.1002/pola.11096.

[5] P. A. Lovell and M. S. El-Aasser, Eds., *Emulsion Polymerization and Emulsion Polymers*. Chichester: John Wiley and Sons, 1981.

[6] N. M. B. Smeets, S. Imbrogno, and S. Bloembergen, "Carbohydrate functionalized hybrid latex particles," *Carbohydrate Polymers*, vol. 173, pp. 233–252, Oct. 2017, doi: 10.1016/j.carbpol.2017.05.075.

[7] M. Khalina, M. Sanei, H. S. Mobarakeh, and A. R. Mahdavian, "Preparation of acrylic/silica nanocomposites latexes with potential application in pressure sensitive adhesive," *International Journal of Adhesion and Adhesives*, vol. 58, pp. 21–27, Apr. 2015, doi: 10.1016/j.ijadhadh.2014.12.007.

[8] A. Romo-Uribe, "Dynamics and viscoelastic behavior of waterborne acrylic polymer/silica nanocomposite coatings," *Progress in Organic Coatings*, vol. 129, no. January, pp. 125–132, Apr. 2019, doi: 10.1016/j.porgcoat.2019.01.017.

[9] P. K. Rana, S. K. Swain, and P. K. Sahoo, "Synthesis, characterization, and properties of intercalated poly(2-ethyl hexylacrylate)/silicate nanocomposites: XRD, TEM, IR, TGA, superabsorbency, pressure-sensitive adhesion, and biodegradation," *Journal of Applied Polymer Science*, vol. 93, no. 3, pp. 1007–1011, 2004, doi: 10.1002/app.20568.

[10] Y. Yamamoto, S. Fujii, K. Shitajima, K. Fujiwara, S. Hikasa, and Y. Nakamura, "Soft polymer-silica nanocomposite particles as filler for pressure-sensitive adhesives," *Polymer*, vol. 70, pp. 77–87, Jul. 2015, doi: 10.1016/j.polymer.2015.06.006.

[11] J. Kajtna and U. Šebenik, "Microsphere pressure sensitive adhesives—acrylic polymer/montmorillonite clay nanocomposite materials," *International Journal of Adhesion and Adhesives*, vol. 29, no. 5, pp. 543–550, Jul. 2009, doi: 10.1016/j.ijadhadh.2009.01.001.

[12] S. Patel, A. Bandyopadhyay, A. Ganguly, and A. K. Bhowmick, "Synthesis and properties of nanocomposite adhesives," *Journal of Adhesion Science and Technology*, vol. 20, no. 4, pp. 371–385, Jan. 2006, doi: 10.1163/156856106776381794.

[13] T. Wang *et al.*, "Waterborne, Nanocomposite Pressure-Sensitive Adhesives with High Tack Energy, Optical Transparency, and Electrical Conductivity," *Advanced Materials*, vol. 18, no. 20, pp. 2730–2734, Oct. 2006, doi: 10.1002/adma.200601335.

[14] B. Sydulu Singu, P. Srinivasan, and K. R. Yoon, "Emulsion polymerization method for polyaniline-multiwalled carbon nanotube nanocomposites as supercapacitor materials," *Journal of Solid State Electrochemistry*, vol. 20, no. 12, pp. 3447–3457, Dec. 2016, doi: 10.1007/s10008-016-3309-1.

[15] H.-X. Wu, X.-Q. Qiu, W.-M. Cao, Y.-H. Lin, R.-F. Cai, and S.-X. Qian, "Polymer-wrapped multiwalled carbon nanotubes synthesized via microwave-assisted in situ emulsion polymerization and their optical limiting properties," *Carbon N Y*, vol. 45, no. 15, pp. 2866–2872, Dec. 2007, doi: 10.1016/j.carbon.2007.10.009.

[16] M. U. Khan, K. R. Reddy, T. Snguanwongchai, E. Haque, and V. G. Gomes, "Polymer brush synthesis on surface modified carbon nanotubes via in situ emulsion polymerization," *Colloid and Polymer Science*, vol. 294, no. 10, pp. 1599–1610, Oct. 2016, doi: 10.1007/s00396-016-3922-7.

[17] C. Bruel, S. Queffeulou, P. J. Carreau, J. R. Tavares, and M. C. Heuzey, "Orienting Cellulose Nanocrystal Functionalities Tunes the Wettability of Water-Cast Films," *Langmuir*, vol. 36, no. 41, pp. 12179–12189, 2020, doi: 10.1021/acs.langmuir.0c01799.

[18] S. A. Kedzior, V. A. Gabriel, M. A. Dubé, and E. D. Cranston, "Nanocellulose in Emulsions and Heterogeneous Water-Based Polymer Systems: A Review," *Advanced Materials*. Wiley-VCH Verlag, 2020. doi: 10.1002/adma.202002404.

[19] H. Sadeghifar, I. Filpponen, S. P. Clarke, D. F. Brougham, and D. S. Argyropoulos, "Production of cellulose nanocrystals using hydrobromic acid and click reactions on their surface," *Journal of Materials Science*, vol. 46, no. 22, pp. 7344–7355, Nov. 2011, doi: 10.1007/s10853-011-5696-0.

[20] S. Camarero Espinosa, T. Kuhnt, E. J. Foster, and C. Weder, "Isolation of Thermally Stable Cellulose Nanocrystals by Phosphoric Acid Hydrolysis," *Biomacromolecules*, vol. 14, no. 4, pp. 1223–1230, Apr. 2013, doi: 10.1021/bm400219u.

[21] O. M. Vanderfleet *et al.*, "Insight into thermal stability of cellulose nanocrystals from new hydrolysis methods with acid blends," *Cellulose*, vol. 26, no. 1, pp. 507–528, Jan. 2019, doi: 10.1007/s10570-018-2175-7.

[22] H.-Y. Yu, D.-Z. Zhang, F.-F. Lu, and J. Yao, "New Approach for Single-Step Extraction of Carboxylated Cellulose Nanocrystals for Their Use As Adsorbents and Flocculants," *ACS Sustainable Chemistry & Engineering*, vol. 4, no. 5, pp. 2632–2643, May 2016, doi: 10.1021/acssuschemeng.6b00126.

[23] E. J. Foster *et al.*, "Current characterization methods for cellulose nanomaterials," *Chemical Society Reviews*, vol. 47, no. 8, pp. 2609–2679, 2018, doi: 10.1039/C6CS00895J.

[24] R. S. Reiner and A. W. Rudie, "Process Scale-Up of Cellulose Nanocrystal Production to 25 kg per Batch at the Forest Products Laboratory," in *Production and Applications of Cellulose Nanomaterials*, no. June 2013, M. T. Postek, R. J. Moon, A. W. Rudie, and M. A. Bilodeau, Eds. Peachtree Corners: TAPPI Press, 2014, pp. 21–24.

[25] S. Beck, J. Bouchard, and R. Berry, "Dispersibility in Water of Dried Nanocrystalline Cellulose," *Biomacromolecules*, vol. 13, no. 5, pp. 1486–1494, May 2012, doi: 10.1021/bm300191k.

[26] S. Beck, M. Méthot, and J. Bouchard, "General procedure for determining cellulose nanocrystal sulfate half-ester content by conductometric titration," *Cellulose*, vol. 22, no. 1, pp. 101–116, Feb. 2015, doi: 10.1007/s10570-014-0513-y.

[27] L. Zhong, S. Fu, X. Peng, H. Zhan, and R. Sun, "Colloidal stability of negatively charged cellulose nanocrystalline in aqueous systems," *Carbohydrate Polymers*, vol. 90, no. 1, pp. 644–649, Sep. 2012, doi: 10.1016/j.carbpol.2012.05.091.

[28] J. Araki, "Electrostatic or steric? – preparations and characterizations of well-dispersed systems containing rod-like nanowhiskers of crystalline polysaccharides," *Soft Matter*, vol. 9, no. 16, p. 4125, 2013, doi: 10.1039/c3sm27514k.

[29] V. Favier, H. Chanzy, and J. Y. Cavaillé, "Polymer Nanocomposites Reinforced by Cellulose Whiskers," *Macromolecules*, vol. 28, no. 18, pp. 6365–6367, Aug. 1995, doi: 10.1021/ma00122a053.

[30] S. Phomrak and M. Phisalaphong, "Reinforcement of Natural Rubber with Bacterial Cellulose via a Latex Aqueous Microdispersion Process," *Journal of Nanomaterials*, vol. 2017, pp. 1–9, 2017, doi: 10.1155/2017/4739793.

[31] M. A. Saïd Azizi Samir, F. Alloin, M. Paillet, and A. Dufresne, "Tangling Effect in Fibrillated Cellulose Reinforced Nanocomposites," *Macromolecules*, vol. 37, no. 11, pp. 4313–4316, Jun. 2004, doi: 10.1021/ma035939u.

[32] P. M. Visakh, S. Thomas, K. Oksman, and A. P. Mathew, "Crosslinked natural rubber nanocomposites reinforced with cellulose whiskers isolated from bamboo waste: Processing and mechanical/thermal properties," *Composites Part A: Applied Science and Manufacturing*, vol. 43, no. 4, pp. 735–741, Apr. 2012, doi: 10.1016/j.compositesa.2011.12.015.

[33] V. Favier, G. R. Canova, J. Y. Cavaille, H. Chanzy, A. Dufresne, and C. Gauthie, "Nanocomposite Materials from Latex and Cellulose Whiskers," *Polymers for Advanced Technologies*, vol. 6, pp. 351–355, 1995.

[34] P. Hajji, J. Y. Cavaillé, V. Favier, C. Gauthier, and G. Vigier, "Tensile Behavior of Nanocomposites From Latex and Cellulose Whiskers," *Polymer Composites*, vol. 7, no. 4, pp. 612–619, 1996.

[35] W. Helbert, J. Y. Cavaillé, A. Dufresne, and U. J. Fourier, "Straw Cellulose Whiskers . Part I : Processing and mechanical behavior," *Polymer Composites*, vol. 17, no. 4, pp. 604–611, 1996.

[36] M. Roohani, Y. Habibi, N. M. Belgacem, G. Ebrahim, A. N. Karimi, and A. Dufresne, "Cellulose whiskers reinforced polyvinyl alcohol copolymers nanocomposites," *European Polymer Journal*, vol. 44, no. 8, pp. 2489–2498, Aug. 2008, doi: 10.1016/j.eurpolymj.2008.05.024.

[37] X. Cao, H. Dong, and C. M. Li, "New Nanocomposite Materials Reinforced with Flax Cellulose Nanocrystals in Waterborne Polyurethane," *Biomacromolecules*, vol. 8, no. 3, pp. 899–904, Mar. 2007, doi: 10.1021/bm0610368.

[38] V. A. Gabriel, E. D. Cranston, and M. A. Dubé, "Pushing the Limits with Cellulose Nanocrystal Loadings in Latex-Based Pressure-Sensitive Adhesive Nanocomposites," *Macromolecular Reaction Engineering*, vol. 14, no. 6, p. 2000027, Dec. 2020, doi: 10.1002/mren.202000027.

[39] Z. Dastjerdi, E. D. Cranston, and M. A. Dubé, "Synthesis of Poly(n -butyl acrylate/methyl methacrylate)/CNC Latex Nanocomposites via In Situ Emulsion Polymerization," *Macromolecular Reaction Engineering*, vol. 11, no. 6, p. 1700013, Dec. 2017, doi: 10.1002/mren.201700013.

[40] Z. Dastjerdi, E. D. Cranston, and M. A. Dubé, "Pressure sensitive adhesive property modification using cellulose nanocrystals," *International Journal of Adhesion and Adhesives*, vol. 81, pp. 36–42, Mar. 2018, doi: 10.1016/j.ijadhadh.2017.11.009.

[41] A. Ouzas, E. Niinivaara, E. D. Cranston, and M. A. Dubé, "Synthesis of poly(isobutyl acrylate/n-butyl acrylate/methyl methacrylate)/CNC nanocomposites for adhesive applications via in situ semi-batch emulsion polymerization," *Polymer Composites*, vol. 40, no. 4, pp. 1365–1377, Apr. 2019, doi: 10.1002/pc.24869.

[42] A. Ouzas, E. Niinivaara, E. D. Cranston, and M. A. Dubé, "In Situ Semibatch Emulsion Polymerization of 2-Ethyl Hexyl Acrylate/ n -Butyl Acrylate/Methyl Methacrylate/Cellulose Nanocrystal Nanocomposites for Adhesive Applications," *Macromolecular Reaction Engineering*, vol. 12, no. 3, p. 1700068, Jun. 2018, doi: 10.1002/mren.201700068.

[43] A. S. Pakdel, V. Gabriel, R. M. Berry, C. Fraschini, E. D. Cranston, and M. A. Dubé, "A sequential design approach for in situ incorporation of cellulose nanocrystals in emulsion-based pressure sensitive adhesives," *Cellulose*, vol. 27, no. 18, pp. 10837–10853, Dec. 2020, doi: 10.1007/s10570-020-03060-6.

[44] F. Cherhal, F. Cousin, and I. Capron, "Influence of charge density and ionic strength on the aggregation process of cellulose nanocrystals in aqueous suspension, as revealed by small-angle neutron scattering," *Langmuir*, vol. 31, no. 20, pp. 5596–5602, 2015, doi: 10.1021/acs.langmuir.5b00851.

[45] X. M. Dong and D. G. Gray, "Effect of counterions on ordered phase formation in suspensions of charged rodlike cellulose crystallites," *Langmuir*, vol. 13, no. 8, pp. 2404–2409, 1997, doi: 10.1021/la960724h.

[46] Y. Zhang, V. Karimkhani, B. T. Makowski, G. Samaranayake, and S. J. Rowan, "Nanoemulsions and Nanolatexes Stabilized by Hydrophobically Functionalized Cellulose Nanocrystals," *Macromolecules*, vol. 50, no. 16, pp. 6032–6042, Aug. 2017, doi: 10.1021/acs.macromol.7b00982.

[47] A. Werner, V. Schmitt, G. Sèbe, and V. Héroguez, "Synthesis of surfactant-free micro- and nanolatexes from Pickering emulsions stabilized by acetylated cellulose nanocrystals," *Polymer Chemistry*, vol. 8, no. 39, pp. 6064–6072, 2017, doi: 10.1039/C7PY01203A.

[48] M. Errezma, A. Ben Mabrouk, A. Magnin, A. Dufresne, and S. Boufi, "Surfactant-free emulsion Pickering polymerization stabilized by aldehyde-functionalized cellulose nanocrystals," *Carbohydrate Polymers*, vol. 202, pp. 621–630, Dec. 2018, doi: 10.1016/j.carbpol.2018.09.018.

[49] J. Glasing, P. G. Jessop, P. Champagne, W. Y. Hamad, and M. F. Cunningham, "Microsuspension Polymerization of Styrene Using Cellulose Nanocrystals as Pickering Emulsifiers: On the Evolution of Latex Particles," *Langmuir*, vol. 36, no. 3, pp. 796–809, Jan. 2020, doi: 10.1021/acs.langmuir.9b03583.

[50] W. Du, J. Guo, H. Li, and Y. Gao, "Heterogeneously Modified Cellulose Nanocrystals-Stabilized Pickering Emulsion: Preparation and Their Template Application for the Creation of PS Microspheres with Amino-Rich Surfaces," *ACS Sustainable Chemistry & Engineering*, vol. 5, no. 9, pp. 7514–7523, Sep. 2017, doi: 10.1021/acssuschemeng.7b00375.

[51] J. Tang, V. L. Dimonie, E. S. Daniels, A. Klein, and M. S. El-Aasser, "Study of the Drying Behavior of Model Latex Blends during Film Formation: Influence of Carboxyl Groups," *Macromolecular Symposia*, vol. 155, pp. 131–161, 2000.

[52] G. Delepierre, O. M. Vanderfleet, E. Niinivaara, B. Zakani, and E. D. Cranston, "Benchmarking Cellulose Nanocrystals Part II: New Industrially Produced Materials," *Langmuir*, vol. 37, no. 28, pp. 8393–8409, Jul. 2021, doi: 10.1021/acs.langmuir.1c00550.

[53] R. J. Moon, A. Martini, J. Nairn, J. Simonsen, and J. Youngblood, "Cellulose nanomaterials review: structure, properties and nanocomposites," *Chemical Society Reviews*, vol. 40, no. 7, p. 3941, Jun. 2011, doi: 10.1039/c0cs00108b.

[54] J. Brandrup, E. H. Immergut, and E. A. Grulke, *POLYMER HANDBOOK*, Fourth Edi. New York: John Wiley & Sons, Inc., 1999.

[55] S. A. Kedzior, H. S. Marway, and E. D. Cranston, "Tailoring Cellulose Nanocrystal and Surfactant Behavior in Miniemulsion Polymerization," *Macromolecules*, vol. 50, no. 7, pp. 2645–2655, 2017, doi: 10.1021/acs.macromol.7b00516.

[56] Y. Moroi, K. Motomura, and R. Matuura, "The critical micelle concentration of sodium dodecyl sulfate-bivalent metal dodecyl sulfate mixtures in aqueous solutions," *Journal of Colloid And Interface Science*, vol. 46, no. 1, pp. 111–117, 1974, doi: 10.1016/0021-9797(74)90030-7.

[57] E. Özdeğer, E. D. Sudol, M. S. El-Aasser, and A. Klein, "Role of the nonionic surfactant Triton X-405 in emulsion polymerization. II. Homopolymerization of n-butyl acrylate," *Journal of Polymer Science, Part A: Polymer Chemistry*, vol. 35, no. 17, pp. 3827–3835, 1997.

[58] A. Modaressi, H. Sifaoui, B. Grzesiak, R. Solimando, U. Domanska, and M. Rogalski, "CTAB aggregation in aqueous solutions of ammonium based ionic liquids; conductimetric studies," *Colloids and Surfaces A: Physicochemical and Engineering Aspects*, vol. 296, no. 1–3, pp. 104–108, Mar. 2007, doi: 10.1016/j.colsurfa.2006.09.031.

[59] M. S. Reid, M. Villalobos, and E. D. Cranston, "Benchmarking Cellulose Nanocrystals: From the Laboratory to Industrial Production," *Langmuir*, vol. 33, no. 7, pp. 1583–1598, Feb. 2017, doi: 10.1021/acs.langmuir.6b03765.

[60] T. Abitbol, H. Marway, and E. D. Cranston, "Surface Modification of Cellulose Nanocrystals with Cetyltrimethylammonium Bromide," *Nordic Pulp & Paper Research Journal*, vol. 29, no. 1, pp. 46–57, 2014.

[61] S. A. Kedzior, M. A. Dubé, and E. D. Cranston, "Cellulose Nanocrystals and Methyl Cellulose as Costabilizers for Nanocomposite Latexes with Double Morphology," *ACS Sustainable Chemistry & Engineering*, vol. 5, no. 11, pp. 10509–10517, Nov. 2017, doi: 10.1021/acssuschemeng.7b02510.

[62] C. Brinatti, J. Huang, R. M. Berry, K. C. Tam, and W. Loh, "Structural and Energetic Studies on the Interaction of Cationic Surfactants and Cellulose Nanocrystals," *Langmuir*, vol. 32, no. 3, pp. 689–698, Jan. 2016, doi: 10.1021/acs.langmuir.5b03893.

[63] S. Bhattacharjee, "DLS and zeta potential - What they are and what they are not?," *Journal of Controlled Release*, vol. 235, pp. 337–351, 2016, doi: 10.1016/j.jconrel.2016.06.017.

[64] S. Alila, S. Boufi, M. N. Belgacem, and D. Beneventi, "Adsorption of a Cationic Surfactant onto Cellulosic Fibers I. Surface Charge Effects," *Langmuir*, vol. 21, no. 18, pp. 8106–8113, Aug. 2005, doi: 10.1021/la050367n.

[65] D. Klemm *et al.*, "Nanocelluloses: A New Family of Nature-Based Materials," *Angewandte Chemie International Edition*, vol. 50, no. 24, pp. 5438–5466, Jun. 2011, doi: 10.1002/anie.201001273.

[66] E. Özdeğer, E. D. Sudol, M. S. El-Aasser, and A. Klein, "Role of the nonionic surfactant Triton X-405 in emulsion polymerization. I. Homopolymerization of styrene," *Journal of Polymer Science Part A: Polymer Chemistry*, vol. 35, no. 17, pp. 3813–3825, Dec. 1997, doi: 10.1002/(SICI)1099-0518(199712)35:17<3813::AID-POLA20>3.0.CO;2-F.

[67] E. Özdeğer, E. D. Sudol, M. S. El-Aasser, and A. Klein, "Role of the nonionic surfactant Triton X-405 in emulsion polymerization. III. Copolymerization of styrene and n-butyl acrylate," *Journal of Polymer Science Part A: Polymer Chemistry*, vol. 35, no. 17, pp. 3837–3846, Dec. 1997, doi: 10.1002/(SICI)1099-0518(199712)35:17<3837::AID-POLA22>3.3.CO;2-N.

[68] D. Colombié, E. D. Sudol, and M. S. El-Aasser, “Role of mixed anionic-nonionic systems of surfactants in the emulsion polymerization of styrene: Effect on particle nucleation,” *Macromolecules*, vol. 33, no. 20, pp. 7283–7291, 2000, doi: 10.1021/ma9920588.

[69] D. Colombié, K. Landfester, E. D. Sudol, and M. S. El-Aasser, “Competitive Adsorption of the Anionic Surfactant SLS and the Nonionic Surfactant Triton X-405 on Polystyrene Latex Particles,” *Langmuir*, vol. 16, no. 21, pp. 7905–7913, Oct. 2000, doi: 10.1021/la9915825.

[70] D. Colombié, E. D. Sudol, and M. S. El-Aasser, “Effect of a Mixed Anionic−Nonionic System of Surfactants on the Entry and Exit of Free Radicals into Polystyrene Particles,” *Macromolecules*, vol. 33, no. 12, pp. 4347–4353, Jun. 2000, doi: 10.1021/ma9920590.

[71] E. Unzueta and J. Forcada, “Semicontinuous emulsion copolymerization of methyl methacrylate and n-butyl acrylate: 1. Effect of mixed emulsifiers in seeded polymerization,” *Polymer*, vol. 36, no. 5, pp. 1045–1052, 1995.

[72] S. Roberge and M. A. Dubé, “The effect of particle size and composition on the performance of styrene/butyl acrylate miniemulsion-based PSAs,” *Polymer*, vol. 47, no. 3, pp. 799–807, Jan. 2006, doi: 10.1016/j.polymer.2005.12.024.

[73] R. M. Fitch, *Polymer Colloids*. Elsevier, 1997. doi: 10.1016/B978-0-12-257745-1.X5000-7.

Chapter 5

Improving Latex-Based Pressure-Sensitive Adhesive Properties using Carboxylated Cellulose Nanocrystals

Vida A. Gabriel,[1] Mathieu N. Tousignant,[1] Sean M.W. Wilson,[2] Marie D.M. Faure,[1] Emily D. Cranston,[3,4] Michael F. Cunningham,[5] Benoît H. Lessard,[1] Marc A. Dubé[1]

[1]Department of Chemical and Biological Engineering, Centre for Catalysis Research and Innovation, University of Ottawa, Ottawa, Ontario, Canada
[2]TerraFixing Inc., Ottawa, Ontario, Canada
[3]Department of Wood Science, University of British Columbia, British Columbia, Canada
[4]Department of Chemical and Biological Engineering, University of British Columbia, Canada
[5]Department of Chemical Engineering, Queen's University, Kingston, Ontario, Canada

This chapter is a manuscript published in Journal of Macromolecular Reaction Engineering (2022; 2100051)

5.1 Abstract

Cellulose nanocrystals (CNCs) are becoming a popular option when producing polymer nanocomposites because they are a green alternative to petroleum-based performance enhancers and provide significant matrix reinforcement at low loadings. DextraCel™ is a commercial grade CNC with carboxylate surface groups that can be dispersed in water without sonication. These carboxylated CNCs (cCNCs) can be incorporated *in situ* via seeded semi-batch emulsion polymerization to produce latexes for adhesive applications. The resulting nanocomposite films exhibit 26x higher peel strength, 4.5x higher tack, and 7.7x higher shear strength relative to base case films. Curiously, adhesives produced from latexes containing cCNCs that did not undergo ultrasonication display greater adhesive property improvements relative to films produced with cCNCs that were ultrasonicated. Atomic force microscopy images reveal that cCNCs have stronger self interactions than their sulfated CNCs counterparts; cCNCs display side-by-side and end-to-end association in films when they are not ultrasonicated, which increases their "apparent" aspect ratio – an important characteristic attributed to matrix reinforcement. Omitting ultrasonication preserves cCNC-cCNC interactions that cause them to behave like nanofibers rather than discrete nanocrystals; this allows them to display greater mechanical

enhancements, similar to reinforcements provided by nanofibrils, without the technical challenges associated with producing composite latexes with nanofibrils.

Keywords: Pressure-sensitive adhesives, latex, nanocomposites, cellulose nanocrystals, carboxylated cellulose nanocrystals

5.2 Introduction

Pressure-sensitive adhesives (PSAs) are a class of polymeric materials that adhere to surfaces with light contact and can be removed without leaving a residue.[1] The demand for PSAs is mainly driven by the packaging industry and in 2018, the global PSA market was valued at 11.1 billion USD.[2] The polymer industry uses predominantly petroleum-based feedstocks and concerns regarding their impact on the world's climate has provided an impetus for change. Thus, researchers and manufacturers are searching for ways to produce eco-friendly polymeric materials and to produce them in more sustainable ways.[3]

Emulsion polymerization is considered a sustainable polymer production technique because it uses water as a dispersing agent instead of the volatile solvents required in other polymerization methods. As was the case several decades ago in the paint industry, there is a shift towards the development of latex-based PSAs as opposed to solvent-based applications. Furthermore, the heterogeneous nature (i.e., the presence of both an organic and an aqueous phase) in an emulsion polymerization reaction provides opportunities for sustainable polymer production by allowing a broader variety of nanomaterials to be incorporated into a given latex formulation. For instance, cellulosic nanomaterials as polymer property modifiers have been gaining popularity because they are sustainably sourced and renewable. Nanocellulose exhibits unique properties due to its structure and surface chemistry, and its ability to assemble at oil-water interfaces has made it particularly useful in heterogeneous systems, such as emulsion polymerization.[4] Cellulose nanocrystals (CNCs) are the crystalline regions in native lignocellulosic fibers and are typically extracted using acid treatments to produce rod-like (i.e., high aspect ratio) nanoparticles. The acid used during their extraction determines CNC surface chemistry and thus, employing different acids for hydrolysis can yield CNCs with unique property

modifying capabilities.[5] For example, CNCs extracted via sulfuric acid hydrolysis possess sulfate half-ester surface groups and can yield improved tack, peel strength and shear strength in latex-based PSA films.[6–11] CNCs are typically available commercially in a powdered form after being spray-dried, and their straightforward dispersibility in water is key to their effectiveness as polymer property modifiers in latex-based systems.[12]

Anomera Inc. (Montreal, QC) produces CNCs with the trade name DextraCel™. Their technology employs a hydrogen peroxide oxidation method for the isolation of the nanocrystals which result in carboxylate groups on the CNC surface. In previous work, we revealed that carboxylated CNC (cCNC) dispersions can be destabilized in high ionic strength conditions. We developed a non-conventional approach to produce stable latexes with cCNCs: a seeded emulsion polymerization using a water-soluble initiator and an anionic surfactant, followed by a semi-batch feed stage using an organic-soluble initiator and a non-ionic surfactant.[13]

The cCNCs are produced in two forms: a “wet” form (a never-dried 4.5 wt.% suspension in water), and a “dry” form (a spray-dried powder, readily redispersible in water). In this study, we examined both forms and dispersed them in various ways as part of their incorporation *in situ* into semi-batch emulsion polymerizations (i.e., adding the cCNCs during the polymerization) to study their effect on the adhesive performance of PSA films. Specifically, cCNCs loadings of 0.5 or 1.0 wt.% were added to 35 wt.% solid content latexes for adhesive applications. The cCNCs were added in the wet form (as received), in the wet form followed by probe ultrasonication, in the dry form dispersed in water, and in the dry form dispersed in water followed by probe ultrasonication. Furthermore, cCNCs in their wet form were added to pre-synthesized base latexes (i.e., latexes without cCNCs) *ex situ* (i.e., after the polymerization), via cold (23 ^{o}C) and hot (60 ^{o}C) blending to compare the adhesive performance of films produced with cCNCs added to emulsion polymerization latexes *in situ* vs. *ex situ*.

5.3 Experimental

5.3.1 Materials

Butyl acrylate (BA) and methyl methacrylate (MMA) (both <99% purity, stabilized by 20-200 ppm hydroquinone) were purchased from Sigma-Aldrich and purified by passing them

dropwise through an inhibitor removal column. The surfactants, sodium dodecyl sulfate (SDS, ACS Reagent >99%) and Triton X-405 (liquid, Sigma-Aldrich, 70% aqueous concentration), were used as received. Potassium persulfate (KPS, >99%) and 2,2'-azobisisobutyronitrile (AIBN, 98%) initiators were purchased from Sigma-Aldrich and used as received. DextraCel™ (i.e., carboxylated CNCs or cCNCs) was obtained from Anomera Inc. (Montreal, QC) in a "wet" form (4.5 wt.% suspension in water) and in a "dry" form (spray-dried redispersible powder). For both forms, the carboxylate groups on the CNC surface were in the sodium-salt form. The "apparent" cCNC length via DLS was 81 ± 0.4 nm, and the carboxylate group content was 141 ± 10 mmol kg^{-1} cCNC.[14] Atomic force microscopy (AFM) images revealed that the cCNCs were 206 ± 36 nm long and 4.6 ±1.4 nm in cross-section.[15] For comparison, the sulfated CNCs (CelluForce Inc., Windsor, QC) were obtained as a spray-dried powder (dimensions: 183 ± 8 nm long and 6 ± 2 nm in cross section) and had nominal sulfate half-ester surface charge of 250 mmol kg^{-1} CNC.[16] Note that the DLS and AFM protocols are detailed in their respective citations. Distilled deionized water (DDW) with a resistivity of 18.0 ± 0.2 MΩ-cm was used for all reactions and characterization.

5.3.2 cCNC dispersion

The cCNCs were added to the emulsion polymerization formulations in multiple ways to study the effect of the type of CNCs (dry vs. wet form) and its dispersion method on the final latex properties. In each case, 203 g of cCNC suspension was prepared at a concentration of 4.2 or 8.4 g_{cCNC}/L_{water} to make latexes with cCNC loadings of 0.5 or 1.0 parts per hundred parts monomer (phm), respectively. Specifically:

"Wet" cCNC: Wet cCNCs (4.5 wt.% dispersion, as received) were diluted in DDW and mixed with a magnetic stir bar before their addition to the formulation.

"Wet ultrasonicated" cCNCs: Wet cCNCs (4.5 wt.% dispersion, as received) were diluted in DDW, mixed with a magnetic stir bar, then ultrasonicated. Probe ultrasonication was performed in an ice bath using a Fisher Scientific 550 sonic dismembrator at 75% amplitude for three intervals of 5 min, with 5 min rest in between.

"Dry dispersed" cCNCs: Dry cCNCs were added to DDW and mixed vigorously with a magnetic stir bar for an hour, or until there were no more visible aggregates.

"Dry ultrasonicated" cCNCs: Dry cCNCs were dispersed in the same way as the "dry dispersed" method followed by three cycles of probe ultrasonication (described above). Sulfated CNCs were also dispersed in this manner.

5.3.3 Seeded semi-batch emulsion polymerization

BA and MMA were used in a 90:10 wt.% ratio to obtain a latex with a low glass transition temperature (T_g) for adhesive applications (-38 °C). In general, copolymer formulations with a 'hard' monomer (i.e., MMA, polymer T_g = 105 °C)[17] and a 'soft' monomer (i.e., BA, polymer T_g = -54 °C)[17] are used when developing latex formulations for PSA applications.

A Mettler-Toledo 500 mL RC1e glass reactor was used to produce all latexes. The reactor was equipped with a Hastelloy stirrer, two feeding pumps, a thermometer and a nitrogen purge line. Because cCNCs are sensitive to high ionic strengths, a non-conventional emulsion polymerization formulation was employed to form stable latexes in which the surfactant-initiator systems in the seed stage and the feed stage were different. Specifically, a seed was formed using ~10% of the total monomer by mass, SDS surfactant and KPS initiator (both anionic). Then, in the feed stage, to avoid increasing the ionic strength of the aqueous phase, the surfactant and initiator were replaced with Triton X-405 (non-ionic) and AIBN (monomer-soluble), respectively. Details for why a non-conventional formulation was needed and why each surfactant and initiator were selected can be found in previous work.[13] One other conclusion from that work was that the cCNCs should be added during the feed stage. Therefore, the reaction sequence was as follows: water and SDS surfactant were loaded into the reactor, purged with nitrogen, and heated to 60 °C under constant mixing (250 rpm). Seed monomer (~10 wt.% of total monomer) was then added and heated while mixing for 5 min. Via a syringe and needle, a shot of initiator solution containing KPS initiator and DDW was injected to the reactor to commence the seeding reaction, which lasted 30 min. At the onset of the feed stage, the mixing rate was increased to 300 rpm and two separate solutions were fed to the reactor for a total of 270 min. The solutions contained: 1- monomer and AIBN initiator, and 2- DDW, Triton X-405 surfactant, and cCNCs when present. The partitioning of components and their addition sequence are summarised in Table 5.1.

Table 5.1 Formulation and reaction sequence for a 40 wt.% solids latex with 1.0 phm dry cCNCs produced via a seeded semi-batch emulsion polymerization.

	Mixture	Description	Component	Amount (g)
Seed stage	Seed emulsifier	Emulsifier solution mixed at 250 rpm and heated to 60 °C over 25 min. Reactor purged with nitrogen and maintained within 1°C of set temperature and mixing at 250 rpm for the seed stage.	DDW	48.25
			SDS	0.43
	Monomer	Seed monomer (~10 wt% of total monomer) added to heated emulsifier solution and left to mix and heat for 5 min.	BA	15.30
			MMA	1.70
	Seed initiator	Initiator dispersed in DDW injected to reactor to initiate seeding reaction, lasting 30 min.	KPS	0.062
			DDW	2.75
Feed stage	Monomer and initiator	Monomer and initiator are fed to reactor at 0.57 g min^{-1} for 270 min after the completion of the seed stage. Reactor mixing rate increased to 300 rpm for the feed stage.	BA	137.70
			MMA	15.30
			AIBN	0.991
	Feed emulsifier	DDW and surfactant are fed to reactor at 0.77 g min^{-1} for 270 min after the completion of the seed stage. When present, cCNCs added to the feed emulsifier. Reactor mixing rate increased to 300 rpm for the feed stage.	DDW	201.3
			Triton X-405	4.74
			Dry cCNC	1.70
Cook stage		Initiator dispersed in DDW injected to reactor to boost final conversion. Reactor contents left to mix at 60 °C for additional 30 min to ensure conversion of residual monomer.	KPS	0.25
			DDW	2.50

5.3.4 Cold and hot blends

Base latexes (i.e., latexes without any cCNCs) were produced to perform hot and cold blending to examine the effects of adding “wet” cCNCs (as received) *ex situ* versus *in situ*. To ensure the same final solids content between all the latexes, the base latexes produced for the blending experiments were of slightly higher solids content such that the addition of the wet

cCNC dispersion would result in a latex with 35 wt.% solids. To perform the hot blends, wet cCNCs were added to the reactor at the end of the feed stage and mixed at 60 ^{o}C for the duration of the cook stage. For the cold blends, wet cCNCs were added to the latex at room temperature (~23 ^{o}C) and mixed with a magnetic stir bar at 300 rpm for 30 min.

5.3.5 Latex characterization

Latex samples (2 mL total) were taken from the reactor using a syringe at 30- or 60-min intervals for characterization. 0.5 to 0.75 mL of sample was used to measure the instantaneous and cumulative conversions (standard gravimetric methods were used)[10] and the remaining sample was used to measure pH, and particle size distribution (PSD).

A Malvern Zetasizer 2000 was used to measure the particle size and PSD. The average particle size of diluted latex samples (0.1 – 0.2 $g_{latex}\ g_{water}^{-1}$) was also measured via dynamic light scattering (DLS) at an angle of 173^{o} and a temperature of 25^{o}C. Three measurements of 12 to 15 scans were obtained and the average value (an intensity weighted mean diameter value, i.e., z-average) was reported. The polydispersity index (PDI, a measure of the breadth of the PSD) was derived from the cumulant analyses.

The pH of the samples and final latexes were measured with a Fisher Scientific/Accumet Research AR50 Dial Channel pH-meter. The viscosity of each final latex was measured at 100 rpm using spindles R2 or R3 on a Thermo Scientific HAAKE Viscotester (Model D).

A TA Instruments Model Q100 DSC was used to measure the T_g of all final latex samples. About 10 mg of dried latex was placed in an aluminum pan and pressed sealed with an aluminum lid. To remove any residual moisture (if any) and to reset the thermal history of the polymer, a first heating cycle was performed by heating the sample from room temperature to 100 °C (at 10 °C min^{-1}). After 3 min at 100 °C, the sample was cooled to -60 °C and maintained there for 3 min before the second heating cycle. Then, the sample was heated to 80°C (at 10 °C min^{-1}) and the inflection point of the reversed heat flow curve was reported as the T_g. All measurements were performed under a nitrogen environment.

5.3.6 Latex film preparation and PSA testing

Adhesive films for PSA testing and characterization were prepared by casting roughly 15 g of latex using a Meyer rod (No. 30) to produce films of approximately 18 g m^{-1}. Films were dried

for 48 h at 50 ± 5% relative humidity at 23 ± 2 °C, and films were tested under these same conditions. Bluehill 2 Materials Testing Software was used on an Instron 3000 Universal Tester, and Pressure Sensitive Tape Council (PSTC) methods were employed for peel strength, loop tack, and shear strength measurements.[18]

Peel strength: the PSTC-101 standard, using Test A for 180° peel, was used. Prepared films were cut into 1" × 12" strips and applied along the centre of a stainless-steel testing plate, adhesive side down. The strips were applied to the testing panel at approximately 10 mm s^{-1} using a weighted steel roller (2040 ±45 g) rolling twice in each lengthwise direction. All samples displayed adhesive, as opposed to cohesive, failure.

Loop tack: the PSTC-16 standard was employed. Prepared films were cut into 1" × 5" strips and formed into a loop with the adhesive side facing outward. A piece of 1" masking tape was used to secure the loop and to create a thicker edge for the Instron tester grips. The loop was lowered on the stainless-steel testing panel at a rate of 2 mm s^{-1} until there was a 1" contact. The strip was lifted by the tester at a rate of 5 mm s^{-1} and the maximum force required to remove the strip was recorded. All samples displayed adhesive, as opposed to cohesive, failure.

Shear strength: the PSTC-107A standard was used but a modification to the test area was made because adhesive strips exhibited unreasonably long failure times. Instead of 1" × 1" areas, 1" × 0.5" testing areas were used. Adhesive strips were cut into 1" × 5" strips and placed in such a way that a 1" × 0.5" adhesive surface was in contact with the testing panel. A weighted steel roller (2040 ±45 g) was used to apply the adhesive to the test plate by rolling twice in each lengthwise direction at a rate of approximately 10 mm s^{-1}. A 500 g mass was affixed to each tape and the time to shear failure was recorded. All samples displayed cohesive, as opposed to adhesive, failure.

5.3.7 Latex film preparation for AFM

Stock latexes (35 wt.% solids) were diluted by a factor of 1 and 100 to make samples of 17.5 and 0.35 wt.% solids, respectively. The base latex (49 wt.% solids), was diluted by a factor of 2.8 and 140 to yield samples of the same concentrations, for comparison (i.e., 17.5 wt.% and 0.35 wt.% solids, respectively). Silicon dioxide wafers (SiO_2) were cleaned with isopropyl alcohol and acetone sequentially and then dried under a nitrogen stream. 500 µL of each of the diluted

sample was spin coated dynamically (i.e., latex was deposited on the wafer as it was spinning) at 3000 rpm for 30 s onto the cleaned SiO_2 wafers using a Laurell WS-650-23 spin coater.

The spin coated latex films were imaged using ScanAsyst tapping mode in air, with a Bruker dimension Icon AFM. A LAXCO™ microscope (Model LMC-4000) was used to obtain a series of 4K images of the 0.35 wt.% and 17.5 wt.% films to illustrate which part of the samples were imaged. The ScanAsyst tips have a nominal spring constant of 0.4 N m^{-1} and resonance frequency of 70 KHz. Imaging was carried out at a scan rate of 0.975 Hz with a resolution of 512 measurements per line. Images were processed using the Nanoscope Analysis software by Bruker and flattened using high order plane fits. Height and in-phase images were analyzed using a computer vision approach implemented in python 3.7;[19] AFM images were processed using OpenCV python module and segmented using a local Otsu approach implemented using the Scikit Image python package. Finally, the segmented images were solved for surface coverage and particle size, where applicable. Detailed descriptions of the full algorithm process can be found elsewhere.[19] In addition, a plugin called "Ridge Detection" in ImageJ was used to measure the CNC aspect ratios from in-phase images which were manually cleaned to remove any artifacts of AFM prior to processing.

5.4 Results and discussion

5.4.1 cCNCs and emulsion polymerization reactions

In the design of PSAs, polymer microstructure is an important determining factor for adhesive properties. The molecular weight (M_w) and molecular weight distribution are governed by the chemical nature of the monomer system and can be modified using chain-transfer agents (CTAs) and/or crosslinkers. Nevertheless, employing CTAs and crosslinkers for the improvement of adhesive properties can be challenging because the two governing attributes, adhesion and cohesion, require opposing properties. Generally speaking, the M_w should be limited to lower values for polymers intended for adhesive applications to retain their mobility – increasing the M_w of polymers in an emulsion tends to decrease their mobility by increasing chain entanglements, which increases the cohesive forces (i.e., shear strength) to the detriment of adhesive forces (i.e., tack and peel strength).[20, 21] However, the addition of CNCs simultaneously

improve the peel strength, tack, and shear strength of a PSA because the mechanisms by which CNCs enhance adhesion and cohesion does not impact the polymer microstructure. For sulfated CNCs in particular, the network created by their rod-like structure in the water phase enhances the mechanical strength of the polymer matrix, and increases the film formation abilities and surface wettability of a composite latex. This provides an avenue for polymer particle tethering and/or entanglement.[4, 10, 11] Thus, cohesion can be enhanced through CNC-polymer networks in the water phase of the latex, improving the adhesive forces. This phenomena is due to the increase in the work of adhesion between the adhesive and the substrate caused by the polar hydroxy groups of the CNCs with the substrate, and an increase in film wettability via hydrogen bonding.[9–11] In other words, using CNCs in a latex for adhesive applications can improve the tack, peel strength and shear strength simultaneously, compared to using a crosslinker and/or CTA where improvements in one property result in decreased performance of another property. One caveat of these property improvements related to the quality of the CNC dispersion in the latex; a uniform distribution of the CNCs in the matrix is a prerequisite for predictable and reproducible properties in the nanocomposite.[4, 11]

As noted in the experimental methods section, cCNCs were incorporated *in situ* and *ex situ* (i.e., blended) into latex formulations (BA:MMA 90:10) to evaluate their effect on the properties PSA films. A total of six different addition methods were tested. The “wet” cCNCs were added to a latex formulation *in situ* in two different ways: as received or after ultrasonication. The dry cCNCs were likewise added to the latexes *in situ* in two ways: after simple dispersion or after simple dispersion followed by ultrasonication. Finally, the “wet” cCNCs were added *ex situ* to base latexes via hot and cold blends. Latexes of 0.5 and 1.0 phm cCNC loading were prepared with each of the six addition methods. The conversion, solids content, particle size and pH trajectories of the emulsion polymerization experiments followed the same trends for all experiments regardless of the cCNC loading and the cCNC dispersion method, which suggests that the cCNCs did not participate in the polymerization reaction and therefore, their dispersion method and loading did not have an effect on the reaction kinetics. Furthermore, the polymer T_gs remained unchanged (-38 ± 1 °C) regardless of cCNC loading. An example of typical conversion, solids content, particle size and pH trajectories is presented in Figures 1(A)-(D), resp-

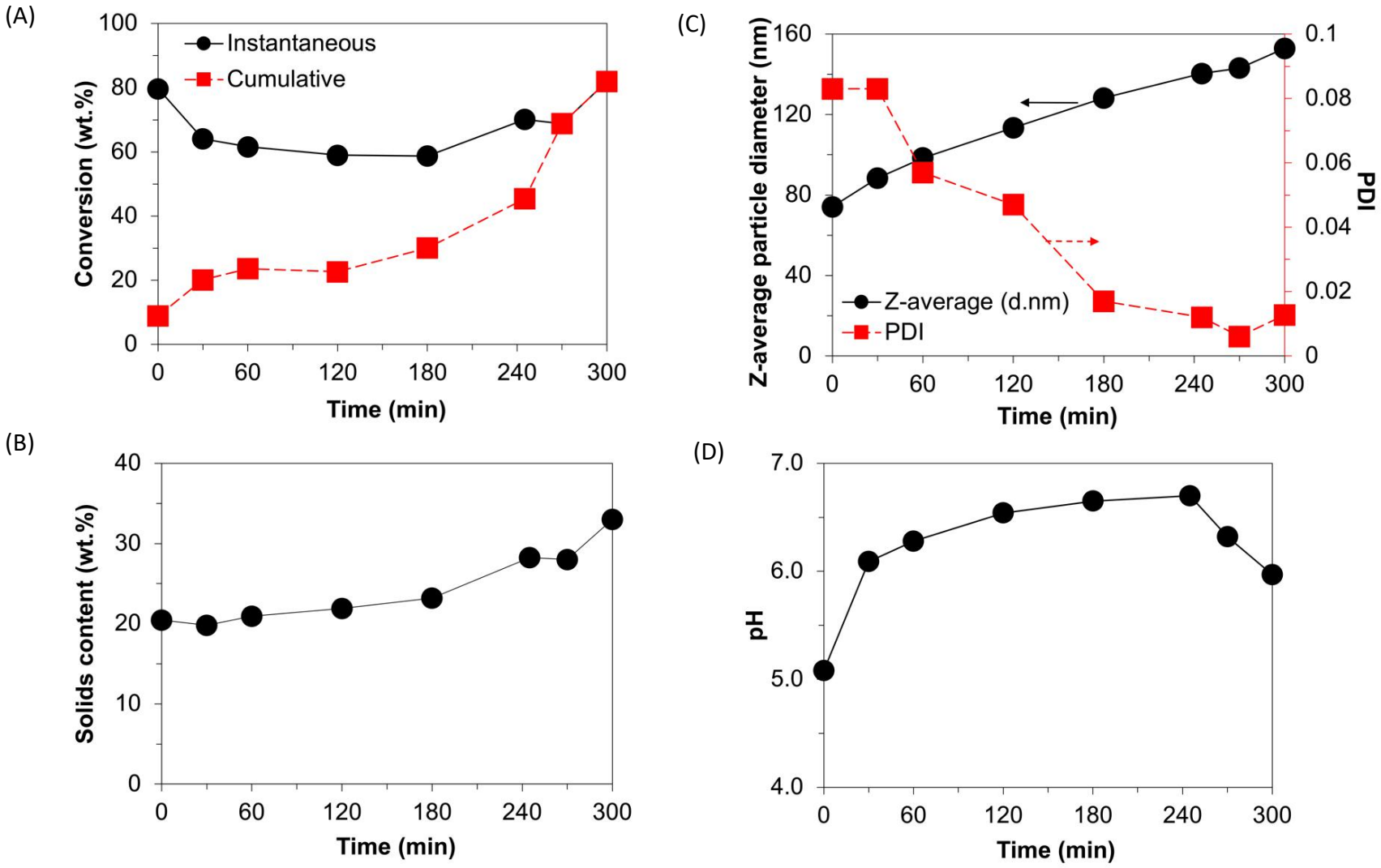

Figure 5.1 (A) conversion, (B) solids content, (C) z-average particle diameter, and (D) pH versus time trajectories for a 35 wt.% solids latex produced with 1.0 phm 'Dry dispersed' cCNCs. Similar profiles were observed for latexes with cCNCs added wet or dry, with simple mixing or ultrasonication (i.e., the 4 in situ addition methods). Lines drawn between points are provided as a guide.

ectively, and a table containing details from other experiments can be found in Table AII.1 of the Appendix II.

5.4.2 Microscopy of cCNC nanocomposite latexes

Stock latex was diluted, spin coated on SiO_2 wafers, and imaged via AFM to observe the cCNC dispersion in the polymer matrix, their position relative to the latex polymer particles, and their behaviour in the films. While AFM can have high precision and resolution, low T_g polymer films are particularly challenging to image. The main concerns when imaging soft polymer particles is the problem of tip contamination, and the phenomenon of particle flattening due to excessive tapping force, which can lead to exaggerated particle sizes. To attain a truly representative image, a cantilever with an appropriate spring constant should be employed; the spring constant should be high enough to withstand the adhesive nature of the PSA film while being low enough to prevent significant indentation of the polymer particles.

In accordance with previous AFM imaging of soft CNC-doped polymer films, some areas of the films were rich in CNCs, and others showed fewer CNCs.[8] A series of 4K images of the 0.35 wt.% and 17.5 wt.% films to illustrate which part of the samples were imaged (Figure AII.1 of the Appendix II). Focusing on polymer-rich areas in the spin coated films proved useful to detect cCNCs, because the CNCs tend to be closely associated with, or adsorbed onto, the surface of the polymer particles.[8, 9, 15, 22] Selected AFM images are presented in the manuscript to guide the discussion.

For the base latex, irrespective of the dilution factor, AFM images revealed that the spin coated films produced were not continuous (Figure 5.2A and 5.3A). For the base latex at 0.35 wt.% solids (Figure 5.2A), the average particle diameter calculated from the AFM image is 167 $\pm$ 16 nm, which is close to the average particle diameter obtained via DLS (164.4 nm).[13] When cCNCs were added, the particle diameters were much bigger than those recorded via DLS, ranging from 114-860 nm for the 0.5 phm loading (Figure 5.2B). The larger diameters observed via AFM, as well as the loss of sphericity, suggest that the polymer particles were packing together, and at higher cCNC loadings (1.0 phm, Figure 5.2C), the polymer was beginning to form a film. Note that all three AFM images from Figure 5.2 were taken from samples diluted to the same solids content (0.35 wt.%).

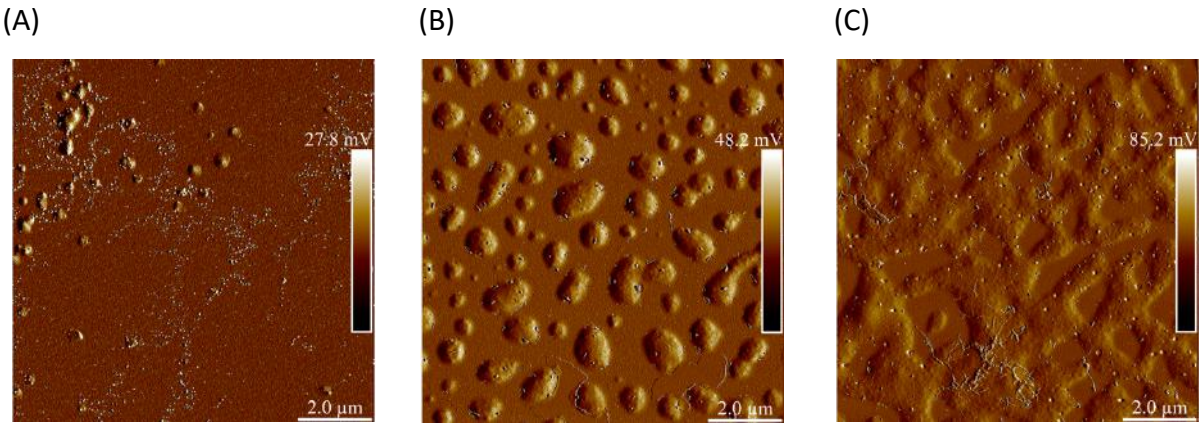

Figure 5.2 In-phase AFM images of films cast from 0.35 wt.% latexes containing (A) no cCNCs, (B) 0.5 phm dry dispersed cCNCs, and (C) 1.0 phm dry dispersed cCNCs.

According to film formation theory, the formation of latex-based films occurs in three stages.[23] Stage I consists of water evaporation and subsequent particle ordering and packing. In Stage II, particle deformation occurs as a result of an imbalance between the attractive forces amid particles and their mechanical resistance. Once particles are in sufficient proximity to one another, Stage III ensues where polymer chains inter-diffuse across particle-particle boundaries, leading to coalescence, and the formation of a uniform, continuous polymer film. There are reports that sulfated CNCs lower the solids content threshold for latex particle coalescence, thereby promoting film formation.[24] The same phenomenon was observed in this work as can be seen from the larger polymer islands on AFM images of samples with increasing cCNC loadings (Figure 5.2B and 2C) versus those without (Figure 5.2A). Processing these AFM images through a computer vision approach[19] revealed that the films produced from 0.35 wt.% latex samples containing 0.5 phm cCNCs (regardless of cCNC type or dispersion method) displayed between 10.8 and 14.6% surface coverage, whereas the film without cCNCs only had a surface coverage of 6.1% (Table 5.2). When increasing the cCNC loading to 1.0 phm, the size of the polymer islands grew, and the range of surface coverages increased to 27.8 – 40.9% (Table 5.2). This surface coverage data support the hypothesis that adding cCNCs to a latex formulation promotes the coalescence of polymer particles, thereby facilitating film formation.

Table 5.2 Surface coverage of 0.35 wt.% spin coated films. AFM height images used for analysis can be found in Figure AII.2 of Appendix II.

	Surface coverage (%)	
Base latex	6.1[a]	
	0.5 phm cCNCs	1.0 phm cCNCs
Wet	13.8	27.8
Wet ultrasonicated	10.8	25.1
Dry dispersed	14.6	40.9
Dry ultrasonicated	13.2	32.8
Sulfated	19.8	36.6

[a]At 17.5 wt.% solids, the surface coverage is 11.4%

When observing the spin coated films produced from 17.5 wt.% latex samples (Figure 5.3), those containing 0.5 and 1.0 phm cCNCs produced continuous films (i.e., 100% surface coverage), whereas the base latex only had a surface coverage of 11.4%. In fact, the 0.35 wt.% films containing 0.5 phm cCNCs had, on average, surface coverages of 13.1% which is roughly 2% higher than that of the base latex at 17.5 wt.%; once again, this illustrates the magnitude to which the cCNCs promote polymer coalescence and enhance film formation. According to film formation theory, there is a minimum solids content threshold at which a uniform polymer film is formed.[23] In our case, a 17.5 wt.% solids base latex sample could not form a continuous film, but with the addition of as little as 0.5 phm cCNCs, a continuous polymer film was achieved. Moreover, carboxyl groups can improve the phase compatibility between hard and soft polymer particles in a polymer matrix,[25] and their addition in latexes produced for coating applications slowed the drying rate of latex-based films, which provided more time for polymer chains to interpenetrate and create continuous films, thereby improving film quality.[26] Though the drying rate was not specifically measured in this work, the higher surface coverage in the cCNC nanocomposites suggests that the carboxylate groups play a role in film coalescence. Note that for the base case latex, increasing the solids content from 0.35 wt.% to 17.5 wt.% only increased the surface coverage from 6.1 to 11.4%.

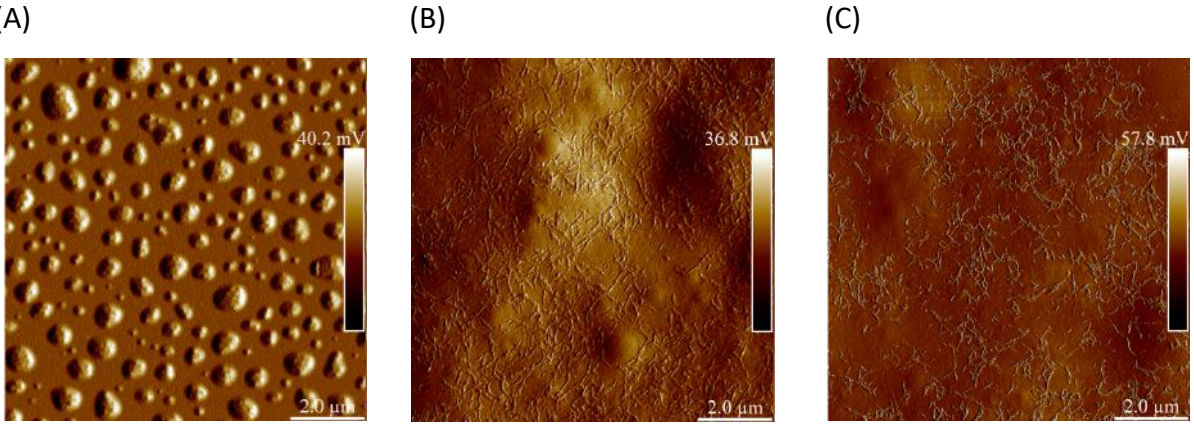

Figure 5.3 In-phase AFM images of films cast from 17.5 wt.% latexes containing (A) no cCNCs, (B) 0.5 phm dry dispersed cCNCs, and (C) 1.0 phm dry dispersed cCNCs.

Overall, there are very few instances of 'free-floating' cCNCs in the AFM images (i.e., cCNCs that do not contact any polymer particles). Instead, as observed many times in the literature with other types of CNCs, cCNCs appear on, around, and in between the polymer islands, indicating many polymer-cCNC interactions.[8, 9, 15, 22] A good CNC dispersion (i.e., CNC individualization, discrete individual CNCs) is critical to the final performance properties of a given nanocomposite because one of the key attributes that render CNCs effective for property improvement in latex-based systems is their high aspect ratio and high surface to volume ratio.[4] Their rigid and whisker-like morphology enables them to act as bridges between soft polymer particles to promote film formation and strengthen the polymer matrix, which improves cohesive forces in PSA nanocomposites. If CNCs are not well dispersed in water prior to their addition, CNC agglomeration can occur in the latex rendering the nanocomposite and the integrity of its films heterogeneous, ultimately affecting performance.[4, 27] Curiously the capacity for property improvement was greater when the ultrasonication step to "fully" disperse the cCNCs was omitted.

Like sulfated CNCs, cCNCs can stack side-by-side when not fully redispersed. However, cCNCs also line-up end-to-end. The cCNCs' distinctive behaviour leads to an increase in their "apparent" aspect ratio in the nanocomposite, which contributes to particle-particle branching,[28] promotes stress transfer between fillers and polymer matrices,[27] and can form

entangled networks at low concentrations.[4] The cCNCs used here have an aspect ratio of 30 ± 10[14] and that of the sulfated CNCs is 31 ± 10;[29] those aspect ratios were determined using length and width data from individual CNCs in AFM images (i.e., the CNCs that were imaged were not touching any other CNC – determining reliable CNC dimensions by AFM and transmission electron microscopy is a heavily studied topic).[30] However, CNCs in latexes inevitably interact with each other and with the polymer film, which can affect their "apparent" aspect ratio. To that end, the "apparent" aspect ratios of the cCNCs were calculated from the AFM images. Traditional methods for determining the 'true' lengths and widths of CNCs are done on height images manually and only individualized CNCs (i.e., CNCs that do not touch any other CNCs) are measured.[30] In this work, the "apparent" aspect ratios were sought and therefore all cCNCs, including those that were aligned and touching, were measured. However, manual determination of the cCNC lengths was challenging because cCNCs in the AFMs were 'curved', resembling nanofibrils, as a result of their end-to-end and side-by-side interactions. Furthermore, the "apparent" cCNC widths were not always consistent from one end of a cCNC 'nanofibril' to the other and therefore manual width estimations proved too subjective. To eliminate these errors, AFMs were processed using the "Ridge Detection" plugin in ImageJ (Table 5.3). In-phase images were used instead of height images because the former showed better contrast between the hard (i.e., cCNC) and soft (i.e., polymer) materials in the spin coated films. This made the cCNCs stand out, and they were therefore more easily detected by the Ridge Detection plugin. Because the aspect ratio data were not normally distributed (skewed to the right) the mode of the "apparent" aspect ratios was more representative of the data and was used for comparison instead of the mean. An example of the "apparent" aspect ratio distribution curve can be found in Appendix II (Figure AII.3).

For all nanocomposite films, the "apparent" cCNC aspect ratios were much smaller than the aspect ratios reported in the literature, but the trends were informative. In latexes with low cCNC loadings (i.e., 0.5 phm, far from the threshold for the formation of a percolation network), AFM images revealed that sonication breaks up loose and end-to-end agglomerates and yields smaller "apparent" aspect ratios. On the other hand, dried CNCs have more side-to-side aggregation and therefore, smaller "apparent" aspect ratios (Table 5.3).

Table 5.3 “Apparent” aspect ratios for cCNCs at 0.5 and 1.0 phm loadings in latex films spin coated from 0.35 wt.% and 17.5 wt.% solids suspensions.

	“Apparent” aspect ratio of cCNCs	
	17.5 wt.% films	
cCNC type	0.5 phm	1.0 phm
Wet	5.8	2.7
Wet ultrasonicated	5.0	2.8
Dry dispersed	2.3	3.2
Dry ultrasonicated	2.1	3.0
Sulfated CNCs	3.0	2.6

In the films produced with 1.0 phm CNC loadings, the difference between “apparent” aspect ratios of ultrasonicated vs. non ultrasonicated CNCs is less pronounced (Table 5.3). At higher concentrations, cCNCs tend to form interconnected networks (Figure 5.4B) rather than the long fibre-like structures observed at the 0.5 phm loading (Figure 5.4A). The (ultrasonicated) sulfated CNCs on the other hand do not display the same degree of end-to-end association and show individualized particles at both loadings (Figure 5.4C-D).

Finally, to confirm these results, DLS measurements were conducted on the cCNC suspensions at 0.1 wt.%. In general, DLS is better suited to characterize spherical particles, hence, measuring rod-like particles (like cCNCs) is not accurate. Nonetheless, DLS can deliver an “apparent” diameter of suspended nanoparticles and can be used as a point of comparison within a study. Thus, DLS measurements revealed that the “apparent” size of the cCNCs varied based on the dispersion method. When ultrasonicated, the “apparent” z-average of the cCNCs via DLS was roughly 81 nm whereas the “wet” and “dry dispersed” cCNCs exhibited higher “apparent” z-averages, at 130 and 186 nm, respectively (Table 5.4). This confirms that there were significant cCNC-cCNC interactions, which rendered their “apparent” lengths longer when they were not redispersed via ultrasonication.

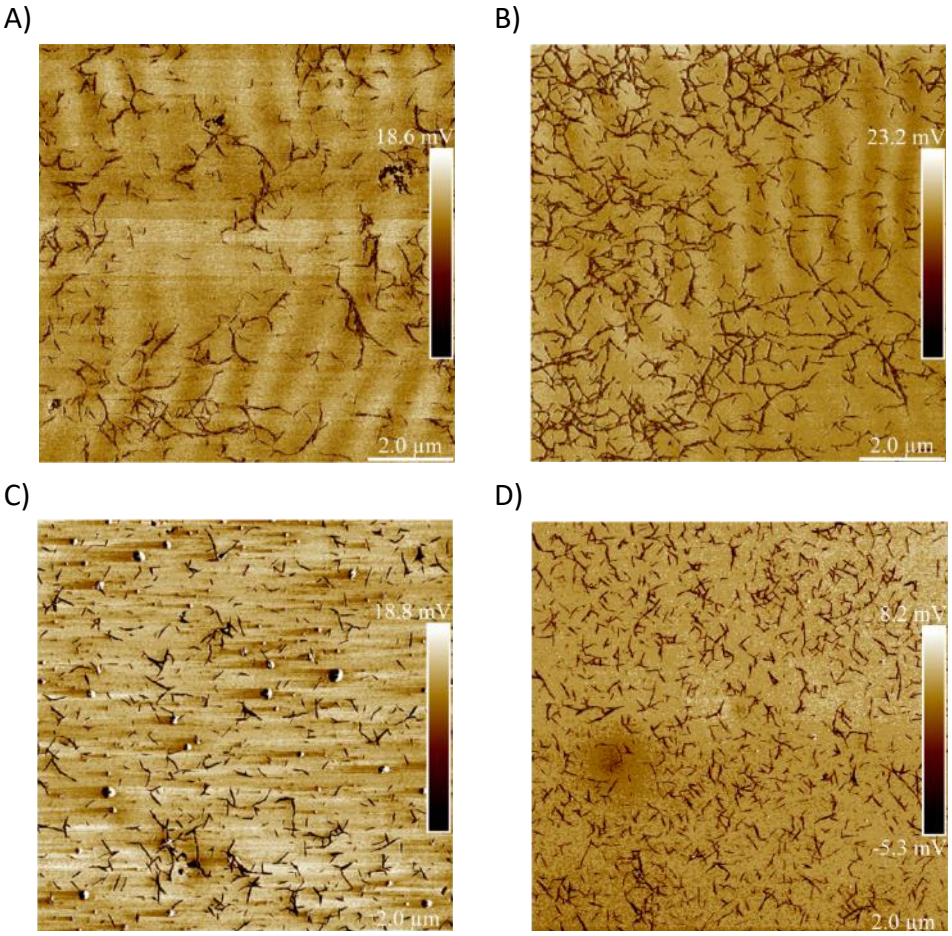

Figure 5.4 In phase AFM images of 17.5 wt.% films with A) 0.5 phm wet cCNCs, B) 1.0 phm wet cCNCs, C) 0.5 phm sulfated CNCs, and D) 1.0 phm sulfated CNCs.

Table 5.4 "Apparent" z-average (via DLS) of 0.1 wt.% cCNC suspensions according to their different dispersion methods.

	"Apparent" z-average size (nm)
Wet	130
Wet ultrasonicated	81
Dry dispersed	186
Dry ultrasonicated	82

5.4.3 PSA properties of cCNC nanocomposite latex films

With the addition of any amount of cCNC, regardless of the addition method (*in situ* vs. *ex situ*), the type of CNC (dry cCNCs, wet cCNCs), or the use of ultrasonication, the peel strength,

tack and shear strength improved relative to the base latex (Figures 5.5, 5.6, and 5.7). For comparison, Post-it notes (Post-it™ "Super Sticky Big Notes"), a commercial masking tape (Uline™ general purpose 1" masking tape), and a latex produced with sulfated CNCs were tested and plotted on the same graph.

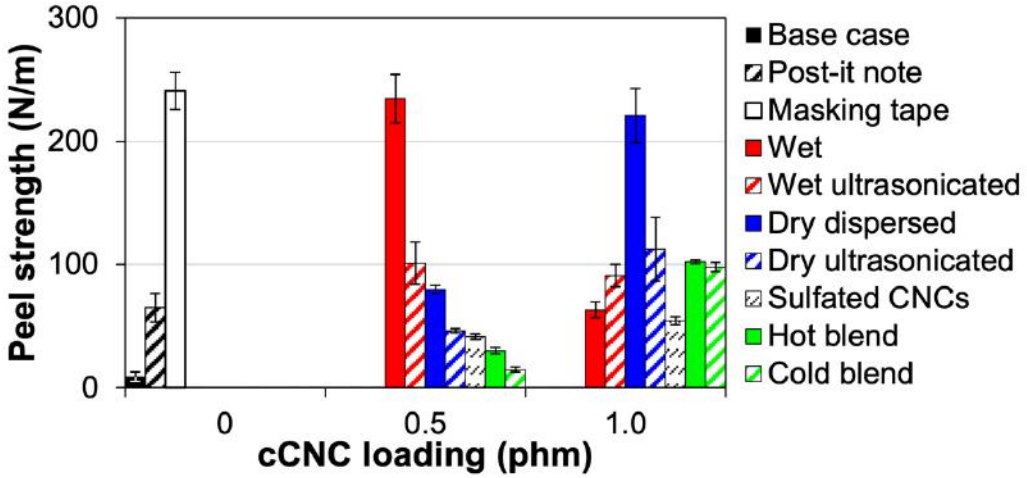

Figure 5.5 Peel strength of latexes produced with 0.5 and 1.0 phm cCNC with various cCNC addition methods (wet, wet ultrasonicated, dry dispersed, dry ultrasonicated, hot blend, cold blend, and sulfated CNCs). Post-it™ notes and masking tape were measured for comparison and the error bars represent the standard deviation of six measurements.

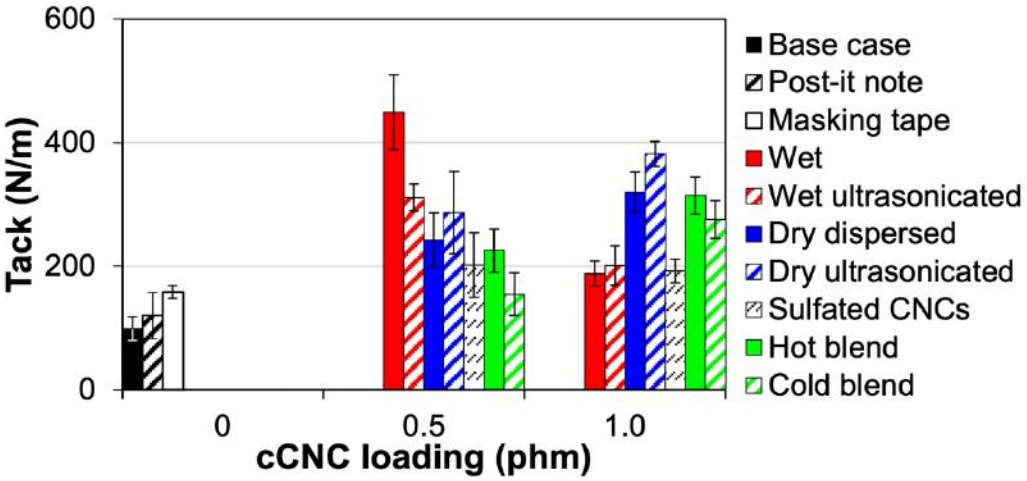

Figure 5.6 Tack of latexes produced with 0.5 and 1.0 phm cCNC with various cCNC addition methods (wet, wet ultrasonicated, dry dispersed, dry ultrasonicated, hot blend, cold blend, and sulfated CNCs). Post-it™ notes and masking tape were measured for comparison and the error bars represent the standard deviation of six measurements.

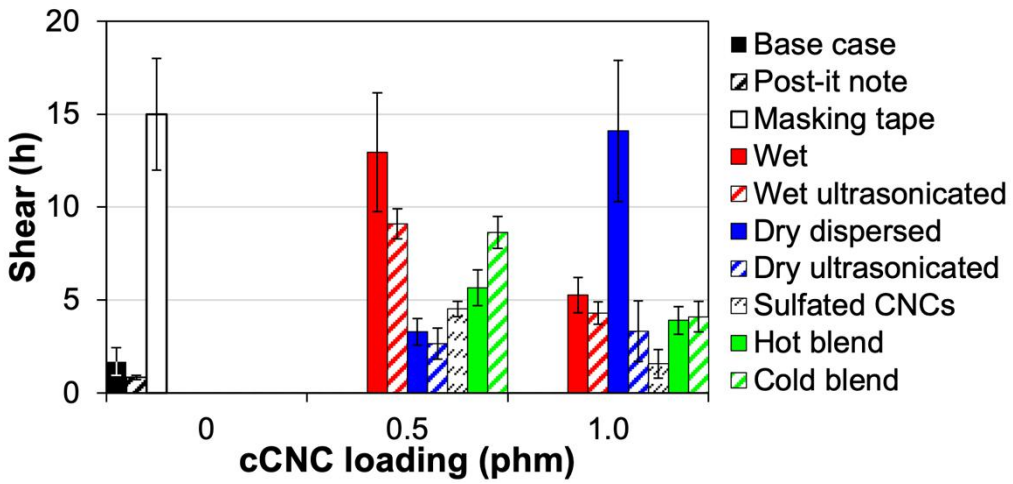

Figure 5.7 Shear strength of latexes produced with 0.5 and 1.0 phm cCNC with various cCNC addition methods (wet, wet ultrasonicated, dry dispersed, dry ultrasonicated, hot blend, cold blend, and sulfated CNCs). Post-it™ notes and masking tape were measured for comparison and the error bars represent the standard deviation of six measurements.

A number of factors influence how CNCs improve adhesive and cohesive properties simultaneously. Without considering surface groups, the addition of a crystalline nanoparticle is known to improve PSA performance because of the added mechanical strength provided by the nanorods.[4] CNCs have high aspect ratios allowing them to form percolating networks within polymer composites.[31–35] The formation of these networks can increase the rigidity of the polymer matrix thereby improving cohesive forces (i.e., shear strength) and strength without affecting the polymer microstructure, e.g., polymer T_g.[4, 6–11, 15] Moreover, when considering surface groups, the abundance of hydroxy or carboxylate moieties render the nanocrystals hydrophilic. Thus, their addition to a latex containing some hydrophilic components (e.g., acrylic acid, vinyl acetate, methyl methacrylate) can promote film formation and increase film smoothness.[25, 28] Finally, the presence of surface groups can provide an avenue for hydrogen bonding within the polymer, which improves cohesion.[6–9, 15]

Both the physical and chemical properties of the cCNCs play a role in the PSA improvements because of the synergy between the cCNCs and the functional monomers in the formulation. As a result of their extraction and production method, the cCNCs have a higher normalized mass of bound water than their sulfated counterparts[14] (i.e., they are more hydrophilic) which likely facilitates their re-dispersion in water relative to the sulfated CNCs. The

cCNCs' greater hydrophilicity was observed experimentally: when preparing 0.5 and 1.0 phm dispersions (4.2 and 8.6 g_{CNC} L_{water}^{-1}, respectively), the dry cCNCs 'dispersed' completely after 30 min of mixing with a stir bar at room temperature whereas sulfated CNCs required 2 (or more) hours of vigorous mixing before the disappearance of visible CNC aggregates. Furthermore, the carboxylate groups provide additional property enhancing characteristics via hydrophilic surface interactions: the cCNCs improve the film wettability via hydrogen bonding between the nanocomposite film and the substrate (i.e., improved adhesion) and the cCNCs help form bridges in the polymer film and reinforce the matrix (i.e., improved cohesion).

With the addition of the "wet" and "wet ultrasonicated" cCNCs (Figures 4-6) the peel strength, tack and shear strength of the adhesive films increased at 0.5 phm compared to the base latex but decreased at the higher loading. This same trend was observed elsewhere with the addition of sulfated CNCs when a classical emulsion polymerization formulation (i.e., using anionic surfactant and persulfate initiator) was employed.[11] Intriguingly, we observed that the cCNCs that did not undergo ultrasonication (i.e., "wet") provided more significant adhesive enhancements than cCNCs that were probe sonicated (i.e, "wet ultrasonicated). The "wet" cCNCs demonstrated the greatest property improvements among all the forms of cCNCs and addition methods at a loading of 0.5 phm, and the adhesive properties rivaled (and sometimes surpassed) those of the commercial masking tape (Figure 4-6). Relative to the base latex, the films with 0.5 phm "wet" cCNCs showed over 26x higher peel strength, 4.5x higher loop tack, and 7.7x greater shear strength. The "wet ultrasonicated" cCNCs also showed PSA improvements, and had 11.2x, 3.1x, and 5.4x higher peel strength, tack and shear strength respectively, relative to the base case.

The peel strength, loop tack and shear strengths of the PSAs produced with the "wet" cCNCs were 2.3x, 1.4x and 1.4x higher than the PSAs produced with the "wet ultrasonicated" cCNCs. AFM images revealed that the cCNCs can interact together (side-by-side and end-to-end stacking), which can affect the cCNCs' "apparent" aspect ratios in the films. In water-based systems, increasing the aspect ratio of CNCs leads to more CNC-CNC entanglement which can form fibrils that are able to bridge neighbouring particles. For instance, Kalashnikova et al.[36] observed that high aspect ratio CNCs were similar in morphology to cellulose nanofibrils (CNFs),

which can entangle and reinforce polymer matrices at much lower concentrations than CNCs. Likewise, our AFM images revealed that the cCNCs resembled nanofibrils more than nanocrystals when added *in situ* to the polymerization without sonication. Their fibre-like appearance allowed them to behave like nanofibrils, which have superior particle anchoring, bridging, and entangling capabilities due to their higher aspect ratio.[37, 38] The benefit of using CNCs rather than CNFs lies in their ease of use: CNCs are rigid nanorods that do not entangle; this makes them easier to homogeneously distribute in a latex. On the other hand, CNFs are harder to successfully and homogenously incorporate into polymer matrices (without extremely high shear processing) because they can entangle permanently and have high viscosities at low concentrations in water which can interfere with the emulsion polymerization. CNFs can also not be redispersed from dry. cCNCs can provide the benefits of both nanocrystals and nanofibrils because they are easily dispersed in a water-based system and can interact with each other to form longer filaments that behave as nanofibrils. Thus, we can reap the benefits of fibre-like nanoparticles without the risk of permanent fibril entanglements. The films produced with the "wet" cCNCs demonstrated the greatest property improvements because the quality of their dispersion was ideal for PSA applications, that is, they were dispersed enough to be homogeneously distributed in the latex while still exhibiting superior "apparent" aspect ratios, branching and networking behaviour, like CNFs.

The "dry dispersed" and "dry ultrasonicated" cCNCs showed increasing peel strength, tack, and shear strength with increasing cCNC loading (Figures 4-6). Similar to the trend observed between the "wet" and "wet ultrasonicated" cCNCs, the absence of probe ultrasonication generally led to better adhesive property improvements. Specifically, the peel and shear strengths at 0.5 and 1.0 phm loadings were higher for the "dry dispersed" films vs. the "dry ultrasonicated" films, and the tack for both methods were within experimental error, but still were higher than the base case. Typically, sonication is required to redisperse dry CNCs in water before adding them to a latex formulation *in situ* or *ex situ* to obtain a homogeneous final product. But, omitting the ultrasonication step is beneficial to the cCNCs when using them to improve PSA properties because of its effect on the "apparent" aspect ratio.

Finally, the wet 4.5 wt.% cCNC dispersion was added to latexes *ex situ* in hot and cold blends (Figures 2-4). Similar to results in the literature, adhesive properties were superior in films cast from latexes produced with cCNCs added *in situ* rather than with the *ex situ* method.[7–9] In our case, regardless of the CNC loading, the peel strength, tack and shear strengths were higher for the 1.0 phm loading than for the 0.5 phm loading, and adhesive strengths between the hot and cold blends at each of the loadings were statistically alike. However, because the cCNCs were being added in an already well dispersed form (i.e., the "wet" 4.5 wt.% dispersion, as received from the manufacturer), there was no statistical difference between the adhesive properties of films cast from the latexes produced via hot and cold blends. The shear strength of the cold blend film at 0.5 phm loading was slightly superior to that of the hot blend at that loading.

5.5 Conclusion

cCNCs improve both the adhesive and cohesive qualities of latex nanocomposite films when incorporated at low loadings (0.5 – 1.0 wt.%). Although PSA films can be enhanced by performing latex-cCNC blends, incorporating cCNCs *in situ* (i.e., during the emulsion polymerization) provides much larger peel strength, tack, and shear strength improvements.

After using the cCNCs in both their wet and dried forms *in situ* to produce PSA films, adhesive testing revealed that cCNCs provided greater property improvements when they were not ultrasonicated. Without sonication, the cCNCs can be adequately dispersed in water and their networking behaviour (i.e., end-to-end and side-by-side interactions) is preserved. Because of this, their "apparent" aspect ratios in the spin coated films were higher, which had a positive effect on the adhesive strength. PSAs produced with 0.5 phm "wet" (unsonicated) cCNCs performed best, surpassing the adhesive performance of a commercial masking tape. The "dry" (unsonicated) cCNCs likewise produced high performance PSAs and could match or outperform a commercial masking tape at a loading of 1.0 phm.

In general, the adhesive improvements that CNCs can provide are in part due to their high aspect ratio. AFM images revealed that cCNCs interact strongly with each other, relative to sulfated CNCs, due to their surface chemistry; the cCNCs resemble nanofibrils more than nanocrystals due to their side-by-side and end-to-end association in the films. When

incorporating the cCNCs without ultrasonication, there was a higher degree of nanocrystal elongation which induced a higher "apparent" aspect ratio of the nanoparticles in the films, which gave the cCNCs a fibre-like appearance. These cCNC-cCNC interactions led to greater improvements in PSA performance relative to films produced from latexes where the cCNCs were added after ultrasonication. The cCNCs may be able to provide similar mechanical improvements to PSA films as nanofibrils (i.e., higher particle-particle bridging and improved film formation) but without the complications associated with the addition of nanofibrils in polymer matrices (e.g., nanoparticle entanglement). Finally, cCNC measurements from AFM images indicated that ultrasonication can decrease the "apparent" aspect ratio of the cCNCs in the PSA films, which was less beneficial to PSA properties.

Finally, cCNCs can be adequately dispersed in water without the need for sonication. From experimental, industrial, and health and safety standpoints, omitting the sonication step is desirable because it is expensive, energy intensive, and hazardous. This paves the way for a more straightforward use of cCNCs in industrial applications.

5.6 Acknowledgements

The authors thank Anomera Inc. (Montreal, QC) for providing the DextraCel (i.e., cCNCs, carboxylated CNCs), and for technical input from their staff: Dr. Amir Khabibullin, Dr. Timothy Morse, Dr. Nathan Hordy, Dr. Zhen (Justin) Hu, and Michael Kiriakou. The authors thank Dr. Pascale Champagne for helpful discussions. V.A.G thanks Dr. Elina Niinivaara for her guidance with the "apparent" aspect ratio measurements for the cCNCs. This work was funded through the MITACS Accelerate program. V.A.G. is a recipient of a NSERC CGS-D Scholarship.

5.7 References

[1] I. Benedek, *Pressure-Sensitive Adhesives and Applications*. 2004.

[2] Grand View Research, "Global Pressure Sensitive Adhesives Market Size Report, 2019-2025." https://www.grandviewresearch.com/industry-analysis/pressure-sensitive-adhesives-market (accessed May 2021).

[3] M. A. Dubé, V. A. Gabriel, A. S. Pakdel, and Y. Zhang, "Sustainable polymer reaction engineering: Are we there yet?," *The Canadian Journal of Chemical Engineering*, vol. 99, no. 1, pp. 31–60, Jan. 2021, doi: 10.1002/cjce.23865.

[4] S. A. Kedzior, V. A. Gabriel, M. A. Dubé, and E. D. Cranston, "Nanocellulose in Emulsions and Heterogeneous Water-Based Polymer Systems: A Review," *Advanced Materials*. Wiley-VCH Verlag, 2020. doi: 10.1002/adma.202002404.

[5] O. M. Vanderfleet and E. D. Cranston, "Production routes to tailor the performance of cellulose nanocrystals," *Nature Reviews Materials*, vol. 6, no. 2. Nature Publishing Group, pp. 124–144, Oct. 13, 2021. doi: 10.1038/s41578-020-00239-y.

[6] Z. Dastjerdi, E. D. Cranston, and M. A. Dubé, "Synthesis of Poly(n -butyl acrylate/methyl methacrylate)/CNC Latex Nanocomposites via In Situ Emulsion Polymerization," *Macromolecular Reaction Engineering*, vol. 11, no. 6, p. 1700013, Dec. 2017, doi: 10.1002/mren.201700013.

[7] Z. Dastjerdi, E. D. Cranston, and M. A. Dubé, "Pressure sensitive adhesive property modification using cellulose nanocrystals," *International Journal of Adhesion and Adhesives*, vol. 81, pp. 36–42, Mar. 2018, doi: 10.1016/j.ijadhadh.2017.11.009.

[8] A. Ouzas, E. Niinivaara, E. D. Cranston, and M. A. Dubé, "In Situ Semibatch Emulsion Polymerization of 2-Ethyl Hexyl Acrylate/ n -Butyl Acrylate/Methyl Methacrylate/Cellulose Nanocrystal Nanocomposites for Adhesive Applications," *Macromolecular Reaction Engineering*, vol. 12, no. 3, p. 1700068, Jun. 2018, doi: 10.1002/mren.201700068.

[9] A. Ouzas, E. Niinivaara, E. D. Cranston, and M. A. Dubé, "Synthesis of poly(isobutyl acrylate/n-butyl acrylate/methyl methacrylate)/CNC nanocomposites for adhesive applications via in situ semi-batch emulsion polymerization," *Polymer Composites*, vol. 40, no. 4, pp. 1365–1377, Apr. 2019, doi: 10.1002/pc.24869.

[10] A. S. Pakdel, V. Gabriel, R. M. Berry, C. Fraschini, E. D. Cranston, and M. A. Dubé, "A sequential design approach for in situ incorporation of cellulose nanocrystals in emulsion-based pressure sensitive adhesives," *Cellulose*, vol. 27, no. 18, pp. 10837–10853, Dec. 2020, doi: 10.1007/s10570-020-03060-6.

[11] V. A. Gabriel, E. D. Cranston, and M. A. Dubé, "Pushing the Limits with Cellulose Nanocrystal Loadings in Latex-Based Pressure-Sensitive Adhesive Nanocomposites," *Macromolecular Reaction Engineering*, vol. 14, no. 6, p. 2000027, Dec. 2020, doi: 10.1002/mren.202000027.

[12] S. Beck, J. Bouchard, and R. Berry, "Dispersibility in Water of Dried Nanocrystalline Cellulose," *Biomacromolecules*, vol. 13, no. 5, pp. 1486–1494, May 2012, doi: 10.1021/bm300191k.

[13] V. A. Gabriel, P. Champagne, M. F. Cunningham, and M. A. Dubé, "In-situ addition of carboxylated cellulose nanocrystals in seeded semi-batch emulsion polymerization," *The Canadian Journal of Chemical Engineering*, vol. 100, no. 4, pp. 767–779, Apr. 2022, doi: 10.1002/cjce.24299.

[14] G. Delepierre, O. M. Vanderfleet, E. Niinivaara, B. Zakani, and E. D. Cranston, "Benchmarking Cellulose Nanocrystals Part II: New Industrially Produced Materials," *Langmuir*, vol. 37, no. 28, pp. 8393–8409, Jul. 2021, doi: 10.1021/acs.langmuir.1c00550.

[15] A. S. Pakdel, E. Niinivaara, E. D. Cranston, R. M. Berry, and M. A. Dubé, "Cellulose Nanocrystal (CNC)–Latex Nanocomposites: Effect of CNC Hydrophilicity and Charge on Rheological, Mechanical, and Adhesive Properties," *Macromolecular Rapid Communications*, vol. 42, no. 3, p. 2000448, Feb. 2021, doi: 10.1002/marc.202000448.

[16] M. S. Reid, M. Villalobos, and E. D. Cranston, "Cellulose nanocrystal interactions probed by thin film swelling to predict dispersibility," *Nanoscale*, vol. 8, no. 24, pp. 12247–12257, 2016, doi: 10.1039/c6nr01737a.

[17] J. Brandrup, E. H. Immergut, and E. A. Grulke, *POLYMER HANDBOOK*, Fourth Edi. New York: John Wiley & Sons, Inc., 1999.

[18] Pressure Sensitive Tape Council, "Test Methods for Pressure Sensitive Adhesive Tapes," 2014.

[19] B. Mirka *et al.*, "Excess Polymer in Single-Walled Carbon Nanotube Thin-Film Transistors: Its Removal Prior to Fabrication Is Unnecessary," *ACS Nano*, vol. 15, no. 5, pp. 8252–8266, 2021, doi: 10.1021/acsnano.0c08584.

[20] S. Roberge and M. A. Dubé, "The effect of particle size and composition on the performance of styrene/butyl acrylate miniemulsion-based PSAs," *Polymer*, vol. 47, no. 3, pp. 799–807, Jan. 2006, doi: 10.1016/j.polymer.2005.12.024.

[21] R. Jovanović and M. A. Dubé, "Emulsion-Based Pressure-Sensitive Adhesives: A Review," *Journal of Macromolecular Science - Polymer Reviews*, vol. 44, no. 1, pp. 1–51, 2004, doi: 10.1081/MC-120027933.

[22] S. A. Kedzior *et al.*, "Incorporating Cellulose Nanocrystals into the Core of Polymer Latex Particles via Polymer Grafting," *ACS Macro Letters*, vol. 7, no. 8, pp. 990–996, 2018, doi: 10.1021/acsmacrolett.8b00334.

[23] J. L. Keddie, "Reports : A Review Journal Film formation of latex," *Materials Science and Engineering*, vol. 21, no. 97, pp. 101–170, 1997.

[24] E. Niinivaara, A. Ouzas, C. Fraschini, R. M. Berry, M. A. Dubé, and E. D. Cranston, "How latex film formation and adhesion at the nanoscale correlate to performance of pressure sensitive adhesives with cellulose nanocrystals," *Philosophical Transactions of the Royal Society A: Mathematical, Physical and Engineering Sciences*, vol. 379, no. 2206, p. 20200330, 2021, doi: 10.1098/rsta.2020.0330.

[25] J. Tang, E. S. Daniels, V. L. Dimonie, A. Klein, and M. S. El-Aasser, "Influence of carboxyl groups on the morphology and surface properties of films prepared from model carboxylated latex blends," *ACS Symposium Series*, vol. 790, pp. 212–232, 2001, doi: 10.1021/bk-2001-0790.ch012.

[26] J. Tang, V. L. Dimonie, E. S. Daniels, A. Klein, and M. S. El-Aasser, "Study of the Drying Behavior of Model Latex Blends during Film Formation: Influence of Carboxyl Groups," *Macromolecular Symposia*, vol. 155, pp. 131–161, 2000.

[27] S. Mondal, "Review on Nanocellulose Polymer Nanocomposites," *Polymer - Plastics Technology and Engineering*, vol. 57, no. 13, pp. 1377–1391, 2018, doi: 10.1080/03602559.2017.1381253.

[28] I. Kalashnikova, H. Bizot, P. Bertoncini, B. Cathala, and I. Capron, "Cellulosic Nanorods of Various Aspect Ratios for Oil in Water Pickering Emulsions," *Soft Matter*, vol. 9, no. 3, pp. 952–959, 2013, doi: 10.1039/c2sm26472b.

[29] M. S. Reid, M. Villalobos, and E. D. Cranston, "Benchmarking Cellulose Nanocrystals: From the Laboratory to Industrial Production," *Langmuir*, vol. 33, no. 7, pp. 1583–1598, Feb. 2017, doi: 10.1021/acs.langmuir.6b03765.

[30] M. Bushell *et al.*, "Particle size distributions for cellulose nanocrystals measured by atomic force microscopy: an interlaboratory comparison," *Cellulose*, vol. 28, no. 3, pp. 1387–1403, 2021, doi: 10.1007/s10570-020-03618-4.

[31] F. Bettaieb, R. Khiari, A. Dufresne, M. F. Mhenni, and M. N. Belgacem, "Mechanical and thermal properties of Posidonia oceanica cellulose nanocrystal reinforced polymer," *Carbohydrate Polymers*, vol. 123, pp. 99–104, 2015, doi: 10.1016/j.carbpol.2015.01.026.

[32] M. Mariano, N. El Kissi, and A. Dufresne, "Cellulose nanocrystal reinforced oxidized natural rubber nanocomposites," *Carbohydrate Polymers*, vol. 137, pp. 174–183, 2016, doi: 10.1016/j.carbpol.2015.10.027.

[33] W. P. Flauzino Neto *et al.*, "Mechanical properties of natural rubber nanocomposites reinforced with high aspect ratio cellulose nanocrystals isolated from soy hulls," *Carbohydrate Polymers*, vol. 153, pp. 143–152, 2016, doi: 10.1016/j.carbpol.2016.07.073.

[34] A. Dufresne, *Cellulose-Based Composites and Nanocomposites*. Elsevier, 2008. doi: 10.1016/B978-0-08-045316-3.00019-3.

[35] M. Roohani, Y. Habibi, N. M. Belgacem, G. Ebrahim, A. N. Karimi, and A. Dufresne, "Cellulose whiskers reinforced polyvinyl alcohol copolymers nanocomposites," *European Polymer Journal*, vol. 44, no. 8, pp. 2489–2498, Aug. 2008, doi: 10.1016/j.eurpolymj.2008.05.024.

[36] I. Kalashnikova, H. Bizot, B. Cathala, and I. Capron, "Modulation of cellulose nanocrystals amphiphilic properties to stabilize oil/water interface," *Biomacromolecules*, vol. 13, no. 1, pp. 267–275, 2012, doi: 10.1021/bm201599j.

[37] X. Xu, F. Liu, L. Jiang, J. Y. Zhu, D. Haagenson, and D. P. Wiesenborn, "Cellulose nanocrystals vs. Cellulose nanofibrils: A comparative study on their microstructures and effects as polymer reinforcing agents," *ACS Applied Materials and Interfaces*, vol. 5, no. 8, pp. 2999–3009, 2013, doi: 10.1021/am302624t.

[38] M. A. Saïd Azizi Samir, F. Alloin, M. Paillet, and A. Dufresne, "Tangling Effect in Fibrillated Cellulose Reinforced Nanocomposites," *Macromolecules*, vol. 37, no. 11, pp. 4313–4316, Jun. 2004, doi: 10.1021/ma035939u.

Chapter 6

Towards a Fully Biobased Pressure-Sensitive Adhesive

Vida A. Gabriel, Marc A. Dubé
University of Ottawa, 161 Louis Pasteur Pvt, Ottawa, K1N 6N5, Canada

Email: Marc.dube@uottawa.ca

This chapter is a manuscript submitted to ACS Sustainable Chemistry & Engineering journal.

6.1 Abstract

The development of adhesive polymers derived from renewable materials is a rapidly emerging research field driven by the rising demands for polymer sustainability. The use of bio-based and biodegradable feedstock to produce commodity polymers often yields products that are outperformed by their petroleum-based equivalents due to various synthetic challenges. To date, the drawbacks of polymers produced from renewable materials in terms of their application properties, ease of production and cost are still too great for their complete commercial adoption. In this work, 12% of the monomer used in the formulation of a latex-based pressure-sensitive adhesive (PSA) was replaced with starch nanoparticles (SNPs), a biodegradable material. To reduce the potential for negative effects to be imparted on the adhesive properties, the SNPs were encapsulated as latex particle cores, within acrylic particle shells, which govern the PSA properties, made from a model system for an ~80% bio-sourced acrylic monomer formulation. The core-shell latexes, produced via seeded semi-batch emulsion polymerization, yielded bimodal particle size distributions, which played an important role in the PSA properties. To address any performance challenges related to substituting petroleum- with bio-based components, cellulose nanocrystals (CNCs), a bio-based material, were incorporated as property performance enhancers. Herein, the challenges of combining SNPs and CNCs in an emulsion-based PSA were overcome and the SNP and CNC loadings were varied to tune the adhesive properties of the PSA films within the performance range of various commercial tapes.

Keywords: Emulsion polymerization, starch nanoparticles, cellulose nanocrystals, pressure-sensitive adhesives, latex, core-shell particles

6.2 Introduction

Since the early 1970's, concerns about plastic pollution on land and in oceans have been on the rise. Although the positive impacts of polymers on our quality of life are incontestable (e.g., medicine, transportation, electronic technologies), the same properties that render plastics useful (e.g., strength, durability, water resistance, low cost) result in their accumulation in nature leading to harm to animal and plant life. In addition, their production methods often require the use of solvents, which are likewise polluting the environment.[1] Due to stringent societal demands for environmental justice, scientists and engineers have been developing better plastic waste management strategies.

In a way similar to the pulp and paper industry's push to use recycled paper to manufacture their products, there have been efforts to recycle plastics to produce new materials. One of the main challenges of plastic recycling is that the separation of polymers into their respective components (monomers, fillers, etc.) is not straightforward. In addition, the polymeric material quality often deteriorates with processing. Upcycling, the production of a material of higher value/quality than the originating material, has been proposed as a more economical way of managing waste from single-use plastics.[2] However, as with many polymeric materials, upcycled plastics will ultimately end up as landfill or be incinerated at their end of life stage because these traditional disposal practices are simpler and less costly.

Due to public pressure and government regulations, the paper industry has developed many innovations to replace single-use plastics in a variety of settings; e.g., paper cups, paper straws and wooden stirrers in coffee shops; paper bags in grocery stores; paper padded mailers and shipping containers. Nonetheless, these paper products almost always contain a polymeric binder or adhesive that can at best pose challenges in recycling equipment fouling and at worst, risk being toxic.[3] Thus, the production of non-toxic and/or biobased adhesives is of interest.

Pressure-sensitive adhesives (PSAs) are viscoelastic polymers that have unique properties – PSAs should simultaneously display high molecular mobility and flow at room temperature while also exhibiting a certain degree of cohesiveness (i.e., flow resistance). The specific balance between flowability/wettability (i.e., adhesion) and strength (i.e., cohesion) can be attained by using a combination of monomers and property modifiers. Due to the increasingly urgent

demand for more sustainable products, adhesive production methods are moving towards water-based methods (i.e., emulsion polymerization) rather than solvent-based ones (i.e., solution polymerization). Furthermore, their composition is moving towards sustainably sourced, bio-based, raw materials, resulting in hopefully biodegradable products (note: it should be acknowledged that degradability is not necessarily the result of using biobased materials). The use of bio-based or bio-sourced feedstock for the production of resins, paints and coatings is a classic example.[4–6] (We distinguish bio-based and bio-sourced as follows: bio-based refers to a naturally occurring resource whereas bio-sourced implies a derivatization of the naturally occurring resource).

The use of bio-feedstock in PSAs has been the subject of many recent studies and include bio-based materials such as lignin, tannins, starch, soybean oil, and sugar-cane.[7–9] Badía et al. synthesized PSAs from 72% bio-sourced materials via emulsion or latex polymerization.[10] In their work, they used 2-octyl acrylate (2OA, 73% bio-sourced) and isobornyl methacrylate (IBOMA, 71% bio-sourced) derived from castor oil and pine resin, respectively. In later work, they produced latex-based coatings containing 2OA and IBOMA along with a sugar-based vinyl monomer (EcoMer©, EcoSynthetix) to introduce a biodegradable element to their formulation.[11] Though work to replace petroleum-derived monomers with bio-based ones is advancing rapidly, the resulting polymeric materials can underperform compared to their petrochemical counterparts.[10, 12] Moreover, additives such as rheology modifiers, cross-linkers and chain transfer agents are commonly used to strengthen the bio-based PSAs to achieve the same performance for the compared to their conventional competitors. However, these additives are often the most toxic and polluting components in a latex polymer.[13–15] Thus, to avoid these toxic additives, nontoxic fillers can be used to modify the polymer properties.

Composites are materials made of two or more components, notably, a matrix (e.g., polymer, binder) and a filler. The matrix serves to distribute any applied load within a composite while surrounding and protecting the filler. The filler serves to enhance the chemical, mechanical or physical properties of the composite material. Nanomaterials have been gaining popularity as fillers in polymer composites because they come in different shapes (e.g., spherical, rod-like, tube), diameters (e.g., nanometers to microns), and can provide significant physical and chemical

enhancements with their addition in very small amounts.[16–19] Starch, a commonly used filler, is a naturally occurring and biodegradable material that can be physically or chemically modified to alter its shape and size or to introduce functionality.[20–24] For example, as a nanocrystal, starch has been used as a Pickering stabilizer[25, 26] or a reinforcing agent,[20, 27, 28] and as a nanoparticle, it has been used as a filler for polymer matrix reinforcement.[29] Nanostarch has been used to displace up to 25% monomer in an emulsion polymerization when used as a reactive copolymer or filler.[30] Using starch in these ways not only displaces monomer and increases bio-content, but it takes the sustainability of the resulting latex to a new level because starch is also biodegradable.

Cellulose, the building block for starch, has gained favour in the production of polymer composites. Cellulose has crystalline regions that can be extracted to yield cellulose nano fibrils or cellulose nanocrystals (CNCs). Like starch nanoparticles, CNCs can be incorporated in emulsion polymer formulations due to their hydrophilicity, and they can improve the mechanical and adhesive properties of a polymeric material.[31, 32] To counteract the potential performance modifications caused by the addition of bio-based materials (compared to their petroleum-based counterparts), CNCs can be added in lieu of rheology modifiers, thickeners, chain-transfer agents or crosslinkers to achieve remarkable adhesive performance.[33–37] Furthermore, when added to a latex-based PSA formulation, CNC loadings of 0.5 – 1% improved both the adhesive and cohesive properties simultaneously[38–44] – an effect that is rarely seen with the addition of a single component to a PSA formulation.[45–47]

The objective of this work was to use all of the available tools and techniques to maximize the bio-content and sustainability of latexes produced for PSAs whilst maintaining the same (or better) performance compared to petrochemical counterparts. To our knowledge, this work presents the first combined use of SNPs and CNCs for emulsion-based PSAs. We explore the combination of these two renewable nanocomposites in a model monomer system for a high bio-content PSA formulation. The model system consists of 91.5 wt.% n-octyl acrylate (nOA), 4.5 wt.% styrene (STY) and 4.0 wt.% acrylic acid (AA). We refer to nOA as a “model” monomer for 2OA because they have the same molecular weight and share a similar molecular structure (Figure 6.1). Because AA and STY can also be biosourced,[48–53] our monomer system models an

acrylic formulation that can be up to 75% biosourced. The focus then, is to explore the displacement of 12% of the monomer in the latex particle cores with functionalized SNPs. Furthermore, the adhesive properties of the resulting PSAs are modified by adding up to 1 wt.% CNCs into the polymer matrix.

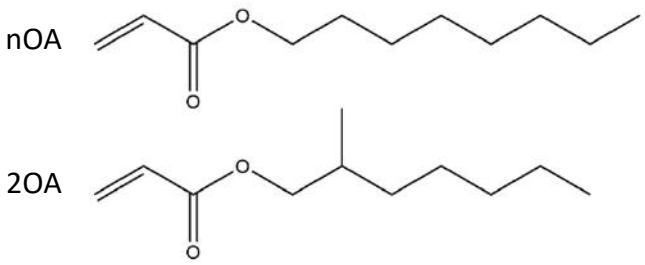

Figure 6.1 Molecular structure of nOA (top) and 2OA (bottom).

6.3 Materials and Methods

6.3.1 Materials

The monomer, n-octyl acrylate (nOA, 99%), was purchased from TCI America. Styrene (STY, >99% stabilized by 20–200 ppm hydroquinone), acrylic acid (AA, 99%, stabilized by 20–200 ppm hydroquinone), potassium persulfate initiator (KPS, >99%) and sodium dodecyl sulfate surfactant (SDS, ACS Reagent >99%) were purchased from Sigma Aldrich. The nOA and STY were purified by passing them dropwise through an inhibitor removal column and the AA was used as received. Experimental grade starch nanoparticles (SNPs) and a functionalized sugar-based monomer (FSM, EcoMer®) were supplied by EcoSynthetix Inc. (Burlington, ON). Sodium trimetaphosphate cross-linker (STMP, food grade, Sigma Aldrich), sodium bicarbonate buffer ($NaHCO_3$, ACS certified, Sigma Aldrich), hydrochloric acid (HCl, 1 M, Fisher Scientific), sodium hydroxide pellets (NaOH, Fisher Scientific) and butyl vinyl ether (BVE, 98%, Sigma Aldrich) were used as received. Sulfated cellulose nanocrystals (CNCs) (CelluForce Inc., Windsor, ON) were obtained as a spray-dried powder (dimensions: 183 $\pm$ 8 nm long and 6 $\pm$ 2 nm in cross section) and had a nominal sulfate half-ester surface charge of 250 mmol kg^{-1} CNC.[54] Distilled deionized water (DDW) with a resistivity of 18.02 $\pm$ 0.2 MΩ-cm was used for all experiments and characterization.

6.3.2 CNC redispersion

The CNCs were redispersed in the DDW reserved for the pre-emulsion solution: 0.75 to 1.5 g CNC powder was mixed in 150 g DDW using a magnetic stir bar and plate overnight. The mixture was probe ultrasonicated in an ice bath using a Fisher Scientific 550 sonic dismembrator at 75% amplitude for three intervals of 5 min, with 5 min rest in between.

6.3.3 Modification of SNPs

The SNPs were modified using a procedure detailed elsewhere[55] but the component amounts were slightly modified to increase the solids content of the modified SNPs (mSNPs) to 20 wt.% (Table 6.1). The steps for the modifications (accompanied by a visual representation in Figure 6.2) are as follows: first, 80 g of SNPs was added to 320 g of DDW and left to fully dissolve overnight (Figure 6.2i). The starch solution, along with 0.8 g of $NaHCO_3$, was added to a 500 mL glass RC1e reaction calorimeter (Mettler-Toledo) equipped with a thermocouple and a Hastelloy stirrer and heated to 60°C under continuous mixing (250 rpm) for 25 min. Once heated, pH was adjusted to 11 using 2.0 – 2.8 g of NaOH pellets to prepare for the SNP crosslinking reaction. To increase the crosslink density of the SNPs, 0.8 g of STMP was added to the reactor (Figure 6.2ii) and left to react for 1h (Figure 6.2ii-iii). Once cross-linked, (Figure 6.2iv) vinyl functionalization was performed by adding 8.0 g of FSM dissolved in 18.5 g DDW (i.e., 26.5 g of a 30% aqueous solution) to the reactor (Figure 6.2v) and reacting for another hour (Figure 6.2vi). To stop the reaction, 2-3 g of HCl was added to adjust the pH to 6.5. Proceeding in this way produced a 20 wt.% functionalized SNP solution. Note that the concentrations of $NaHCO_3$, STMP and FSM relative to the SNPs were 1, 1 and 10 wt.%, respectively. The modified SNPs are henceforth referred to as mSNPs.

Table 6.1 Components and method for the production of functionalized (modified) SNPs.

Step	Description	Component	Amount (g)
Initial charge	$NaHCO_3$ added to SNPs dissolved in water. Mixture loaded into reactor and heated to 60°C and stirred (250 rpm) for 25 min. pH adjusted to 11 by adding NaOH.	SNPs	80.0
		DDW	320.0
		$NaHCO_3$	0.8
		NaOH	2.0 – 2.5
SNP cross linking	STMP added to reactor and left to react 1h.	STMP	0.8
Vinyl functionalization of cross-linked SNPs	FSM aqueous solution added to the reactor and left to react 1h.	FSM	8.0
		DDW	18.5
Reaction termination	pH adjusted to 6.5 using HCl to terminate reaction. mSNPs placed in a glass jar and stored at 4°C.	HCl	2.0 – 3.0

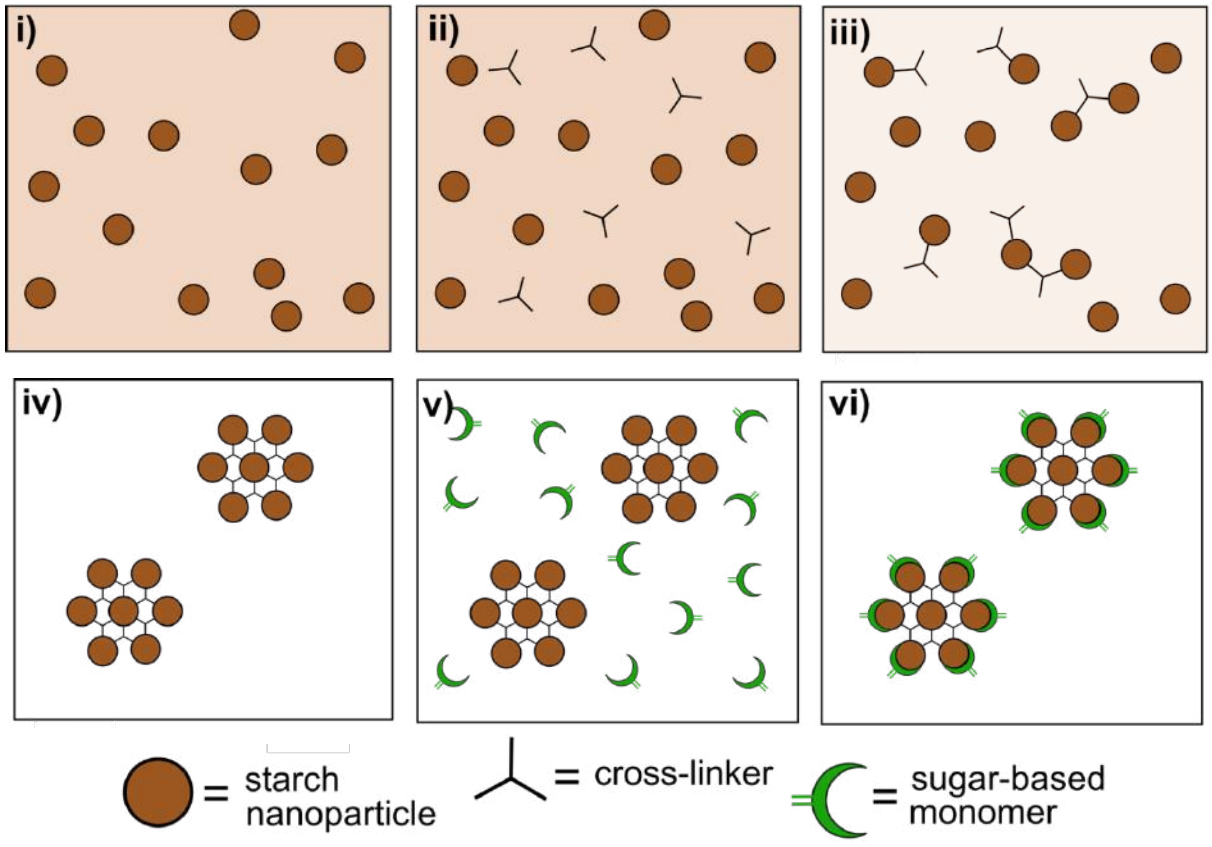

Figure 6.2 Visual representation of the production of modified (i.e., crosslinked and functionalized) starch nanoparticles. Components are not to scale.

6.3.4 Seeded Semi-batch Emulsion Polymerization

The RC1e reactor, equipped with two feed pumps and an inlet for nitrogen purging, was used for the polymerization. An example formulation and procedure is shown in Table 6.2. To begin, the mSNPs (when used), SDS and DDW were loaded to the reactor, heated to 60°C and purged with nitrogen under constant mixing (250 rpm) for ~25 min. Once heated, a small amount of BVE was added as a "tie-layer" monomer and polymerized by injecting an initiator solution (KPS in DDW) to complete the final SNP modification step, which lasted for 45 min; this is referred to as the seed stage. The feed stage consisted of feeding a pre-emulsion solution (monomer, surfactant, and CNC suspension) to the reactor over 240 min, along with an initiator solution (KPS in DDW) which was fed over 270 min. At the end of the feed stage, the latex was left to cook for 1 h.

Table 6.2 Typical formulation and procedure for the production of a 40 wt.% solids latex with 15 wt.% mSNPs and 1 wt.% CNCs. Monomer ratios were 91.5/4.5/4.0 nOA/STY/AA (wt.%) and 1 wt.% surfactant and 1.3 wt.% initiator (relative to total monomer) were used.

	Mixture	Description	Component	Amount (g)
Seed stage	mSNPs and emulsifier	mSNPs DDW and SDS mixed at 250 rpm and heated to 60°C over 25 min. Reactor purged with nitrogen, maintained within 1°C of set temperature and mixed (250 rpm) for the entire reaction.	mSNP	98.0
			DDW	13.8
			SDS	0.40
	Tie-layer Monomer	BVE added to heated solution and left to mix and heat for 5 min.	BVE	10.0
	Seed initiator	Initiator dissolved in DDW injected to reactor to polymerize BVE (45 min).	KPS	0.12
			DDW	2.75
Feed stage	Pre-emulsion	Monomers and surfactant emulsified with CNC + DDW suspension fed to reactor at 0.81 g min^{-1} for 240 min after completion of seed stage.	AA	4.7
			STY	5.3
			nOA	107.3
			SDS	1.32
			CNC	1.6
			DDW	75.3
	Feed initiator	Initiator solution fed to reactor at 0.16 g min^{-1} for 270 min after completion of seed stage.	KPS	1.2
			DDW	41.0

Cook stage		Reactor contents left to mix at 60°C for 1 h to ensure conversion of residual monomer.		

To produce latexes without mSNP cores, the seeding stage was slightly modified: water and surfactant were loaded to the reactor instead of the mSNP solution, and in lieu of the BVE, 20 g of monomer solution (91.5/4.5/4.0 wt.% nOA/STY/AA) was added to form the seed latex. For all reactions, the initiator (KPS) and surfactant (SDS) concentrations were 0.34% and 1.0%, respectively, relative to the monomer weight.

Table 6.3 Typical formulation and procedure for the production of a 40 wt.% solids latex without mSNPs or CNCs (i.e., base-latex). Monomer ratios are 91.5/4.5/4.0 wt.% nOA/STY/AA and 1 wt.% surfactant and 1.3 wt.% initiator (relative to total monomer) were used.

	Mixture	**Description**	**Component**	**Amount (g)**
Seed stage	Seed emulsifier	Emulsifier solution mixed at 250 rpm and heated to 60°C over 25 min. Reactor purged with nitrogen, maintained within 1°C of set temperature and mixed (250 rpm) for the entire reaction.	DDW	100
			SDS	0.25
	Monomer	Seed monomer (~10 wt% of total monomer) added to heated emulsifier solution and left to mix and heat for 5 min.	AA	0.80
			STY	0.90
			nOA	18.30
	Seed initiator	Initiator dispersed in DDW injected to reactor to initiate seed reaction (45 min).	KPS	0.05
			DDW	5.0
Feed stage	Pre-emulsion	Emulsified monomers, water, and surfactant fed to reactor at 0.68 g min^{-1} for 240 min after completion of seed stage.	AA	4.70
			STY	5.30
			nOA	107.5
			SDS	1.33
			DDW	43.75
	Feed initiator	Initiator + water solution fed to reactor at 0.16 g min^{-1} for 270 min after completion of seed stage.	KPS	201.3
			DDW	43.75
Cook stage		Reactor contents left to mix at 60°C for 1 h to ensure conversion of residual monomer.	KPS	0.25
			DDW	2.50

6.3.5 Latex Characterization

Samples were taken throughout the reactions at intervals of 30-60 min to track particle size, pH, conversion and solids content of the latexes. A Malvern Zetasizer 2000 was used to measure the particle size and particle size distribution; the pH was measured using a Fisher Scientific/Accumet Research AR50 Dial Channel pH meter; and the conversion and solids content were calculated via gravimetry. Final latexes were characterized for viscosity using a Thermo Scientific HAAKE Viscotester (Model D), glass-transition temperature (T_g) using a TA Instruments Model Q100 DSC, and gel content via solvent extraction. Details of the above characterization methods can be found elsewhere.[43]

6.3.6 PSA Testing

Adhesive films for PSA testing were prepared by casting ~15 g of latex on a corona treated Mylar sheet (Melinex 462 0.002 MIL, Tekra) using Meyer rods No. 30 and No. 50 to produce films of approximately 18 g m^{-1} and 30 g m^{-1}, respectively. Films were dried for 48 h at 50 $\pm$ 5% relative humidity and at 23 $\pm$ 2°C and tested under the same conditions. Bluehill 2 Materials Testing Software was used with an Instron 3000 Universal Tester, and Pressure Sensitive Tape Council (PSTC) methods[56] were employed to measure the peel strength, loop tack and shear strength of the prepared films. Details of these methods can be found elsewhere.[43]

6.4 Results and Discussion

6.4.1 Producing Latexes with mSNPs and CNCs

PSAs are polymers with a specific balance of fluidity, tackiness and strength. Their practicality (e.g., quick adherence, residue-free removal) and properties (e.g., strength, tackiness) are a direct result of their microstructure, which can be fine-tuned to specific applications. Low T_g acrylic monomers (e.g., butyl acrylate, 2-ethylhexyl acrylate) make up the majority of a PSA formulation because they are soft and tacky at room temperature. To provide some cohesiveness, a lesser amount of high T_g monomer (e.g., methyl methacrylate, styrene) can be used. Monomers with functional groups (e.g., AA) can also be introduced.

To increase the sustainability of PSA films, latex particle cores can be replaced with a filler such as starch; not only does this displace some petroleum-based feedstock but it introduces a

biodegradable component. Zhang et al.[55] developed a method to cross-link and functionalize SNPs (i.e., produce mSNPs) for this very purpose. In their pioneering work, they produced latex particles with a core-shell morphology; mSNPs were encapsulated within the particles (core) and then enveloped with an acrylic polymer shell as illustrated in Figure 6.3. In general, film formation and bulk adhesive properties of latex films are governed by the surface properties of the polymer particles.[57, 58] Thus, with a low T_g polymer shell, the core-shell latexes resulted in PSA films that maintained the tackiness and peel strength of the original base-latex. However, the shear strength slightly decreased.[55]

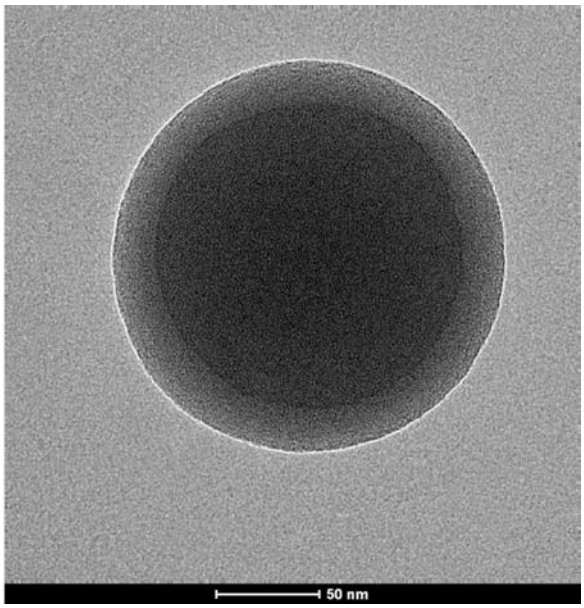

Figure 6.3 TEM image of a core-shell latex particle produced with an SNP core and poly(methyl-methacrylate) shell. Figure reproduced with permission.[55] Copyright 2018 Elsevier.

The addition of nanoparticles to a polymer matrix is advantageous for property modification because of their high surface area to volume ratio and functionality, which leads to significant particle-matrix interactions at low loadings. CNCs are hydrophilic and thus compatible with water-based systems such as emulsion polymerizations. While these extraordinarily efficient additives require energy intensive dispersion (i.e., they require sonication when in powder form) and require significant amounts of water, once redispersed, the suspended CNCs are highly stable and can be added at any stage of a semi-batch emulsion polymerization.[43, 44] To compensate for the decrease in shear strength, such as was noted above for the mSNP core-

shell latexes, we added CNCs because they have been shown to increase the shear strength in latex-based PSA films. In fact, CNCs have been shown to increase all three PSA performance properties simultaneously, which is atypical because the improvement in adhesive strength often corresponds to a decrease in cohesive strength, or vice versa. [45–47] The ability of CNCs to increase the adhesive and cohesive performance of PSA films at low loadings (0.5% - 1% relative to monomer) arises because their reinforcing mechanism does not affect the polymer microstructure.[38–44]

When combining mSNP latexes with CNCs, we were faced with the challenge of limiting the solids concentration in the latex because of the significant water requirements emanating from both the SNP modification and CNC redispersion. For instance, the method to produce mSNPs yields a 13 wt.% suspension in water.[55] Thus, to displace 15% of the monomer in a 40 wt.% solids latex (total mass 350 g), Zhang et al. added 172.2 g of mSNP solution to the seed stage (i.e., 21 g of mSNPs and 151.2 g water). Because high shear mixing (in this case, probe sonication) can alter the mSNPs, the CNCs cannot be redispersed in the presence of mSNPs but should instead be incorporated in the feed solution. Of the remaining water, 78 g was allocated to the initiator solutions thereby leaving 27.8 g of water in the pre-emulsion for CNC redispersion. It is generally advised to limit the concentration of a CNC suspension in the feed stage to 17.87 g L^{-1} to maintain a good quality suspension.[43] Therefore, the maximum mass of CNCs that could be added to the latex is 0.5 g, which amounts to 0.36 wt.% relative to the monomer mass. Recalling that meaningful PSA enhancements were achieved with at least 0.5 wt.% loadings, the SNP modification method was altered in this work to yield 20 wt.% mSNP solutions (as described in the experimental methods section). In this way, a larger amount of water was made available for CNC redispersion. In addition, because the KPS initiator has a high solubility in water at room temperature, we were able to move some water from the initiator solutions to the pre-emulsion solution. Thus, stable 40 wt.% latexes with 15% mSNP cores and 0.5% to 1.0% CNCs in the matrix were produced (percentages relative to monomer).

6.4.2 Effect of mSNP and CNC Loading on Latex Properties

Reaction trajectory

The monomer conversion profile of latexes containing 15% mSNPs was different than that of latexes made with 0-12% mSNPs. For example, there was a significant delay (1.5 h) in conversion for latexes produced with >12% mSNPs and the final conversion was low (80%). More initiator could have been added but this would have resulted in significant latex property changes from run to run and it was therefore decided to limit the mSNP loading to 12%. Consequently, a series of nine experiments were run following a three-level two-factor experimental design (3^2) to study the effects of mSNP and CNC loading on PSA properties (Table 6.4). The mSNP loadings were 0, 6 and 12%, and those of the CNCs were 0, 0.5 and 1.0% (percentages are relative to monomer mass; experiments were conducted in random order). Typical monomer conversion, solids content, particle size and pH evolution for experiments without and with mSNP cores are presented in Figure 6.4 and 6.5, respectively, and are discussed next. In general, the latexes with mSNPs (Figure 6.5D) had a higher pH than those without (Figure 6.4D) because the mSNP solution had a pH of ~6.5.

Table 6.4 3^2 factorial design: mSNP and CNC loadings

Run ID	mSNP loading (%)	CNC loading (%)
0,0	0	0
0,0.5		0.5
0,1		1.0
6,0	6	0
6,0.5		0.5
6,1.0		1.0
12,0	12	0
12,0.5		0.5
12,1		1.0

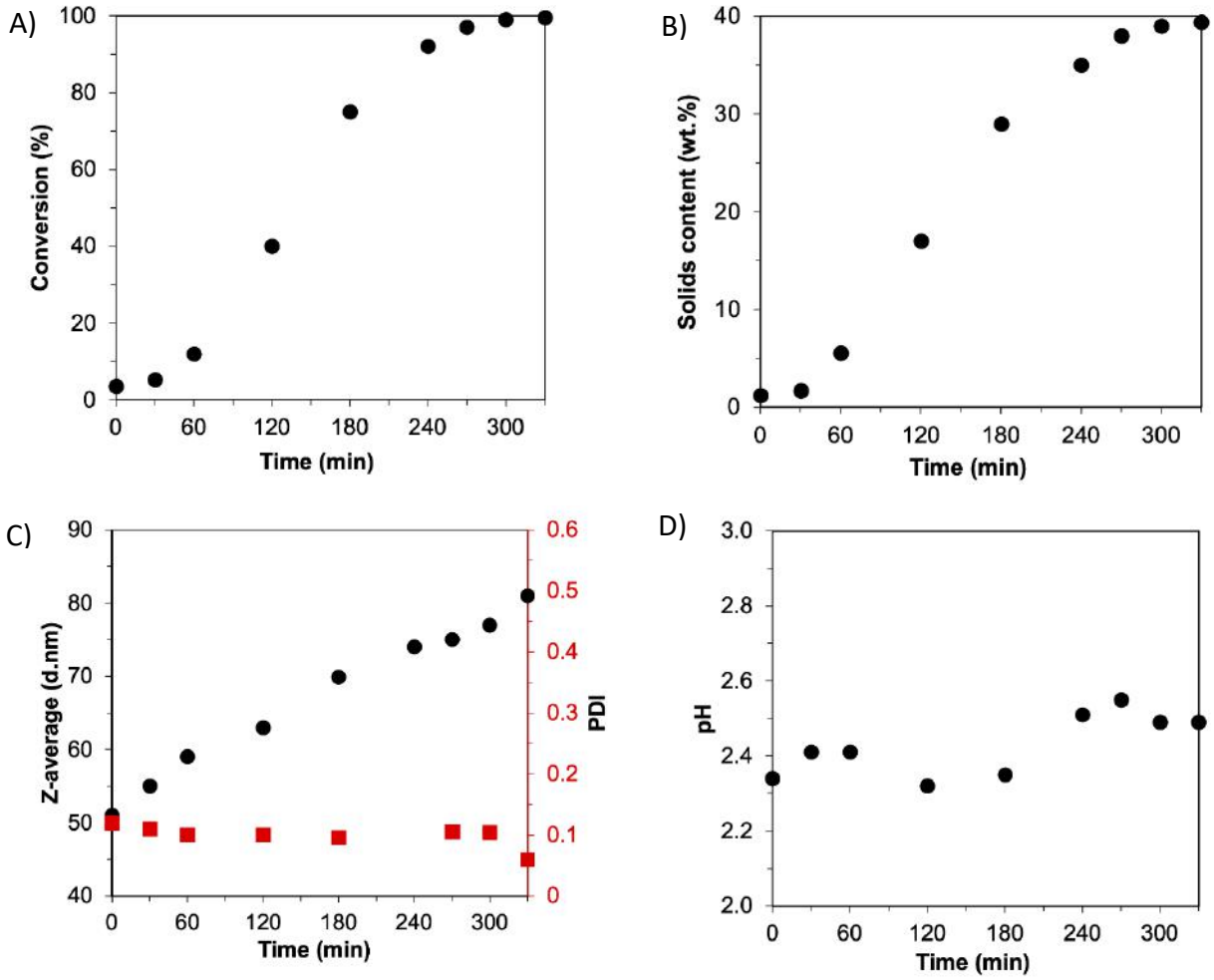

Figure 6.4 Typical A) monomer conversion, B) solids content, C) z-average, and D) pH profiles vs. time for latexes produced with CNCs (Run ID 0,1).

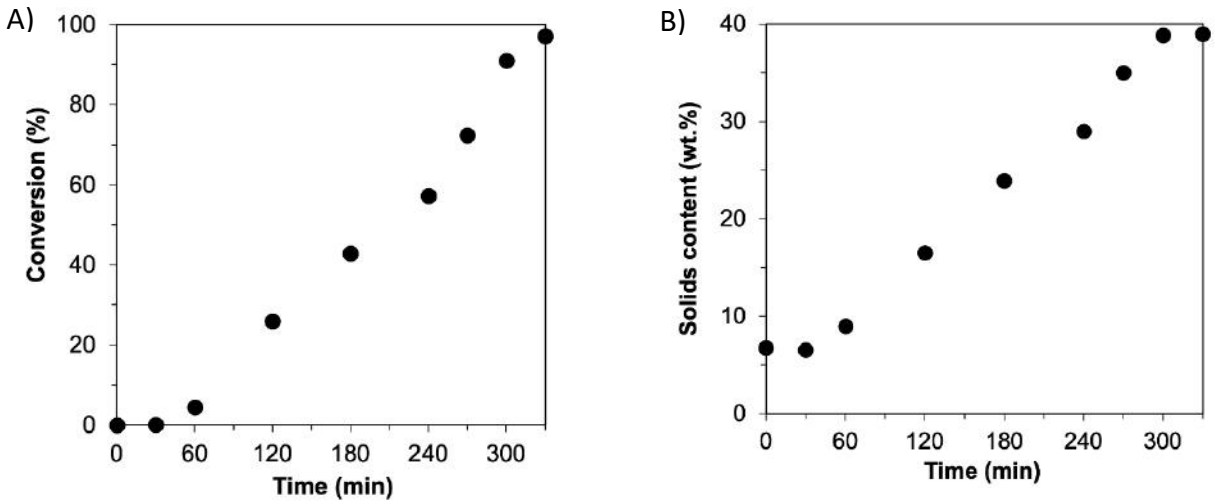

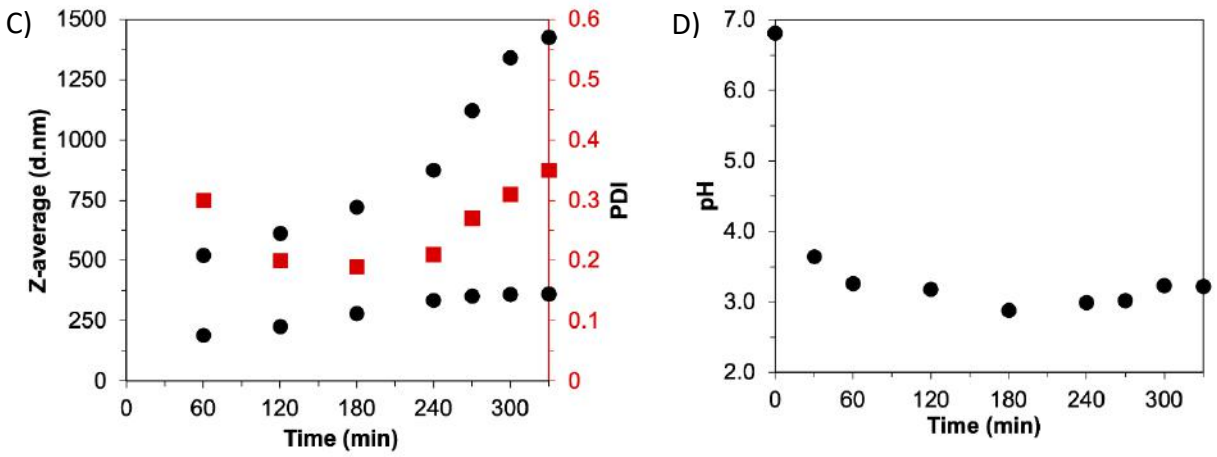

Figure 6.5 Typical A) monomer conversion, B) solids content, C) z-average, and D) pH profiles vs. time for latexes produced with mSNPs (Run ID 6,0).

Particle size

The initial and final particle diameters varied greatly from run to run. Latexes produced without mSNP cores followed traditional conversion and particle size trajectories (Figure 6.4C) and had final particle sizes between 72 – 189 nm depending on CNC loading (Table 6.5). On the other hand, latexes with mSNP cores could not be characterized for particle size at the end of the seeding stage (Figure 6.5C, t = 0) because the monomer conversion was too low to prepare stable samples for DLS. After ~1 h of monomer feeding, the conversion was high enough to measure particle size and the latex displayed a bimodal size distribution (Figure 6.5C, t = 60 min). Due to the changes made to the SNP cross-linking and functionalization reaction protocols compared to previous work, the mSNPs were larger in the current work.[30, 55] Because of this, the same volume of mSNPs generated fewer seed particles, which resulted in an excess of unreacted monomer and surfactant. Consequently, at the onset of the semi-batch feed (t = 0) a second population of particles was nucleated. The larger particle diameters observed in Figure 6.5C (500 – 1500 nm) were particles with mSNP cores, whereas the smaller particles (100 – 300 nm in diameter) were the result of a secondary micellar nucleation. With a loading of 6% mSNPs, between 62 and 69% of the particles were large (i.e., had mSNP cores) and the remaining 31-38% were small (i.e., nucleated from micelles). Latexes produced with 12% mSNPs likewise displayed particle bimodality, however, the ratio of large to small particles was higher because of the higher number of mSNP seed particles; only 10-14% of the particles were fully acrylic. As noted in Table

6.5, particle sizes differed significantly from run to run. The final particle size(s) and intensity of each of the latexes are presented therein.

Table 6.5 Final latex particle diameter and T_g.

Run ID (mSNP% + CNC%)	Z-average particle diameter (d.nm)	
	Peak 1 (volume %)	Peak 2 (volume %)
0,0	189.1 *(100%)*[a]	-
0,0.5	72.2 *(100%)*	-
0,1.0	81.0 *(100%)*	-
6,0	1426.0 *(66%)*	361.2 *(34%)*
6,0.5	878.4 *(69%)*	405.6 *(31%)*
6,1.0	1326.0 *(62%)*	379.4 *(38%)*
12,0	4563.6 *(90%)*	276.1 *(10%)*
12,0.5	4202.7 *(86%)*	289.0 *(14%)*
12,1.0	4309.2 *(87%)*	281.6 *(13%)*

[a]Base-latex was produced at a higher solids content (50 wt.%) to improve film formation.

Minitab™ software was used for statistical modeling to uncover the effects of mSNP and CNC loading on the particle size(s) and the relative peak volume percent. The predictors were standardized using the following equation:

$$Standardized\ variable = \frac{\text{(value of operating variable)} - \text{(average of upper and lower limits)}}{\text{half the range between upper and lower limits}} \quad \text{Eq. 6.1}$$

Regression models were fitted using all first- and second-order variable interactions and subsequently reduced to retain only the statistically significant terms using backwards elimination at a significance level of 5% (i.e., $\alpha = 0.05$). This method was used throughout the work to fit all subsequent regression models. Detailed Minitab outputs can be found in the Supporting Information. The regression equation for the particle diameter of peak 1 (i.e., particle size 1, or PS1) and its adjusted-R^2 value are presented in Eq. 6.2 and the corresponding surface plot is shown in Figure 6.6.

$$\text{PS1 (d.nm)} = 1034 + 2122\ \text{mSNP} - 77\ \text{CNCs} + 1026\ \text{mSNP}^2 + 265\ \text{CNCs}^2 \quad \text{Eq. 6.2}$$
$$(R^2_{adj} = 99.51\%)$$

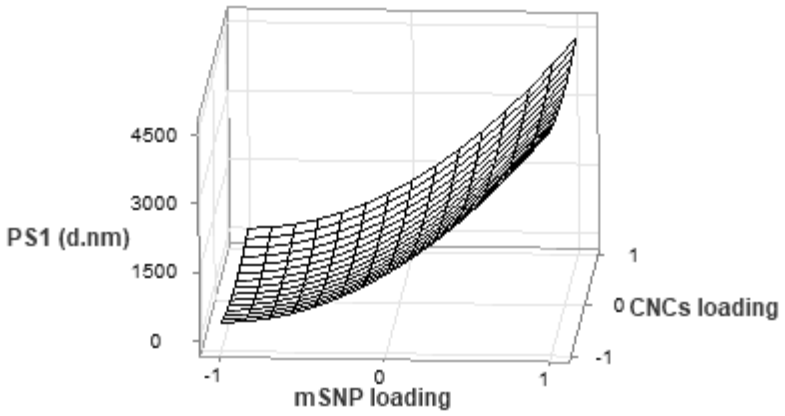

Figure 6.6 Surface plot of the regression model for the particle diameter of peak 1 (PS1) as a function of mSNP and CNC loadings from mSNP = 0 – 12% and CNC = 0 – 1% (R^2_{adj} = 99.51). Note that the mSNP and CNC predictors are standardized on the figure.

Both the mSNP and CNC loadings had a statistically significant effect on PS1. As the mSNP and CNC loadings increased, PS1 increased. With the addition of mSNPs there was a greater number of large particle cores for the polymerization and thus, the particle diameter of the larger particles (i.e., PS1) increased. The effect of the CNCs was slightly nuanced because of the negative CNC and positive CNC^2 terms in the model. At a lower loading (CNC = 0.5%) the effect of the negative term in Eq.2 dominates thereby reducing the particle diameter. In other words, for a given mSNP loading, adding 0.5% CNCs decreased the particle diameter of peak 1 (Table 6.5). This was attributed to CNCs' ability to adsorb to polymer particle surfaces and create particle-particle barriers similar to Pickering stabilizers (CNCs have been used in lieu of surfactant in other work).[59, 60] However, with further increases in CNC loading (CNC = 1 %), the effect of the positive term of the equation dominates and PS1 increases slightly because of increased surfactant/CNC interactions related to ionic strength effects. Because of the mSNPs' lower general reactivity, the KPS loading in this work was high (1% relative to monomer) compared to other work (~0.34% relative to monomer).[40, 41, 43] CNC suspension stability is affected by ionic strength[61] and although the KPS loading remained constant from run to run, CNC/ion interactions increased with CNC loading.

The regression equations for the particle diameters of peak 2 (i.e., particle size 2, or PS2) and the volume fraction of PS1 (i.e., percentage of particles in peak 1, or %PS1) are presented in Eq. 6.3 and 4 (along with their adjusted-R^2 values) and their corresponding fitted lines are shown

in Figure 6.7 and 6.8, respectively. Only the mSNP loading had a statistically significant effect on PS2 and %PS1 (i.e., $p < \alpha$ of 0.05) and therefore all terms involving the CNC loading were removed during the backwards elimination. Without mSNPs, the PSD was unimodal and thus %PS1 was 1 (i.e., 100%) and PS2 was zero (Figure 6.7 and 6.8, respectively). With the addition of 6 wt.% mSNPs, a secondary population of particles was nucleated hence the appearance of PS2. Relative to the 12% loading, latexes with 6% mSNPs had a smaller number of latex particles with mSNP cores (i.e., lower %PS1) and thus, PS2 was higher (discussed previously). In other words, as the mSNP loading increased %PS1 increased (Figure 6.8) and the particle size of PS2 decreased (Figure 6.7).

$$\mathrm{PS2\ (d.nm)} = 382 + 141\,\mathrm{mSNP} - 241\,\mathrm{mSNP}^2\ (R^2_{adj} = 99.39\%) \qquad \text{Eq. 6.3}$$

$$\%\,\mathrm{PS1\ (\%)} = 0.66 - 62 \times 10^{-3}\,\mathrm{mSNP} + 0.38\,\mathrm{mSNP}^2\ (R^2_{adj} = 97.60\%) \qquad \text{Eq. 6.4}$$

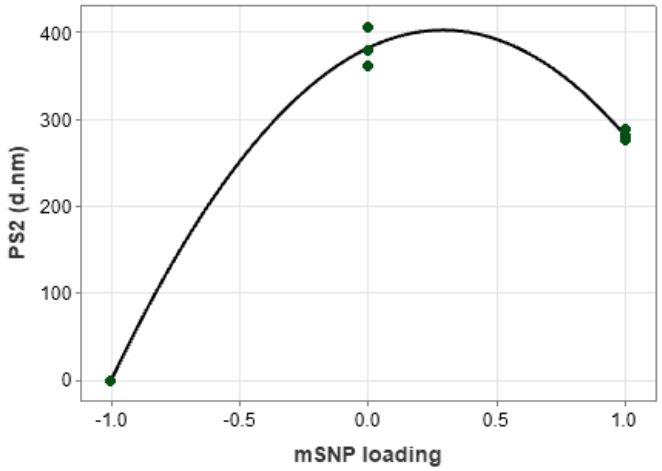

Figure 6.7 Fitted line of the regression model for particle diameter of peak 2 (PS2) as a function of mSNP loading from SNP = 0 – 12% (R^2_{adj} = 99.39%). Data points represent the experimental data. Note that the mSNP predictor is standardized on the figure.

Viscosity and gel content

Variations in particle size, particle size distribution (PSD) and CNC loading can affect latex viscosity. A latex with smaller particles will generally have a higher viscosity than one with larger particles, in a given formulation, because of the increased surface area and therefore, increased particle-particle interactions.[62] Although viscosity trends in latexes with bimodal particle size distributions are more complex, in general, as the particle size or fraction of large particles increases, latex viscosity generally decreases[62, 63] (Table 6.5 and Figure 6.9A). Note that this

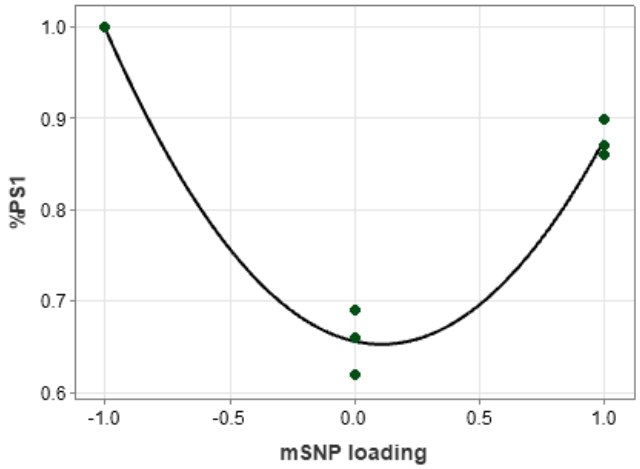

Figure 6.8 Fitted line of the regression model for the intensity of peak 1 (%PS1) as a function of mSNP from SNP = 0 – 12% *(R^2_{adj} = 97.6)*. Data points represent the experimental data. Note that the mSNP predictor is standardized on the figure.

trend cannot be extended to the base-latex because it was produced at a higher solids content (to cast good quality PSA films). CNCs can also cause an increase in latex viscosity because of the increase in CNC-latex particle interactions due to their high surface contact area and functional group interactions.[39, 40, 43] Thus, for a given mSNP loading, an increase in CNC loading increased latex viscosity (Figure 6.9A).

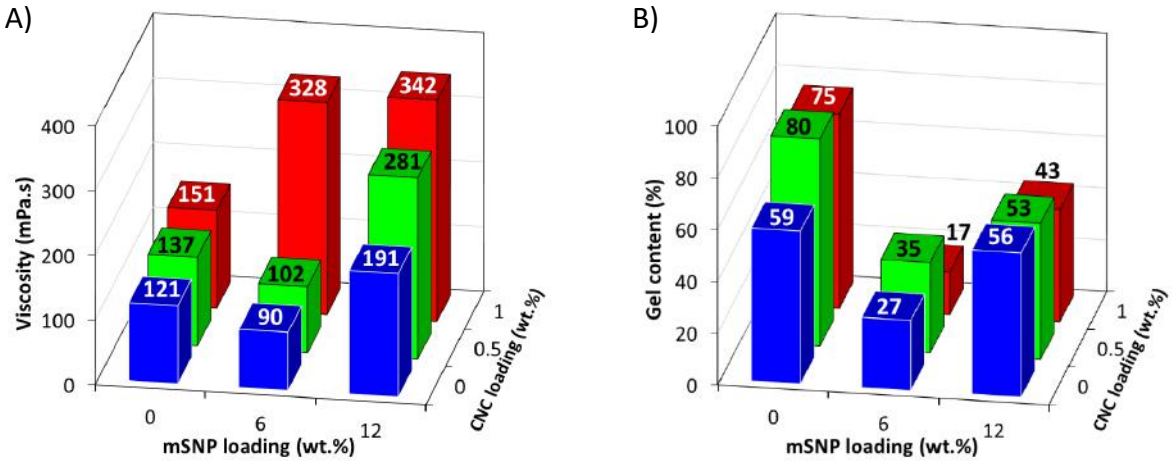

Figure 6.9 Latex viscosity (A) and polymer gel content (B) vs. mSNP and CNC loading.

CNCs have been shown to increase latex gel content without affecting polymer microstructure.[38, 39, 42, 43] However, the effect of CNC loading on the gel content of latexes

produced with mSNP cores was not statistically significant in the present analysis. This was because of the overwhelming effect on gel content due to the particle size and peak distribution which, as discussed above, were the result of the change in mSNP loading. In some cases, latex particle size can affect polymer gel content. For example, higher gel content latexes can be produced with larger particles when using acrylate monomers because of their tendency for intramolecular chain transfer to polymer (i.e., backbiting).[64–67] After standardizing the predictors, gel content was modeled using PS1, PS2 and %PS1 in the regression equation:

$$\text{Gel content}\ (\%) = -28.29\ \text{PS2} * \%\text{PS1} + 46.31\ \text{PS1}^2 \qquad (R^2_{adj} = 98.30\%). \qquad \text{Eq. 6.5}$$

According to Eq. 6.5, PS1 is the largest contributor to the gel content. The polymer gel content was measured using a solvent extraction method in which polymer samples were sealed in poly(vinylidene fluoride) (PVDF) pouches with a pore size of 0.45 μm and soaked in tetrahydrofuran for 48 h. Any soluble polymer would leach out of the pouch and only the insoluble portion (typically, the gel) would be retained. The mSNP cores were much larger (800 – 4000 nm in diameter) than the PVDF pores and thus, were retained in all cases as they too were insoluble. Thus, as the amount of mSNP increased, PS1 increased (Eq. 2) and the gel content increased. The decrease in %PS1, which corresponded to an increase in PS2, led to higher gel contents due to the increased intramolecular chain transfer, as discussed above. The gel content increased with PS1 due to the increased percentage of mSNP cores, which as described above were retained in the PVDF pouches. Finally, the mSNP and CNC loadings did not affect the polymer T_g in a meaningful way; all latexes displayed T_g's of -51.0 ± 2.4°C.

6.4.3 Effect of mSNP and CNC loading on PSA properties

PSA properties of the base-latex (Run ID 0,0) were measured from films prepared from a 50 wt.% solids latex because at 40 wt.%, the latex was not castable. Because latex film thickness has an effect on PSA properties, a smaller Meyer rod (#20 instead of #30) was used to cast the base-latex to yield an equivalent film thickness. Peel strength, tack and shear strength results are presented in Figure 6.10A, B and C, respectively. The PSA properties of other commercial tapes are shown in Figure 9D for comparison.

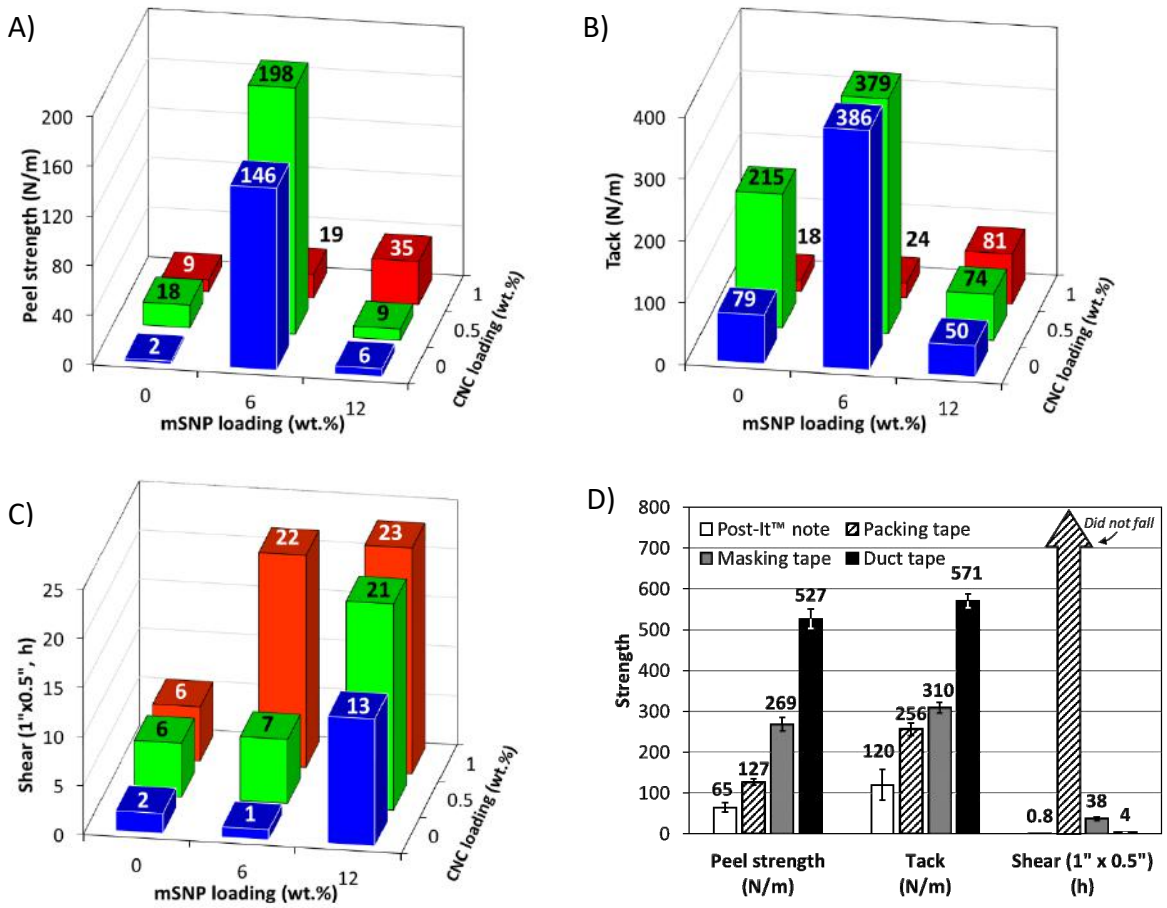

Figure 6.10 A) Peel strength, B) tack, and C) shear strength of films produced from latexes with varying mSNP and CNC loadings (film thickness = 17.6 ± 0.8 g m^{-1}). Adhesive strength of commercial adhesives shown in D) for comparison.

Adding mSNPs and CNCs improved the peel strength, tack, and shear strength of the PSA films relative to the base-latex at most of the load levels (Figure 6.10). The adhesive forces of a PSA (i.e., peel strength and tack) can be enhanced with the addition of hydrophilic components because they can improve the wettability of the films to a substrate.[47] With the exception of experiments with 12 wt.% mSNPs (discussed next), the addition of CNCs resulted in adhesive forces going through a maximum (Figure 6.10A and B). This trend, observed many times before,[33–37] is due to the balance of hydrophilicity and stiffness in the PSA film. At 0.5%, the CNCs' hydrophilicity and hydrogen bonding capabilities improved the films' ability to wet and adhere to the substrate, thereby improving adhesion. At higher loadings, although the material became more hydrophilic, the CNCs contributed to an increase in polymer stiffness, which reduced their mobility to the detriment of the adhesive strength.[40, 47]

Film quality and PSA properties are affected by, among various factors, the ability for the latex particles to deform, pack together, and for their polymer chains to interdiffuse into a continuous film.[68] Smaller particles can deform and fill interstitial voids faster than larger ones because in the larger particles, polymer chains have to flow over greater distances.[69] Broad or multimodal PSDs can produce films with smaller void fractions due to the improved particle organization and bimodal PSDs are known to alter dispersion rheology and facilitate film formation, leading to improved final film properties.[62, 70, 71] Latexes with 6% mSNP cores and 0.5% CNCs displayed the highest peel strength and tack due to the better balance of PSD and particle shell thickness. Increasing the thickness of a soft polymer shell decreases the minimum film formation temperature, which improves the particles' ability to flow and deform during film formation.[57, 68] Finally, the addition of 0.5% CNCs further increased adhesive properties because of film formation facilitation and/or increased film hydrophilicity and film wetting without over-stiffening the films.

The adhesive strength of films containing 12% mSNPs behaved differently than their lower mSNP counterparts due to differences in film formation. Studies on film formation characteristics and film properties of latexes with large, hard particles and small, soft particles, show that there is a critical ratio of small to large particles required to obtain a continuous voidless film.[71] There should be a sufficient number of small particles to fill the voids between the large particles. Even though the mSNP's shells were acrylic, they could not deform as easily as the smaller particles due to their larger, harder cores. Therefore, at the higher mSNP loading (12%), the higher fraction of large, hard particles had a negative effect on film formation and thus, on the adhesive properties (Figure 6.10A and B). Nonetheless, at the 12% mSNP loading, the increasing CNC loading led to increasing peel strength and tack. The morphology (i.e., rod-like) and surface chemistry (polar and hydrophilic sulfate half-ester groups) of CNCs enable them to act as bridges between polymer particles, which improves the homogeneity of PSA films.[44, 72] Thus, for the 12% mSNP films, the CNCs acted as polymer particle bridges and promoted film formation with the resulting positive effect on adhesive strength.

In general, the addition of a stiff filler to otherwise non-linked particles can increase the cohesiveness of a composite material.[47] CNCs improve cohesiveness not only because they are

rigid nanoparticles, but because their surface groups (i.e., sulfate half-esters) introduce the possibility for CNC-CNC, CNC-particle, and CNC-substrate hydrogen bonding.[38, 72, 73] As the CNC loading increased, the film rigidity and the probability of hydrogen bonding increased, leading to higher shear strengths (Figure 6.10C). For the latexes with higher mSNP loadings, not only were the particle cores more rigid (recall, the seed was not a soft acrylic) but the acrylic polymer shell was thinner. Thus, the strengthening effects of higher CNC loadings was more pronounced as the mSNP loading increased because the amount of CNCs relative to polymer surface area was higher.

Although the shear strength was acceptable, the base films' adhesive forces were weaker than that of a 3M™ commercial Post-It™ note (Figure 6.10A-D). However, with the addition of 6% mSNPs and up to 0.5% CNCs, the peel strength increased to 146 – 198 N/m, surpassing that of a commercial packing tape and the tack improved beyond the strength of a commercial masking tape. Moreover, the mSNP and CNC loadings can be used to tune the adhesive strength of a PSA depending on its intended application ranging from Post-It™ notes to masking or duct tapes. Another way that the PSA properties can be fine-tuned is by varying the PSA film thickness. For example, casting thinner films can enable PSAs with 6% mSNPs and 0.5% CNCs to exhibit similar peel and tack to commercial masking tape (Figure S1 of the Supporting Information).

6.5 Conclusion

Growing environmental concerns due to polymer pollution have spurred the development of innovative strategies to increase the sustainability of adhesives. The use of emulsion polymerization for PSA synthesis partly addresses the sustainability of the production step because the technology is water-based as opposed to solvent-based. To improve the sustainability of the PSA materials, fossil fuel-based monomers are being replaced with renewable raw materials derived from biological sources. However, the inherent technical and economic drawbacks of using certain bio-based or bio-sourced feedstock is preventing their widespread commercial implementation. Emulsion polymerization is a more technically challenging polymer production method relative to solvent-based methods due to its heterogeneous nature; small changes in chemical compositions can easily perturb colloidal

stability, ultimately affecting the reaction kinetics and/or product quality. Synthesizing common fossil-based monomers from renewable materials can eliminate some technical challenges because the formulation components, and therefore the reaction kinetics, are preserved. Sourcing monomers from bio-feedstock instead of fossil fuels is a step towards polymer sustainability. Another important consideration in addressing sustainability, is to address the issue of polymer end of life.

In this work, 12% of the monomer was displaced with starch, a bio-based and biodegradable material,[74, 75] as particle cores in a seeded semi-batch emulsion polymerization. To contribute to the commercial viability and widespread adoption of sustainable polymers, they should be able to compete with their highly optimized petroleum-based equivalents. Thus, to improve the adhesive qualities of the starch-filled PSAs, CNCs were used instead of typically hazardous property modifiers. CNCs are not only sustainable, but due to their hydrophilic nature, are compatible with emulsion polymerization. In addition, they have previously been proven to be effective as adhesive and cohesive reinforcing agents in latex-based adhesives.[40–44, 76] The other major component in the PSAs is the monomer forming the acrylic polymer shells. Acrylic acid and methacrylic acid can now be produced as bio-sourced materials and are precursors for the production of a broad range of monomers.[50–53] One such monomer is 2OA, which exhibits the low T_g required for PSA applications. As noted, nOA is a near equivalent model monomer for 2OA and was readily available at lower cost. The other monomer, styrene, is also obtainable from biological sources.[49] Moreover, we have implemented a more sustainable technology (emulsion polymerization) along with bio-sourced components (starch, and acrylic monomers) and a safe, bio-based nanomaterial (CNC) as a property modifier. The resulting adhesive now contains more biodegradable components than typical commercial formulations. Their degree of degradability or compostability has yet to be measured.

The combined effects of mSNPs and CNCs on PSA properties are complex. In the first place, and in part due to the synthetic conditions, the mSNPs contributed to the generation of latexes with bimodal PSDs. The bimodal PSDs led to lower latex viscosity. Under some conditions, the bimodal PSDs led to better particle arrangement and therefore improved film coalescence.[63] However, the latexes consisting of a high ratio of large and hard particles to small and soft

particles yielded PSA films that sometimes underperformed the base-latex (i.e., without starch or CNCs) due to film-formation difficulties. The addition of CNCs led to better adhesive properties due to improvements in film-formation facilitated by CNC-particle bridging, among other effects.[44, 72, 77] Finally, by manipulating the mSNP and CNC loadings, PSAs that rival commercial post-it notes, masking tapes, and duct tapes were produced. Moreover, high performance model PSAs with a bio-sourced content of ~80% were produced.

6.6 Acknowledgements

We acknowledge EcoSynthetix, Inc. (Burlington, ON) and CelluForce, Inc. (Windsor, ON) for providing the SNPs and CNCs, respectively. The Natural Sciences and Engineering Research Council of Canada (NSERC) is acknowledged for financial support for both research project funding and scholarship support for V.A. Gabriel.

6.7 References

[1] E. George Wypych, "Handbook of Solvents: Use, Health, and Environment 3rd ed," 3rd ed., G. B. T.-H. of S. (Third E. Wypych, Ed. ChemTec Publishing, 2019, pp. 1203–1253.

[2] C. Zhuo and Y. A. Levendis, "Upcycling waste plastics into carbon nanomaterials: A review," *Journal of Applied Polymer Science*, vol. 131, no. 4, pp. 1–14, 2014, doi: 10.1002/app.39931.

[3] "Turkey: Alternate Routes to the Table | Food Safety and Inspection Service." https://www.fsis.usda.gov/food-safety/safe-food-handling-and-preparation/poultry/turkey-alternate-routes-table#2 (accessed Mar. 2022).

[4] "Sigma Air Pure Improves Indoor Air Quality | PPG People." https://www.ppgpeople.com/innovations/sigma-air-pure-improves-indoor-air-quality (accessed Mar. 2022).

[5] "Decovery®." https://decovery.covestro.com/en/home.html (accessed Mar. 2022).

[6] "AkzoNobel unlocks more sustainable future for coatings after biomass breakthrough | AkzoNobel." https://www.akzonobel.com/en/media/latest-news---media-releases-/akzonobel-unlocks-more-sustainable-future-for-coatings-after-bio (accessed Mar. 2022).

[7] S. Mapari, S. Mestry, and S. T. Mhaske, "Developments in pressure-sensitive adhesives: a review," *Polymer Bulletin*, vol. 78, no. 7, pp. 4075–4108, Jul. 2021, doi: 10.1007/s00289-020-03305-1.

[8] S. Magalhães *et al.*, "Brief overview on bio-based adhesives and sealants," *Polymers (Basel)*, vol. 11, no. 10, 2019, doi: 10.3390/polym11101685.

[9] P. Antov, V. Savov, and N. Neykov, "Sustainable Bio-Based Adhesives for Eco-Friendly Wood Composites A Review," *Wood Research*, vol. 65, no. 1, pp. 051–062, Mar. 2020, doi: 10.37763/wr.1336-4561/65.1.051062.

[10] A. Badía, J. Movellan, M. J. Barandiaran, and J. R. Leiza, "High Biobased Content Latexes for Development of Sustainable Pressure Sensitive Adhesives," *Industrial and Engineering Chemistry Research*, vol. 57, no. 43, pp. 14509–14516, 2018, doi: 10.1021/acs.iecr.8b03354.

[11] A. Badía, M. Kastelijn, J. Scheerder, and J. R. Leiza, "Development of biobased waterborne coatings containing Ecomer®: An alkyl polyglucoside maleic acid ester monomer," *Progress in Organic Coatings*, vol. 147, no. March, p. 105708, 2020, doi: 10.1016/j.porgcoat.2020.105708.

[12] Y. Zhu, C. Romain, and C. K. Williams, "Sustainable polymers from renewable resources," *Nature*, vol. 540, no. 7633, pp. 354–362, Dec. 2016, doi: 10.1038/nature21001.

[13] R. Vendamme, N. Schüwer, and W. Eevers, "Recent synthetic approaches and emerging bio-inspired strategies for the development of sustainable pressure-sensitive adhesives derived from renewable building blocks," *Journal of Applied Polymer Science*, vol. 131, no. 17, pp. 8379–8394, 2014, doi: 10.1002/app.40669.

[14] M. A. Dubé and S. Salehpour, "Applying the Principles of Green Chemistry to Polymer Production Technology," *Macromolecular Reaction Engineering*, vol. 8, no. 1, pp. 7–28, Jan. 2014, doi: 10.1002/mren.201300103.

[15] M. A. Dubé, V. A. Gabriel, A. S. Pakdel, and Y. Zhang, "Sustainable polymer reaction engineering: Are we there yet?," *The Canadian Journal of Chemical Engineering*, vol. 99, no. 1, pp. 31–60, Jan. 2021, doi: 10.1002/cjce.23865.

[16] M. Holzinger, A. le Goff, and S. Cosnier, "Nanomaterials for biosensing applications: a review," *Frontiers in Chemistry*, vol. 2, pp. 1–10, Aug. 2014, doi: 10.3389/fchem.2014.00063.

[17] C. Santhosh, V. Velmurugan, G. Jacob, S. K. Jeong, A. N. Grace, and A. Bhatnagar, "Role of nanomaterials in water treatment applications: A review," *Chemical Engineering Journal*, vol. 306, pp. 1116–1137, Dec. 2016, doi: 10.1016/j.cej.2016.08.053.

[18] L. A. Kolahalam, I. V. Kasi Viswanath, B. S. Diwakar, B. Govindh, V. Reddy, and Y. L. N. Murthy, "Review on nanomaterials: Synthesis and applications," *Materials Today: Proceedings*, vol. 18, pp. 2182–2190, 2019, doi: 10.1016/j.matpr.2019.07.371.

[19] Q. Wu, W. Miao, Y. Zhang, H. Gao, and D. Hui, "Mechanical properties of nanomaterials: A review," *Nanotechnology Reviews*, vol. 9, no. 1, pp. 259–273, Mar. 2020, doi: 10.1515/ntrev-2020-0021.

[20] D. le Corre, J. Bras, and A. Dufresne, "Starch Nanoparticles: A Review," *Biomacromolecules*, vol. 11, no. 5, pp. 1139–1153, May 2010, doi: 10.1021/bm901428y.

[21] D. Le Corre and H. Angellier-Coussy, “Preparation and application of starch nanoparticles for nanocomposites: A review,” *Reactive and Functional Polymers*, vol. 85, pp. 97–120, 2014, doi: 10.1016/j.reactfunctpolym.2014.09.020.

[22] H. Y. Kim, S. S. Park, and S. T. Lim, “Preparation, characterization and utilization of starch nanoparticles,” *Colloids and Surfaces B: Biointerfaces*, vol. 126, pp. 607–620, 2015, doi: 10.1016/j.colsurfb.2014.11.011.

[23] N. M. B. Smeets, S. Imbrogno, and S. Bloembergen, “Carbohydrate functionalized hybrid latex particles,” *Carbohydrate Polymers*, vol. 173, pp. 233–252, Oct. 2017, doi: 10.1016/j.carbpol.2017.05.075.

[24] N. Lin, J. Huang, P. R. Chang, D. P. Anderson, and J. Yu, “Preparation, modification, and application of starch nanocrystals in nanomaterials: A review,” *Journal of Nanomaterials*, vol. 2011, 2011, doi: 10.1155/2011/573687.

[25] S. B. Haaj, W. Thielemans, A. Magnin, and S. Boufi, “Starch nanocrystal stabilized pickering emulsion polymerization for nanocomposites with improved performance,” *ACS Applied Materials and Interfaces*, vol. 6, no. 11, pp. 8263–8273, 2014, doi: 10.1021/am501077e.

[26] C. Li, P. Sun, and C. Yang, “Emulsion stabilized by starch nanocrystals,” *Starch/Starke*, vol. 64, no. 6, pp. 497–502, 2012, doi: 10.1002/star.201100178.

[27] K. R. Rajisha, H. J. Maria, L. A. Pothan, Z. Ahmad, and S. Thomas, “Preparation and characterization of potato starch nanocrystal reinforced natural rubber nanocomposites,” *International Journal of Biological Macromolecules*, vol. 67, pp. 147–153, 2014, doi: 10.1016/j.ijbiomac.2014.03.013.

[28] E. Kristo and C. G. Biliaderis, “Physical properties of starch nanocrystal-reinforced pullulan films,” *Carbohydrate Polymers*, vol. 68, no. 1, pp. 146–158, 2007, doi: 10.1016/j.carbpol.2006.07.021.

[29] L. Dai, C. Qiu, L. Xiong, and Q. Sun, “Characterisation of corn starch-based films reinforced with taro starch nanoparticles,” *Food Chemistry*, vol. 174, pp. 82–88, 2015, doi: 10.1016/j.foodchem.2014.11.005.

[30] Y. Zhang, M. F. Cunningham, N. M. B. Smeets, and M. A. Dubé, “Increasing Starch Nanoparticle Content in Emulsion Polymer Latexes,” *Industrial & Engineering Chemistry Research*, 2019, doi: 10.1021/acs.iecr.9b00332.

[31] S. Mondal, “Review on Nanocellulose Polymer Nanocomposites,” *Polymer - Plastics Technology and Engineering*, vol. 57, no. 13, pp. 1377–1391, 2018, doi: 10.1080/03602559.2017.1381253.

[32] S. A. Kedzior, V. A. Gabriel, M. A. Dubé, and E. D. Cranston, “Nanocellulose in Emulsions and Heterogeneous Water-Based Polymer Systems: A Review,” *Advanced Materials*. Wiley-VCH Verlag, 2020. doi: 10.1002/adma.202002404.

[33] R. J. Moon, A. Martini, J. Nairn, J. Simonsen, and J. Youngblood, "Cellulose nanomaterials review: structure, properties and nanocomposites," *Chemical Society Reviews*, vol. 40, no. 7, p. 3941, Jun. 2011, doi: 10.1039/c0cs00108b.

[34] F. A. dos Santos, G. C. V. Iulianelli, and M. I. B. Tavares, "The Use of Cellulose Nanofillers in Obtaining Polymer Nanocomposites: Properties, Processing, and Applications," *Materials Sciences and Applications*, vol. 07, no. 05, pp. 257–294, 2016, doi: 10.4236/msa.2016.75026.

[35] Y. C. Ching *et al.*, "Rheological properties of cellulose nanocrystal-embedded polymer composites: a review," *Cellulose*, vol. 23, no. 2, pp. 1011–1030, 2016, doi: 10.1007/s10570-016-0868-3.

[36] H. Kargarzadeh *et al.*, "Recent developments on nanocellulose reinforced polymer nanocomposites: A review," *Polymer*, vol. 132, pp. 368–393, 2017, doi: 10.1016/j.polymer.2017.09.043.

[37] D. Klemm *et al.*, "Nanocellulose as a natural source for groundbreaking applications in materials science: Today's state," *Materials Today*, vol. 21, no. 7, pp. 720–748, 2018, doi: 10.1016/j.mattod.2018.02.001.

[38] Z. Dastjerdi, E. D. Cranston, and M. A. Dubé, "Synthesis of Poly(n -butyl acrylate/methyl methacrylate)/CNC Latex Nanocomposites via In Situ Emulsion Polymerization," *Macromolecular Reaction Engineering*, vol. 11, no. 6, p. 1700013, Dec. 2017, doi: 10.1002/mren.201700013.

[39] Z. Dastjerdi, E. D. Cranston, and M. A. Dubé, "Pressure sensitive adhesive property modification using cellulose nanocrystals," *International Journal of Adhesion and Adhesives*, vol. 81, pp. 36–42, Mar. 2018, doi: 10.1016/j.ijadhadh.2017.11.009.

[40] A. Ouzas, E. Niinivaara, E. D. Cranston, and M. A. Dubé, "In Situ Semibatch Emulsion Polymerization of 2-Ethyl Hexyl Acrylate/ n -Butyl Acrylate/Methyl Methacrylate/Cellulose Nanocrystal Nanocomposites for Adhesive Applications," *Macromolecular Reaction Engineering*, vol. 12, no. 3, p. 1700068, Jun. 2018, doi: 10.1002/mren.201700068.

[41] A. Ouzas, E. Niinivaara, E. D. Cranston, and M. A. Dubé, "Synthesis of poly(isobutyl acrylate/n-butyl acrylate/methyl methacrylate)/CNC nanocomposites for adhesive applications via in situ semi-batch emulsion polymerization," *Polymer Composites*, vol. 40, no. 4, pp. 1365–1377, Apr. 2019, doi: 10.1002/pc.24869.

[42] A. S. Pakdel, V. Gabriel, R. M. Berry, C. Fraschini, E. D. Cranston, and M. A. Dubé, "A sequential design approach for in situ incorporation of cellulose nanocrystals in emulsion-based pressure sensitive adhesives," *Cellulose*, vol. 27, no. 18, pp. 10837–10853, Dec. 2020, doi: 10.1007/s10570-020-03060-6.

[43] V. A. Gabriel, E. D. Cranston, and M. A. Dubé, "Pushing the Limits with Cellulose Nanocrystal Loadings in Latex-Based Pressure-Sensitive Adhesive Nanocomposites," *Macromolecular Reaction Engineering*, vol. 14, no. 6, p. 2000027, Dec. 2020, doi: 10.1002/mren.202000027.

[44] V. A. Gabriel *et al.*, "Improving Latex-Based Pressure-Sensitive Adhesive Properties Using Carboxylated Cellulose Nanocrystals," *Macromolecular Reaction Engineering*, p. 2100051, Jan. 2022, doi: 10.1002/mren.202100051.

[45] D. Satas, Ed., *Handbook of Pressure Sensitive Adhesive Technology*, 2nd ed. New York: Van Nostrand Reinhold, 1989.

[46] C. Creton, "Pressure-sensitive adhesives: an introductory course," *Materials Research Society*, pp. 434–439, Dec. 2003, Accessed: May 13, 2018. [Online]. Available: https://patents.google.com/patent/US4243500A/en

[47] R. Jovanović and M. A. Dubé, "Emulsion-Based Pressure-Sensitive Adhesives: A Review," *Journal of Macromolecular Science - Polymer Reviews*, vol. 44, no. 1, pp. 1–51, 2004, doi: 10.1081/MC-120027933.

[48] J. T. Claypool, D. R. Raman, L. R. Jarboe, and D. R. Nielsen, "Technoeconomic evaluation of bio-based styrene production by engineered Escherichia coli," *Journal of Industrial Microbiology and Biotechnology*, vol. 41, no. 8, pp. 1211–1216, 2014, doi: 10.1007/s10295-014-1469-5.

[49] J. Spekreijse, J. le Nôtre, J. van Haveren, E. L. Scott, and J. P. M. Sanders, "Simultaneous production of biobased styrene and acrylates using ethenolysis," *Green Chemistry*, vol. 14, no. 10, pp. 2747–2751, 2012, doi: 10.1039/c2gc35498e.

[50] R. Beerthuis, G. Rothenberg, and N. R. Shiju, "Catalytic routes towards acrylic acid, adipic acid and ε-caprolactam starting from biorenewables," *Green Chemistry*, vol. 17, no. 3, pp. 1341–1361, 2015, doi: 10.1039/c4gc02076f.

[51] C. v. Pramod, R. Fauziah, K. Seshan, and J. P. Lange, "Bio-based acrylic acid from sugar via propylene glycol and allyl alcohol," *Catalysis Science and Technology*, vol. 8, no. 1, pp. 289–296, 2018, doi: 10.1039/c7cy01416c.

[52] J. G. H. Hermens, A. Jensma, and B. L. Feringa, "Highly Efficient Biobased Synthesis of Acrylic Acid," *Angewandte Chemie*, vol. 134, no. 4, pp. 1–6, 2022, doi: 10.1002/ange.202112618.

[53] T. Dishisha, S. H. Pyo, and R. Hatti-Kaul, "Bio-based 3-hydroxypropionic- and acrylic acid production from biodiesel glycerol via integrated microbial and chemical catalysis," *Microbial Cell Factories*, vol. 14, no. 1, pp. 1–11, 2015, doi: 10.1186/s12934-015-0388-0.

[54] M. S. Reid, M. Villalobos, and E. D. Cranston, "Benchmarking Cellulose Nanocrystals: From the Laboratory to Industrial Production," *Langmuir*, vol. 33, no. 7, pp. 1583–1598, Feb. 2017, doi: 10.1021/acs.langmuir.6b03765.

[55] Y. Zhang, M. F. Cunningham, N. M. B. Smeets, and M. A. Dubé, "Starch nanoparticle incorporation in latex-based adhesives," *European Polymer Journal*, vol. 106, no. June, pp. 128–138, 2018, doi: 10.1016/j.eurpolymj.2018.07.014.

[56] Pressure Sensitive Tape Council, "Test Methods for Pressure Sensitive Adhesive Tapes," 2014.

[57] J. L. Keddie, “Reports : A Review Journal Film formation of latex,” *Materials Science and Engineering*, vol. 21, no. 97, pp. 101–170, 1997.

[58] P. A. Steward, J. Hearn, and M. C. Wilkinson, “Overview of polymer latex film formation and properties,” *Advances in Colloid and Interface Science*, vol. 86, no. 3. Elsevier, pp. 195–267, Jul. 28, 2000. doi: 10.1016/S0001-8686(99)00037-8.

[59] A. MacKie, S. Gourcy, N. Rigby, J. Moffat, I. Capron, and B. Bajka, “The fate of cellulose nanocrystal stabilised emulsions after simulated gastrointestinal digestion and exposure to intestinal mucosa,” *Nanoscale*, vol. 11, no. 6, pp. 2991–2998, 2019, doi: 10.1039/c8nr05860a.

[60] A. Ben Mabrouk, A. Dufresne, and S. Boufi, “Cellulose nanocrystal as ecofriendly stabilizer for emulsion polymerization and its application for waterborne adhesive,” *Carbohydrate Polymers*, vol. 229, no. October 2019, p. 115504, 2019, doi: 10.1016/j.carbpol.2019.115504.

[61] V. A. Gabriel, P. Champagne, M. F. Cunningham, and M. A. Dubé, “In-situ addition of carboxylated cellulose nanocrystals in seeded semi-batch emulsion polymerization,” *The Canadian Journal of Chemical Engineering*, vol. 100, no. 4, pp. 767–779, Apr. 2022, doi: 10.1002/cjce.24299.

[62] M. Do Amaral, A. Roos, J. M. Asua, and C. Creton, “Assessing the effect of latex particle size and distribution on the rheological and adhesive properties of model waterborne acrylic pressure-sensitive adhesives films,” *Journal of Colloid and Interface Science*, vol. 281, no. 2, pp. 325–338, 2005, doi: 10.1016/j.jcis.2004.08.142.

[63] A. C. I. A. Peters, G. C. Overbeek, A. J. P. Buckmann, J. C. Padget, and T. Annable, “Bimodal dispersions in coatings applications,” *Polymers Paint Colour Journal*, vol. 186, no. 4380, pp. 38–42, 1996.

[64] C. Plessis, G. Arzamendi, J. R. Leiza, H. A. S Schoonbrood, D. Charmot, and J. M. Asua, “Modeling of Seeded Semibatch Emulsion Polymerization of n-BA”, doi: 10.1021/ie000427e.

[65] C. Plessis, G. Arzamendi, J. M. Alberdi, M. Agnely, J. R. Leiza, and J. M. Asua, “Intramolecular Chain Transfer to Polymer in the Emulsion Polymerization of 2-Ethylhexyl Acrylate”, doi: 10.1021/ma0018190.

[66] V. A. Gabriel and M. A. Dubé, “Bulk Free-Radical Co- and Terpolymerization of n-Butyl Acrylate/2-Ethylhexyl Acrylate/Methyl Methacrylate,” *Macromolecular Reaction Engineering*, vol. 13, no. 2, 2019, doi: 10.1002/mren.201800057.

[67] J. A. Gómez-Reguera, E. Vivaldo-Lima, V. A. Gabriel, and M. A. Dubé, “Modeling of the free radical copolymerization kinetics of n-butyl acrylate, methyl methacrylate and 2-ethylhexyl acrylate using PREDICI®,” *Processes*, vol. 7, no. 7, p. 395, Jun. 2019, doi: 10.3390/pr7070395.

[68] J. L. Keddie, “Fundamentals of Latex Film Formation,” *Materials Science and Entineering*, vol. 21, pp. 101–170, 1997, doi: 10.1007/978-90-481-2845-7.

[69] G. E. Fonseca, T. F. L. McKenna, and M. A. Dubé, "Effect of bimodality on the adhesive properties of pressure sensitive adhesives: Role of bimodal particle size and molecular weight distributions," *Industrial and Engineering Chemistry Research*, vol. 49, no. 16, pp. 7303–7312, 2010, doi: 10.1021/ie100204x.

[70] J. M. Geurts, M. Lammers, and A. L. German, "The effect of bimodality of the particle size distribution on film formation of latices," *Colloids and Surfaces A: Physicochemical and Engineering Aspects*, vol. 108, no. 2–3, pp. 295–303, 1996, doi: 10.1016/0927-7757(95)03404-8.

[71] A. Tzitzinou, J. L. Keddie, J. M. Geurts, A. C. I. A. Peters, and R. Satguru, "Film formation of latex blends with bimodal particle size distributions: Consideration of particle deformability and continuity of the dispersed phase," *Macromolecules*, vol. 33, no. 7, pp. 2695–2708, 2000, doi: 10.1021/ma991372z.

[72] E. Niinivaara, A. Ouzas, C. Fraschini, R. M. Berry, M. A. Dubé, and E. D. Cranston, "How latex film formation and adhesion at the nanoscale correlate to performance of pressure sensitive adhesives with cellulose nanocrystals," *Philosophical Transactions of the Royal Society A: Mathematical, Physical and Engineering Sciences*, vol. 379, no. 2206, p. 20200330, 2021, doi: 10.1098/rsta.2020.0330.

[73] V. Favier, G. R. Canova, J. Y. Cavaille, H. Chanzy, A. Dufresne, and C. Gauthie, "Nanocomposite Materials from Latex and Cellulose Whiskers," *Polymers for Advanced Technologies*, vol. 6, pp. 351–355, 1995.

[74] D. Schlemmer, M. J. A. Sales, and I. S. Resck, "Degradation of different polystyrene/thermoplastic starch blends buried in soil," *Carbohydrate Polymers*, vol. 75, no. 1, pp. 58–62, 2009, doi: 10.1016/j.carbpol.2008.06.010.

[75] K. Leja and G. Lweandowicz, "Polymer Biodegradation and Biodegradable Polymers – a Review," *Polish Journal of Environmental Studies*, vol. 19, no. 2, pp. 255–266, 2010, doi: 10.1111/j.1469-8749.1985.tb04573.x.

[76] A. S. Pakdel, E. Niinivaara, E. D. Cranston, R. M. Berry, and M. A. Dubé, "Cellulose Nanocrystal (CNC)–Latex Nanocomposites: Effect of CNC Hydrophilicity and Charge on Rheological, Mechanical, and Adhesive Properties," *Macromolecular Rapid Communications*, vol. 42, no. 3, p. 2000448, Feb. 2021, doi: 10.1002/marc.202000448.

[77] E. Niinivaara, J. Desmaisons, A. Dufresne, J. Bras, and E. D. Cranston, "Thick Polyvinyl Alcohol Films Reinforced with Cellulose Nanocrystals for Coating Applications," *ACS Applied Nano Materials*, 2021, doi: 10.1021/acsanm.1c01244.

Chapter 7

Polymer End-of-Life

7.1 Sustainable end-of-life polymer management

Sustainability is a practice in which current actions are examined considering their future consequences. The idea is to develop ecological methods that can be used indefinitely to meet present needs without impeding future generations' ability to meet theirs. In our pursuit for sustainability, each step of the polymer lifecycle (i.e., material extraction, manufacturing, packaging and transportation, use, and end-of-life) should be addressed. Although there can be some overlap, decoupling each of the stages and addressing them individually, enables us to be more effective in designing for sustainability. Admirable work in academia and industry have led to the development of more sustainably sourced feedstock for polymer formulations (e.g., bio-based and bio-sourced monomers) and advancements in their sustainable synthesis – the topic of this thesis. When considering polymer end-of-life, recycling and degradation are the two most considered routes.

Recycling offers economic and environmental benefits if the costs of resources used are not greater than the resources saved. Waste collection, sorting, cleaning and reprocessing are cost intensive, and the recycling of household waste plastics can be difficult due to biological residue contamination or when they contain a mixture of different plastics.[1] Furthermore, the quality of many polymeric materials deteriorates with processing, making recycling and reuse of limited value in addressing sustainable end-of-life practices for polymers. Therefore, researchers have been turning to polymer degradation in the last few decades as a more promising and sustainable avenue for plastic end-of-life management.

7.2 Polymer (bio)degradation

Photodegradation by natural daylight, oxidation by chemical additives, thermal degradation by heat, mechanical degradation by physical means and biodegradation by microorganisms are five possible polymer degradation pathways.[2, 3] Because our goal is to design polymers with sustainable end-of-life outcomes, biodegradation is the most promising

pathway because of their reintegration into nature. The definition and specifications of biodegradability have been the subject of some debate in the literature so, for the purposes of this chapter, biodegradability will be defined as the carbon chain deterioration and ultimate mass loss of a material due to the action and metabolism of microorganisms. During the biodegradation process, high molecular weight polymer molecules break down into low molecular weight compounds, and eventually into carbon dioxide, methane and water for example by exo- and endo-enzymes or secreted byproducts.[4]

Biodegradable polymers have received considerable attention due to the decline in available fossil resources and the increasing preference for environmentally friendly products.[5] When designing more sustainable synthetic polymers, a common misconception is that incorporating renewably, or bio-sourced materials can improve biodegradability. For example, bio-sourced and petroleum sourced monomers will behave identically at the end-of-life stage because their molecular structure remains the same. Similarly, entirely bio-based polymers do not equate to biodegradable polymers as they do not necessarily degrade in short time frames. For example, lignin is a naturally occurring and relatively inert macromolecule but its degradability can be lower than a synthetic polymer which has hydrolysable functional groups, such as aliphatic polyesters.[6] Note that in the design of biodegradable plastics, a common first factor to consider is the hydrolysable linkages that the polymer backbone has.[2] Some bio-based materials such as starch and cellulose are biodegradable and thus, researchers postulate that utilising them in polymer formulations will render the material more prone to degradation. Although the reasoning is sound, the effect of including bio-based materials in synthetic polymers on biodegradation has not been thoroughly examined.

The main challenge with biodegradability is the measurement of the extent of degradation and the creation of toxic by-products. Test methods have been developed by standards organizations such as the American Society for Testing and Materials (ASTM), the International Organization of Standardization (ISO), and the British Standards Institution, to name a few. Despite the large number of respected testing standards for degradability and biodegradability, to our knowledge, there have been few reports of their application to adhesives, excluding for medical applications. For example, in a study where adhesives were

synthesized from plant oil-derived acrylated methyl oleate, the materials were reported to have completely disappeared when exposed to soil for a few months. However, the specific testing conditions were not mentioned despite statements that they were biocompatible as determined from cytotoxicity tests and were found to support the growth of human tissue, opening a door for biomedical applications.[7] In another example, double-sided adhesives comprising a starch carrier were synthesized and it was noted that the acrylic-based adhesive was partly degradable; few details about the degradation were provided.[8]

The ASTM and ISO have developed standard test methods for water-insoluble polymer and plastic material biodegradability in liquid media (e.g., sewage water, activated sludge) or solid media (e.g., petri dish, soil).[9] Their standards include aerobic and anaerobic decomposition and require the measurement of gaseous emissions (e.g., CO_2, H_2O, CH_4) to evaluate the extent of degradation. The two main methods for solid biodegradability testing are in petri dishes or in soil, the latter including composting methods.[2]

Biodegradation studies using petri dishes can be useful for biodegradability screening and are most effective to determine degradation pathways for polymeric materials with low water solubility.[10] Testing materials in soil is more desirable, but experiments for the biodegradation of plastic materials in soil are much longer (2-12 months) and more complex.[2, 11–13] Although tests in soils and petri dishes are interesting from a biological perspective as they can provide insights about which bacterial or fungal strains are capable of degrading the material, one of the biggest challenges is that the controlled testing conditions are not scalable. For instance, if the right microorganisms from petri dish or soil studies could be identified and introduced in a landfill, their chances of survival and reproduction is low due to competition with other microorganisms. If they do survive, the probability that these microorganisms will feed from more readily accessible carbohydrates (e.g., food scraps, plant matter) is high, and the probability of these microorganisms landing specifically on the targeted plastic is low. Composting is a promising avenue for polymer biodegradation because it provides an environment with a multitude of healthy and active bacterial and fungal colonies. In addition, the industrial composting process is conducive to degradation because it also comprises thermal, mechanical and chemical degradation.

7.2.1 Composting

Composting is an aerobic biological process in which organic matter is decomposed by the action of microorganisms to produce a biologically stable product with no phytotoxic effects on plants.[14] Composting yields a mixture rich in plant nutrients (e.g., nitrogen, phosphorus, potassium) and microorganisms (e.g., microbes, fungal mycelium, worms) called 'humus', which can be used to fertilize soil. Humus is produced when materials rich in nitrogen (e.g., plant matter, food scraps) and carbon (e.g., wood chips, leaves, other yard waste) are broken down over many months. The decomposition process can be facilitated via composting, which is a multi-step process in which the temperature, oxygen and moisture levels are controlled. Although there are very many practiced composting methods, they can be divided into two categories: passively and actively aerated composting. The sub-classification of the methods largely depends on the specific method used to provide aeration and the size and shape of the composting vessel. Actively aerated composting is often preferred because aerating the compost pile helps to regulate its temperature and maintain aerobic degradation conditions, thereby expediting the composting process. This approach is also conducive to the production of high-quality pathogen free compost.[14, 15]

A first step in the industrial composting process involves shredding the organic matter. Aside from shredding and aerating the compost pile, the decomposition process is aided by adding water. Aerobic detritivores such as bacteria and fungi chemically break down organic matter by converting them into CO_2, ammonium, nitrate, nitrite and humus-like products while generating heat. Different communities of microorganisms (e.g., bacteria, actinomyces, mildews) dominate depending on the pile temperature. For example, mesophilic microorganisms dominate in the initial decomposition when temperatures are between 25 and 35°C which break down soluble and other readily degradable matter causing the temperature to rise. Above 40°C, the colonies of mesophilic microorganisms start to decline and are replaced by thermophilic microorganisms. The thermophilic phase is marked by temperatures of 55-60°C which accelerates the decomposition of fats, protein and complex hydrocarbons (e.g., cellulose and hemicellulose). In addition, these temperatures eliminate plant and human pathogens. After the decomposition in complete, the pile can be left to mature for several days, weeks, or months.

In a municipal composting plant, the moisture content, oxygen availability and nitrogen- and carbon-rich inputs are appropriately maintained to promote biological activity of the microbes, fungi, earthworms, and other detritivores. Thus, a composting environment is an extremely species-rich source of inoculum for evaluation of the biodegradability of plastics. In this work, we adapted published standards and consulted with an industrial composter (Renewi Canada Ltd., Ottawa) to design an apparatus to measure polymer biodegradability under aerobic composting conditions at the lab scale.

7.3 Design of a lab scale composting test apparatus

Carbon dioxide measurements and visual observations are typically used to estimate the degree of biodegradation.[16] Determination of the percent dry weight of the material after burial in soil, in agar culture or in bioreactors, is considered a quantitative measure for biodegradability.[17, 18] Gravimetric methods are the most widely used and are easy to carry out however, they cannot be used independently for our materials because weight loss methods require that the material should not be sensitive to moisture (e.g., swellable) or easily hydrolyzed upon exposure in a short period of time.[9] PSAs tend to be sensitive to moisture and thus, gravimetric methods would not be sufficient in our case.

Because our goal was to design a polymer that could biodegrade using existing infrastructure and industrial methods, the biodegradability set-up was designed to simulate the composting conditions of Ottawa's municipal composting facility (Renewi Canada Ltd.). The facility is designed as an enclosed aerated static pile in the shape of a tunnel that has an aerated floor, which provides positive aeration (i.e., aeration that pushes air from the ground upwards, through the compost pile, and into the environment). The aeration floor and composting pile are housed in a long narrow concrete tunnel typically 3 to 6 m wide, 6 to 10 m high, and upwards of 50 m in length. The tunnels are designed to allow large loaders to drive in and out to load and unload materials and during the active composting, the tunnel is closed with an airtight seal.

We designed and built a series of 15 bioreactors capable of simulating the enclosed aerated static pile, common to municipal composting facilities, to measure the aerobic degradation based on the D5338 ASTM standard.[19] The apparatus also includes sensors, a

temperature control bath, and ventilation system. A data acquisition software was developed using LabVIEW to automate communication with sensors to measure temperature, humidity and CO_2 concentrations and infer the degree and rate of aerobic degradation.

7.3.1 ASTM D5338

Test method ASTM D5338 determines the rate and degree of aerobic biodegradation of plastic materials when exposed to a controlled composting environment.[19] It was designed to yield reproducible and translatable test results under conditions that simulate composting conditions where thermophilic temperatures are achieved. According to the standard, aerobic composting should take place in a controlled environment where temperature, aeration and humidity are controlled within certain limits. In essence, polymer samples are exposed to inoculum derived from compost from municipal solid waste. The CO_2 evolution as a function of time is measured and used to assess the rate of biodegradation. The degree of biodegradability is obtained by calculating the total percentage of carbon in the test substance that is converted to CO_2 during the composting experiment.

A series of at least 12 composting vessels, 2 to 5 L in volume, are required: one test substance, one blank, one positive control and one negative control, all in triplicate. The blank consists of the inoculum only, the positive control consists of inoculum with a thin-layer chromatography cellulose, and the negative control consists of inoculum with polyethylene.

7.3.2 Bioreactor design

To obtain a suitable lab scale set-up and to reduce overall costs, the bioreactors were custom built in-house in the University of Ottawa's Chemical Engineering Department workshop. The bioreactors (Figure 7.1) were designed to be robust (e.g., made from durable materials, able to withstand temperatures and pressures far greater than required) and the bioreactor prototyping was done with the help of Dr. Sean M.W. Wilson (TerraFixing Inc.). Detailed SolidWorks sketches of the bioreactor tube, flange, base, lid and O-ring used to machine the vessels can be found in Appendix III. The bioreactor body was made from a 4.5" outer diameter stainless steel tube (thickness = ⅛") cut to 12" in height and has a total inner volume of approximately 3.1 L. The tube has two port holes for ¼" Yor-Lok adaptors suitable for the tubing used for the active aeration (discussed later). The lid, made from ½" thick polycarbonate, was

secured to the flange via six bolts and wing nuts passing through ¼" holes drilled into the flange and lid. Note that there is a 0.06" deep groove that was etched into the lid to house an O-ring to ensure an airtight seal. The sensor (described later) was affixed to the underside of the lid and the cable used to power the sensor and transmit data to the computer was passe through the lid via a compression fitting sealed with silicone (Figure 7.2).

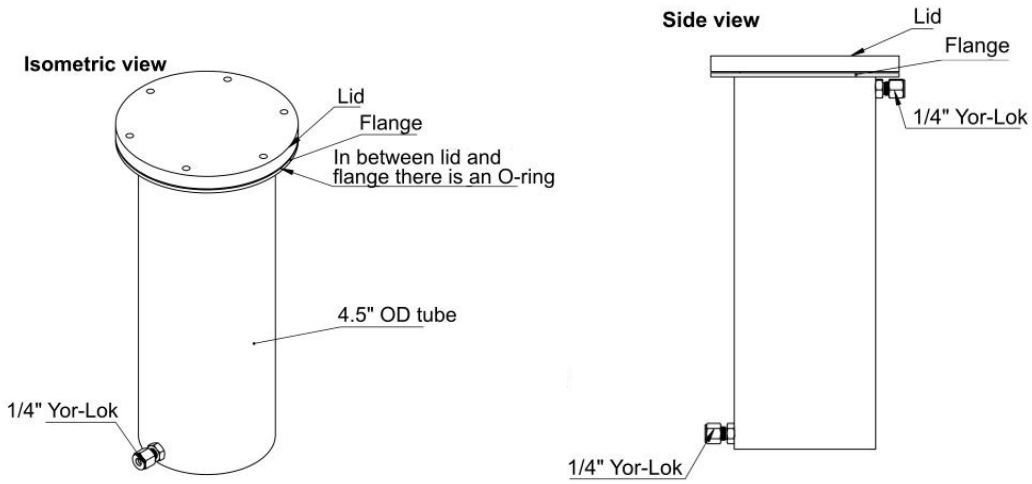

Figure 7.1 Isometric and side views of the bioreactor.

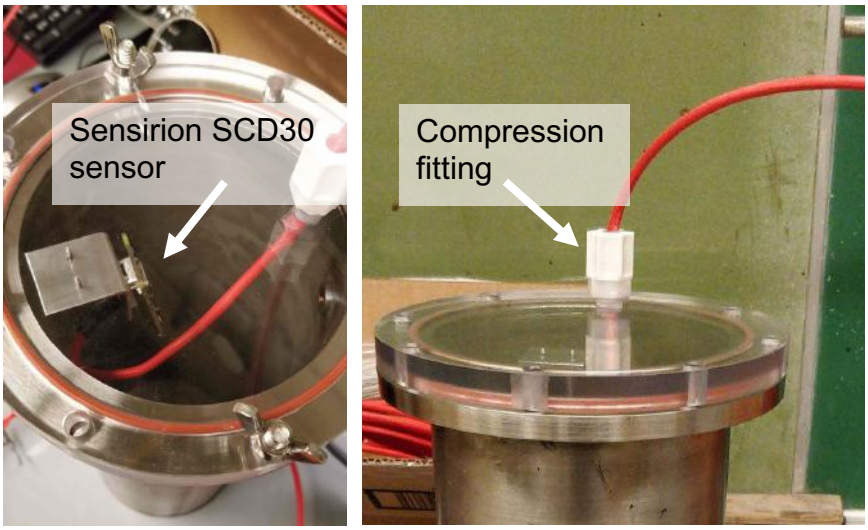

Figure 7.2 Image of Sensirion SCD30 sensor affixed to lid (left) and the compression fitting used to secure cable in place.

At the start of testing, a predetermined amount of compost is added to each bioreactor while ensuring that no more than 75% of the volume of the test vessel is filled; sufficient

headspace is required to provide enough space for CO_2, humidity and temperature readings as well as manual mixing. The CO_2 concentration in ppm, relative humidity and temperature data measured by a Sensirion SCD30 sensor are transmitted in real time to LabVIEW via a microcontroller board (data acquisition platform and electronics setup is described later). To calculate the number of moles of CO_2 from the ppm values, the exact volume of the bioreactor after it has been filled with the sample and inoculum should be known. Thus, before initializing testing, a secondary container with a known volume and pressure gauge is used with the relationship of Boyle's law (i.e., $P_1V_1 = P_2V_2$) to calculate the exact volume of each of the vessels' headspace.

7.3.3 Temperature-control bath

During mid- and large-scale composting, the bulk temperature increases naturally to about 58°C due to the biological activity of the microorganisms. By monitoring the carbon:nitrogen ratio and aeration rate, the compost temperature is naturally maintained within 2°C. Because of the small overall volume of inoculum in each reactor, a temperature control bath is required to simulate the natural temperature cycles of composting. Environmental chambers can also be used to simulate these temperatures. To reduce costs, a temperature control bath made from a 60-gallon galvanized steel stock-tank (McMaster Carr, Figure 7.3) and a heating element were used. To ensure that the desired temperatures are reached and maintained throughout the experiment, the stock tank was wrapped with a ½" thick layer of isoprene insulation, and to avoid bulk water evaporation and heat loss, the bioreactors and temperature-control bath are covered with a Plexiglas lid (to be designed).

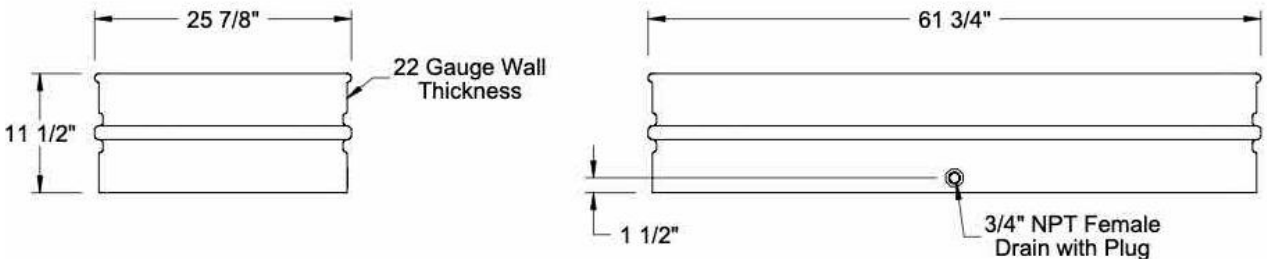

Figure 7.3 Sketch of the 60-gallon stock tank used as the temperature control bath.

7.3.4 CO_2, relative humidity, and temperature sensor

Instead of using cumbersome methods for determining CO_2 evolution (e.g., titrating a caustic solution periodically), an automatic data acquisition platform was designed in LabVIEW to record the CO_2 evolution in real time, thereby reducing manual labour for the duration of the experiment. Each bioreactor is equipped with a measurement device comprised of a Sensirion SCD30 sensor (which measures CO_2 concentration in ppm, relative humidity, and temperature) and an Adafruit 5V microcontroller board called a Trinket. The Trinket transmits the data from the sensor to LabVIEW via a standard I2C protocol through the Arduino integrated development environment (Arduino IDE). The code used to program the SCD30 (i.e., the library manager in the Arduino IDE) was obtained online[20] and the Toolkit needed to establish communication between the Trinket and LabVIEW was downloaded from the National Instruments website. Cables capable of withstanding the experimental conditions (e.g., high temperatures, humidity) were purchased form McMaster Carr and a diagram of the sensor-Trinket connection is shown in Figure 7.4. Note that the Trinket is plugged directly into the computer via a micro USB cable which provides power to and transmits data from the sensor.

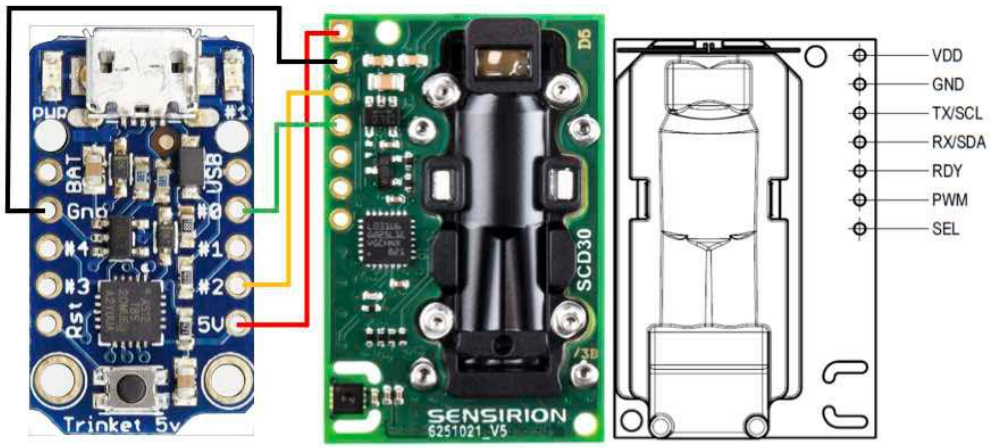

Figure 7.4 Diagram representing how the Trinket microcontroller (left) and Sensirion SCD30 sensor (right) are wired together.

7.3.5 Positive aeration system

The ASTM D5338 standard requires that the vessels be opened and aerated periodically to ensure that the microorganisms have sufficient oxygen. During that time, the caustic solutions used to capture the CO_2 emitted during the tests (e.g., $Ba(OH)_2$) are titrated to calculate the

number of moles of CO_2 emitted. To minimize experimental error, reduce the amount of labour, and to eliminate unpleasant odours that are released every few days during aeration and titrations, an airflow system designed to mimic the positive aeration used in municipal composting facilities will be used which vents directly into a fume hood. Briefly, CO_2-free air (Zero Air, Messer) is flowed through the vessels and purged via a series of tubes and valves (Figure 7.5). To determine the degree of biodegradation, we can calculate the number of moles of CO_2 by taking the integral of the CO_2 curve between each reactor purge. These calculations were automated in LabVIEW.

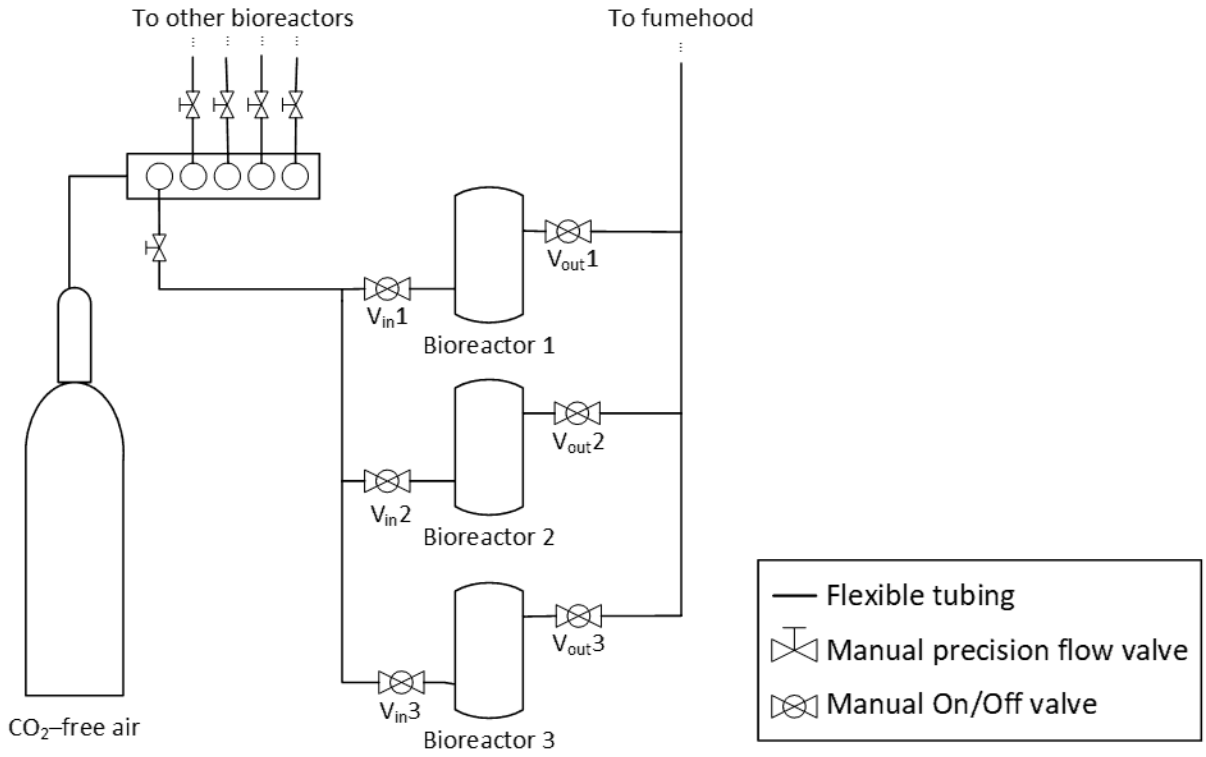

Figure 7.5 Bioreactor aeration set-up.

7.3.6 Determination of the rate of biodegradation and biodegradability

The percent biodegradation is calculated by dividing the average net CO_2 production of the sample by the original average amount of carbon in the sample, and multiplying by 100 as follows:

$$\%\ biodegradation = \frac{\bar{C}_{bioreactor} - \bar{C}_{blank}}{C_{sample}} \quad \text{Eq. 7.1}$$

where $\bar{C}_{bioreactor}$ is the average net CO_2 produced in the three bioreactors with the test sample and $\bar{C}_{blank}$ is the average net CO_2 produced from the three bioreactors with compost only. C_{sample} is the amount of carbon in the sample itself, which is readily calculated because the exact chemical composition of the samples is known. The standard error, s_e, and the 95% confidence interval of the percentage of biodegradation should also be reported and are calculated as follows:

$$s_e = \frac{\sqrt{\left(\frac{s_{bioreactor}^2}{3}\right) + \left(\frac{s_{blank}^2}{3}\right)}}{C_{sample}} \times 100 \quad \text{Eq. 7.2}$$

$$95\%\ confidence\ interval = \%\ biodegradation \pm (2.132 \times s_e) \quad \text{Eq. 7.3}$$

where $s_{bioreactor}^2$ and s_{blank}^2 are the variances in the calculated averages of the CO_2 concentration in the bioreactor containing the test sample and the blank, respectively. These calculations are automated in LabVIEW at the end of the test which lasts 45 days.

7.4 Conclusions and future work

In this chapter, the design and construction of an affordable lab scale composting test apparatus capable of determining the aerobic biodegradation of plastic materials under composting conditions per the ASTM D 5338 standard was reported. Using sensors and microcontrollers, CO_2 data can be automatically collected via LabVIEW to calculate both the rate and degree of biodegradation of our test samples. The following tasks to complete the construction and testing are pending:

- design and construct fitted lid for the temperature control bath,
- connect flexible tubing for the aeration system and test for leaks,
- test temperature control bath,
- write LabVIEW code for automatic calculation of rate of biodegradation, and
- test long-term sensor reliability.

Once these tasks are completed, the lab-scale composting apparatus can be validated by measuring the rate and extent of biodegradation of a known material (e.g., chromatography cellulose).

7.5 References

[1] F. Flintoff, "The Disposal of Town Refuse," *Royal Society of Health Journal*, pp. 241–245, 1971.

[2] R. Jayasekara, I. Harding, I. Bowater, and G. Lonergan, "Biodegradability of a selected range of polymers and polymer blends and standard methods for assessment of biodegradation," *Journal of Polymers and the Environment*, vol. 13, no. 3, pp. 231–251, 2005, doi: 10.1007/s10924-005-4758-2.

[3] Calmon-Decriaud, V. Bellon-Maurel, and F. Silvestre, "Standard Methods for Testing the Aerobic Biodegradation of Polymeric Materials. Review and Perspectives," in *Advances in Polymer Science*, vol. 135, 2011, pp. 209–227. doi: 10.1524/zpch.1974.92.1-3.167.

[4] S. Karlsson and A. C. Albertsson, "Biodegradable polymers and environmental interaction," *Polymer Engineering and Science*, vol. 38, no. 8, pp. 1251–1253, 1998, doi: 10.1002/pen.10294.

[5] J. Ma, Q. Xu, J. Zhou, D. Gao, J. Zhang, and L. Chen, "Nano-scale core-shell structural casein based coating latex: Synthesis, characterization and its biodegradability," *Progress in Organic Coatings*, vol. 76, no. 10, pp. 1346–1355, 2013, doi: 10.1016/j.porgcoat.2013.04.006.

[6] A.-C. Albertsson and S. Karlsson, "Chemistry and biochemistry of polymer biodegradation," *Department of Polymer Technology, Royal Institute of Technology*. 1994.

[7] R. P. Wool, *Pressure-Sensitive Adhesives, Elastomers, and Coatings from Plant Oil*, no. 2005. Elsevier, 2012. doi: 10.1016/B978-1-4557-2834-3.00012-4.

[8] Z. Czech, K. Wilpiszewska, B. Tyliszczak, and X. Jiang, "Biodegradable self-adhesive tapes with starch carrier," *International Journal of Adhesion and Adhesives*, vol. 44, pp. 195–199, 2013, doi: 10.1016/j.ijadhadh.2013.03.002.

[9] E. Rudnik, *Biodegradability Testing of Compostable Polymer Materials*, no. 2008. Elsevier, 2012. doi: 10.1016/B978-1-4557-2834-3.00011-2.

[10] R. D. Fields, F. Rodriguez, and R. K. Finn, "Microbial degradation of polyesters: Polycaprolactone degraded by P. pullulans," *Journal of Applied Polymer Science*, vol. 18, no. 12, pp. 3571–3579, 1974, doi: 10.1002/app.1974.070181207.

[11] S. Gartiser, M. Wallrabenstein, and G. Stiene, "Assessment of Several Test Methods for the Determination of the Anaerobic Biodegradability of Polymers," *Journal of Environmental Polymer Degradation*, vol. 6, no. 3, pp. 159–173, 1998, doi: 10.1023/a:1021869530253.

[12] R. Jayasekara, G. T. Lonergan, I. Harding, I. Bowater, P. Halley, and G. B. Christie, "An automated multi-unit composting facility for biodegradability evaluations," *Journal of Chemical Technology and Biotechnology*, vol. 76, no. 4, pp. 411–417, 2001, doi: 10.1002/jctb.388.

[13] ASTM Standard D5988, "Standard Test Method for Determining Aerobic Biodegradation of Plastic Materials in Soil," *ASTM International*. pp. 1–6, 2012. doi: 10.1520/D5988-12.2.

[14] F. Schuchardt, "Composting of Organic Waste," in *Environmental Biotechnology*, Weinheim, FRG: Wiley-VCH Verlag GmbH & Co. KGaA, 2005, pp. 333–354. doi: 10.1002/3527604286.ch13.

[15] *Technical Document on Municipal Solid Waste Organics Processing*. 2013. doi: 10.1002/14651858.CD004265.pub3.

[16] R. Bartha and A. V Yabannar, "Methods for Assessment of Biodegradability of Plastic Films in Soil," *Applied and Environmental Microbiology*, vol. 60, no. 10, pp. 3608–3614, 1994.

[17] A. Gandini and T. M. Lacerda, "From monomers to polymers from renewable resources: Recent advances," *Progress in Polymer Science*, vol. 48, pp. 1–39, 2015, doi: 10.1016/j.progpolymsci.2014.11.002.

[18] M. de Geus, I. van der Meulen, B. Goderis, K. van Hecke, M. Dorschu, and H. van Der, "Performance polymers from renewable monomers : high molecular weight poly (pentadecalactone) for fiber applications," pp. 525–533, 2010, doi: 10.1039/b9py00360f.

[19] ASTM International, "ASTM D5338-15 : Standard Test Method for Determining Aerobic Biodegradation of Plastic Materials Under Controlled Composting Conditions, Conditions, Incorporating Thermophilic Temperatures," *ASTM Standards.* pp. 1–7, 2015. doi: 10.1520/D5338-15.2.

[20] "SparkFun SCD30 Arduino Library." https://www.arduino.cc/reference/en/libraries/sparkfun-scd30-arduino-library/ (accessed Mar. 2020).

Chapter 8

General Discussion and Conclusion

8.1 General discussion

The goal of this thesis was to develop and implement as many sustainable engineering practices as possible to make a fully sustainable adhesive. To that end, the formulation, polymerization process, and end-of-life fate of the polymers were considered at the design stage.

8.1.1 Polymer additives

Relative to their solvent-based equivalents, manufacturers often rely on additives and rheology modifiers in latex-based paints, coatings, and adhesives to achieve a specific balance of application viscosity, flow and levelling, and anti-settling properties – it is not unusual to use 3-4 different additives at a time.[1–4] For latex-based adhesives in particular, cross-linkers and chain transfer agents are commonly added to tune the polymer microstructure and ultimately, the adhesive properties.[5] One conundrum faced in the adhesives industry is that changes to the microstructure that improve adhesion will weaken cohesion, and vice-versa.[6] In this work, we replaced these additives with cellulose nanocrystals (CNCs), a bio-based and biodegradable material.[7, 8] When added to our formulations, the CNCs acted as latex rheology modifiers and improved all PSA properties (tack, peel strength and shear strength) simultaneously, thus resolving the opposing actions of cohesion and adhesion.

CNCs need to be fully redispersed in water if they are to be properly incorporated into a latex polymerization. In Chapter 3, we overcame the ~1.5% CNC loading threshold in latexes by developing a method of incorporating them while maintaining colloidal stability and without impacting the reaction kinetics. Hence, CNCs were loaded into both the emulsifier solution (used for the seed stage) and in the pre-emulsion solution (used for the feed stage) thereby using all of the available water in the formulation for CNC redispersion. We demonstrated that 0.5-1% loadings gave the best balance of PSA properties, whereas higher loadings of CNCs (up to 4%) led to monotonical increases in cohesive forces (Figure 8.1). That work provided a pathway for higher loadings which may be beneficial in other applications (e.g., latex paints and coatings).[9]

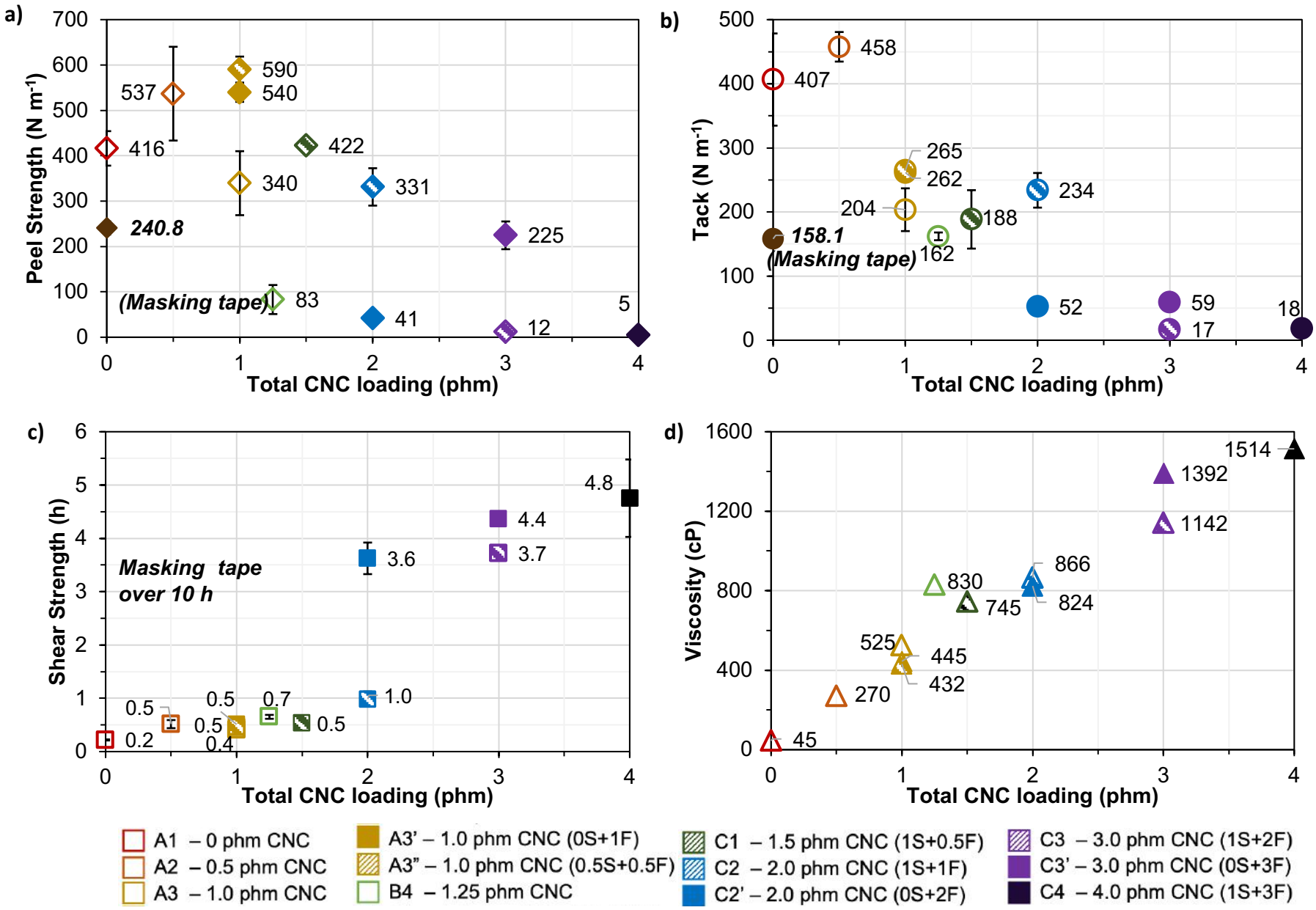

Figure 8.1 a) Peel strength, b) tack c) shear strength of adhesive films and d) latex viscosity with increasing CNC loading ("S" = seed and "F" = feed). Hollow symbols = latexes prepared by dispersing CNCs in the seed stage only; striped symbols = latexes prepared by dispersing CNCs in both the seed and feed stages; solid symbols = latexes prepared by dispersing CNCs in the feed stage only. Error bars represent the standard deviation.

Because our objective was to increase the sustainability of our polymers, we explored a novel nanomaterial, cCNCs (DextraCel™) in Chapter 4. Relative to sulfated CNCs (used in Chapter 3), cCNCs are extracted via an eco-friendly process (using hydrogen peroxide instead of sulfuric acid) and can be obtained as a spray-dried powder or as a 4.5 wt.% suspension in water.[10] When incorporating cCNCs into our latexes via traditional methods,[11, 12] the nanoparticle suspension was destabilized causing catastrophic coagulation. After carefully studying the cCNCs' interactions with the other components in the formulation, we overcame the colloidal instabilities and developed a reproducible method to incorporate the cCNCs *in situ* via a semi-batch emulsion polymerization to produce stable, high quality latexes for PSA applications.[13] This marks the first instance of *in situ* incorporation of cCNCs in a latex-based composite.

In Chapter 5, PSA testing revealed that cCNCs improved the adhesive and cohesive strengths of films simultaneously, and to a greater degree than the sulfated CNCs (Figure 8.2). In addition, films produced with unsonicated cCNCs outperformed those that were sonicated prior to addition to the latex. AFM imaging revealed that cCNCs stacked side-by-side and end-to-end, which resulted in an elongated appearance, i.e., a higher 'apparent' aspect ratio in the films. Omitting sonication preserved the cCNCs' networking behaviour and enabled them to provide similar mechanical improvements to PSA films as would nanofibrils but without the difficulties in dispersion associated with the addition of nanofibrils in polymer matrices.

Impact

Chapters 3 to 5 reveal our efforts to uncover how one bio-based additive, CNCs, can be used to displace hazardous/petroleum-based additives and rheology modifiers. CNC surface groups (sulfate half-ester or carboxylate) coupled with their high aspect ratios decreased the solids content threshold at which latex particles coalesced into a continuous film. This enhanced interaction between the CNCs and the latex particles facilitated film casting, improved film formation and increased PSA properties without impacting the latex solids content. Henceforth, cCNCs can be used in the place of rheology modifiers to make an otherwise non-castable film castable, or to tailor the adhesive strength of a latex-based adhesive. Although the benefits of using CNCs in polymer composites is now well-established, their widespread use in industry has

been hampered by the need to sonicate them prior to addition.[12] Thus, this work has paved the way for more straightforward addition of cCNCs in industrial applications beyond adhesives.[14]

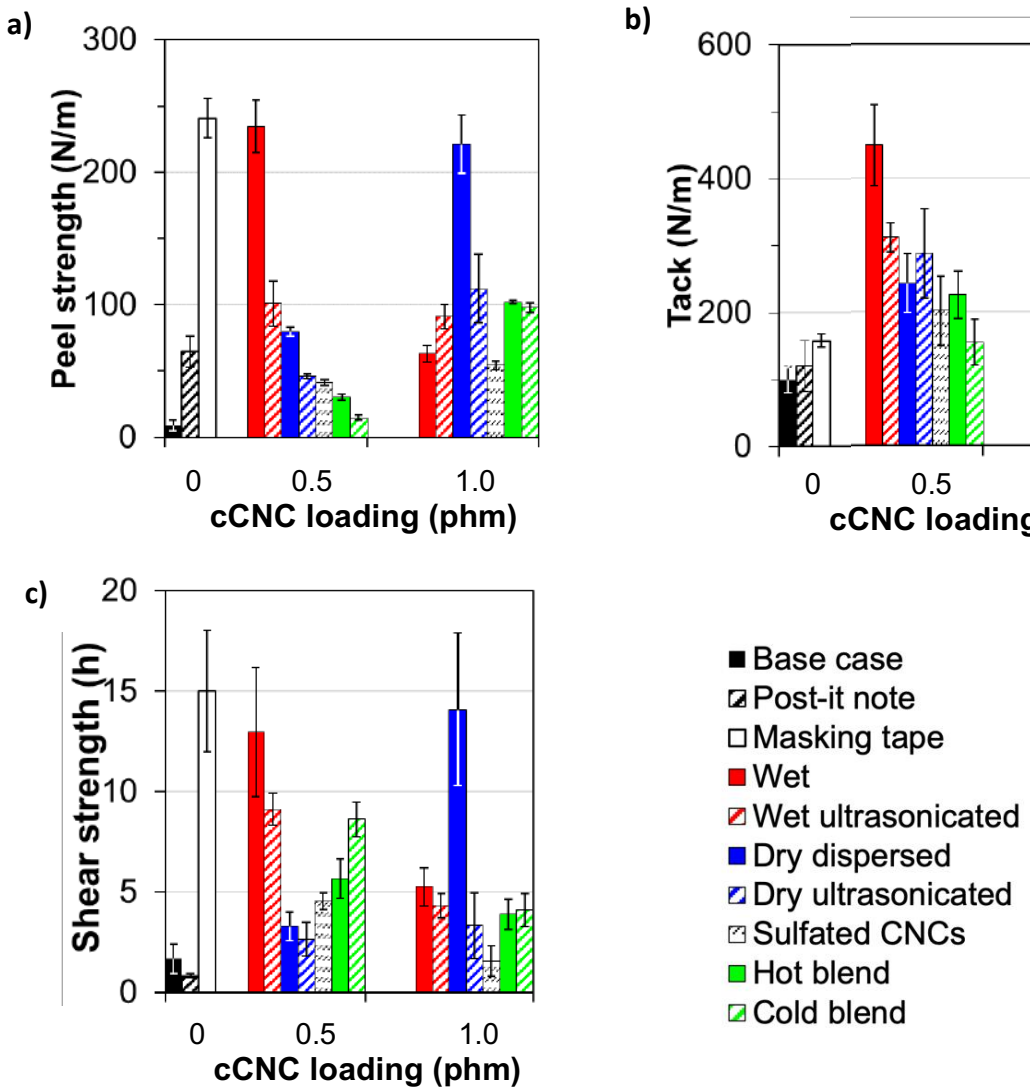

Figure 8.2 a) Peel strength, b) tack, and c) shear strength of latexes produced with 0.5 and 1.0 phm cCNC with various cCNC addition methods (wet, wet ultrasonicated, dry dispersed, dry ultrasonicated, hot blend, cold blend, and sulfated CNCs). Post-it™ notes and masking tape were measured for comparison and the error bars represent the standard deviation of six measurements.

The work from Chapters 4 and 5 is enormously beneficial to Anomera Inc. because it provided their scientist and engineers with invaluable insights on how their material behaves with latexes and how it compares to other commercially available CNCs. We developed a method

to overcome the colloidal instabilities encountered whilst adding their material to typical latex formulations thereby widening the scope of potential applications (e.g., latex-based paints and coatings). The resulting peer-reviewed publications are being used to showcase Anomera's cCNCs (aka DextraCel™) and has resulted in a spin-off project between the University of Ottawa, the University of British Columbia, Queen's University, Anomera, BASF and Rayonier Advanced Materials.

8.1.2 Monomer

Replacing all the petroleum-based components in PSA formulations with bio-based ones (i.e., materials that are obtained directly from natural resources) would be ideal, however, polymerization kinetics and resulting product properties are increasingly affected as key components (e.g., monomers) are replaced.

Bio-based materials can be derivatized or modified to increase their likelihood of polymerizing. However, one must consider avoiding extensive chemical derivatization and modification due to their negative impact on cost, waste, atom economy, energy and the introduction of additional chemical hazards. Starch nanoparticles (SNPs), a bio-based material, were functionalized and used to displace monomer in latex formulations (Chapter 6). To preserve the adhesive properties of the films, the SNPs were encapsulated to produce core-shell particles whose bulk properties (e.g., T_g, adhesive forces) were governed by the acrylic shell. Petroleum-based materials often outperform their greener counterparts so, in lieu of enhancing our PSA properties with typical petroleum-based additives, we developed a method to introduce another renewable material, sulfated CNCs, to tune the PSA properties to rival commercial, fully acrylic PSAs (Chapter 6). In Chapter 3, we examined the effects of higher CNC loadings (< 4 wt.%) and concluded that the best adhesive and cohesive improvements were achieved at loadings of 0.5 – 1%. Consequently, the core-shell latexes discussed in Chapter 6 were enhanced with 0.5 – 1% CNCs. As the formulation components were changed, the application performance unsurprisingly also changed. Thus, due to performance limitations, we were limited to displacing only 12% of the monomer with SNPs. To address the sustainability of the remaining monomer, we developed a formulation which modeled an ~80% bio-sourced acrylic formulation comprising 91.5% n-octyl acrylate (nOA), 4.5% styrene (STY) and 4.0% acrylic acid (AA). Note that nOA was used to model

2-octyl acrylate (2OA), which can be 73% bio-sourced,[15] while AA and STY can both be bio-sourced.[16–21]

Impact

The objective of this thesis was to use sustainable methods to produce high-performance PSAs composed of a maximal amount of renewable materials. Thus, the work culminated in the production of PSAs that rival commercial Post-It™ notes, masking tape, and duct tape in which 13% of the monomer was replaced with starch and cellulose, and whose acrylic formulation modeled that of an ~80% bio-sourced polymer.

8.1.3 Polymer end-of-life

A key element in polymer sustainability is the notion of sustainable polymer end-of-life management. In Chapter 7, we explored available degradation pathways and hypothesized that composting conditions provide the environment most conducive to polymer biodegradation because it includes the elements of mechanical degradation, thermal degradation, chemical degradation and biodegradation. Because lab-scale testing facilities for polymer biodegradation in compost do not exist in Canada, we designed an apparatus capable of measuring the aerobic biodegradability of polymers in a composting environment, modeled after Ottawa's municipal composting facility (Renewi Ltd.). Although mostly constructed, the unit has yet to be thoroughly tested and validated against materials with known extents and rates of biodegradation. Thereafter, we will be able to evaluate the effects of our sustainable polymer reaction engineering practices on the end-of-life of our PSAs.

8.2 Perspective on future directions

The future of sustainable polymer reaction engineering will likely address and develop techniques to promote post-use biodegradation of polymers and their reintegration to the environment. During processing, storage and use, (bio)degradable polymers must remain stable and only disintegrate at the end of their intended lifetime. Ideally, they should completely break down into molecules that can be reintegrated to the environment without having any adverse effects on human health or the environment. To design practical, economical, and commercially competitive biodegradable polymers, selecting the right formulation components that cater to

the applications and provide a degradability pathway is key. Microorganisms degrade starch and cellulose more readily than petroleum-based materials, therefore, introducing them in polymeric materials can introduce degradation pathways therein.[22] From a polymer reaction engineering perspective, we hypothesize that increasing the polymer hydrophilicity and improving polymer chain accessibility to microorganisms are key in promoting polymer biodegradation.

8.2.1 Polymer hydrophilicity

Most synthetic polymers are hydrophobic and water insoluble making them inaccessible to microorganisms or enzymatic activity. To that end, increasing the hydrophilicity of the polymers can increase the susceptibility to enzymatic attack.[23] The addition of AA (bio-sourced, bio-degradable) as a co-monomer, for instance, would help to improve polymer polarity and hydrophilicity due to the carboxyl groups which are also known to improve the peel adhesion of elastomers.[5] Adding other components that can swell with water can also promote biodegradability because high moisture content can foster biological activity (as discussed in the composting section of Chapter 7). CNCs can improve a polymer's ability to swell with water and the addition of biodegradable components such as starch and cellulose can increase the biodegradation of the material under compositing conditions, due to the priming effect (when large amounts of the organic matter present in the mature compost undergo polymer-induced degradation).[24] Starch and cellulose are biodegradable in many environments, and neither are toxic or hazardous.[25–29] A final important caveat, however, is that the intended application of the polymeric material must allow for a limited level of hydrophilicity.

8.2.2 Polymer chain accessibility

In comparison with small organic molecules, polymers are long-chained high molecular weight materials with unique physical and chemical properties. They play essential and ubiquitous roles in everyday life and fulfill many applications due to their versatile structures and morphologies which impart a wide range of chemical, mechanical, optical and electrical properties. A significant portion of commercial polymers are produced via chain-growth polymerization and have high molecular weights which give rise to their desirable properties. However, this very same property is what causes them to persist and accumulate in nature.

Modifying the molecular weight alters polymer properties significantly; this phenomenon can be used to our advantage to design materials that can degrade at the end of their useful life.

Many biodegradable polymers used in medical applications are produced via step-growth polymerization. Polymers produced via step-growth mechanisms can be made biodegradable by introducing hydrolysable components in the polymer backbone, which is not the case with chain-growth polymerization where the backbone typically contains only carbon-carbon bonds. In industry, free-radical (i.e., chain-growth) polymerization is a widely used polymer synthesis method because of its fast reaction kinetics, high yields, and absence of by-products. The challenge is to produce a polymer with hydrolysable linkages like oxygen (i.e., ester bonds) in the backbone using free-radical polymerization. When copolymerized with acrylic monomers via radical ring-opening polymerization, cyclic monomers such as cyclic ketene acetals can introduce ester bonds in polymer backbones, making them more susceptible to enzymatic attack.[30, 31] This is another interesting avenue worth investigating.

8.3 Concluding remarks

In this thesis, we explored the possibility of synthesizing a fully sustainable polymer for adhesive applications. While we haven't achieved a 100% sustainable PSA, this work demonstrates the feasibility of producing ~80% bio-sourced and commercially competitive adhesives via emulsion polymerization. It should be clear, however, that a transition to fully sustainable polymers is an enormous challenge. In the first place, identifying suitable alternative materials is complicated by the many constraints we face: cost, availability, properties, polymerizability, etc. Secondly, as demonstrated in this work, any changes to a polymer formulation can result in significant property changes and may even require substantial process modifications. While this may seem like an insurmountable problem, we are heartened by the transition made by the paints and coatings industry many decades ago when they moved from a solvent-based to latex-based (water-based) process.

8.4 References

[1] D. D. Braun and M. R. Rosen, *Rheology Modifiers Handbook: Practical Use and Application*. New York: Andrew Publishing.

[2] S. Thorp, R. E. van Doren, and A. J. Whitton, "Rheological Additives for Latex Paints," *Surface Coatings*, pp. 581–591, 1993, doi: 10.1007/978-94-011-1220-8_32.

[3] "Coatings Technology Handbook, 3rd edition," *Pigment & Resin Technology*, vol. 35, no. 1, pp. 147–156, 2006, doi: 10.1108/prt.2006.12935aac.004.

[4] J. J. Florio and D. J. Miller, *Handbook of Coating Additives*, 2nd editio. New York: CRC Press, 2004. doi: 10.1201/9781482276671.

[5] I. Benedek, *Pressure-Sensitive Adhesives and Applications*. 2004.

[6] R. Jovanović and M. A. Dubé, "Emulsion-Based Pressure-Sensitive Adhesives: A Review," *Journal of Macromolecular Science, Part C: Polymer Reviews*, vol. 44, no. 1, pp. 1–51, Dec. 2004, doi: 10.1081/MC-120027933.

[7] N. Rescignano *et al.*, "Use of alginate, chitosan and cellulose nanocrystals as emulsion stabilizers in the synthesis of biodegradable polymeric nanoparticles," *Journal of Colloid and Interface Science*, vol. 445, pp. 31–39, 2015, doi: 10.1016/j.jcis.2014.12.032.

[8] Y. Lu, J. Huang, L. Ge, W. Xie, and D. Wu, "Selective localization of cellulose nanocrystals in the biodegradable poly(vinyl alcohol)/poly(ε-caprolactone) blend composites prepared by Pickering emulsions," *Polymer*, vol. 156, no. August, pp. 136–147, 2018, doi: 10.1016/j.polymer.2018.10.005.

[9] V. A. Gabriel, E. D. Cranston, and M. A. Dubé, "Pushing the Limits with Cellulose Nanocrystal Loadings in Latex-Based Pressure-Sensitive Adhesive Nanocomposites," *Macromolecular Reaction Engineering*, vol. 14, no. 6, p. 2000027, Dec. 2020, doi: 10.1002/mren.202000027.

[10] M. P. Andrews, T. Morse, A. Khabibullin, M. Farooque, and M. Rak, "WO 2020/163948 A1 Nanoredispersible microparticles of dried cellulose nanocrystals and method of production thereof," 2020

[11] Z. Dastjerdi, E. D. Cranston, and M. A. Dubé, "Synthesis of Poly(n -butyl acrylate/methyl methacrylate)/CNC Latex Nanocomposites via In Situ Emulsion Polymerization," *Macromolecular Reaction Engineering*, vol. 11, no. 6, p. 1700013, Dec. 2017, doi: 10.1002/mren.201700013.

[12] S. A. Kedzior, V. A. Gabriel, M. A. Dubé, and E. D. Cranston, "Nanocellulose in Emulsions and Heterogeneous Water-Based Polymer Systems: A Review," *Advanced Materials*. Wiley-VCH Verlag, 2020. doi: 10.1002/adma.202002404.

[13] V. A. Gabriel, P. Champagne, M. F. Cunningham, and M. A. Dubé, “In-situ addition of carboxylated cellulose nanocrystals in seeded semi-batch emulsion polymerization,” *The Canadian Journal of Chemical Engineering*, vol. 100, no. 4, pp. 767–779, Apr. 2022, doi: 10.1002/cjce.24299.

[14] V. A. Gabriel *et al.*, “Improving Latex-Based Pressure-Sensitive Adhesive Properties Using Carboxylated Cellulose Nanocrystals,” *Macromolecular Reaction Engineering*, p. 2100051, Jan. 2022, doi: 10.1002/mren.202100051.

[15] A. Badía, J. Movellan, M. J. Barandiaran, and J. R. Leiza, “High Biobased Content Latexes for Development of Sustainable Pressure Sensitive Adhesives,” *Industrial and Engineering Chemistry Research*, vol. 57, no. 43, pp. 14509–14516, 2018, doi: 10.1021/acs.iecr.8b03354.

[16] R. Beerthuis, G. Rothenberg, and N. R. Shiju, “Catalytic routes towards acrylic acid, adipic acid and ε-caprolactam starting from biorenewables,” *Green Chemistry*, vol. 17, no. 3, pp. 1341–1361, 2015, doi: 10.1039/c4gc02076f.

[17] T. Dishisha, S. H. Pyo, and R. Hatti-Kaul, “Bio-based 3-hydroxypropionic- and acrylic acid production from biodiesel glycerol via integrated microbial and chemical catalysis,” *Microbial Cell Factories*, vol. 14, no. 1, pp. 1–11, 2015, doi: 10.1186/s12934-015-0388-0.

[18] C. v. Pramod, R. Fauziah, K. Seshan, and J. P. Lange, “Bio-based acrylic acid from sugar via propylene glycol and allyl alcohol,” *Catalysis Science and Technology*, vol. 8, no. 1, pp. 289–296, 2018, doi: 10.1039/c7cy01416c.

[19] J. G. H. Hermens, A. Jensma, and B. L. Feringa, “Highly Efficient Biobased Synthesis of Acrylic Acid,” *Angewandte Chemie*, vol. 134, no. 4, pp. 1–6, 2022, doi: 10.1002/ange.202112618.

[20] J. T. Claypool, D. R. Raman, L. R. Jarboe, and D. R. Nielsen, “Technoeconomic evaluation of bio-based styrene production by engineered Escherichia coli,” *Journal of Industrial Microbiology and Biotechnology*, vol. 41, no. 8, pp. 1211–1216, 2014, doi: 10.1007/s10295-014-1469-5.

[21] J. Spekreijse, J. le Nôtre, J. van Haveren, E. L. Scott, and J. P. M. Sanders, “Simultaneous production of biobased styrene and acrylates using ethenolysis,” *Green Chemistry*, vol. 14, no. 10, pp. 2747–2751, 2012, doi: 10.1039/c2gc35498e.

[22] A. Gandini and T. M. Lacerda, “From monomers to polymers from renewable resources: Recent advances,” *Progress in Polymer Science*, vol. 48, pp. 1–39, 2015, doi: 10.1016/j.progpolymsci.2014.11.002.

[23] R. F. Kirk, D. F. Othmer, and M. Grayson, *Concise encyclopedia of chemical technology*, 5th ed., vol. 12. New York: John Wiley and Sons, 1985.

[24] E. Rudnik, *Biodegradability Testing of Compostable Polymer Materials*, no. 2008. Elsevier, 2012. doi: 10.1016/B978-1-4557-2834-3.00011-2.

[25] D. Schlemmer, M. J. A. Sales, and I. S. Resck, “Degradation of different polystyrene/thermoplastic starch blends buried in soil,” *Carbohydrate Polymers*, vol. 75, no. 1, pp. 58–62, 2009, doi: 10.1016/j.carbpol.2008.06.010.

[26] K. Leja and G. Lweandowicz, “Polymer Biodegradation and Biodegradable Polymers – a Review,” *Polish Journal of Environmental Studies*, vol. 19, no. 2, pp. 255–266, 2010, doi: 10.1111/j.1469-8749.1985.tb04573.x.

[27] A. L. Andrady, “Assessment of Environmental Biodegradation of Synthetic Polymers Assessment of Environmental Biodegradation of Synthetic Polymers,” vol. 1797, 2006, doi: 10.1080/15321799408009632.

[28] S. Gartiser, M. Wallrabenstein, and G. Stiene, “Assessment of Several Test Methods for the Determination of the Anaerobic Biodegradability of Polymers,” *Journal of Environmental Polymer Degradation*, vol. 6, no. 3, pp. 159–173, 1998, doi: 10.1023/a:1021869530253.

[29] R. Jayasekara, G. T. Lonergan, I. Harding, I. Bowater, P. Halley, and G. B. Christie, “An automated multi-unit composting facility for biodegradability evaluations,” *Journal of Chemical Technology and Biotechnology*, vol. 76, no. 4, pp. 411–417, 2001, doi: 10.1002/jctb.388.

[30] F. Wenzel, S. Hamzehlou, L. Pardo, M. Aguirre, and J. R. Leiza, “Kinetics of Radical Ring Opening Polymerization of the Cyclic Ketene Acetal 2-Methylene-1,3-dioxepane with Vinyl Monomers,” *Industrial and Engineering Chemistry Research*, vol. 60, no. 29, pp. 10479–10488, 2021, doi: 10.1021/acs.iecr.0c04117.

[31] J. B. Lena and A. M. van Herk, “Toward Biodegradable Chain-Growth Polymers and Polymer Particles: Re-Evaluation of Reactivity Ratios in Copolymerization of Vinyl Monomers with Cyclic Ketene Acetal Using Nonlinear Regression with Proper Error Analysis,” *Industrial and Engineering Chemistry Research*, vol. 58, no. 46, pp. 20923–20931, 2019, doi: 10.1021/acs.iecr.9b02375.

Appendix I

Supporting Information for "Pushing the Limits with Cellulose Nanocrystal Loadings in Latex-based Pressure-Sensitive Adhesive Nanocomposites"

Supporting Information for

Pushing the limits with cellulose nanocrystal loadings in latex-based pressure-sensitive adhesive nanocomposites

Vida A. Gabriel,[a] Emily D. Cranston,[b] and Marc A. Dubé[a]

[a]Department of Chemical and Biological Engineering, Centre for Catalysis Research and Innovation, University of Ottawa, 161 Louis Pasteur Pvt, Ottawa, Ontario K1N 6N5, Canada
[b]Department of Wood Science, University of British Columbia, 2424 Main Mall, Vancouver, British Columbia V6T 1Z4, Canada

AI.1 Developing a high-performance PSA formulation

AI.1.1 Formulation

A terpolymer latex formulation of BA/STY/AA (91.5/4.5/4.0 wt%) was inspired by a patent,[1] which purports to deliver an adhesive with high peel strength, tack and shear strength, and a T_g lower than -40 °C. To improve the adhesive strength of the base-case (Figure AI.1), a chain-transfer agent, n-dodecyl mercaptan (NDM) was added to the formulation. After a number of screening experiments (Table AI.1), a maximum loading of 0.25 parts-per-hundred monomer (phm) NDM was added to the formulation. Higher NDM concentrations resulted in cohesive failure of the PSA (i.e., when residual PSA remains on the substrate after testing). A 0.25 phm NDM loading was added to the formulation and showed significant improvement to the tack and peel strength of the films (Figure AI.1 Tack and peel strength of the base-case PSA produced with and without NDM compared to that of a commercial masking tape.). Due to the addition of 0.25 phm NDM, the adhesive strength exceeded that of a commercial masking tape (Uline™ general purpose 1" masking tape).

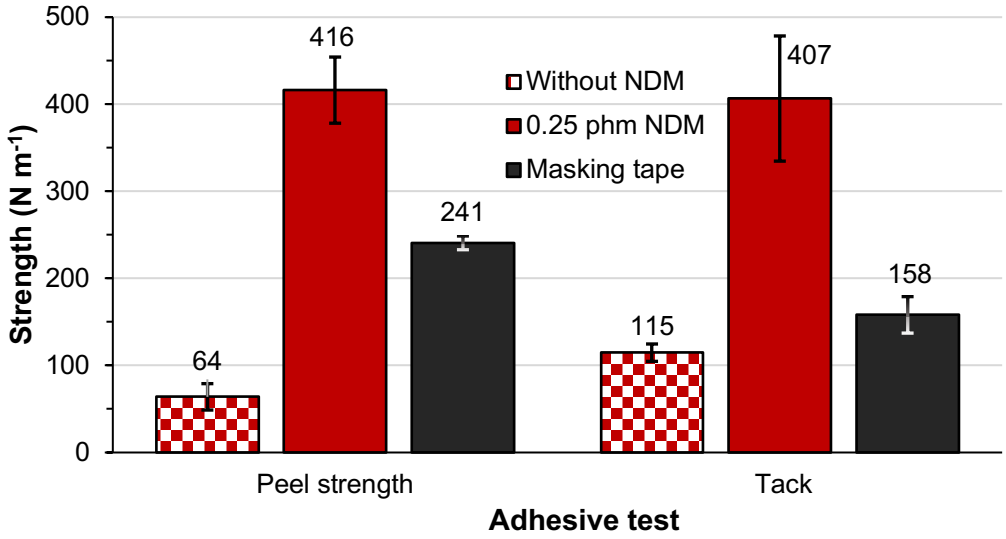

Figure AI.1 Tack and peel strength of the base-case PSA produced with and without NDM compared to that of a commercial masking tape.

Table AI.1 Latex status for the determination of NDM loading (40 wt% solids).

NDM (phm)	Latex status	PSA test
0.40	Good	Failed
0.30	Good	Failed
0.2	Could not cast film due to low viscosity	N/A
0.25	Good	Good

AI.1.2 AA addition

Previous work showed that BA and high T_g monomers were compatible with CNCs,[2] yet coagulation would occur at the onset of the reaction when CNCs were added to the base-case. To overcome these instabilities, the component addition sequence and concentrations of the monomer, buffer, and surfactant were studied (Table AI.2.).

Table AI.2. List of troubleshooting experiments to obtain a stable latex with AA and CNCs (40 wt% solids).

Experiment	AA addition		CNC	[SDS]	Buffer		Latex status
	Seed	Feed	(1 phm)	(phm)	Seed	Feed	
1	✓	✓	X	2.0	X	X	Good
2	✓	✓	✓	2.0	X	X	Failed
3	X	X	✓	2.5	X	X	Unstable
4	X	X	✓	3.0	X	X	Good
5	✓	✓	✓	3.0	X	X	Failed
6	✓	✓	✓	3.5	X	X	Failed
7	✓	✓	✓	3.0	✓	✓	Failed
8	✓	✓	✓	3.0	X	✓	Failed
9	X	✓	✓	**3.0**	X	✓	**Good**

The use of AA in the formulation was thought to cause the coagulation. Thus, to evaluate the CNC-AA interaction, the monomer addition step was studied by adding the AA to i) the seed stage, ii) the feed stage, and iii) added to both the seed and feed stages. The CNCs were obtained from a sulfuric acid hydrolysis treatment which produces rod-like crystals with nominal sulfate half-ester groups on their surface. The ester groups can react with the carboxylic acid groups of the AA in a saponification reaction, thus interfering with the CNC surface charges and therefore, the CNC-polymer network stability.[3] Although the CNCs reside in the water phase isolated from monomer droplets, the AA-CNC interaction is unavoidable because the AA is highly water-soluble. It was decided to omit AA from the latex seed, and instead feed all of the desired AA with the pre-emulsion after the end of the seed stage.

AI.1.3 Buffer concentration

Sodium bicarbonate buffer was added to the formulation in order to increase the latex's shelf life. Without buffer, the latex would destabilize after a few weeks (e.g., formation of grit or polymer sedimentation). After trying different buffer concentrations and addition methods (e.g., in the seed stage, feed stage, or both), a 1.0:0.5 (mol:mol) initiator:buffer solution mixed into the

initiator feed increased the latex shelf life significantly (>8 months) and improved the adhesive strength of cast films (Figure AI.2).

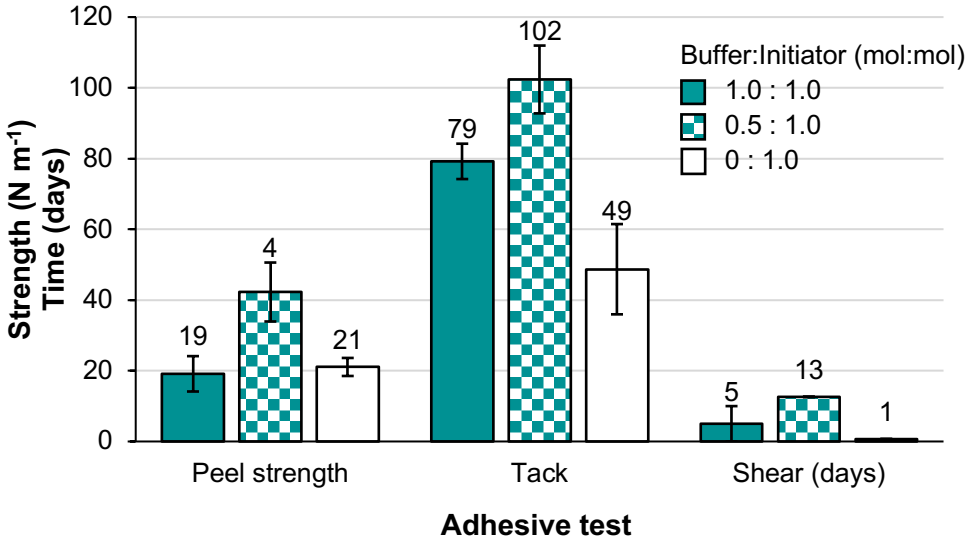

Figure AI.2 Effect of buffer on the peel strength, tack, and shear strength of films cast from latexes with 0.5 phm CNCs added in the seed (without NDM in the formulation).

1.4. Surfactant concentration

Surfactant is key in maintaining the stability of growing latex particles, yet in excess, PSA film performance diminishes[4–6] (Figure AI.3). During preliminary experiments, coagulation would occur towards the end of the polymerization likely due to mixing limitations caused by the increase in latex viscosity due to the presence of CNCs. In other words, the higher viscosity and the CNC-particle interactions reduce particle mobility in the reactor. The overall slower movement causes the particles to interact longer and more intimately, thereby increasing the chances of particle agglomeration. This was confirmed by the sudden increase in large particles observed by DLS toward the end of the reaction. Thus, SDS levels needed to be increased for higher CNC levels to help promote good particle movement (i.e., mixing) relative to the CNC matrix.

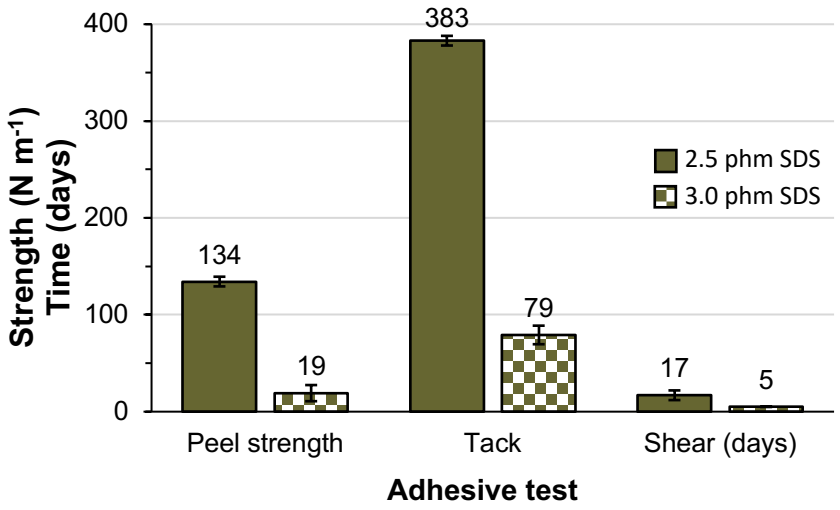

Figure AI.3 Effect of surfactant concentration on adhesive properties for latexes containing 0.5 phm CNC and a 0.5:1 (mol:mol) of buffer:initiator (without NDM in the formulation).

It is important to note that CNCs have shown stabilizing characteristics when used in an emulsion. For example, Mabrouk et al.[7] produced stable polymer nanocomposite dispersions with CNCs in lieu of surfactant in an emulsion polymerization. However, CNCs do not interact with the anionic SDS used here and are shown to displace anionic CNCs from the monomer-water interface.[8] In the present study, CNCs showed similar stabilizing characteristics. In the seed stage, less surfactant was necessary for runs with CNCs to attain the targeted initial particle diameter (~70 nm). However, emulsions with more CNCs needed more surfactant in the later stages of the reaction to remain stable. This can be explained due to the overall concentrations: relative to the whole reaction mixture, the concentration of CNCs was high during the seed stage; thus, less surfactant was required to stabilize the seed particles. During the feed stage however, the concentration of CNCs relative to the emulsion volume was continually decreasing; thus, the stabilizing effects of the CNCs were less significant and more surfactant was necessary to stabilize the polymer particles. To obtain seed particles of ~73 nm (±5 nm), roughly 0.65, 0.62 and 0.60 g of SDS were needed for CNC loadings of 0, 0.5 and 1 phm, respectively. The total required SDS concentration for those CNC loadings were 2.0, 2.5 and 3.0 phm, respectively, to obtain a final latex particle size of 130 nm (±5 nm).

AI.2 Characterization

AI.2.1 Sample characterization

Conversion: the overall conversion ($C_{overall}$) was calculated gravimetrically based on the total dried polymer relative to the sample weight and overall monomer present in the reaction formulation.

$$C_{overall} = \frac{mass\ of\ dry\ polymer}{total\ mass\ of\ monomer\ in\ the\ reaction} \quad \text{(Eq AI.1)}$$

Particle size: a Malvern NanoS Zetasizer was used to measure the particle size and particle size distribution (PSD) of all samples and the final latex using dynamic light scattering (DLS). One drop of sample was diluted in roughly 5 mL of distilled deionized water (DDW) and tested thrice at an angle of 173° and 25°C in a cuvette. The particle sizes reported are intensity-weighted mean diameter (z-average) and the PDI is a measure of the breadth of the PSD derived from cumulative analyses and is dimensionless.

pH: The pH was measured for all samples and the final latexes using a Fisher Scientific/Accumet Research AR50 Dual Channel pH/Ion/Conductivity meter.

Viscosity: The final latex viscosity was measured at 200 rpm using a Thermo Scientific HAAKE Viscotester (Model D). The appropriate spindle was selected to ensure sufficient drag to perform the measurements.

AI.2.2 PSA characterization

Glass transition temperature (T_g): T_g was measured for the final latexes using dynamic scanning calorimetry (DSC, TA Instruments, Model Q1000). Between 10-15 mg of dry latex were measured in an aluminum dish and the heating/cooling cycles were as follows: samples were initially heated to 100 ^oC and isothermal for 3 min to ensure the evaporation of any moisture. The sample was then cooled to -80 °C at 10 °C min^{-1} and held for 3 min. A final heating to 20 °C at 10 °C min^{-1} was performed. The T_g was calculated at the inflection point of the reverse heat flow curve of the cooling cycle.

Gel content: Gel content was measured the final latexes. Approximately 0.03 g of dry samples were placed in poly(vinylidene fluoride) Durapore (47 mm diameter, 5 µm-pores, Millipore) membrane pouch. Each membrane was heat sealed and placed in a 475 ml glass jar

filled with approximately 250 ml of THF. The jars were left to shake for 48 h in a wrist action shaker after which the THF was decanted and the pouches dried in a fume hood. The gel content was calculated as follows:

$$Gel\ content = \frac{weight\ of\ retained\ gel}{weigt\ of\ polymer\ sample} \quad \text{(Eq AI.21)}$$

Contact angle measurements: The DDW and diiodomethane (Sigma) contact angle of the adhesive films were measured using a VCA Optima (AST Productions Inc.). Adhesive films were prepared in same manner as for adhesive testing (detailed below). 1 µL droplets of solvent were dropped onto the surface of the film, followed by immediate measurement of the contact angle. Measurements were repeated 6 times with each solvent for each sample and contact angle was calculated by VCA OptimaXE software.

Adhesive properties: Films were prepared on 14" × 14" corona treated Mylar sheets by casting roughly 20 g of latex using a Meyer rod (No. 50). Films were dried at 50 ± 5% relative humidity at 23 ± 2 °C for 48 h. These conditions were maintained during adhesive testing. Bluehill 2 Materials Testing Software was used on an Instron 3000 Universal Tester, and Pressure Sensitive Tape Council (PSTC) methods[9] were employed. Each one of the methods described were performed for each formulation in quintuplets.

Peel strength was measured using the PSTC-101 standard using Test A for 180° peel. Dried films were cut into 1" × 12" strips and applied along the center of a testing plate, adhesive side down. The strips were applied to the testing panel at approximately 10 mm s^{-1} using a weighted steel roller (2040 ± 45 g) rolling twice in each lengthwise direction. Note that a piece of 1" masking tape was affixed to the edge of the film to form a thicker edge for the Instron tester grip and that the specimen was discarded if any air bubbles were visible.

Loop tack was measured using the PSTC-16 standard. Dried films were cut into 1" × 5" strips and formed into a loop with the adhesive site facing outward. A piece of 1" masking tape was used to secure the loop and to create a thicker grip for the Instron tester grips. The loop was lowered on the testing panel at a rate of 2 mm s^{-1} until there was a 1" contact. The strip was lifted by the tester at a rate of 5 mm s^{-1} and the maximum force requited to remove the strip was recorded.

Shear strength was measured with the PSTC-107A standard. A modification to the test area was made since the preliminary formulations exhibited unreasonably long time to failure times. Instead of 1" × 1" areas, 0.5" × 1" testing areas were used. Adhesive strips were cut into 1" × 5" strips and placed in such a way that a 0.5" × 1" adhesive surface was in contact with the testing panel. A weighted steel roller (2040 ± 45 g) was used to apply the adhesive to the test place by rolling twice in each lengthwise direction at a rate of approximately 10 mm s^{-1}. A 500 g mass was affixed to each tape and the time to shear failure was recorded.

Work of adhesion: Using two probe liquids with known surface tensions, a harmonic mean equation[10] can be used to evaluate the surface free energy of a PSA film:

$$(1+\cos\theta_1)\gamma_1 = 4\left(\frac{\gamma_1^d\gamma_p^d}{\gamma_1^d+\gamma_p^d}+\frac{\gamma_1^p\gamma_p^p}{\gamma_1^p+\gamma_p^p}\right) \text{ (Eq AI.3)}$$

$$(1+\cos\theta_2)\gamma_2 = 4\left(\frac{\gamma_2^d\gamma_p^d}{\gamma_2^d+\gamma_p^d}+\frac{\gamma_2^p\gamma_p^p}{\gamma_2^p+\gamma_p^p}\right) \text{ (Eq AI.4)}$$

$$\gamma_p = \gamma_p^d+\gamma_p^p \qquad \text{(Eq AI.5)}$$

where γ is the surface tension (in mN m^{-1}) and θ is the measured contact angle. The superscripts d and p designate the polar component and the dispersive component of the surface tension, respectively, and the subscripts 1 and 2 specify the probe liquids, which are DDW and diiodomethane, respectively. Note that γ_p^p is the polar component of the PSA film and γ_p^d is the dispersive component of the PSA film.

Using solver in Microsoft Excel, equations AI.3 – AI.4 can be solved for γ^p, γ^d and γ_p. The results for each of the latexes are summarized in Table S3. Using these results, the work of adhesion can be calculated using the Owens-Wendt relation:[10]

$$W_{AD} = 0.5\gamma(1+cos\theta) = (\gamma_{ss}^d\gamma_p^d)^{0.5}(\gamma_{ss}^p\gamma_p^p)^{0.5} \text{ (Eq AI.6)}$$

where γ_{ss}^d is the dispersive component of stainless steel (26.6 mN m^{-1}) and γ_{ss}^p is the polar component of stainless steel (18.8 mN m^{-1}). The work of adhesion is reported in Table AI.3.

Table AI.3 Water contact angle, diiodomethane contact angle and work of adhesion of PSA films.

Run #	[CNC] (phm)			Contact angle (°)		Surface tension (mN m^{-1})			W_{AD} (mN m^{-1})	T_g (°C)
	[Seed]	[Feed]	*[Tota]*	DDW[a)]	Diiodo-methane	γ^d_P	γ^p_P	γ_P		
A1	-	-	*0*	54.99	72.48	14.6	32.6	47.2	488	-40.7
A2	0.5	-	*0.5*	52.76	66.06	17.1	31.9	49.0	522	-40.9
A3	1	-	*1*	55.05	69.18	15.9	31.4	47.3	500	-40.9
A3'	0	1	*1*	56.61	72.59	14.6	31.4	46.1	480	-40.8
A3”	0.5	0.5	*1*	5.25	77.59	14.6	32.4	47.0	486	-39.6
B4	1.25	-	*1.25*	56.58	71.12	14.6	31.5	46.1	480	-40.2
C1	1	0.5	*1.5*	72.06	83.50	11.1	24.3	35.4	367	-39.9
C2	1	1	*2*	71.07	67.08	17.7	19.9	37.6	419	-39.5
C2'	0	2	*2*	66.47	68.02	16.9	23.1	40.1	443	-39.8
C3	1	2	*3*	61.40	77.14	13.0	29.7	42.7	440	-40.2
C3'	0	3	*3*	58.59	67.39	16.8	28.3	45.1	487	-40.2
C4	1	4	*4*	59.48	75.16	13.7	30.3	44.1	456	-38.6

[a)] Distilled deionized water

3. Experimental results: conversion, particle size, pH and solid content evolution

Conversion, solids content, particle size and pH evolution for all experiments detailed in the main text are shown in Figure AI.4 to AI.15. Note that for run C4 with 4.0 phm CNCs (Figure S15), samples could not be characterized between 150 and 270 min due to difficulties encountered with sample preparation.

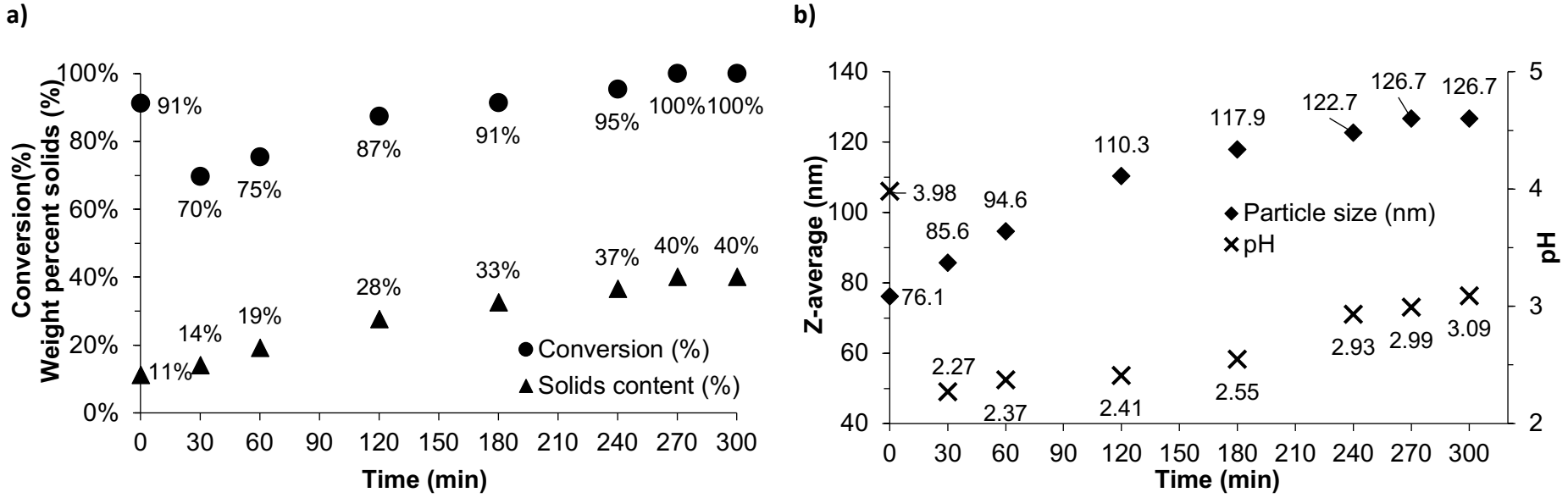

Figure AI.4 a) Conversion and solids content evolution, and b) particle size and pH evolution run A1 (base case, 0 phm CNCs).

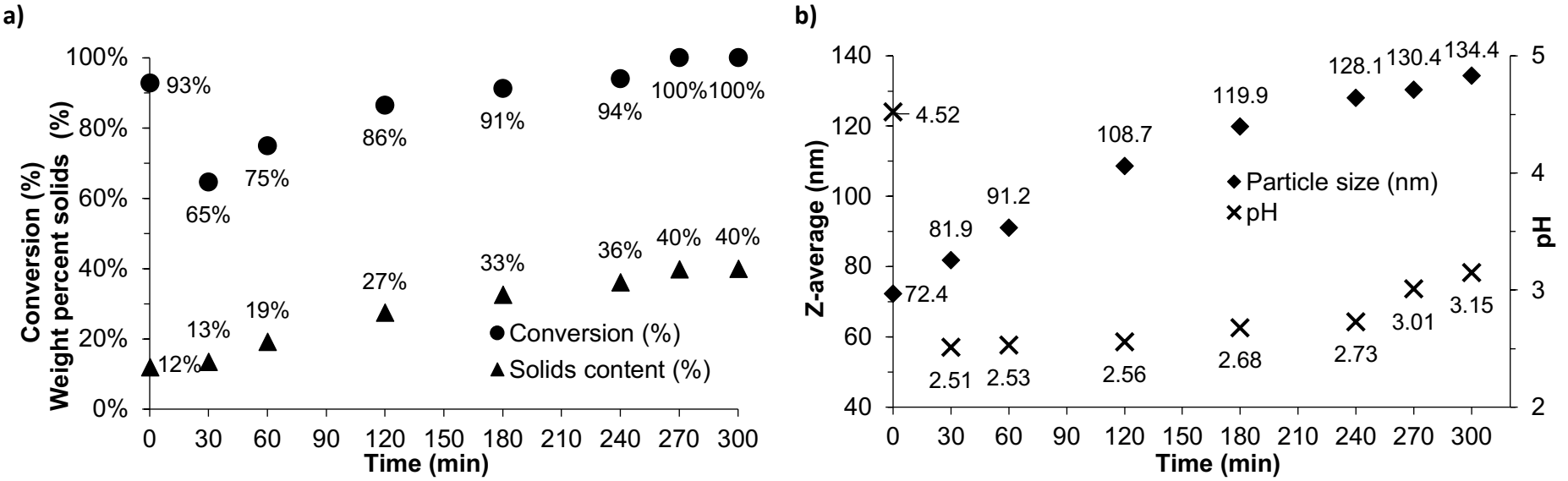

Figure AI.5 a) Conversion and solids content evolution, and b) particle size and pH evolution of run A2 with 0.5 phm CNCs in the seed.

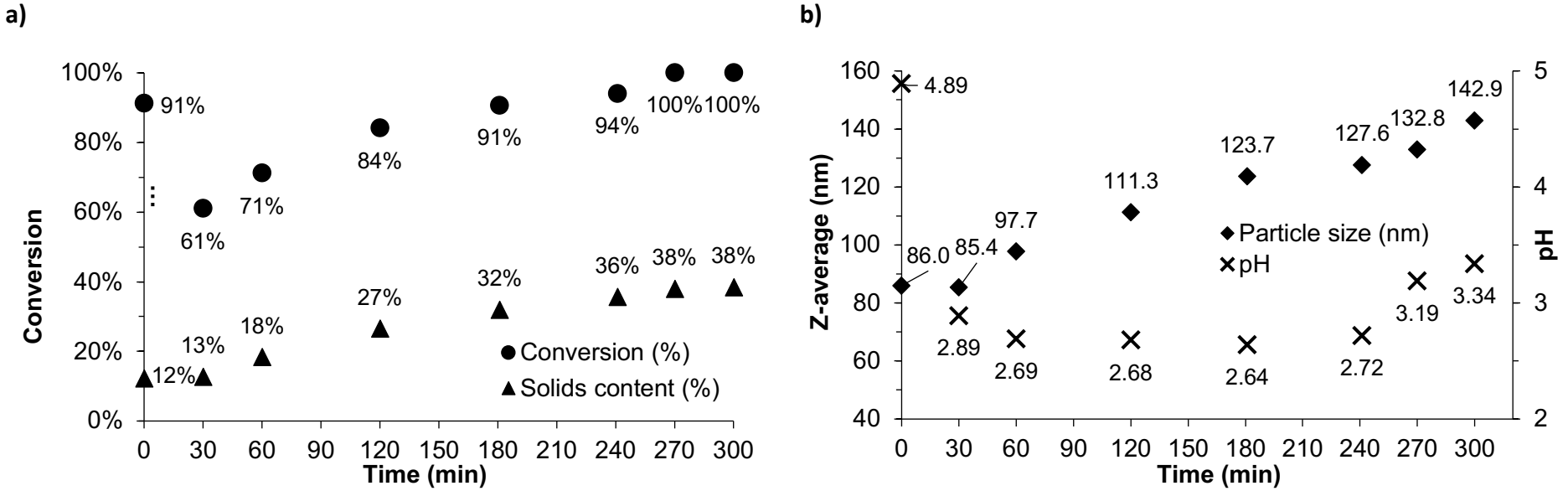

Figure AI.6 a) Conversion and solids content evolution, and b) particle size and pH evolution of run A3 with 1.0 phm CNCs in the seed.

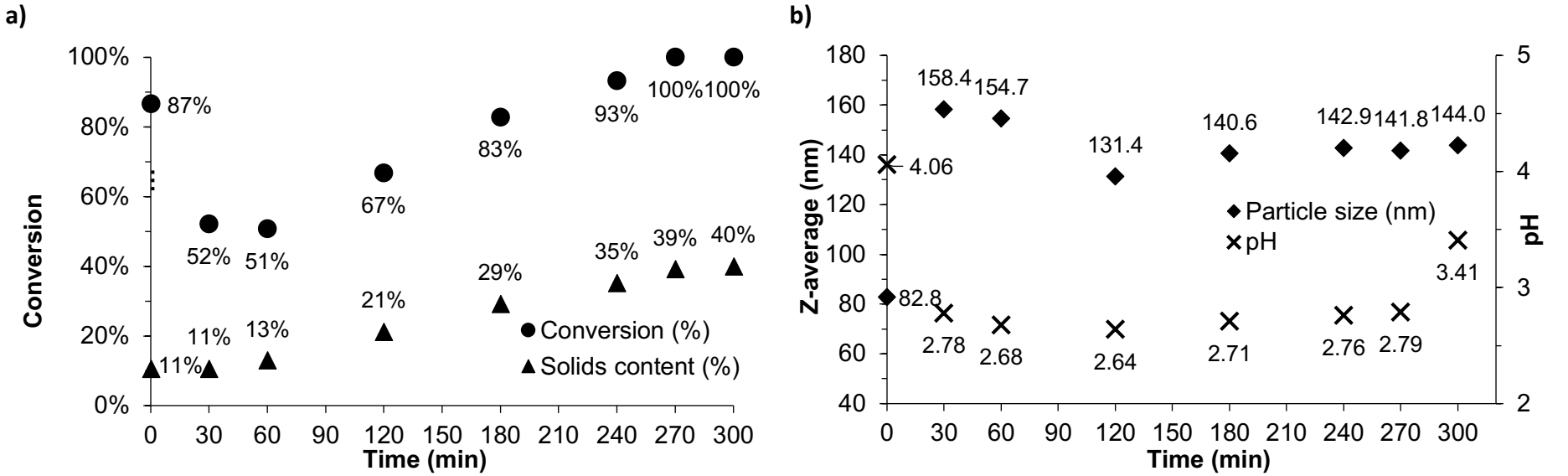

Figure AI.7 a) Conversion and solids content evolution, and b) particle size and pH evolution of run A3' with 1.0 phm CNCs in the feed.

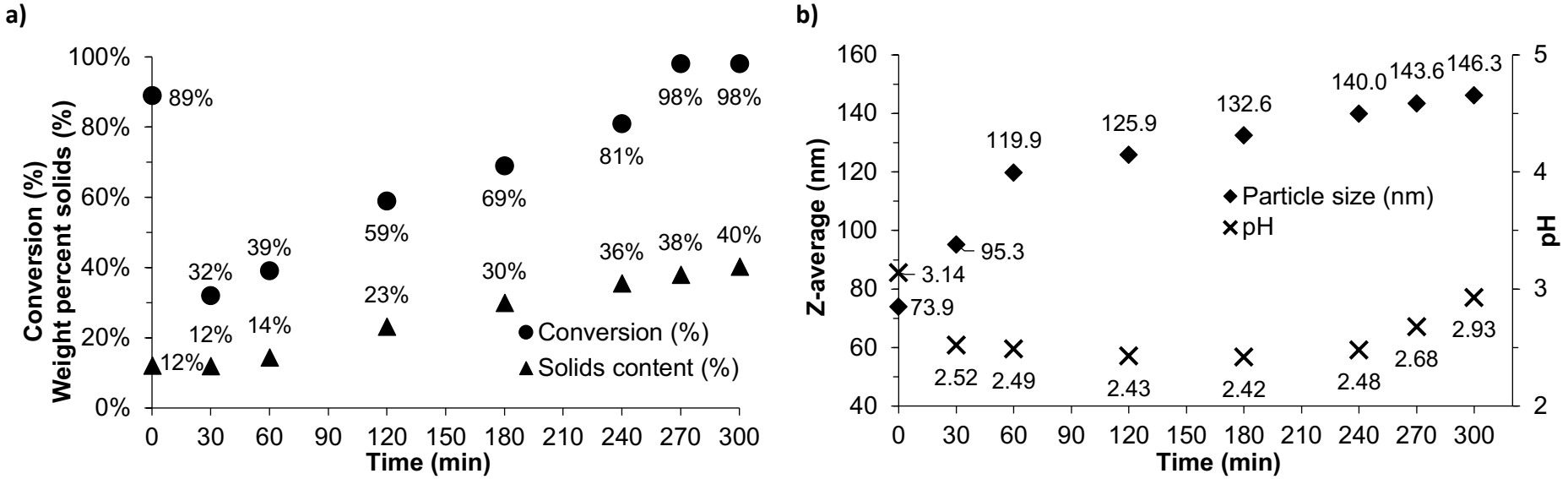

Figure AI.8 a) Conversion and solids content evolution, and b) particle size and pH evolution of run A3" with 1.0 phm CNCs, 0.5 phm in the seed and 0.5 phm in the feed.

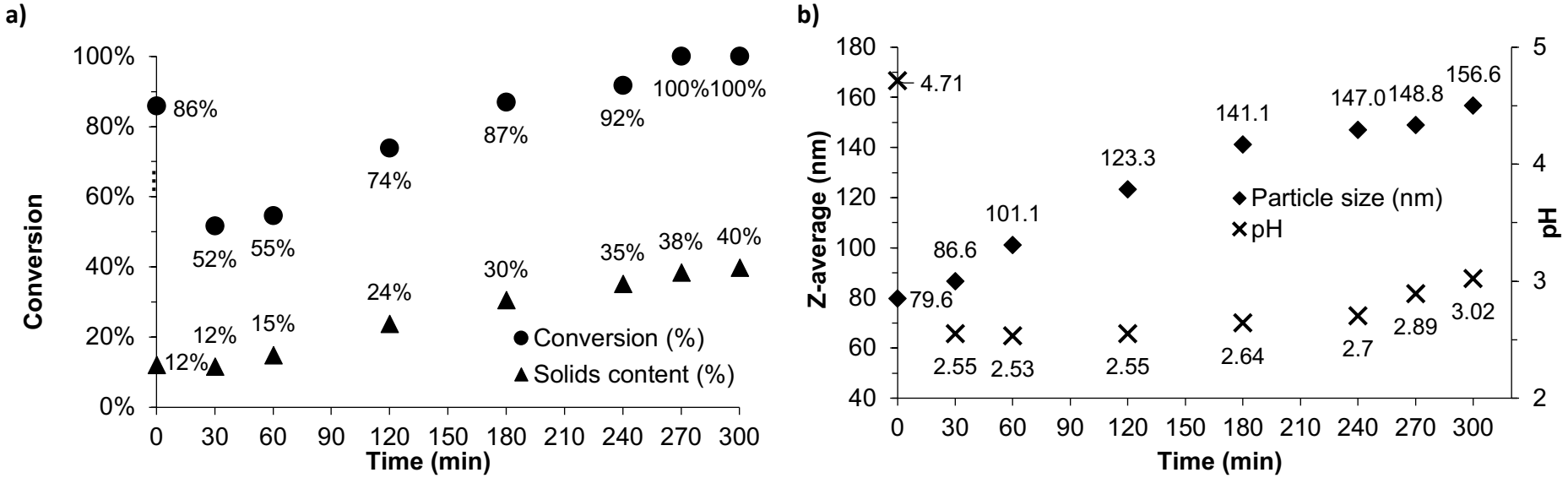

Figure AI.9 a) Conversion and solids content evolution, and b) particle size and pH evolution of run B4 with 1.25 phm CNCs in the seed.

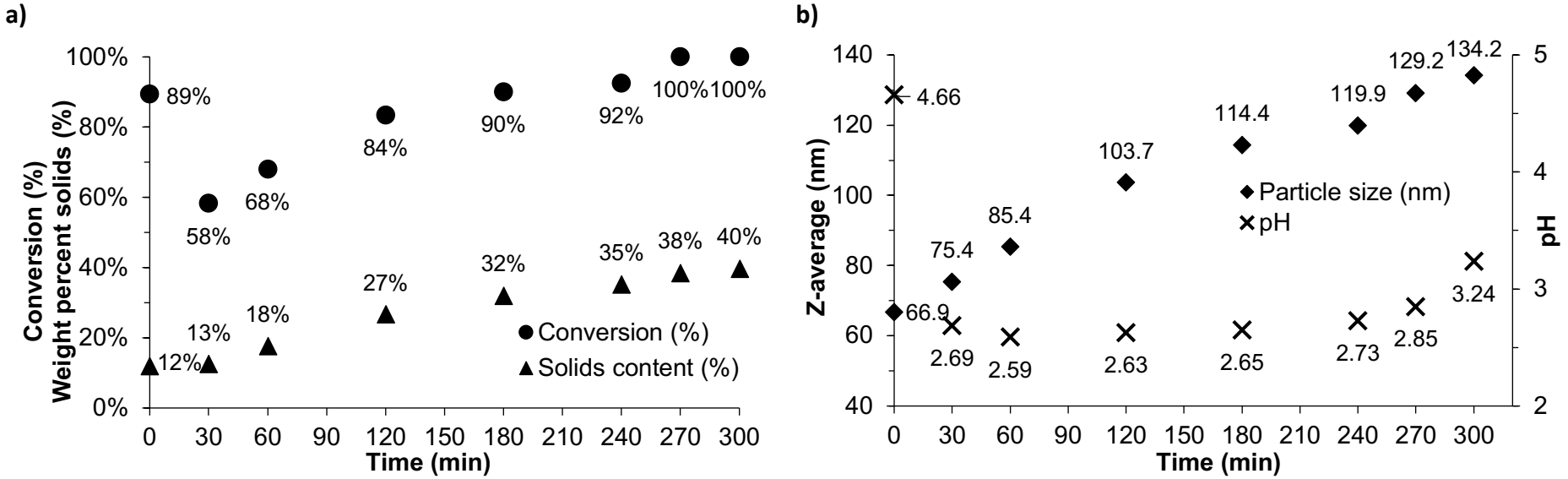

Figure AI.10 a) Conversion and solids content evolution, and b) particle size and pH evolution of run C1 with 1.5phm CNCs (1.0 phm in the seed and 0.5 phm in the feed).

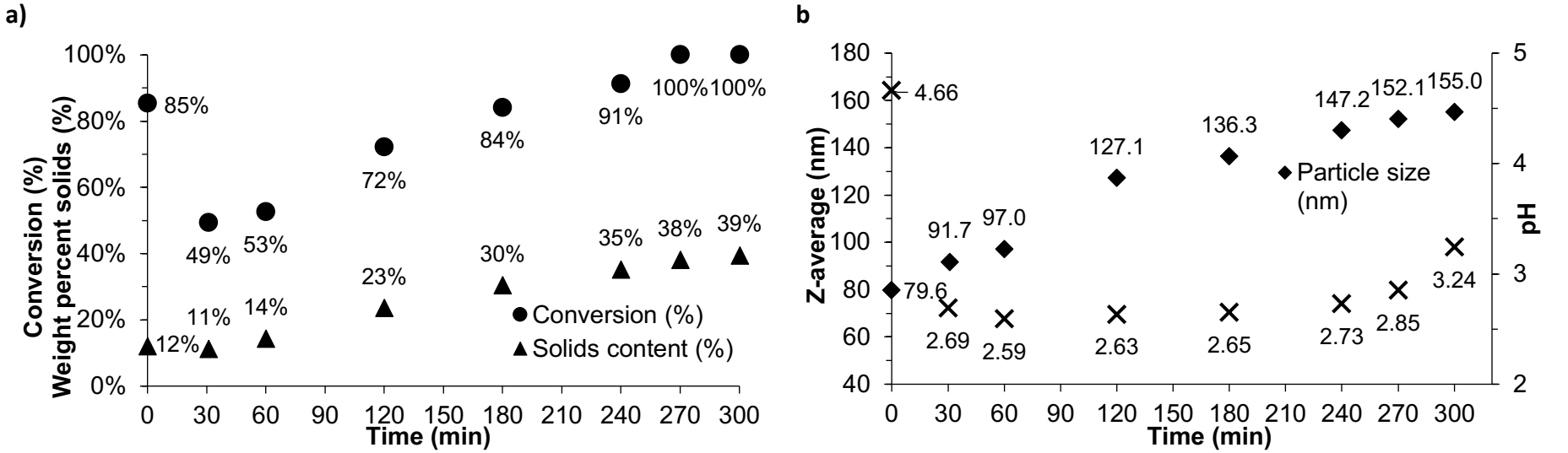

Figure AI.11 a) Conversion and solids content evolution, and b) particle size and pH evolution of run C2 with 2.0 phm CNCs (1.0 phm in the seed and 1.0 phm in the feed).

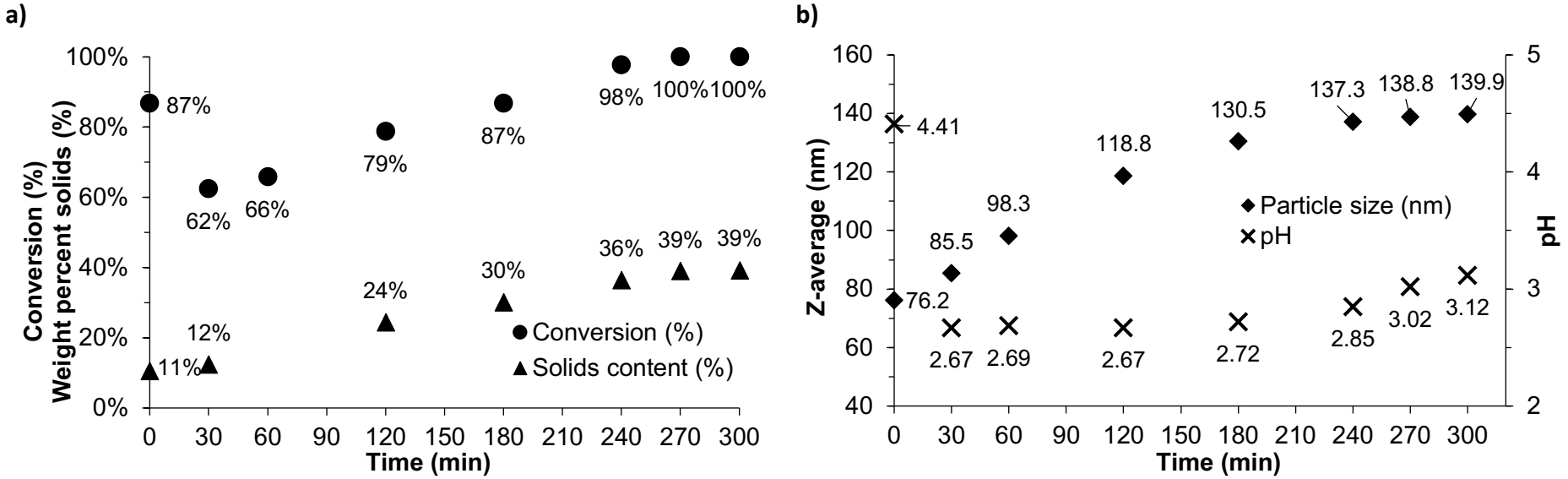

Figure AI.12 a) Conversion and solids content evolution, and b) particle size and pH evolution of run C2' with 2.0 phm CNCs in the feed.

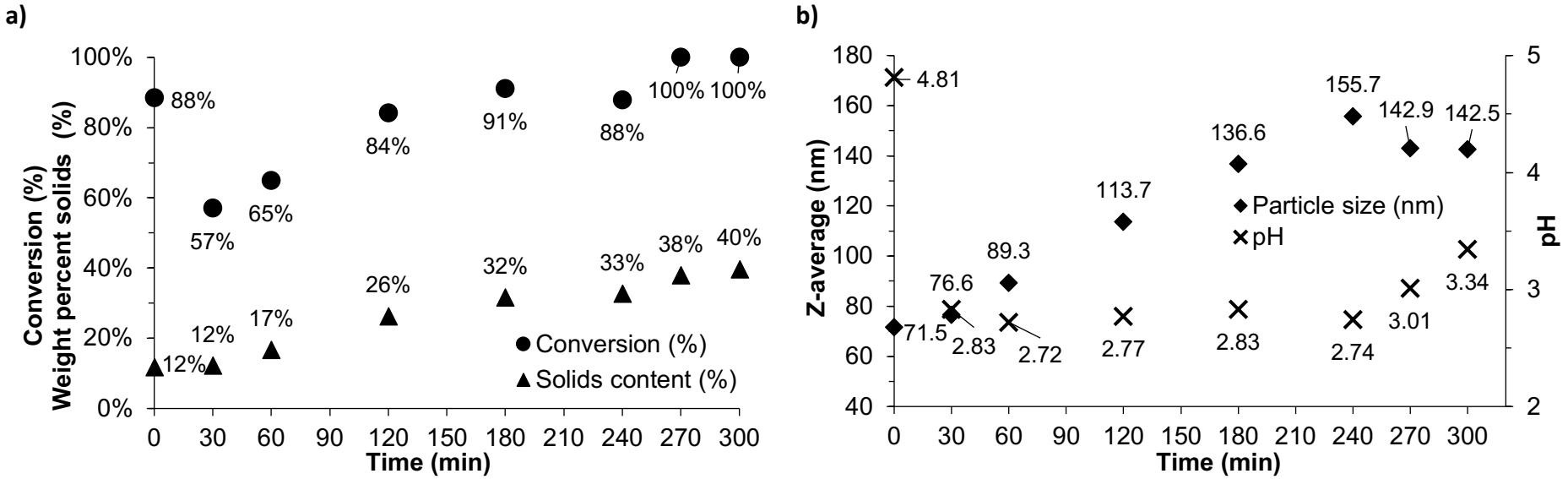

Figure AI.13 a) Conversion and solids content evolution, and b) particle size and pH evolution of run C3 with 3.0 phm CNCs (1.0 phm in the seed and 2.0 phm in the feed).

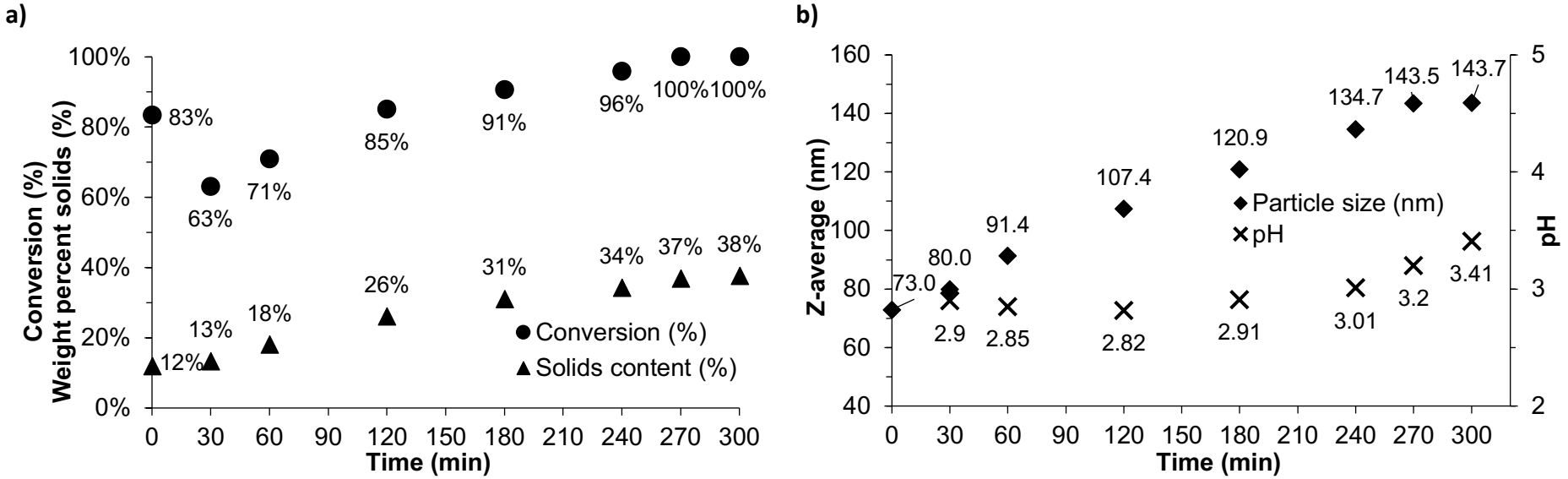

Figure AI.14 a) Conversion and solids content evolution, and b) particle size and pH evolution of run C3' with 3.0 phm CNCs in the feed.

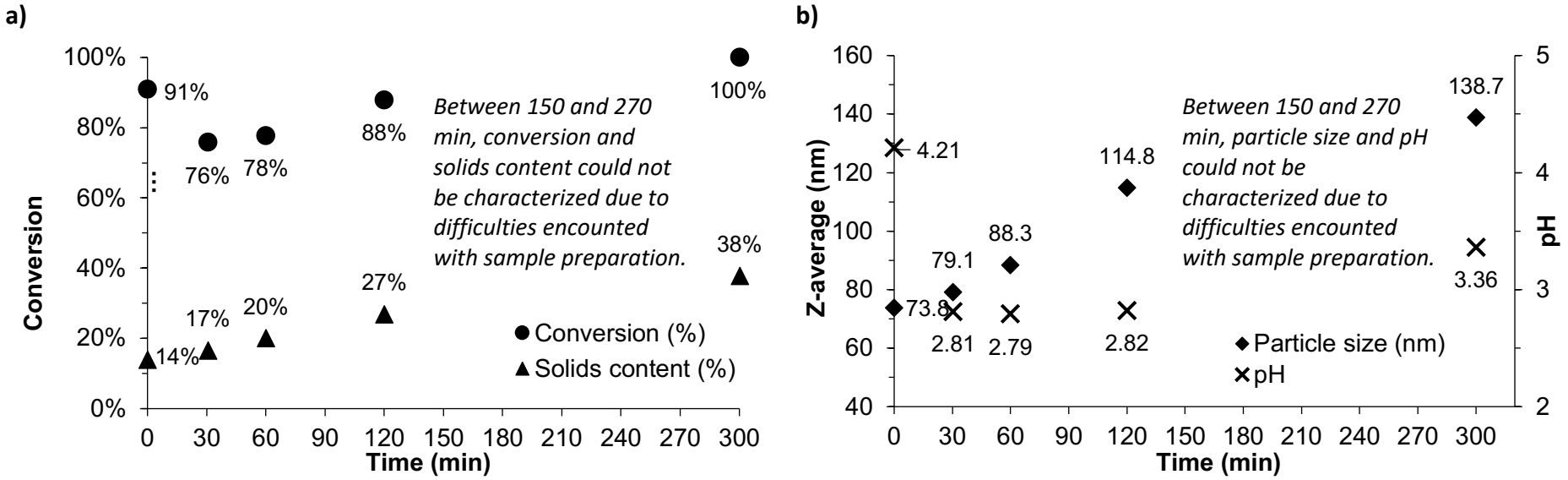

Figure AI.15 a) Conversion and solids content evolution, and b) particle size and pH evolution of run C4 with 4.0 phm CNCs (1.0 phm in the seed and 3.0 phm in the feed).

AI.3 References

[1] M. J. Skoglund, “US Patent number 5,416,134,” 5416134, 1995

[2] A. Ouzas, E. Niinivaara, E. D. Cranston, and M. A. Dubé, “In Situ Semibatch Emulsion Polymerization of 2-Ethyl Hexyl Acrylate/ n -Butyl Acrylate/Methyl Methacrylate/Cellulose Nanocrystal Nanocomposites for Adhesive Applications,” *Macromolecular Reaction Engineering*, vol. 12, no. 3, p. 1700068, Jun. 2018, doi: 10.1002/mren.201700068.

[3] A. Ben Mabrouk, A. Dufresne, and S. Boufi, “Cellulose nanocrystal as ecofriendly stabilizer for emulsion polymerization and its application for waterborne adhesive,” *Carbohydrate Polymers*, vol. 229, no. October 2019, p. 115504, 2019, doi: 10.1016/j.carbpol.2019.115504.

[4] J. Mallégol, J.-P. ; Gorce, O. Dupont, C. ; Jeynes, P. J. ; McDonald, and J. L. Keddie, “Origins and Effects of a Surfactant Excess near the Surface of Waterborne Acrylic Pressure-Sensitive Adhesives,” *Langmuir*, vol. 18, pp. 4478–4487, 2002, doi: 10.1021/LA0117698.

[5] A. Zosel and B. Schuler, “The Influence of Surfactants on the Peel Strength of Water-based Pressure Sensitive Adhesives,” *The Journal of Adhesion*, vol. 70, no. 1–2, pp. 179–195, May 1999, doi: 10.1080/00218469908010494.

[6] S. Bunker, C. Staller, N. Willenbacher, and R. Wool, “Miniemulsion polymerization of acrylated methyl oleate for pressure sensitive adhesives,” *International Journal of Adhesion and Adhesives*, vol. 23, no. 1, pp. 29–38, 2003, doi: 10.1016/S0143-7496(02)00079-9.

[7] A. Ben Mabrouk, M. C. B. Salon, A. Magnin, M. N. Belgacem, and S. Boufi, “Cellulose-based nanocomposites prepared via mini-emulsion polymerization: Understanding the chemistry of the nanocellulose/matrix interface,” *Colloids and Surfaces A: Physicochemical and Engineering Aspects*, vol. 448, no. 1, pp. 1–8, 2014, doi: 10.1016/j.colsurfa.2014.01.077.

[8] S. A. Kedzior, H. S. Marway, and E. D. Cranston, “Tailoring Cellulose Nanocrystal and Surfactant Behavior in Miniemulsion Polymerization,” *Macromolecules*, vol. 50, no. 7, pp. 2645–2655, 2017, doi: 10.1021/acs.macromol.7b00516.

[9] *Pressure Sensitive Tape Council : Test Methods for Pressure Sensitive Adhesive Tapes*, 16th ed. Oakbrook Terrace, IL: Pressure Sensitive Tape Council, 2014.

[10] D. Sowa, Z. Czech, and Ł. Byczyński, “Peel adhesion of acrylic pressure-sensitive adhesives on selected substrates versus their surface energies,” *International Journal of Adhesion and Adhesives*, vol. 49, pp. 38–43, 2014, doi: 10.1016/j.ijadhadh.2013.12.013.

Appendix II

Supporting Information for: "Improving Latex-Based Pressure-Sensitive Adhesive Films using Carboxylated Cellulose Nanocrystals"

Supporting Information for

Improving Latex Based Pressure-Sensitive Adhesive Films using Carboxylated Cellulose Nanocrystals

Vida A. Gabriel,[1,2] Mathieu N. Tousignant,[1] Sean M.W. Wilson,[2] Marie D.M. Faure,[1] Emily D. Cranston,[3,4] Michael F. Cunningham,[5] Pascale Champagne,[5] Benoît H. Lessard,[1] Marc A. Dubé[1]

[1]Department of Chemical and Biological Engineering, Centre for Catalysis Research and Innovation, University of Ottawa, Ottawa, Ontario, Canada
[2]TerraFixing Inc., Ottawa, Ontario, Canada
[3]Department of Wood Science, University of British Columbia, British Columbia, Canada
[4]Department of Chemical and Biological Engineering, University of British Columbia, Canada
[5]Department of Chemical Engineering, Queen's University, Kingston, Ontario, Canada
Email: marc.dube@uottawa.ca

AII.1 Summary of experimental details

Table AII.1 Solid's content, conversion, particle size, pH, zeta-potential, and T_g of latexes produced in this study.

Run ID	cCNC loading (phm)	Final solids content	Final conversion	Z-average (d.nm)		Final PDI	pH Range		Final zeta-potential (mV)	Standard deviation for zeta-potential	T_g (°C)
				Initial (seed)	Final		Initial (seed)	Final			
Base case	0	49%	99%	81.8	164.0	0.032	5.1	4.5	-46.3	7.09	-37.0
Wet	0.5	35%	93%	75.6	178.4	0.016	5.2	5.1	-49.9	4.94	-36.7
	1.0	35%	93%	75.0	160.4	0.100	5.1	5.7	-49.1	5.82	-37.5
Wet ultrasonicated	0.5	35%	93%	76.1	161.2	0.023	5.1	5.4	-50.1	7.31	-37.6
	1.0	35%	93%	75.2	162.1	0.017	5.1	5.6	-50.3	7.99	-37.4
Dry dispersed	0.5	35%	93%	78.9	159.9	0.017	5.0	5.3	-51.8	8.18	-39.1
	1.0	35%	93%	74.1	152.9	0.013	5.1	6.0	-50	5.07	-38.9
Dry ultrasonicated	0.5	35%	93%	78.9	160.2	0.070	5.2	5.4	-49.6	8.42	-38.5
	1.0	35%	93%	75.2	162.1	0.002	5.2	6.1	-54.8	6.89	-37.8
Sulfated CNCs	0.5	35%	93%	74.5	163.2	0.023	4.8	4.4	-67.7	9.77	-37.0
	1.0	35%	93%	69.4	161.2	0.053	5.2	4.2	-54.2	8.21	-37.1
Hot Blend	0.5	48%	98%	73.2	149.4	0.002	4.4	5.4	-61.6	6.23	-38.2
	1.0	48%	98%	67.4	141.6	0.011	4.0	6.4	-60.4	7.74	-37.9
Cold blend	0.5	48%	98%	71.2	155.6	0.042	4.5	5.7	-56.2	7.87	-38.4
	1.0	48%	98%	75.7	156.1	0.060	5.1	6.3	-53.7	8.51	-37.3

AII.2 AFM imaging

A LAXCO™ microscope (Model LMC-4000) was used to obtain a series of 4K images of the 0.35 wt.% and 17.5 wt.% films to illustrate which part of the samples were imaged (Figure AII.1). In general, areas that appeared smoother (i.e., 'valleys' in the polymer film) had a limited number of cCNCs whereas parts of the film which showed more significant topological heterogeneity (i.e., polymer 'mountains') proved more successful when searching for cCNCs. In other words, focusing on polymer-rich areas in the spin-coated films proved useful to detect cCNCs, because the CNCs tend to be more closely associated with, or adsorbed to, the surface of the polymer particles.[1–4] Examples of areas used for AFM images can be found in Figure AII.1.

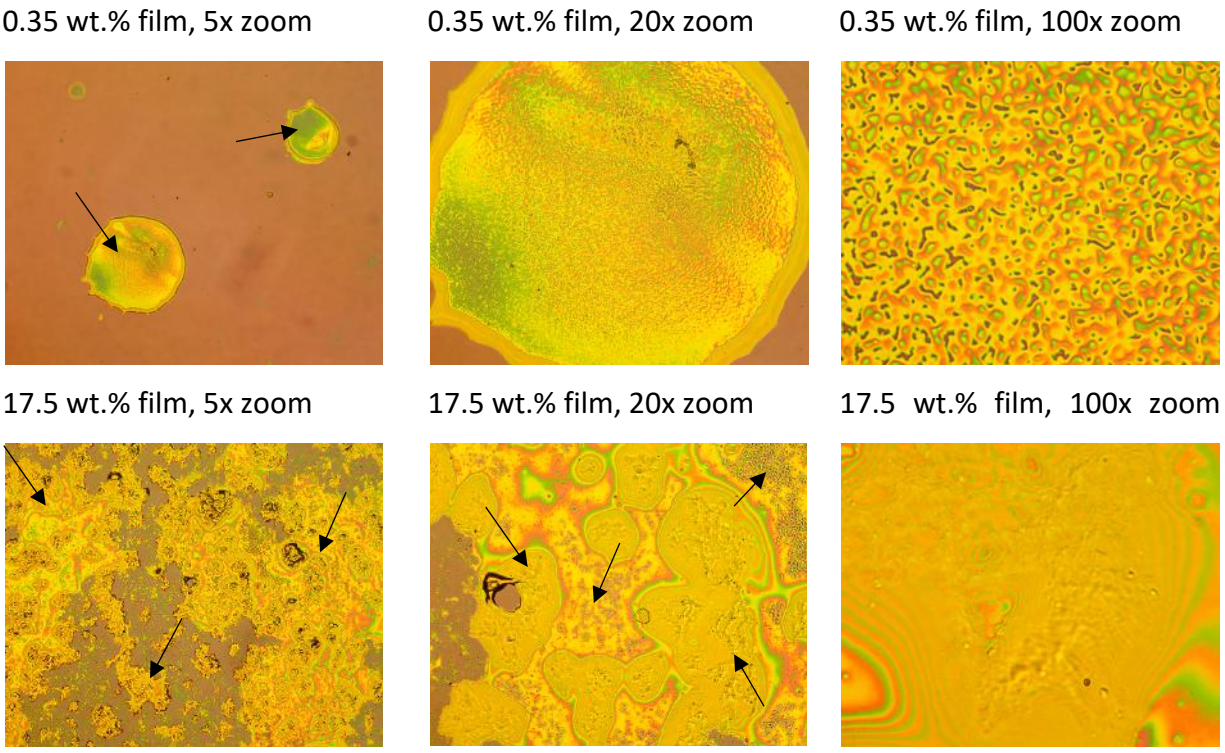

Figure AII.1 Microscopy images (visual representation) of latex films containing 1.0 phm 'wet' cCNCs on SiO_2 wafers. Arrows represent where probe was lowered to collect AFM images.

AII.2.1 AFM image characterisation

Height images were used to determine the films' surface coverage on the SiO_2 wafers. The data from Table 5.2 in the main manuscript were obtained from the images in Figure AII.2.

	0.5 phm cCNCs	1.0 phm cCNCs
Wet	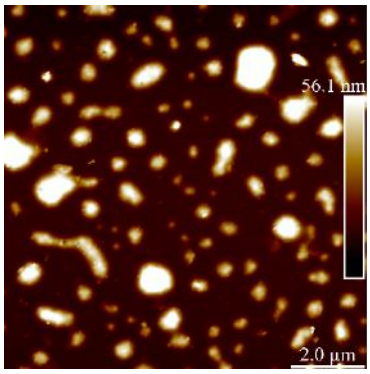	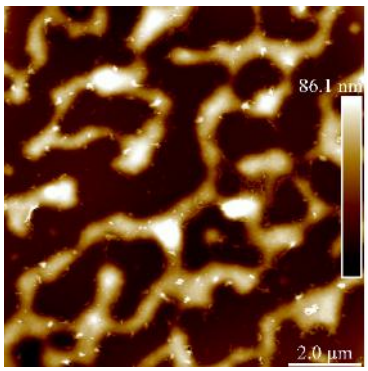
Wet ultrasonicated	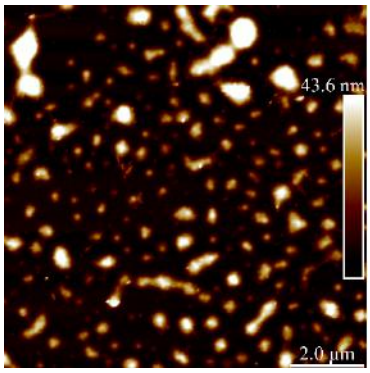	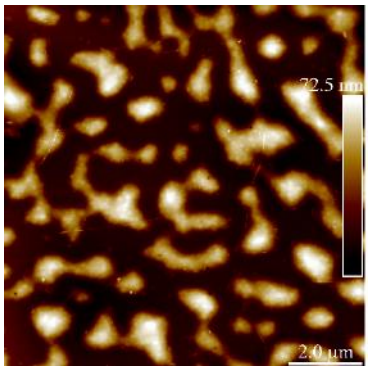
Dry dispersed	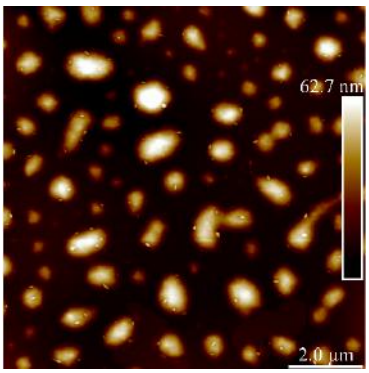	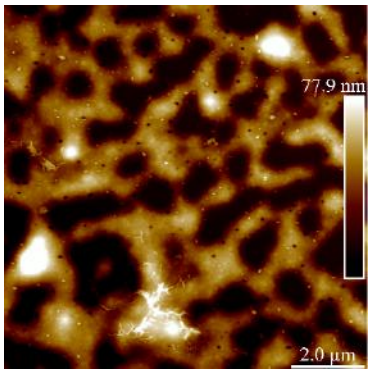
Dry ultrasonicated	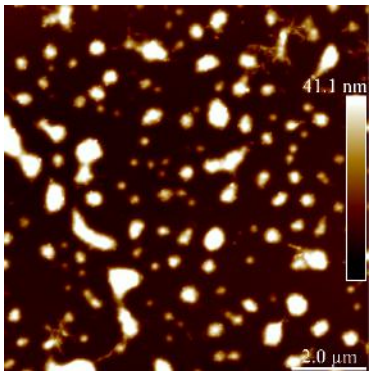	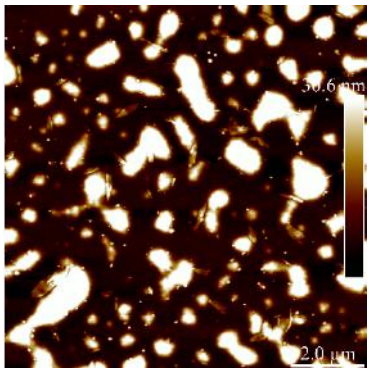

Sulfated CNCs

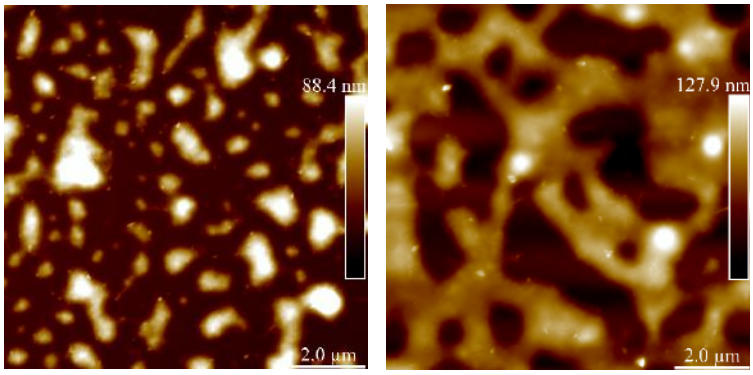

Figure AII.2 AFM height images of PSA films with 0.5 and 1.0 phm cCNC loadings used to calculate polymer surface coverages.

AII.2.2 Frequency curve from “apparent” aspect ratio calculations

In phase images were analyzed in ImageJ using the “Ridge Detection” plugin. An example of a an “apparent” aspect ratio distribution curve is presented in Figure AII.3.

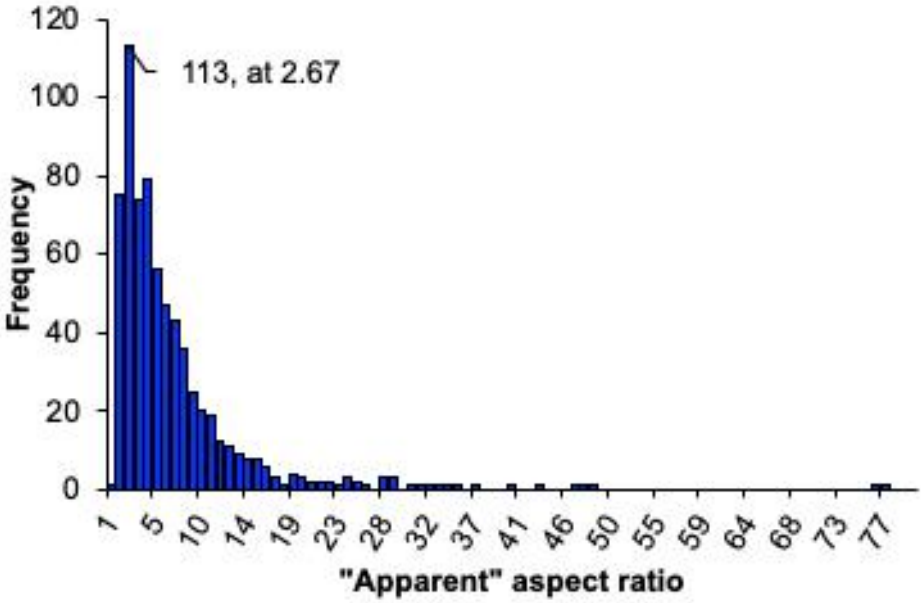

Figure AII.3 Frequency curve or the "apparent" aspect ratios of cCNCs in films produced from a latex with 1.0 phm wet cCNCs.

AII.3 Additional latex characterization

The latex gel content was measured via gravimetry. Approximately 0.03 g of dried latex was weighed and heat-sealed in 47 mm diameter poly(vinylidene fluoride) (PVDF) membrane pouches with a pore size of 0.45 microns (Durapore, Millipore). Prepared pouches were placed in 4 oz jars and filled with ~100 mL of THF and left to soak and stir for 24 h in a wrist-action mechanical shaker. After decanting the THF, the pouches were left to dry in a fume hood for 24 h, or until their mass was constant. The gel content was calculated as the mass of retained gel divided by the mass of polymer sample.

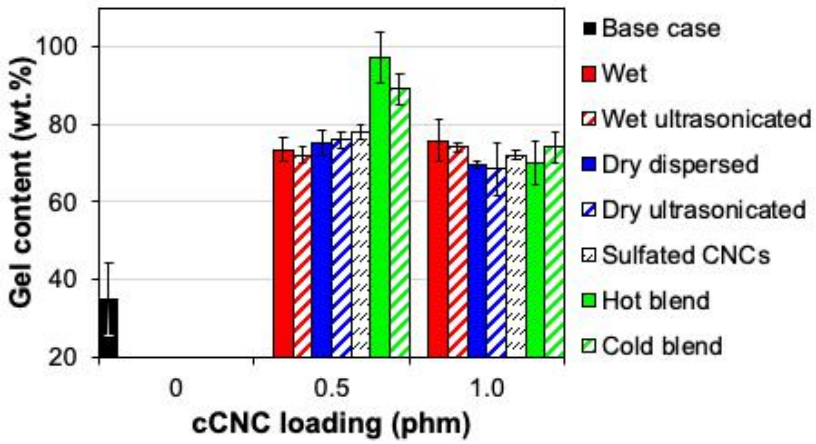

Figure AII.4 Gel content of latexes produced with 0.5 and 1.0 phm cCNCs.

AII.4 References

[1] A. Ouzas, E. Niinivaara, E. D. Cranston, and M. A. Dubé, "In Situ Semibatch Emulsion Polymerization of 2-Ethyl Hexyl Acrylate/ n -Butyl Acrylate/Methyl Methacrylate/Cellulose Nanocrystal Nanocomposites for Adhesive Applications," *Macromolecular Reaction Engineering*, vol. 12, no. 3, p. 1700068, Jun. 2018, doi: 10.1002/mren.201700068.

[2] A. Ouzas, E. Niinivaara, E. D. Cranston, and M. A. Dubé, "Synthesis of poly(isobutyl acrylate/n-butyl acrylate/methyl methacrylate)/CNC nanocomposites for adhesive applications via in situ semi-batch emulsion polymerization," *Polymer Composites*, vol. 40, no. 4, pp. 1365–1377, Apr. 2019, doi: 10.1002/pc.24869.

[3] S. A. Kedzior *et al.*, "Incorporating Cellulose Nanocrystals into the Core of Polymer Latex Particles via Polymer Grafting," *ACS Macro Letters*, vol. 7, no. 8, pp. 990–996, 2018, doi: 10.1021/acsmacrolett.8b00334.

[4] A. S. Pakdel, E. Niinivaara, E. D. Cranston, R. M. Berry, and M. A. Dubé, “Cellulose Nanocrystal (CNC)–Latex Nanocomposites: Effect of CNC Hydrophilicity and Charge on Rheological, Mechanical, and Adhesive Properties,” *Macromolecular Rapid Communications*, vol. 42, no. 3, p. 2000448, Feb. 2021, doi: 10.1002/marc.202000448.

Appendix III

Supporting Information for "Chapter 7: Polymer End-of-Life"

AIII.1 SolidWorks sketches for Bioreactor machining

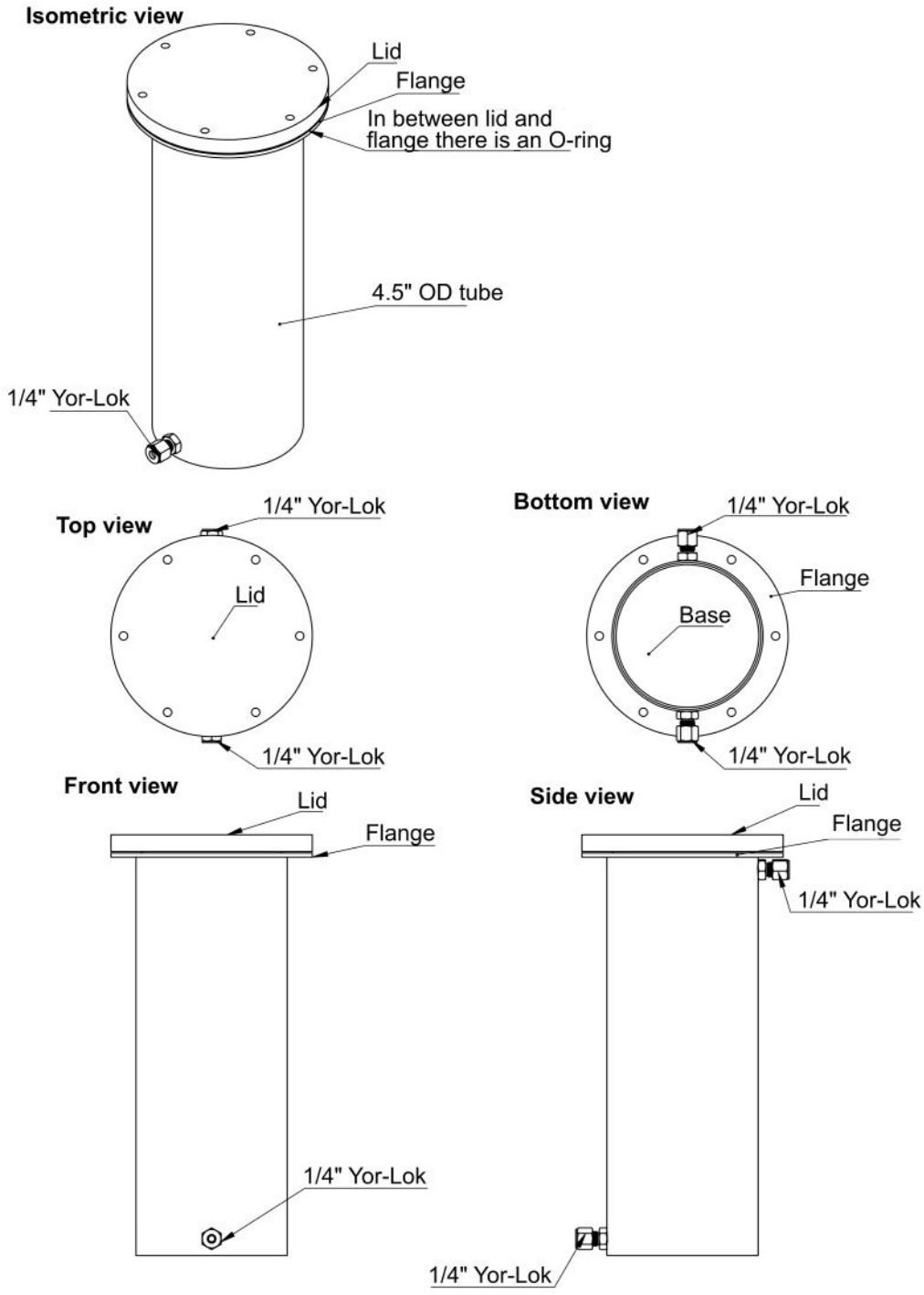

Figure AIII.1 Solidworks design for Bioreactor vessels

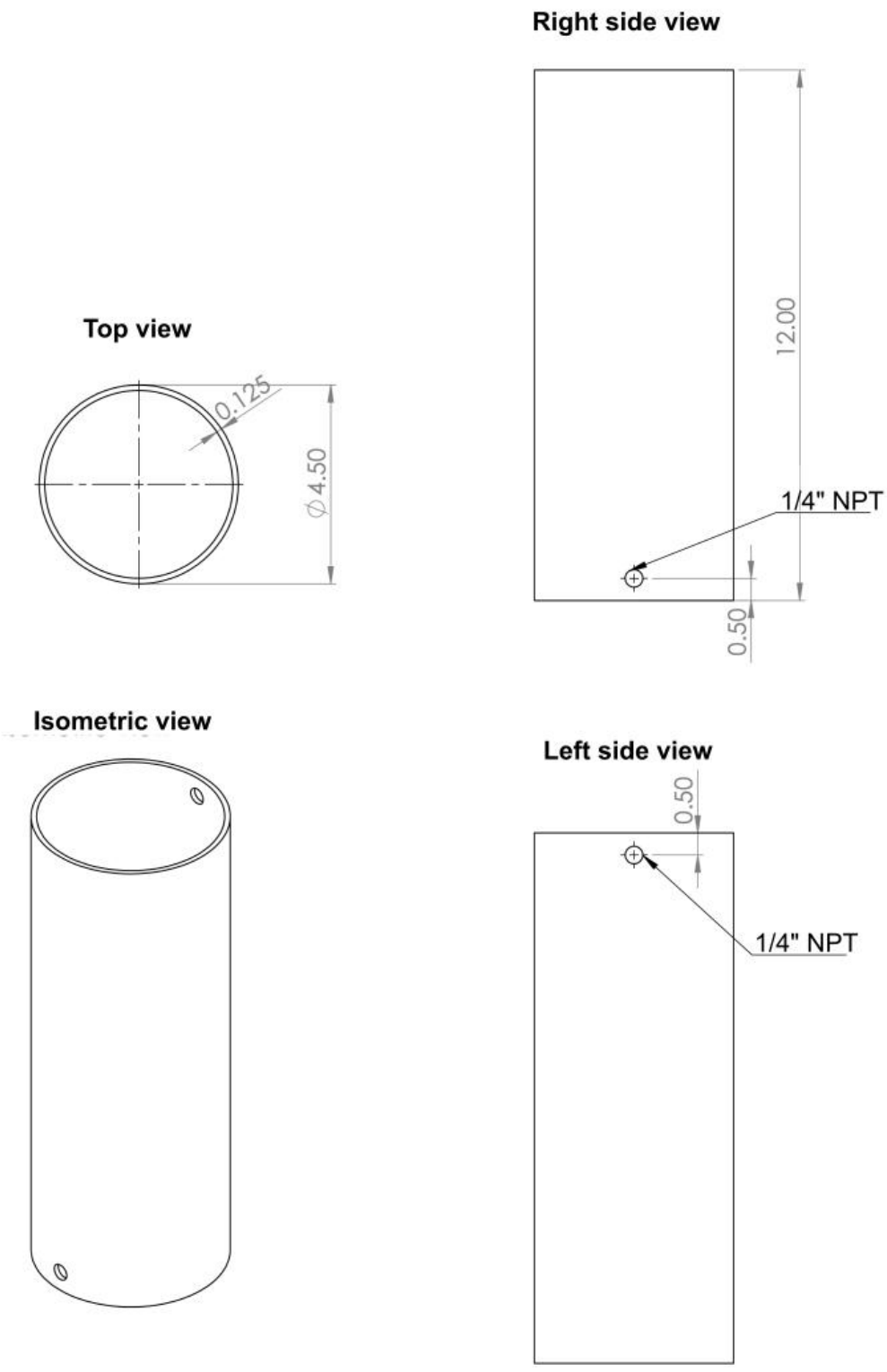

Figure AIII.2 Solidworks design for Bioreactor body

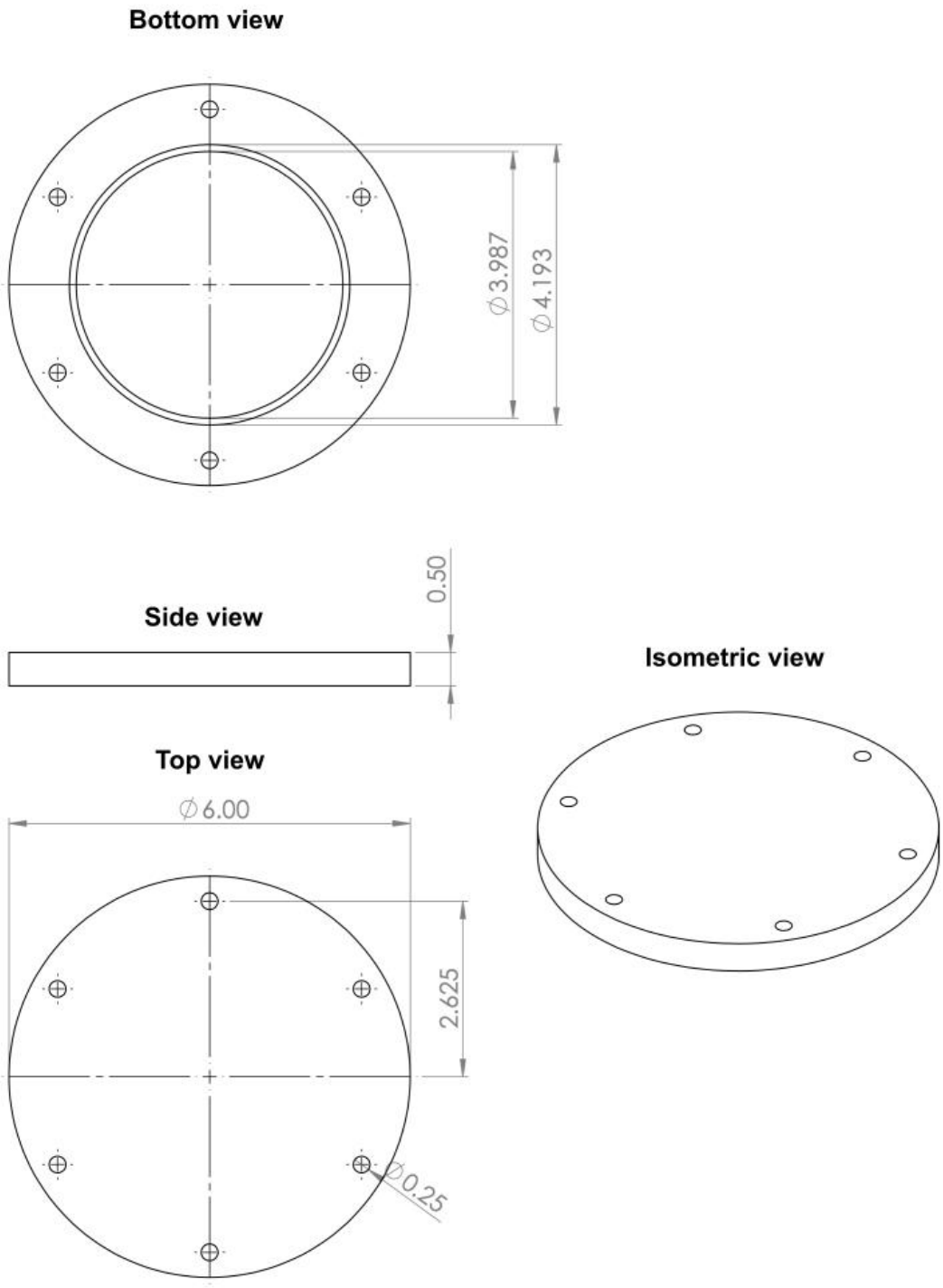

Figure AIII.3 Solidworks design for Bioreactor lid.

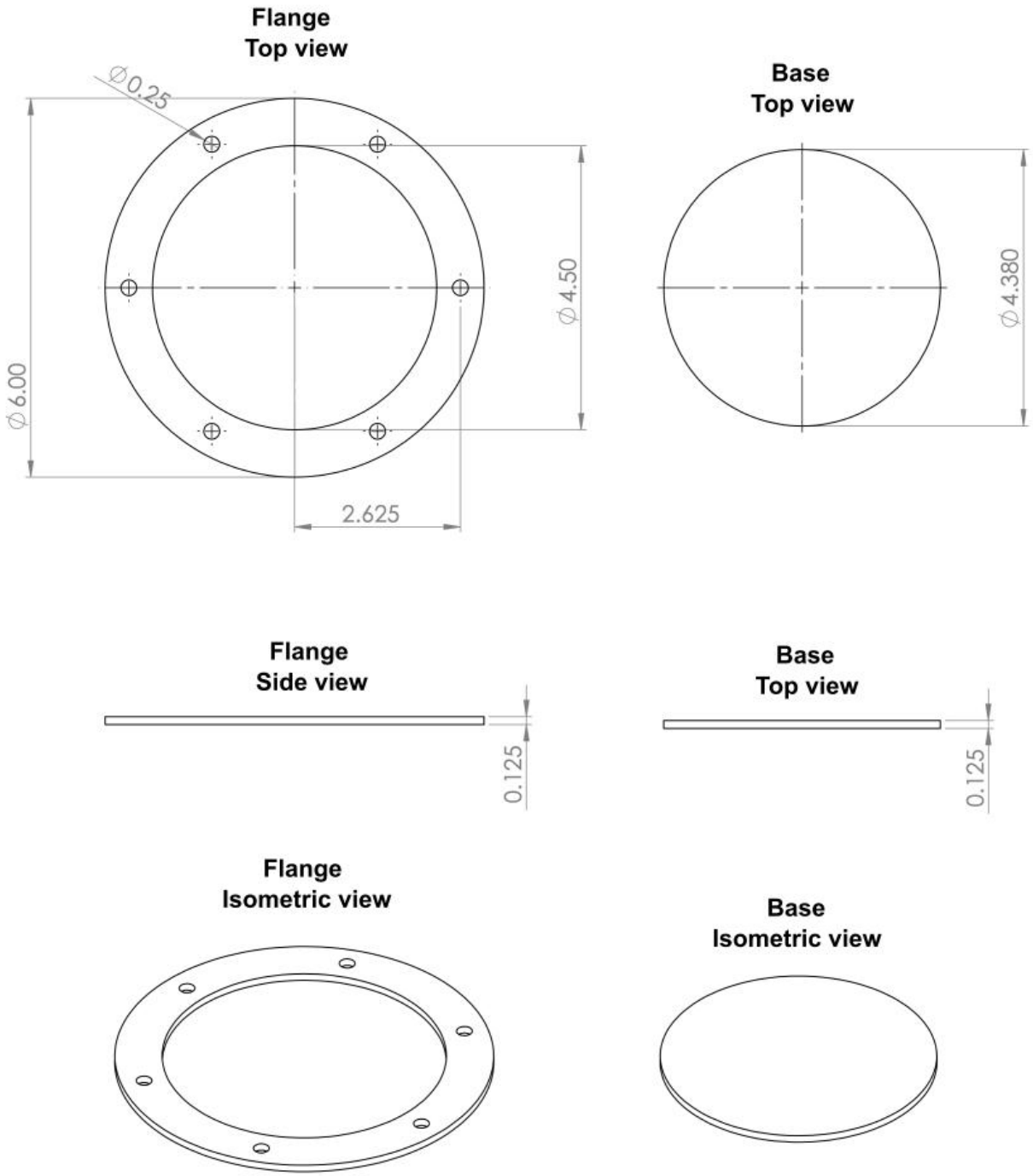

Figure AIII.4 Solidworks design for Bioreactor flange and base

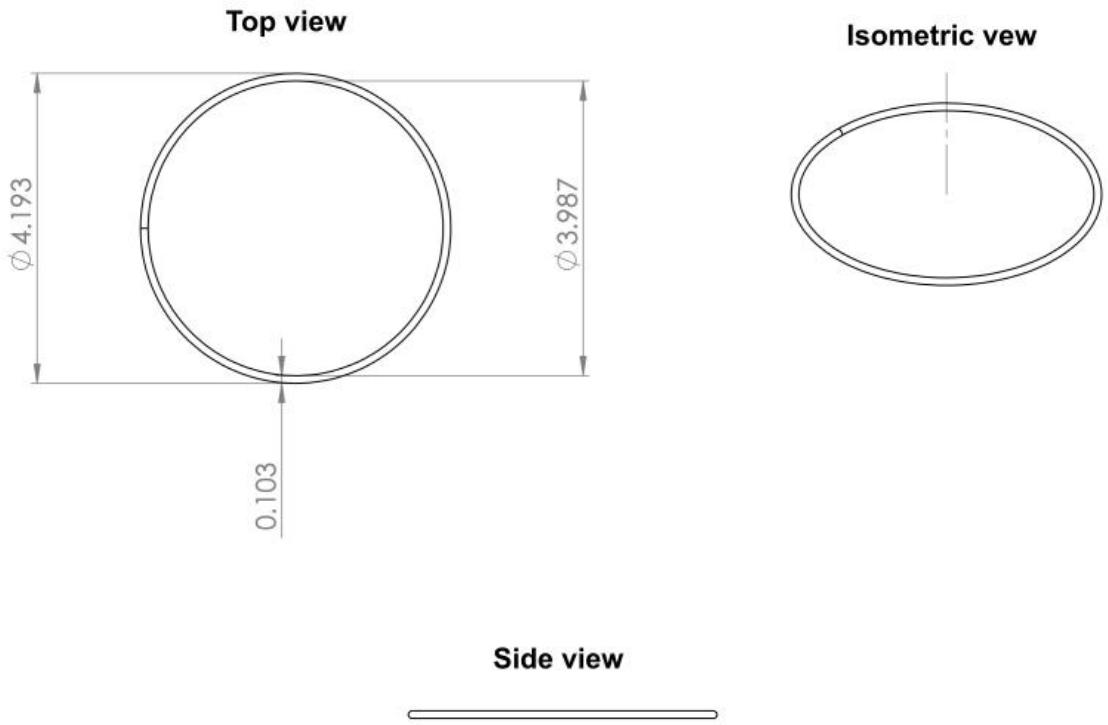

Figure AIII.5 Solidworks design for Bioreactor O-ring

Appendix IV

Laboratory Safety Considerations

The hazards and required PPEs for all the chemicals used in this project were obtained from the manufacturer's safety data sheets and are summarised below. In general, solutions were prepared in a fume hood and personal protective equipment (PPE) including respiratory mask, safety goggles, gloves, and lab coat were used during reaction preparation and polymerization because of possible contact with monomer vapours (during reactor charging and sampling). The reactor temperature is automatically controlled (max ~ 65-70 °C) in a jacketed stainless-steel reactor, connected to a condenser which liquefies the monomer vapours.

Table AIV.1 Hazards and personal protective equipment required for chemicals in this project.

Chemicals	Manufacturing company	Hazards	Personal protective equipment (PPE)
Acrylic Acid (AA)	Sigma-Aldrich	Flammable liquid and vapour. Harmful if swallowed, in contact with skin or if inhaled. Causes severe skin burns and eye damage. May cause respiratory irritation.	Tightly fitting safety goggles. Gloves, complete suit, a full-face respirator Handle in fumehood
Acrylated epoxidized soybean oil (AESO)	Sigma-Aldrich	May cause allergic skin reaction	Protective gloves, eye protection
Acetone	Fischer Scientific	Highly flammable liquid and vapor Causes serious eye irritation May cause drowsiness	Protective clothing and gloves, eye protection
2,2'-Azobis isobutyronitrile (AIBN)	Sigma-Aldrich	Flammable Toxic if swallowed Skin, eye and respiratory irritation	Protective clothing and gloves, eye protection, and full face respirator
Butyl Acrylate (BA)	Sigma-Aldrich	Flammable liquid and vapour Cause skin irritation	Protective clothing and gloves, eye protection, and full face respirator
Butyl vinyl ether (BVE)	Sigma-Aldrich	Flammable liquid and vapour, fatal in contact with skin	Protective clothing and gloves, eye protection, and full face respirator
Carboxylated cellulose nanocrystals (cCNCs)	Anomera Inc.	No significant hazard	Protective clothing and gloves, eye protection
Cetyltrimethylammonium bromide (CTAB)	Fisher Scientific	Causes serious eye damage Acute oral toxicity Causes skin irritation	Protective clothing and gloves, eye protection, and respirator

		May cause respiratory irritation	
EcoMer® (sugar-based monomer)	EcoSynthetix	Causes skin irritation	Protective clothing and gloves, eye protection
Sodium hydroxide pellets (NaOH)	Sigma-Aldrich	Corrosive material, may cause severe skin burns, eye and resperatory irritation. Poisonous if ingested. Reactive with water and bases	Protective clothing and gloves, eye protection
Sulfated cellulose nanocrystals (CNCs)	CelluForce	No significant hazard	Protective clothing and gloves, eye protection
Hydrochloric acid (HCL)	Sigma-Aldrich	Corrosive material, causes severe skin burns and eye damage, may cause repertory irritations	Protective clothing, gloves, eye protection, and full face respirator. Manipulate in fume hood
N-dodecyl mercaptan (NDM)	Sigma-Aldrich	Highly flammable liquid and vapor May cause skin and eye irritation and damage to organs	Protective clothing and gloves, eye protection, and full face respirator
Nitrogen gas (N_2)	Messer	High pressure May cause suffocation by displacing the oxygen in air	Storage upright and secure cylinders all time while in use and use appropriate hand truck designed for cylinder
N-octyl acrylate (nOA)	TCI America	Combustible liquid Flammable liquid Causes skin and eye damage/irritation,	Protective clothing and gloves, eye protection, and full face respirator
Potassium persulfate (KPS)	Sigma-Aldrich	Oxidizing solids May cause eye, skin, and respiratory irritation	Protective clothing and gloves, eye protection
Sodium bicarbonate ($NaHCO_3$)	Sigma Aldrich	No Hazard. May cause eye and skin irritation	Protective clothing and gloves, eye protection
Sodium trimetaphosphate (STMP)	Sigma-Aldrich	Not a hazardous substance or mixture. May be harmful if inhaled, or absorbed through skin. May cause eye irritation	Handle with gloves and eye protection
Sodium dodecyl sulfate (SDS)	Sigma-Aldrich	Flammable and toxic in contact with skin May cause serious eye damage and may cause skin and respiratory irritation	Protective clothing and gloves, eye protection

Sodium hydroxide (NaOH)	Sigma-Aldrich	Causes severe skin burns and eye damage	Protective clothing and gloves, eye protection and respirator
Starch nanoparticles (SNPs)	ExoSynthetix Inc.	May produce slight irritation to respiratory tract. Prolonged exposure to eyes and skin may cause slight irritation	Protective clothing and gloves, eye protection. Avoid breathing dust
Styrene (STY)	Sigma-Aldrich	Flammable liquid and vapour, causes skin and serious eye irritation, harmful if inhaled.	Tightly fitting safety goggles. Gloves, Complete suit, a full-face respirator
Tetrahydrofuran (THF)	Caledon chemicals	Flammable May cause mild skin and serious eye irritation	Protective clothing and gloves, eye protection
Triton X-405, 70% solution in water	Fisher Scientific	Not considered hazardous by the 2012 OSHA Hazard Communication Standard	Protective clothing, gloves, eye protection

Appendix V

List of Publications and Conferences

AV.1 List of Publications

1. **V.A. Gabriel**, M.A. Dubé, "Towards a Fully Biobased Pressure-Sensitive Adhesive," *ACS Sustainable Chemistry and Engineering*, (2022) Submitted.
2. **V.A. Gabriel**, M.N. Tousignant, S.M.W. Wilson, M.D.M. Faure, E.D. Cranston, M.F.Cunningham, B.H. Lessard, M.A. Dubé, "Improving Latex-Based Pressure-Sensitive Adhesive Properties Using Carboxylated Cellulose Nanocrystals," *Macromolecular Reaction Engineering*, (2022) 2100051. **Front cover article.**
3. **V.A. Gabriel**., P. Champagne, M.F. Cunningham, M.A. Dubé, "In-situ addition of carboxylated cellulose nanocrystals in seeded semi-batch emulsion polymerization," *The Canadian Journal of Chemical Engineering* (2021) **100**, 767-779.
4. M.A. Dubé, **V.A. Gabriel**, A.S. Pakdel, Y. Zhang, "Sustainable polymer reaction engineering: Are we there yet?" *The Canadian Journal of Chemical Engineering,* (2021) **99**, 31–60.
5. A.S. Pakdel, **V.A. Gabriel**, R.M. Berry, C. Fraschini, E.D. Cranston, M.A. Dubé, "A sequential design approach for in situ incorporation of cellulose nanocrystals in emulsion-based pressure sensitive adhesives," *Cellulose,* (2020) **27**, 10837–10853.
6. **V.A. Gabriel**, E.D. Cranston, M.A. Dubé, "Pushing the Limits with Cellulose Nanocrystal Loadings in Latex-Based Pressure-Sensitive Adhesive Nanocomposites," *Macromolecular Reaction Engineering,* (2020) **14**, 2000027.
7. S.A. Kedzior, **V.A. Gabriel**, M.A. Dubé, E.D. Cranston, "Nanocellulose in Emulsions and Heterogeneous Water-Based Polymer Systems: A Review," *Advanced Materials,* (2020) **5,** 10509-10517.
8. S.M.W. Wilson, **V.A. Gabriel**, F.H. Tezel, "Adsorption of components from air on silica aerogels," *Microporous and Mesoporous Materials,* (2020) **305**, 110297.

9. A.J. Scott, **V.A. Gabriel**, M.A. Dubé, A. Penlidis, "Making the most of parameter estimation: Terpolymerization troubleshooting tips," *Processes,* (2019) **7**, 7.
10. J.A. Gómez-Reguera, E. Vivaldo-Lima, **V.A. Gabriel**, M.A. Dubé, "Modeling of the free radical copolymerization kinetics of n-butyl acrylate, methyl methacrylate and 2-ethylhexyl acrylate using PREDICI®," *Processes,* (2019) **7**, 395.
11. **V.A. Gabriel**, M.A. Dubé, "Bulk Free-Radical Co- and Terpolymerization of n-Butyl Acrylate/2-Ethylhexyl Acrylate/Methyl Methacrylate," *Macromolecular Reaction Engineering*, (2019) **13**, 1800057.

AV.2 List of Conference Presentations

1. **V.A. Gabriel**,* E.D. Cranston, M.A. Dubé, "*Dried vs. Never-Dried Carboxylated Cellulose Nanocrystals: Branching Out to Sticker Nanocomposite Adhesives*," Oral presentation, International Conference on Nanotechnology for Renewable Materials, TAPPI Nano 2022, Helsinki, Finland, June 2022.
2. J. Antoniw,* **V.A. Gabriel**, M.A. Dube, E.D. Cranston, "*The sticky road to understanding the effect of cellulose nanocrystal surface chemistry on the performance of latex-based pressure-sensitive adhesives,*" Oral presentation, International Conference on Nanotechnology for Renewable Materials, TAPPI Nano 2022, Helsinki, Finland, June 2022.
3. **V.A. Gabriel**,* M.A. Dubé (2021), "*Improving latex-based adhesives with carboxylated cellulose nanocrystals (cCNCs),*" Oral presentation, Canadian Chemical Engineering Conference, CCEC 2021, National, Ottawa, ON, October 2021.
4. **V.A. Gabriel,*** M.A. Dubé, E.D. Cranston, E.D., (2020), "*How much is 'too much'? Using cellulose nanocrystals for pressure-sensitive adhesive enhancement,*" Oral presentation, Canadian Chemical Engineering Conference CCEC 2020, National, Ottawa, ON, October 2020.
5. **V.A. Gabriel,*** M.A. Dubé, E.D. Cranston, C. Frashini, R. Berry, "*Adhesive property improvement via CNC incorporation,"* Poster presentation, PAPTAC 2019, BIOFOR, International 2019, Montréal, QC, February 2019.

6. S.M.W. Wilson,* **V.A. Gabriel**, F.H. Tezel, (2019), "*Silica Aerogel Adsorption of Components in Air,"* Poster presentation, Fundamentals of Adsorption XIII (FOA XIII), international, Cairns Australia, May 2019.
7. **V.A. Gabriel,*** M.A. Dubé, "*Predicting Terpolymer Composition using Copolymer Reactivity Ratios,"* Oral presentation, 68th Canadian Chemical Engineering Conference (CCEC), national, Toronto, ON, October 2018.
8. **Gabriel, V.A.*** and Dubé, M.A, "*Reactivity Ratio Estimation for Co- and Terpolymer Systems,"* Poster presentation, Polymer Reaction Engineering X (PRE X) Conference, international, Punta Cana, Dominican Republic, May 2018.